MicroRNAs as molecular targets for non-viral gene therapy of glioblastoma: development of a lipid-based nanosystem for nucleic acid delivery to brain tumor cells

MicroRNAs como alvos moleculares para terapia génica não viral de glioblastoma: desenvolvimento de um nanosistema de base lipídica para entrega de ácidos nucleicos a células de tumores cerebrais

Thesis presented to the Department of Life Sciences, Faculty of Science and Technology, University of Coimbra, in partial fulfillment of the requirements for obtaining a Doctoral degree in Biochemistry, in the speciality of Biochemical Technology, under supervision of Professor Dr. Maria da Conceição Pedroso de Lima (Department of Life Sciences, Faculty of Science and Technology, University of Coimbra) and Professor Dr. Luís Pereira de Almeida (Faculty of Pharmacy, University of Coimbra).

Tese apresentada ao Departamento de Ciências da Vida, Faculdade de Ciências e Tecnologia, Universidade de Coimbra, para prestação de provas de Doutoramento em Bioquímica, na especialidade de Tecnologia Bioquímica, sob supervisão da Professora Doutora Maria da Conceição Pedroso de Lima (Departamento de Ciências da Vida, Faculdade de Ciências e Tecnologia, Universidade de Coimbra) e do Professor Doutor Luís Pereira de Almeida (Faculdade de Farmácia, Universidade de Coimbra).
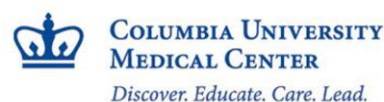
Front cover:

MicroRNA-21 staining in U87 human glioblastoma cells by fluorescence in situ hybridization. MicroRNA-21 staining (red dots) is detected in the cytoplasm of glioblastoma cells, while no staining is observed in the cell nucleus, stained with the DNA-intercalating probe Hoechst (blue). Image obtained by confocal microscopy.

À Aneta

Aos meus pais

Ao meu irmão

Eles não sabem, nem sonham,

que o sonho comanda a vida,

que sempre que um homem sonha

o mundo pula e avança

como bola colorida

entre as mãos de uma criança.

Acknowledgements/Agradecimentos

À Professora Doutora Maria da Conceição Pedroso de Lima gostaria de dedicar um agradecimento muito especial pela qualidade da sua orientação cíentifica, desde o meu estágio de licenciatura até esta etapa académica. O seu rigor, conhecimento científico, apoio e incentivo contribuíram decisivamente para o sucesso deste Trabalho e para a minha formação científica. Agradeço também toda a sua disponibilidade, toda a confiança que depositou em mim e acima de tudo a amizade que sempre demonstrou e a qual prezo muito.

Ao Professor Doutor Luís Pereira de Almeida, pela qualidade da sua orientação científica, pela constante disponibilidade, pelo apoio e amizade e por todas as excelentes sugestões que em muito enriqueceram e melhoraram este Trabalho, e me ajudaram a crescer cientificamente.

To Professor Jeffrey Bruce, for receiving me at his laboratory at the Columbia University Medical Center (CUMC), New York, USA, for his support and for giving me all the conditions to work efficiently during my stay at his laboratory.

To Professor Peter Canoll, for his help and support, for the interesting discussions that greatly increased my knowledge about glioblastoma and for the suggestions that contributed to improve the quality of this Work.

À Professora Doutora Catarina Resende de Oliveira, por me permitir realizar a maior parte deste Trabalho no Centro de Neurociências e Biologia Celular da Universidade de Coimbra.

À Fundação para a Ciência e Tecnologia, pelo financiamento concedido, sem o qual não seria possível a realização deste trabalho.

To Orlando Gil, for all the support with the experiments performed at the CUMC and for the help during my stay in New York City.

A todos os meus colegas do grupo de Vectores e Terapia Génica e do Centro de Neurociências e Biologia Celular, pela ajuda e por todos os momentos de boa disposição partilhados ao longo destes anos. Em especial, gostaria de agradecer à Ana Luísa Cardoso, pela amizade, pelo auxílio e pelas interessantes discussões e sugestões que

contribuiram bastante para melhorar este Trabalho. És para mim uma referência como jovem cientista. Gostaria também de agradecer ao Carlos Custódia por toda a ajuda na realização das experiências e pelos momentos de boa disposição, à Liliana Mendonça pelos ensinamentos sobre SNALPs, e à Mariana Conceição pela ajuda com os procedimentos envolvendo animais.

Aos meus colegas do curso de Bioquímica, em especial ao/à Tiago, Diogo, Nair, Maria Inês, Telmo, Ludgero, Rui Costa e João Costa, pela amizade e por todos os momentos partilhados ao longo destes últimos anos.

Um agradecimento profundo aos meus pais, Eduardo e Maria, por todos os ensinamentos, toda a confiança e todo o apoio que sempre demonstraram ao longo deste caminho. Obrigado por me mostrarem que com esforço e determinação conseguimos alcançar todos os nossos objectivos. A pessoa que sou hoje é o reflexo da educação, amor e carinho que sempre me deram.

Um agradecimento muito especial à Aneta, minha esposa e minha melhor amiga, não só pela ajuda na elaboração desta tese, mas acima de tudo pelo amor, carinho, apoio, compreensão e incentivo constantes, que muito me ajudaram nos momentos mais difíceis. Obrigado por acreditares sempre em mim e por fazeres de mim uma pessoa melhor.

Esta tese é-vos dedicada!

INDEX

Abbreviations

2'-F: fluorine
2'-MOE: methoxyethyl
2'-OMe: methyl
2-IT: 2-iminothiolane
3'/5' UTR: 3'/5'-terminal untranslated region
5-FC/FU: 5-fluorocytosine/fluorouracil

A:

AAVs: adeno-associated viruses
Ago: argonaute protein
Ago2: argonaute protein 2
AIB1: amplified in breast cancer 1
Akt (PKB): protein kinase B
AML: acute myeloid leukemia
AMOs: anti-miRNA oligonucleotides
AP-1: activator protein 1
APAF-1: apoptotic protease activating factor 1
ARF: alternative reading frame
ASOs: antisense oligonucleotides

B:

BBB: blood-brain barrier
Bcl-2: B-cell lymphoma 2
BCL2L: B-Cell CLL/Lymphoma 2 like protein
BCNU: 1,2-bis(2-chloroethyl)-1-nitrosourea
BL: Burkitt's lymphoma
Bmi-1: B lymphoma mouse Moloney leukemia virus insertion region 1
BMP: bone morphogenic protein
BSA: bovine serum albumin

C:

CAF1: chromatin assembly factor 1
CAGRs: cancer-associated genomic regions
CALR: calreticulin
CCR4-NOT: C-C chemokine receptor type 4-NOT
CD: cytosine deaminase
CDK1/2/4/6: cyclin-dependent kinase 1/2/4/6
CDKN1A: cyclin-dependent kinase inhibitor 1A

CDKs: cyclin-dependent protein kinases
CED: convection-enhanced delivery
CENTG1: Arf-GAP with GTPase, ANK repeat and PH domain-containing protein 2
CerC16-PEG2000: N-palmitoyl-sphingosine-1-(succinyl(methoxypolyethylene glycol) 2000)
CHI3L1: chitinase-3-like protein 1
CLL: chronic lymphocytic leukemia
CMV: cytomegalovirus
CN-AML: cytogenetically normal acute myeloid leukemia
CNOT7: CCR4-NOT transcription complex subunit
CPP: cell-penetrating peptide
CSCs: cancer stem cells
CSF: cerebrospinal fluid
CTX: chlorotoxin

D:

DAXX: death-associated protein 6
DC-Chol: 3β-(N-(N′, N′-dimethylaminoethane)-carbamoyl)-cholesterol
DCP1-DCP2: mRNA-decapping enzyme 1/2
DFS: disease-free survival
DGCR8: DiGeorge syndrome criticical region gene 8
DIG: digoxigenin
DLS: liposomal delivery system
DMSO: dimethylsulfoxide
DNA: deoxyribonucleic acid
DNMT3A/B: DNA methyltransferases 3A/B
DODAP: 1,2-dioleoyl-3-dimethylammonium-propane
DOGS: dioctadecylamidoglycylspermidine
DOPE: L-α-dioleoylphosphatidylethanolamine
ds: double-stranded
DSPC: 1,2-dioleoyl-sn-glycero-3-phosphocholine
DSPE-PEG-MAL: 1,2-distearoyl-sn-glycero-3-phospatidylethanolamine-N-(maleimide (polyethylene glycol)-2000) ammonium salt
DTT: dithiothreitol

E:

EDD/ubr5: E3 ligase identified by differential display/ ubiquitin protein ligase E3 component n-recognin 5
EDTA: ethylenediaminetetraacetic acid
EGF: epidermal growth factor
EGFR: epidermal growth factor receptor
EGFRvIII: epidermal growth factor receptor variant III
EHCO: (1-aminoethyl)iminobis(N-(oleicylcysteinylhistinyl-1-aminoethyl)propionamide
eIF: eukaryotic initiation factor
eIF2/3: eukaryotic initiation factor 2/3
eIF4A/E /G: eukaryotic initiation factor 4A/E/G
ERBB2: human epidermal growth factor receptor 2 gene
ERK1/2: extracellular-signal-regulated kinase 1/2

F:

FAM: 6-carboxyfluorescein
FFPE: formalin-fixed paraffin embedded
FHIT: fragile histidine triad protein
FISH: fluorescence in situ hybridization
FITC: fluorescein isothiocyanate
FMRP: fragile X mental retardation protein

G:

GBM: glioblastoma
GDP: guanosine diphosphate
GFP: green fluorescent protein
Grb2: growth factor receptor-bound 2
GSCs: GBM stem-like cells
GTP: guanosine triphosphate
GW182 (TNRC6A-C): trinucleotide repeat-containing gene 6A protein

H:

HBS: HEPES buffered saline
HC: hepatitis C
HCV: hepatitis C virus
HDAC: histone deacetylases
HER2: human epidermal growth factor receptor 2
HGF: hepatocyte growth factor
HIF-1α: hypoxia-inducible factor 1
HMGA2: high-mobility group AT-hook 2

HNRNPK: heterogeneous nuclear ribonucleoprotein K
HOXD10: homeobox D10
HPRT1: hypoxanthine-guanine phosphoribosyltransferase
HSV: herpes simplex virus
HSV-tk: herpes simplex virus type 1 thymidine kinase
hTERT: enzyme telomerase reverse transcriptase

I:

IDH1: isocitrate dehydrogenase
IFN-β: interferon-β
IGFR: insulin-like growth factor receptor
IL13Rα2: interleukin-13 receptor α2
IL-2/6/12/13: interleukin-2/6/12/13
INK4: cyclin-dependent kinase inhibitor 2A isoform p16gamma
INK4aARF: cyclin-dependent kinase inhibitor 2A
IRES: internal ribosome entry sites
IRS-1/2: insulin receptor substrate ½

J:

JMY: junction-mediating and -regulatory protein
JNK: c-Jun N-terminal kinase

L:

LNA: locked nucleic acid
LOH: loss of heterozygosity

M:

m7Gppp: 7-methylguanosine
MA: myristic acid
MAGE-A3: melanoma-associated antigen 3
MAPK: mitogen-activated protein kinase
MBS: miRNA binding sites
MDM2/4: mouse double minute 2/4 homolog
MEK: mitogen-activated protein kinase kinase
MET (HGFR): hepatocyte growth factor receptor
MGMT: O(6)-methyguanine methyltransferase
MHC: major histocompatibility complex
miRNA: microRNA

miRNP: miRNA-containing ribonucleoprotein
mirtrons: short-hairpin intron
MMP: matrix metalloproteinase
mRNA: messenger RNA
MSCs: mesenchymal stem cells
MSH6: mutS homolog 6
mTOR: mammalian target of rapamycin

N:

NBD-PE: 1,2-dipalmitoyl-sn-glycero-3-phosphoethanolamine-N-(7-nitro-2-1,3-benzoxadiazol-4-yl) ammonium salt
ncRNAs: noncoding RNAs
NF1: neurofibromin 1
NF-kB: nuclear factor kB
NK: natural killer
NLE: neutral lipid emulsion
NRVs: non-replicating viruses
NSCLC: small-cell lung cancer
NSCs: neural stem cells
NT: nontargeted
nt: nucleotide

O:

ORF: open reading frame
OS: overall survival
OVs: oncolytic viruses

P:

p21: cyclin-dependent kinase inhibitor 1
p27Kip1: cyclin-dependent kinase inhibitor 1B
PABP: poly(A)-binding protein
PAMAM: polyamidoamine
PAN2-PAN3: PAB-dependent poly(A)-specific ribonuclease subunit 2/3
PBS: phosphate buffered saline
PCR: polymerase chain reaction
PDCD4: programmed cell death protein 4
PDGF-A/B: platelet-derived growth factor AA/BB
PDGFR: platelet-derived growth factor receptor
PDGFRA: platelet-derived growth factor receptor alpha
PDK: phosphatidylinositol-dependent kinase
PEG: polyethylene glycol
PEI: polyethylenimine
Pex: pseudomonas exotoxin

PFA: paraformaldehyde
PFS: progression-free survival
PGE2: prostaglandin E2
PI: propidium iodide
PI3K: phosphoinositide-3 kinase pathway
PIK3CA: phosphatidylinositol-4,5-bisphosphate 3-kinase, catalytic subunit alpha
PIK3R1: phosphoinositide-3-kinase, regulatory subunit 1
PIP2: phosphatidylinositol 4,5-bisphosphate
PIP3: phosphatidylinositol 3,4,5-triphosphate
piRNAs: Piwi-interacting RNAs
PLGA: poly(lactic-co-glycolic acid
PMSF: phenylmethylsulfonyl fluoride
PNAs: peptide nucleic acids
PRC1: polycomb repressor complex
pre-miRNAs: precursor miRNAs
pri-miRNAs: primary miRNAs
PTBP1/2: polypyrimidine tract-binding protein ½
PTEN: phosphatase and tensin homolog
PU: polyurethane
PVDF: polyvinylidene fluoride

Q:

qPCR: real-time PCR

R:

R9: nona-arginine
RAF: murine leukemia viral oncogene homolog 1
Ras: rat sarcoma viral oncogene homologue
RB: retinoblastoma protein
RCK/p54: human DEAD-box/RNA unwindase RCK/p54
RCRs: replication-competent retroviruses
RECK: reversion-inducing-cysteine-rich protein with kazal motifs
RHOC: Ras homolog gene family member C
Rho-PE: L-α-phosphoethanolamine-N-(lissamine rhodamine B sulfonyl)
RIPA: radioimmunoprecipitation assay
RNA: ribonucleic acid
RNAi: RNA interference
RTK: receptor tyrosine kinase

S:

S6K: ribosomal protein S6 kinase
SCs: stem cells
SDS: sodium dodecyl sulfate
SGs: stress granules
SHIP1: phosphatidylinositol-3,4,5-trisphosphate 5-phosphatase 1
shRNAs: short hairpin RNAs
siRNAs: small interference RNAs
SLN: solid lipid nanoparticles
SMAD3/4: Mothers against decapentaplegic homolog 3/4
SNALP: stable nucleic acid lipid particle
ss: single-stranded
Stat3: signal transducer and activator of transcription 3

T:

TATp: trans-activating transcriptional activator peptide
TBS/T: Tris buffered saline with 0.1% tween-20
TCGA: The Cancer Genome Atlas
TFAP2C: transcription factor AP-2 gamma
TGF-β: transforming growth factor β
TGFβR: transforming growth factor beta receptor
TIA: T-cell-restricted intracellular antigen 1
TIAR: TIA-related RNA-binding protein
TIMP3: tissue inhibitor of metalloproteinases 3
TMZ: temozolomide
TNF: tumor necrosis factor
TOPORS: topoisomerase I binding ligase
TP53: tumor protein 53
TP53BP2: tumor suppressor p53-binding protein 2
TRAIL: tumor necrosis factor-related apoptosis-inducing ligand
TRBP: RNA-binding protein TAR
TSC: tuberous sclerosis complex

V:

VEFGR: vascular endothelial growth factor receptor
VEGF: vascular endothelial growth factor
VEGF-A: vascular endothelial growth factor A

W:

WT1: Wilms tumor protein 1
WWOX: WW domain containing oxidoreductase

X:

XRN1: 5'-3' exoribonuclease 1

Abstract

Glioblastoma (GBM) is the most common and aggressive primary brain tumor associated with a high degree of mortality. Despite the recent advances in cancer therapy, GBM almost always recurs and patient survival remains under the year mark, thus emphasizing the need for new and effective therapeutic strategies, as well as a better understanding of the molecular alterations that occur in this malignancy. The development of successful GBM therapies faces two major challenges. The first concerns the identification of cellular effectors involved in cancer surgence and progression, which may constitute important targets for an effective therapeutic approach. MicroRNAs (miRNAs), a small class of noncoding gene-regulator RNAs, have been implicated in the intricate carcinogenic process, including GBM pathogenesis. In this regard, the modulation of dysregulated miRNAs has been associated with anti-tumor activities, including reduced cell proliferation and increased apoptosis, which indicates that miRNAs could be explored as targets for treatment of cancer. The second major challenge relates to the delivery of the therapeutic molecules to the brain tumor cells. The complex structure of the blood-brain barrier (BBB) strongly restricts the type and amount of molecules that can reach the brain. Therefore, development of safe and efficient delivery systems, able to surpass the BBB and improve the delivery of anti-tumoral agents to the brain, could significantly contribute to increase the efficacy of GBM therapies.

Aiming at generating an effective therapy to GBM with clinical relevance, one of the main purposes of this Thesis consisted in the development of a non-viral gene therapy approach towards GBM, based on stable nucleic acid lipid particles (SNALPs), which were designed for systemic delivery of antisense oligonucleotides (ASOs) targeting dysregulated miRNAs in GBM.

Initial studies, described in Chapter 3, involved the identification of abnormally expressed miRNAs in GBM through real-time PCR quantification of miRNAs in tumor samples from patients and GBM mouse models, and control non-cancer tissues. MicroRNA-21 (miR-21) was found to be upregulated and microRNA-128 (miR-128) was downregulated in tumor samples, when compared to their expression in different control tissues, a finding that was corroborated by the analysis of a large set of human GBM data from The Cancer Genome Atlas. The therapeutical potential of a miRNA-based approach was evaluated by assessing the cellular and molecular alterations associated with the repression of miR-21, by Western blot, apoptosis and cell viability assays. A significant increase in both the expression of tumor suppressors PTEN and PDCD4 and the activation of apoptose effectors caspase 3/7

were observed in cells with reduced miR-21 expression. Importantly, miR-21 silencing enhanced the cytotoxic effect of the tyrosine kinase inhibitor sunitinib, whereas no therapeutic benefit was observed when combining miR-21 silencing with the first line drug temozolomide.

The second part of this Work, described in Chapter 4, was focused on the development and application of a lipid-based nanosystem - SNALPs - for targeted delivery of nucleic acids to GBM. To achieve specific tumor delivery, as well as to enhance particle internalization, the peptide chlorotoxin (CTX), which was reported to bind selectively to glioma cells while showing no affinity for non-cancer cells, was covalently coupled to the liposomal surface. Initial studies, addressing the physicochemical characteristics of the developed nanoparticles, revealed that the targeted (CTX-coupled) SNALPs exhibit suitable features for *in vivo* application, including small size (below 180 nm) and neutral surface charge. Moreover, high ASO-encapsulation efficiencies were obtained for both targeted and nontargeted formulations. Cellular association (flow cytometry) and internalization (confocal microscopy) studies revealed that CTX coupling onto the liposomal surface enhanced SNALP internalization into glioma cells, while no significant internalization was observed in non-cancer cells. Importantly, CTX was also shown to enhance particle internalization into established intracranial tumors. Furthermore, increased expression of PTEN and PDCD4, caspase 3/7 activation and increased tumor cell sensitivity to sunitinib were observed in U87 human GBM and GL261 mouse glioma cells when incubated with CTX-coupled liposomes encapsulating anti-miR-21 oligonucleotides.

Finally, in Chapter 5, the effect of the angiogenic platelet-derived growth factor-B (PDGF-B) on the expression of miRNAs in GBM was investigated, aiming at understanding its role in GBM tumorogenesis. Initial studies demonstrated that miR-21 and miR-128 were downregulated in U87 cells overexpressing PDGF-B (U87-PDGF), which was associated with increased cell proliferation. Curiously, siRNA-mediated PDGF-B silencing led to increased levels of miR-21 and miR-128, whereas miR-21 overexpression did not affect the expression of PDGF-B. Microarray analysis was performed to ascertain whether the expression profiling of other miRNAs would be affected by the exposure to increased levels of PDGF-B. In this regard, increased expression of pro-oncogenic miRNAs (including members of the miR-106b family) and decreased expression of tumor suppressor miRNAs (including let-7b) were observed in U87-PDGF cells.

Overall, the findings gathered in this Work demonstrate the therapeutic relevance of a multimodal approach towards GBM, combining targeted and efficient delivery of anti-miRNA

oligonucleotides, via CTX-coupled SNALPs, with the receptor tyrosine kinase inhibitor sunitinib, with potential to be successfully applied in future clinical translational studies.

Resumo

O glioblastoma (GBM) é o tipo de tumor cerebral mais comum e mais agressivo que afecta os humanos. Apesar dos recentes avanços no estudo do cancro, as opções de tratamento para este tipo de tumor permanecem limitadas e pouco eficazes, com taxas de sobrevivência de 9 a 12 meses após diagnóstico. Assim, é urgente desenvolver novas estratégias terapêuticas que conduzam à morte das células tumorais e à erradicação do tumor, aumentando assim a esperança de vida dos doentes.

O desenvolvimento de abordagens terapêuticas para tratamento do GBM apresenta dois grandes desafios. O primeiro está relacionado com a identificação de moléculas efectoras envolvidas no aparecimento e desenvolvimento do GBM, que poderão constituir alvos importantes para uma eficaz abordagem terapêutica. Inúmeros estudos demonstraram que microRNAs (miRNAs), uma classe de pequenas moléculas de RNA não codificante com capacidade de regular a expressão genética, estão envolvidos no processo carcinogénico, incluindo o desenvolvimento do GBM. Para além disso, vários estudos demonstraram que a modulação de miRNAs expressos em níveis anormais nas células tumorais resulta em actividade anti-tumoral, incluindo a redução da proliferação celular e o aumento da apoptose, o que indica que os miRNAs poderão ser explorados como alvos numa terapia anti-cancerígena. O segundo grande desafio está relacionado com a entrega de agentes anti-cancerígenos ás células tumorais cerebrais. A complexa estrutura da barreira hematoencefálica restringe drasticamente o tipo e quantidade de moléculas que podem alcançar o tecido cerebral. Assim sendo, o desenvolvimento de veículos que possam ultrapassar esta barreira e entregar de forma segura e eficiente agentes terapêuticos às células tumorais cerebrais poderá contribuir para o aumento de eficácia das terapias direccionadas ao GBM.

Com o objectivo de gerar uma terapia eficaz para GBM, com relevância clínica, um dos principais objectivos desta Tese consistiu no desenvolvimento de uma estratégia de terapia génica não viral, baseada em partículas lipídicas estáveis encapsulando ácidos nucleícos (SNALPs), que foram concebidas para entrega sistémica de oligonucleótideos antisense direccionados para miRNAs desregulados em GBM.

Estudos iniciais, descritos no Capítulo 3, envolveram a identificação de miRNAs anormalmente expressos em GBM, através da quantificação por PCR em tempo real de miRNAs em amostras tumorais de doentes e modelos animais de GBM, e em diferentes amostras de tecido não tumoral. Os resultados obtidos demonstraram que o microRNA-21 (miR-21) se encontra sobre-expresso e o microRNA-128 (miR-128) se encontra sob-

expresso nas amostras tumorais, quando comparado com os níveis de expressão em amostras não tumorais. A análise de dados relativos a aproximadamente 200 amostras de GBM, disponíveis na base de dados TCGA (The Cancer Genome Atlas, USA), corroborou os resultados obtidos. Para avaliar o potencial de uma abordagem terapêutica baseada em miRNAs, oligonucleótideos antisense foram utilizados para silenciar o miR-21 em células de GBM em cultura. Ensaios para detectar a expressão de proteínas (Western blot), activação de apoptose e viabilidade celular foram realizados para avaliar as alterações celulares e moleculares associadas à repressão do miR-21. Um aumento significativo da expressão dos supressores tumorais PTEN e PDCD4 e a activação dos efectores apoptóticos caspase 3/7 foram detectados em células com níveis baixos de miR-21. Importantemente, o silenciamento do miR-21 aumentou o efeito citotóxico do sunitinib, um inibidor de receptores com actividade de cinase de tirosina, enquanto que nenhum benefício terapêutico foi observado quando o silenciamento do miR-21 foi combinado com temozolomide, o fármaco que é actualmente utilizado no tratamento do GBM.

A segunda parte deste trabalho, descrita no Capítulo 4, focou-se no desenvolvimento e aplicação de nanopartículas de base lipídica – SNALPs – para a entrega direccionada de oligonucleótideos antisense contra o miR-21. De forma a entregar os oligonucleótidos de forma específica às células tumorais e aumentar a internalização das nanopartículas, clorotoxina (CTX), um peptídeo que se liga especificamente a células tumorais e que revela baixa afinidade para células não tumorais, foi ligado covalentemente à superfície das nanopartículas. Estudos iniciais avaliaram as características fisico-químicas das nanopartículas desenvolvidas e revelaram que estas possuem características ideais para administração *in vivo*, incluindo tamanho reduzido (inferior a 180 nm) e carga superficial neutra. Para além disso, uma elevada taxa de encapsulação de oligonucleótideos foi obtida para as nanopartículas com e sem CTX associada. Estudos de associação (citometria de fluxo) e internalização celular (microscopia confocal) revelaram que o acoplamento de CTX à superfície das nanopartículas permitiu o aumento da sua internalização em células de GBM, enquanto que reduzida internalização foi detectada em células não cancerígenas. Importantemente, a associação de CTX ás nanopartículas permitiu também aumentar a internalização destas em tumores de murganho, desenvolvidos após implantação intracraniana de células de glioma. Um aumento significativo da expressão dos supressores tumorais PTEN e PDCD4, activação das caspases 3 e 7 e aumento da citotoxicidade do sunitinib foram também detectados após exposição de células de GBM humano (U87) e

glioma de murganho (GL261) a nanopartículas com clorotoxina encapsulando oligunucleótideos contra o miR-21.

Na última parte deste Trabalho, descrita no Capítulo 5, o efeito do factor de crescimento angiogénico derivado de plaquetas B (PDGF-B), na expressão de miRNAs em GBM, foi investigado com o objectivo de compreender o seu papel na carcinógenese do GBM. Estudos iniciais demonstraram que o miR-21 e o miR-128 estão sob-expressos em células U87 que sobre-expressam PDGF-B (U87-PDGF), estando esta sob-expressão dos miRNAs associada a um aumento da proliferação celular. Curiosamente, o silenciamento do PDGF-B, via siRNAs, resultou num aumento da expressão do miR-21 e do miR-128, enquanto que a sobre-expressão do miR-21, mediada por plasmídeos, não afectou significamente os níveis de PDGF-B. Importantemente, a quantificação de miRNAs utilizando miRNA "arrays" revelou que vários miRNAs pró-oncogénicos, incluindo membros da família do miR-106b, estão sobre-expressos em células U87-PDGF, enquanto que vários miRNAs com funções de supressão tumoral, incluíndo let-7b, estão sob-expressos nestas células.

Em conclusão, os resultados apresentados nesta Tese demonstram a relevância terapêutica de uma abordagem multi-modal direccionada a GBM, combinando um nanosistema de base lipídica para entrega específica e eficiente de oligonucleótideos antisense contra miRNAs com o fármaco sunitinib, com potencial para ser aplicada em estudos clínicos.

Chapter 1

General introduction

1. Glioblastoma (GBM)

The central nervous system is composed primarily of two broad classes of cells: neurons and glia. While neurons are functionally the most important cells due to their ability to transmit signals to specific target cells over long distances, glial cells (namely astrocytes, oligodendrocytes and microglia) play a number of critical roles, including structural and metabolic support, insulation, and neuronal protection. Tumors arising from glial cells or glial precursors - designated gliomas - represent approximately 50% of all diagnosed primary brain tumors (neoplasms originated in the brain) and are presently classified according to the cell of origin, morphology of the cells within the tumors and the presence of endothelial proliferation and necrosis within tumor samples (1).

GBM is not only the most common type of malignant glioma but also one of the deadliest forms of human cancer, with a median patient survival of 12 to 15 months after diagnosis (2, 3). It is a highly heterogeneous and aggressive type of tumor, characterized by hallmark features of uncontrolled cellular proliferation, diffuse infiltration throughout the brain parenchyma, extensive angiogenesis, resistance to apoptosis and development of necrosis (2).

1.1 Classification and risk factors

Based on the origin of the tumor, GBMs can be classified as primary subtype, when tumors develop *de novo* i.e. without evidence of prior less-maligant lesions, or secondary subtype, when tumors develop from the progression of lower grade astrocytomas (4) (Fig. 1). Despite being morphologically and clinically indistinguishable, primary and secondary GBMs are genetically distinct entities. Phosphatase and tensin homolog (*PTEN*)[1] mutations and epidermal growth factor receptor (*EGFR*) amplification are genetic alterations generally observed in primary GBMs, while tumor protein 53 (*TP53*)[2] mutations are early and frequent genetic alterations in the pathway leading to secondary GBMs (4) (Fig. 1). Secondary GBMs are relatively rare when compared to primary GBMs, accounting for approximately 10% of all the tumors that are classified as GBM, and generally affecting patients at younger ages since the mean age of secondary GBM patients is approximately 45 years, whereas primary GBMs develop in older patients (62 years) (4).

---

[1] *PTEN* codes for a tumor suppressor protein, PTEN, which is usually downregulated in GBM.
[2] The protein encoded by the TP53 gene is designated p53.
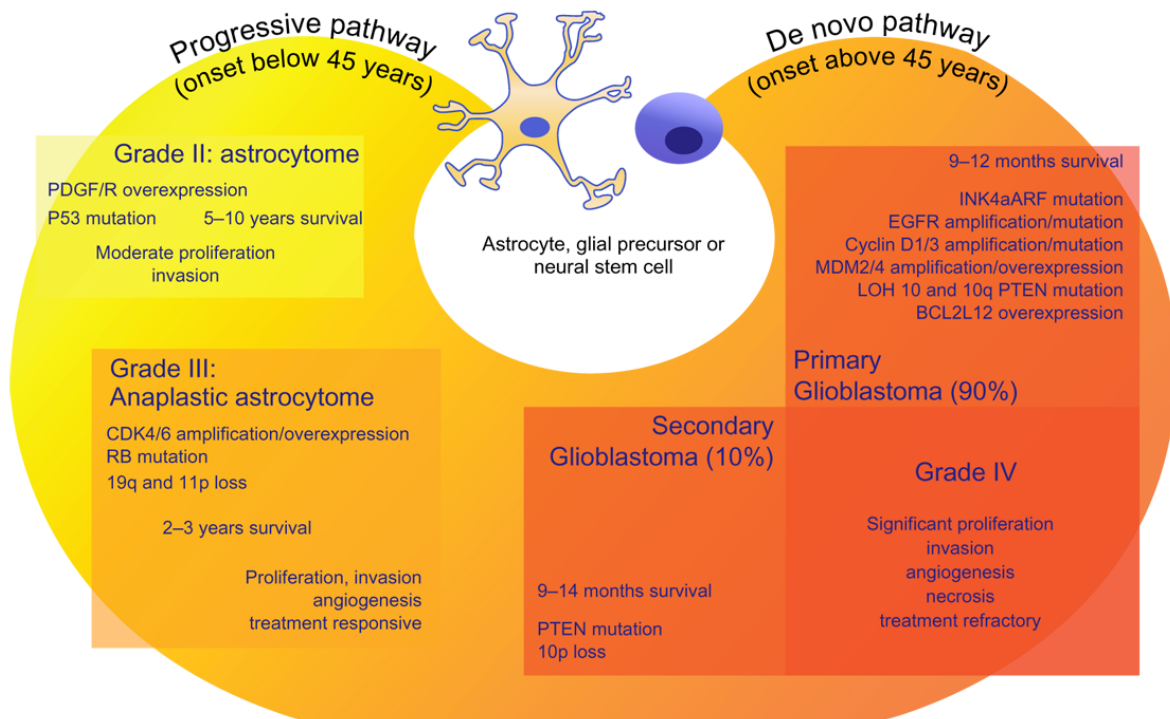
Figure 1. Genetic pathways to primary and secondary glioblastomas at the population level. Tumor protein 53 (*TP53*) mutations are early and frequent genetic alterations in the pathway leading to secondary GBM, while phosphatase and tensin homolog (*PTEN*) mutations are more frequent in the primary subtype. Loss of heterozygosity (LOH) at the chromosome 10q is frequent in both primary and secondary subtypes. *PDGF/R*: platelet-derived growth factor receptor; *CDK4/6*: cyclin-dependent kinase 4/6; *RB*: retinoblastoma protein; *INK4aARF*: cyclin-dependent kinase inhibitor 2A; *MDM2/4*: mouse double minute 2/4 homolog; *BCL2L*: B-cell CLL/lymphoma 2 like protein. Adapted from (5).

Although extensive research has focused on the potential role of environmental hazards play a role in the development of brain tumors, exposure to high-doses of therapeutic ionizing radiation and occurrence of mutations in highly penetrant genes associated with certain rare syndromes are, to date, the only confirmed risk factors for the development of GBM (6). Interestingly, a recent study involving the bioinformatic evaluation of gene-environment interactions, identified 173 genes that may be important in the development of GBM, sixty-five of which, display considerable potential for response to chemicals and subsequent disease related actions (7). However, research is necessary to evaluate the effect of long-term environmental exposure on the identified genes.

1.2 Molecular and genetic abnormalities involved in GBM pathogenesis

One of the hallmark characteristics of GBM is its heterogeneity. In general, GBMs contain a large mass of cancerous cells and recruited astrocytes, microglia and precursor cells; they present a considerable genetic variability, not only within the tumors but also among patients (2, 4). Tumor heterogeneity constitutes one of the main challenges in the treatment of GBM, because different cells within an individual tumor may respond differently to a particular therapy (8).

Different theories try to explain how tumor heterogeneity develops and is maintained (9). Tumor heterogeneity may arise from clonal evolution, in which tumor progression (from the cancer-initiating cell) results from the accumulation of different mutations that promote genetic variability and increased heterogeneity. Under selective pressures (like drug treatment), the most aggressive clones survive (9, 10). A more recent theory proposes that tumors develop and are maintained by a small subpopulation of stem-like cells – designated cancer stem cells (CSCs) – which are capable of dividing indefinitely and give rise to distinct cell types that compose the bulk of the tumor (9). Mutations in CSCs may also contribute to the increase of tumor heterogeneity. However, this is a controversial issue in the cancer field, including GBM, where CSCs have been isolated and characterized, but their role in tumor development and progression is still unclear.

Despite the intrinsic heterogeneity of GBM, insights from a large number of studies provided a clearer picture of the critical genomic abnormalities and molecular pathways that contribute to GBM pathogenesis (addressed below).

1.2.1 GBM subtypes

Over the last few years, a concerted effort has been made to identify and characterize all the genomic and signaling abnormalities driving GBM tumorigenesis. In this regard, the creation of The Cancer Genome Atlas (TCGA) Research Network presented a major advantage as it allowed researchers to gather and share tremendous amount of information on gene expression, copy number, DNA methylation and even miRNA expression from hundreds of human GBM samples (11). Findings from integrated genomic analysis of TCGA data (12) and targeted proteomic analysis (13) revealed not only the existence of molecular subclasses of GBM, driven by different genetic alterations, but also common pathways mutated in this disease. Accordingly, the majority of GBM tumors harbor abnormalities in p53,

RB and receptor tyrosine kinase (RTK) pathways[3], suggesting that this is a core feature of GBM pathogenesis (12). Chromosome 7 amplification and chromosome 10 deletion are also common chromosomal aberrations found in GBM, whereas alterations in the genes coding for the protein neurofibromin 1 (NF1) and the isocitrate dehydrogenase (IDH1) are associated with specific GBM subtypes.

Overall, the findings from the abovementioned studies depict GBM as "a heterogeneous collection of distinct diseases with multiple dependencies both within and across each particular subtype" (14).

1.2.1.1 Classical subtype

The classical subtype of GBM displays several of the most common genomic aberrations found in GBM, such as chromosome 7 amplifications, chromosome 10 deletions, *EGFR* amplification or mutation and homozygous deletion of the *Ink4a/ARF* locus, located at chromosome 9p21 (12).

Amplifications or mutations involving *EGFR*, a gene coding for a class of membrane receptors with intrinsic tyrosine kinase activity, lead to its hyper (or permanent) activation and consequent induction of signaling pathways that promote cell proliferation and angiogenesis. INK4 and the alternative reading frame (ARF) are tumor suppressors involved in the control of cell cycle. While INK4 proteins (INK4a and INK4b) prevent cell cycle progression through the inhibition of cyclin-dependent kinases (CDKs) (15), ARF initiates p53-dependent cell cycle arrest and apoptosis (16). Although *TP53* is the most frequently mutated gene in GBM (11), no significant alterations are found in *TP53, PDGFRA* or *IDH1* in the classical subtype (Table 1).

Neural precursor and stem cell marker nestin, as well as components of the pro-oncogenic Notch and Sonic hedgehog signaling pathways (17, 18), are highly expressed in this GBM subtype (12, 13). Increased Notch signaling was also observed by Brennan and colleagues in a subset of tumors characterized by mutations or amplifications in *EGFR* (13), which suggests that alterations in the EGF signaling pathway increase Notch activation.

---

[3] Alterations in the RTK pathways encompass not only abnormal EGFR and PDGFR expression, but also alterations in the downstream signaling cascades, including Ras and PI3K.

1.2.1.2 Proneural subtype

Tumors with a proneural profile generally occur in younger patients and are characterized by focal amplification concomitant with high expression levels of PDGFR subunit alpha (PDGFRA), as well as *IDH1*[4] and *TP53* mutations (Table 1) (12), all being alterations previously associated with secondary GBM (2).

PDGFRA overexpression, in combination with the increased levels of platelet-derived growth factor BB (PDGF-B) detected in this class of tumors (13), generates an autocrine signaling loop that promotes cell proliferation and tumor growth (19). In opposition, IDH1 is likely to function as a tumor suppressor in GBM. Studies by Zhao and colleagues demonstrated that a reduction in IDH1 activity results in the upregulation of hypoxia-inducible factor 1 (HIF-1α), a pro-oncogenic protein that promotes cell proliferation in hypoxic conditions, which are commonly found within the tumor core (20). The classical GBM event, chromosome 7 amplification paired with chromosome 10 loss, is less prevalent in the proneural subtype (12).

Proneural GBM tumors also display high expression of oligodendrocytic development genes, which suggests that this subtype of tumors may arise from a progenitor or neural stem cell that can also give rise to oligodendrocytes (12).

1.2.1.3 Mesenchymal subtype

Focal deletions or mutations in *NF1*, a gene coding for a protein (neurofibromin-1) that acts as a negative regulator of the pro-oncogenic Ras[5] signaling pathway (21), in combination with reduced NF1 messenger RNA (mRNA) expression, are the main characteristics of this GBM subtype (12) (Table 1). Inherited mutations in *NF1* were previously associated with a variety of tumors, including neurofibromas (22). Reduced NF1 activity, also detected by proteomic analysis in a specific subset of GBMs (13), may contribute to the development of a tumorigenic phenotype by enhancing Ras signaling.

Tumors in the mesenchymal subtype also displayed high expression of the pro-oncogenic mesenchymal markers chitinase-3-like protein 1 (CHI3L1) and MET, as well as of microglial markers and genes in the tumor necrosis factor (TNF) and NF-κB pathway, probably as a consequence of the elevated number of inflammatory infiltrates and overall necrosis found in tumors from this class (12).

---

[4] This gene codes for an enzyme involved in the conversion of isocitrate to α-ketoglutarate.
[5] Rat sarcoma viral oncogene homologue.

1.2.1.4 Neural subtype

As opposed to the other three GBM subtypes, neural tumors do not display a specific genomic signature, abnormalities in TP53, IDH1, NF1 and EGFR being observed in several tumors of this class. The expression patterns of neural tumors are the most similar to that of samples derived from normal brain tissue, and their signature is suggestive of a cell with a differentiated phenotype (12). The neural class also shows a strong enrichment of genes differentially expressed by neurons (12).

Table 1. Distribution of frequently mutated genes across GBM subtypes

Gene	Proneural (n=37)	Neural (n=19)	Classical (n=22)	Mesenchymal (n=38)	Total #Mut
TP53	**20 (54%)**	4 (21%)	**0 (0%)**	12 (32%)	36
PTEN	6 (16%)	4 (21%)	5 (23%)	12 (32%)	27
NF1	2 (5%)	3 (16%)	1 (5%)	**14 (37%)**	20
EGFR	6 (16%)	5 (26%)	7 (32%)	2 (5%)	20
IDH1	**11 (30%)***	1 (5%)	0 (0%)	0 (0%)	12
PIK3R1	7 (19%)	2 (11%)	1 (5%)	0 (0%)	10
RB1	1 (3%)	1 (5%)	0 (0%)	5 (13%)	7
ERBB2	2 (5%)	3 (16%)	1 (5%)	1 (3%)	7
EGFRvIII	1 (3%)	0 (0%)	5 (23%)	1 (3%)	7
PIK3CA	3 (8%)	1 (5%)	1 (5%)	1 (3%)	6
PDGFRA	4 (11%)	0 (0%)	0 (0%)	0 (0%)	4

Bolded entries indicate p-values significant at 0.1 level. Asterisk indicates p-values significant at 0.01 level. *TP53*: tumor protein 53; *PTEN*: phosphatase and tensin homolog; *NF1*: neurofibromin 1; *EGFR*: epidermal growth factor receptor; *IDH1*: isocitrate dehydrogenase; *PIK3R1*: phosphoinositide-3-kinase, regulatory subunit 1; *ERBB2*: human epidermal growth factor receptor 2; *EGFRvIII*: EGFR variant III; *PIK3CA*: phosphatidylinositol-4,5-bisphosphate 3-kinase, catalytic subunit alpha; *PDGFRA*: platelet-derived growth factor receptor alpha. Adapted from (12).

1.2.1.5 Disease prognosis associated with the different GBM subtypes

The studies by Verhaak and colleagues (integrated genomic analysis of TCGA data) also addressed whether tumors from different subtypes would respond differently to aggressive therapy[6]. Although a significant survival advantage following aggressive therapy was observed for patients with tumors fitting the classical and mesenchymal subtypes (which

---

[6] Defined as concurrent chemotherapy and radiotherapy or more than three subsequent cycles of chemotherapy.

was not visible for patients with tumors of the proneural subtype), a trend towards longer survival (independent of treatment) was observed for patients of the proneural subtype. Moreover, promoter hypermethylation of the O(6)-methyguanine methyltransferase (*MGMT*) gene, which has been correlated with a better response to alkylating agents such as temozolomide (23), was not associated with any specifc subtype (12).

1.3 Therapeutic approaches for GBM

Due to the highly infiltrative nature of GBM, cancer cells from the tumor core usually spread into the surrounding brain tissue. For this reason, complete surgical resection is nearly impossible, although partial tumor removal decreases the symptoms associated with the presence of an intracranial mass, and allows tissue collecting for histopathological and genomic characterization. Radiation and chemotherapy are then used to treat the remaining tumor. Alternative therapeutic approaches, including gene therapy and immunotherapy are currently being tested in advanced clinical trials.

1.3.1 Standard treatment for newly diagnosed patients

The standard post-surgery treatment for GBM consists of concomitant administration of the alkylating drug temozolomide (TMZ) with fractionated radiotherapy, followed by up to six cycles of adjuvant TMZ (24). Although this treatment regimen has shown to provide a slight increase in overall patient survival (14.6 months), when compared to that of radiotherapy *per se* (12.1 months) (25), tumor resistance to this drug usually occurs, due to the action of different DNA repair mechanisms that can restore the structural integrity of the methylated DNA bases before they cause extensive DNA damage (14). One of those mechanisms involves MGMT, a suicide enzyme that repairs O(6)-methylguanine DNA adducts caused by environmental exposure or treatment with alkylating drugs (26). *MGMT* promoter hypomethylation, commonly observed in GBM patients, allows the expression of this enzyme and consequent repair of the DNA adducts, which counteracts the biological action of the alkylating TMZ (23). Additional mechanisms of treatment resistance include the loss of the mismatch repair gene mutS homolog 6 (MSH6) (27) and the silencing of the base excision repair enzyme alkylpurine-DNA-N-glycosylase (28).

Despite surgical resection followed by intensive radiotherapy with concomitant and adjuvant TZM, GBM relapse is nearly universal (25). However, as opposed to the newly

diagnosed GBM, there is currently no standard treatment for recurrent GBM (29). Several ongoing clinical trials are expected to bring effective therapeutic modalities that can significantly increase patient survival.

1.3.2 Alternative chemotherapeutic approaches

1.3.2.1 TMZ rechallenge

The treatment of relapsed tumors with TMZ (also known as TMZ rechallenge) remains one of the therapeutic options available for patients with recurrent disease. Initial studies addressed whether different TMZ doses and administration intervals would provide any therapeutic benefit from TMZ therapy. It was shown that a continuous dose-dense treatment regimen is effective in surpassing MGMT-mediated TMZ resistance (30), this effect being observed in patients with or without methylated *MGMT*. Nevertheless, a dose-dense regimen is also associated with increased side-effects that limit the efficacy of this approach. Moreover, recent results from a randomized phase III trial comparing standard adjuvant TMZ with a dose-dense schedule failed to show significant differences in patient survival between these two approaches, which raises concern about the efficacy of this alternative therapeutic regimen[7].

1.3.2.2 Anti-angiogenic therapy

GBM is characterized by robust microvasculature proliferation, driven primarily by the vascular endothelial growth factor (VEGF). However, as opposed to the normal brain blood vessels, GBM presents a heterogeneous, disorganized tumor vascular network composed of highly abnormal and permeable blood vessels, which create a hostile pro-hypoxic microenvironment that contributes to cell proliferation and migration (31).

To date, clinical studies involving anti-angiogenesis monotherapy for the treatment of GBM have shown little efficacy. Small tyrosine kinase inhibitors targeting the VEGF receptors (VEGFR), such as AZD2171 (32) and the multiple receptor tyrosine kinase inhibitor sunitinib (33), failed to demonstrate sufficient antitumor activity for use in single-agent regimens. Anti-angiogenesis drugs may be, however, more effective when combined with cytotoxic therapy (5). Phase II clinical trials involving administration of bevacizumab, a humanized monoclonal

---

[7] http://www.asco.org/ascov2/Meetings/Abstracts?&vmview=abst_detail_view&confID=102&abstractID=79659

antibody that inhibits the highly expressed vascular endothelial growth factor A (VEGF-A), in combination with chemotherapy, revealed an increase in patient progression-free survival[8] (PFS) over those treated with the drug (34, 35). Although few severe side effects have been reported as a consequence of bevacizumab therapy, including intracranial hemorrhage, deep venous thrombosis and ischemic stroke (36), phase III trials are being conducted[9].

Despite the encouraging results arising from several clinical trials, the response to anti-VEGF therapy appears to be transient and the majority of patients eventually relapse (37). Several biological mechanisms have been associated with the development of resistance to this therapy and tumor recurrence, such as the activation of parallel pro-angiogenic signaling pathways (29) and the capacity of GBM cells to form vessel-like structures, thus allowing the tumors to maintain vascular perfusion (38).

1.3.2.3 Targeting of growth-promoting pathways

As referred to in section 1.2.1, alterations in the RTK pathways are among the most common genetic abnormalities found in GBM. Upon binding to their receptors, growth factors activate different signaling cascades that induce nuclear transcription of genes involved in cell cycle control, apoptosis and metabolism. One of the intracellular second-messenger systems activated is the phosphoinositide-3 kinase pathway (PI3K), which leads to the downstream activation of Akt (also known as protein kinase B, PKB) and mammalian target of rapamycin (mTOR) (39) (Fig. 2). In GBM (and in most cancers), the PI3K pathway is overactive and induces cellular proliferation and survival. So far, only modest non-durable responses have been observed in clinical trials involving targeted therapy to the PI3K/Akt/mTOR pathway (40, 41), which appear to be highly dependent on the functional status of PTEN (42). PTEN, a tumor suppressor that is usually mutated or downregulated in GBM, suppresses PI3K-driven Akt phosphorylation, thus blocking the downstream signaling cascade and consequent cellular effects (43).

---

[8] PFS is the length of time during and after medication or treatment during which the disease being treated does not get worse.
[9] http://clinicaltrials.gov/ct2/show/NCT00943826?term=glioblastoma?bevacizumab&phase=2&rank=2;
http://clinicaltrials.gov/ct2/show/NCT00884741?term=glioblastoma?bevacizumab&phase=2&rank=1.
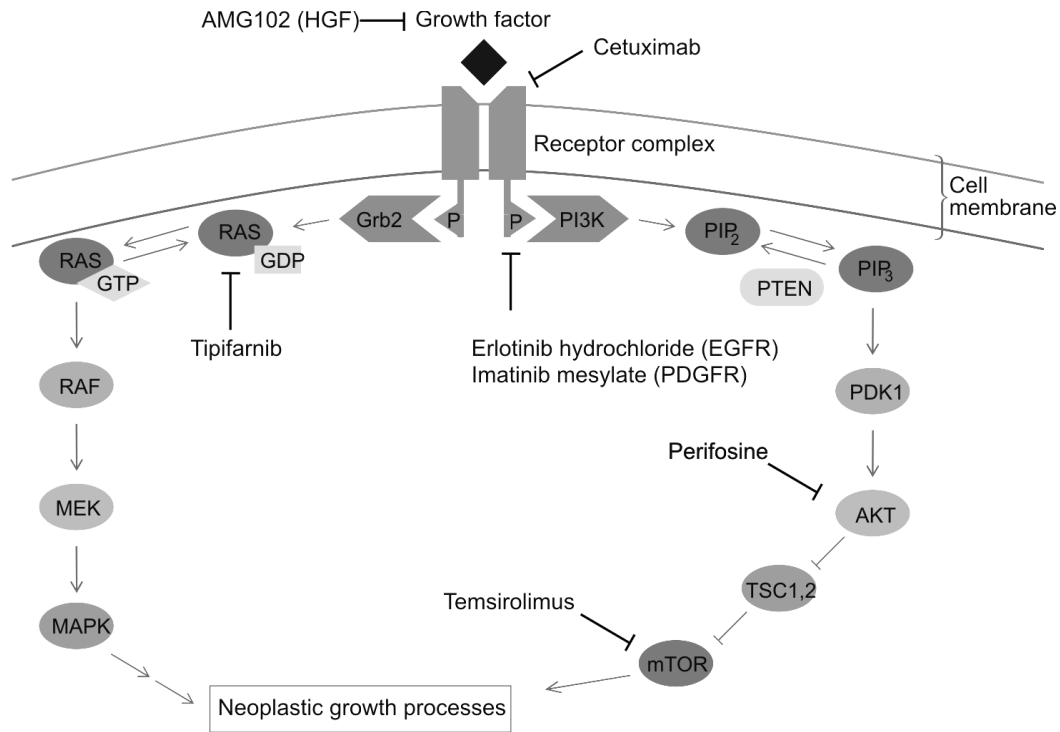
Figure 2. Growth factor pathways targeted in different therapeutic approaches for GBM. Both PI3K/Akt/mTOR and Ras/MAPK signaling pathways are represented. Several drugs that are being (or were) tested in clinical trials are also indicated in the figure. HGF: hepatocyte growth factor; EGFR: epidermal growth factor receptor; PDGFR: platelet-derived growth factor receptor; Grb2: growth factor receptor-bound 2; GDP: guanosine diphosphate; GTP: guanosine triphosphate; Ras: rat sarcoma viral oncogene homologue; RAF: murine leukemia viral oncogene homologue 1; MAPK: mitogen-activated protein kinase; MEK: MAPK kinase; PI3K: phosphoinositide-3 kinase; PIP2: phosphatidylinositol 4,5-bisphosphate; PIP3: phosphatidylinositol 3,4,5-triphosphate; PTEN: phosphate and tensin homologue; PDK: phosphatidylinositol-dependent kinase; Akt: protein kinase B; TSC: tuberous sclerosis complex; mTOR: mammalian target of rapamycin. Adapted from (39).

1.3.3 Overcoming the blood-brain barrier (BBB)

One of the limitations associated with the treatment of GBM is related to the complex structure of the brain capillary endothelial cells, which form the BBB (Fig. 3). The presence of tight junctions between endothelial cells, as well as of xenobiotic transporters that extrude substrates from the brain into the systemic circulation, strongly restricts the type and amount of molecules that can reach the brain (44). Although GBM is associated with a heterogeneous vascular network, composed of different microvessel populations with distinct permeabilities (31, 45, 46), several drugs used in the treatment of cancer do not readily cross the BBB, or do it only at concentrations that are systemically toxic.

Aiming to increase the delivery of therapeutic agents into the tumors, different approaches have been developed: alteration of the BBB permeability, intratumoral implantation of devices for local release or nanoparticle-mediated drug delivery.

1.3.3.1 Physical or chemical alteration of the BBB permeability

The BBB permeability can be increased by either chemical or physical methods. Intra-arterial or intracarotidal infusion of a hypertonic solution of arabinose or mannitol (for 30 seconds) promotes endothelial cell shrinkage and vascular dilatation associated with removal of water from brain, which increases the permeability of the BBB for water-soluble drugs and macromolecules (47). This approach is currently used in clinics (48), although its application is limited to short periods of time (approximately 30 minutes) as it exposes normal brain cells to the chemotherapeutic drug that is being administered, thus promoting adverse side effects.
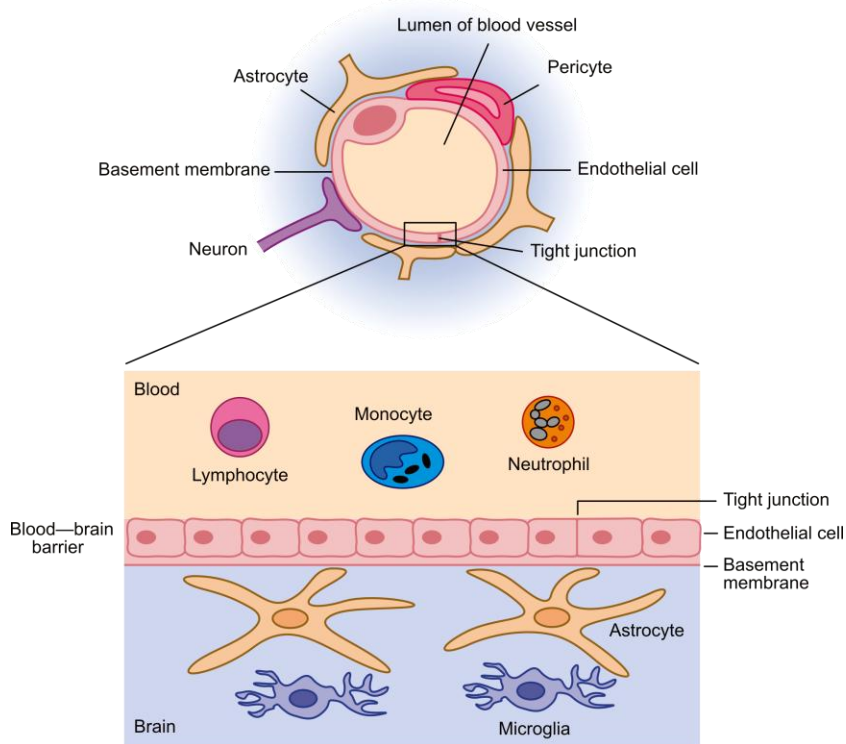
Figure 3. The blood-brain barrier. The endothelial cells that line the blood vessels within the brain are functionally different from those lining the normal blood vessels. The presence of transmembranar protein complexes, designated tight junctions, join together the cytoskeletons of adjacent cells and severely restrict the movement of molecules into the brain. Moreover, the endothelial cell membranes express several xenobiotic transporters (not shown in the figure) that actively pump substrates from the brain into the cerebrospinal fluid and systemic circulation. Adapted from "*The blood-brain barrier, Cambridge University Press, 2003*"[10].

---

[10] http://journals.cambridge.org/fulltext_content/ERM/ERM5_15/S1462399403006252sup001.pdf

Another approach that is currently being tested in pre-clinical models involves the application of high-intensity focused sonic energy (focused ultrasound) to increase the local permeability of the endothelial cells. Although increased drug delivery to has been observed in both rodent and monkey disease models (49, 50), the feasibility and safety of this technique must be tested before application in a clinical setting.

1.3.3.2 Intratumoral delivery of therapeutic agents

In order to surpass the limitations imposed by the BBB, several strategies based on the intratumoral delivery of therapeutic agents were also explored, including the use of biodegradable wafers and CED.

The implantation of biodegradable carmustine (1,2-bis(2-chloreoethyl)-1-nitrosourea, BCNU) wafers was the first approved local treatment for patients with newly diagnosed and relapsed GBM (29, 51). After surgical resection of the tumor, these tiny devices are placed in the resection site and the chemotherapeutic agent is continuously released (29). This therapeutic modality was shown to provide a small patient survival benefit (approximately 2 months) when administered either *per se,* compared to that of a placebo-treated group (52), or in combination with TMZ and radiation followed by rotational chemotherapy, compared to that of single radiation therapy (53). Nevertheless, the implantation of intratumoral wafers has inherent limitations, including the delay in wound healing and the increased risk of edema (54), which restrict their widespread application.

CED is a method for infusion of therapeutic agents directly into the brain in which a catheter is stereotactically inserted into the area to be treated and the therapeutic agent is delivered through the catheter, via pressure gradient-assisted diffusion (55). Although this technique has been shown to increase local delivery of various agents, including anti-neoplastic drugs and toxins (56, 57), its clinical application has not resulted in significant patient survival benefit yet (29).

1.3.3.3 Nanoparticle-mediated drug delivery

The development of stable nanoparticles by association/encapsulation of drugs with (or into) lipid or polymer-based carriers offered several advantages for intratumoral and systemic administration of the therapeutic agent. In addition to promote the local distribution and half-life of delivered agents (58, 59), CED of camptothecin-loaded or paclitaxel

nanoparticles was shown to increase animal survival in intracranial rodent tumor models, when compared to that observed in animals treated with the plain drug (60, 61). Similarly, the combination of nanoliposomal topotecan with polyethylene glycol (PEG)-coated liposomal doxorubicin was shown to increase the median animal survival (90 days) in a rat xenograft tumor model, when compared to that observed in animals treated with the plain drugs (30 days) (57).

Interestingly, the intravenous administration of PEG-coated paclitaxel nanoparticles or liposomal doxorubicin was also shown to increase bioavailability, while conferring a small but significant therapeutical advantage in rodent glioma models (62, 63). Unfortunately, the promising results obtained in pre-clinical studies have yet to translate into significant clinical effects, especially when the nanoparticles are delivered intravenously. It has been shown that combination of CED of herpes simplex virus thymidine kinase (HSV-tk) gene-bearing liposomal vector with systemic administration of ganciclovir is safe and provides some therapeutic benefit (64). However, the combination of TMZ with systemic pegylated liposomal doxorubicin, although well tolerated, does not appear to add significant clinical benefit in the treatment of newly diagnosed GBM (65). Ongoing clinical trials should provide new insights about the efficacy of this therapeutic modality.

1.3.4 Immunotherapy

One of the features that contribute to the extreme lethality of GBM is the capacity of the tumor cells to evade and suppress the immune system by creating a local immunosuppressive environment which severely restricts immune cell activation and tumor cell recognition. GBM cells were found to express low levels of class I major histocompatibility complex (MHC) and no class II MHC (66), which may result from autocrine production of different immunoinhibitory factors, including transforming growth factor β (TGF-β) and prostaglandin E2 (PGE2), that decrease the expression of class II MHC in tumor cells (67). GBM can also repress the production of co-stimulatory molecules required for lymphocyte T (T-cell) activation (68) or induce accumulation of immunosuppressive cells in its microenvironment (5).

Conceptually, immunotherapy seeks to boost the capacity of the immune system to recognize the tumor cells and organize a response against them, while leaving the normal tissue intact. For this reason, most immunotherapeutic approaches that are currently in clinical trials target tumor-specific antigens, such as the EGFRvIII, in the case of GBM. While its expression is not detected in normal cells, approximately one third of GBMs express this

truncated isoform (69). A vaccine targeting this receptor was tested in a multi-center phase II trial of 18 patients with newly diagnosed EGFRvIII-expressing GBM, a significant survival advantage being observed in vaccinated patients (26 months), when compared to that reported for patients treated with TMZ[11] (n=17) (15 months) (70). Although phase III trials are currently in progress, the clinical application of this vaccine would be nevertheless limited to patients expressing the EGFRvIII.

Other immunotherapeutic approaches that are currently being tested for GBM include autologous dendritic-cell-based tumor-targeted preparations (71), vaccines targeting tumor-associated WT1 (Wilms tumor protein 1) or cancer stem cell antigens (72, 73) and an autologous heat shock protein vaccine (HSPPC-96) that seeks to promote an antitumor T-cell-mediated immune response (74). Despite the encouraging results in a few clinical trials, many experts in the field consider that immunotherapy, on its own, "does not represent the magic bullet in glioma therapy" (5, 75).

1.3.5 Gene therapy

Gene therapy involves the delivery of nucleic acids to either replace a defective gene or to express/modulate a specific gene in a target cell/tissue. The choice of a vector that can efficiently and specifically deliver nucleic acids that sensitize or kill tumor cells, is crucial towards the development of effective gene therapy approaches for the treatment of cancer. As reported in the Wiley database (June 2012) on gene therapy clinical trials (Fig. 4), the majority of gene therapy clinical trials have been addressed to cancer (76), among which fifty-seven were specifically designed for the treatment of high grade gliomas, including GBM.

Cancer diseases 64.4% (n=1186)
Monogenic diseases 8.7% (n=161)
Cardiovascular diseases 8.4% (n=155)
Infectious diseases 8% (n=147)
Neurological diseases 2% (n=36)
Ocular diseases 1.5% (n=28)
Inflammatory diseases 0.7% (n=13)
Other diseases 1.4% (n=25)
Gene marking 2.7% (n=50)
Healthy volunteers 2.3% (n=42)
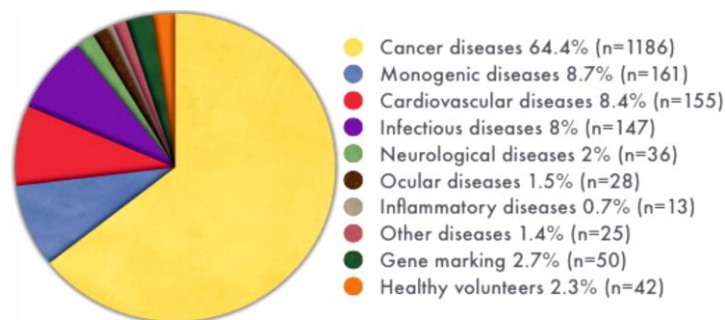
Figure 4. Distribution of completed or ongoing gene therapy clinical trials according to the targeted diseases. Adapted from (76) (http://www.abedia.com/wiley/index.html).

---

[11] A control TMZ-treated group was not included in the clinical trial, and the authors compared the survival rate with a TZM-matched, historical group (n=17).

1.3.5.1 Naked nucleic acids

The delivery of unconjugated nucleic acids has been tested for the treatment of high grade gliomas (77). So far, the most promising approach involves a phosphorothioate-modified antisense oligonucleotide targeting the mRNA of TGF-β2[12], a protein that is highly overexpressed in high grade gliomas and induces tumor cell proliferation, angiogenesis, invasion and metastasis (78). Phase I/II clinical trials involving the CED of this agent in high grade gliomas patients revealed that this approach is safe, well tolerated and significantly increases patient survival, when compared to that observed for patients treated with standard chemotherapy (79). Phase III clinical trials are currently ongoing for the treatment of high grade glioma patients[13].

As viruses remain the most efficient vectors in transducing tumor cells, it is not surprising that the majority of gene therapy trials for high grade gliomas have involved these carriers (80). To date, both non-replicating and oncolytic (replication-competent) viruses have been tested in clinic trials for the treatment of GBM.

1.3.5.2 Non-replicating viruses (NRVs)

As opposed to oncolytic viruses, NRVs lack the genes that are involved in the viral replication and therefore cannot produce new virions and induce target cell death. For this reason, NRVs are engineered to incorporate conditional or direct cytotoxic transgenes in their genome (81).

The most widely used conditional cytotoxic transgene is the HSV-tk[14], which codes for the enzyme thymidine kinase that converts the prodrug ganciclovir into the metabolite deoxyguanosine monophosphate. This metabolite is further phosphorylated by cellular kinases to the corresponding nucleoside triphosphate, a highly toxic nucleotide analog that incorporates into the DNA strands causing early chain termination (82). This enzyme/prodrug combination has the capacity to promote cell death not only in the recipient cells, but also in the neighboring cells, by the so-called "bystander effect". Such effect may occur via different mechanisms, including the passage of phosphorylated ganciclovir metabolites through intercellular gap junctions (83), thus compensating for the low efficacy of vectors in

---

[12] This molecule is being tested by the company Antisense Pharma, under the designation of trabedersen (AP12009).
[13] www.antisense-pharma.com/fileadmin/data_antisense/PDF_Dokumente/Pressemitteilungen/EN_2010_04_18_Press_Release.pdf
[14] Herpes simplex virus type 1 thymidine kinase.

transferring genes into the tumor cells. Despite the encouraging results from pre-clinical studies, numerous clinical trials for GBM involving non-replicating adenoviral/retroviral-mediated HSV-tk delivery demonstrated, at best, a modest increase in patient survival[15], when compared to that observed with standard radiotherapy and chemotherapy (84-87). The limited efficacy of this therapeutic approach may be explained by the difficulties for ganciclovir to cross the BBB and reach the tumor, inefficient local viral dispersion and low transduction of tumor cells (80).

Among the direct cytotoxic therapeutic approaches, human toxin-based chimeric proteins have shown potential to be used in the treatment of several human diseases, including cancer (88). An interesting approach for GBM took advantage of the transduction efficiency of non-replicating adenoviral vectors to deliver a transgene encoding the highly toxic Pseudomonas exotoxin (PEx), which inhibits protein translation in the target cell leading to cell death (89). The authors constructed doxycycline-dependent adenoviral vectors encoding the PEx fused with a mutated human interleukin-13 (IL-13), in order to target the chimeric protein to a variant of the IL-13 receptor (IL13Rα2) which is overexpressed in GBM. In pre-clinical experiments with human xenografts, the intratumoral delivery of the adenoviral construct resulted in significant antitumoral activity and increased animal survival, in comparison to that observed for intratumoral administration of protein formulations (89). Indeed, earlier phase I-III trials involving the protein formulations failed to provide significant survival benefits due to short half-life and poor local distribution (90, 91), which indicates that the adenoviral administration may confer an important advantage towards a therapeutical effect. Future clinical trials should clarify whether this approach is clinically safe and provides significant therapeutic benefit.

NRVs were also shown to efficiently deliver non-cytotoxic genes, including small interference and short hairpin RNAs (siRNAs and shRNAs, respectively) to glioma cells. Saydam and colleagues developed a herpes simplex virus 1 (HSV-1)-construct expressing anti-EGFR siRNAs, which was shown to promote efficient knockdown of EGFR and significant decrease in proliferation of human GBM cells, both in culture and upon subcutaneous implantation of the transduced cells in athymic mice (92). Similarly, Kock and colleagues developed lentivirally-based constructs that encode an anti-Bcl-2 shRNA, to

---

[15] The longest median patient survival was reported by Immonen and colleagues, an increase in survival from 37.7 to 62.4 weeks being observed in patients treated with virally-delivered HSV-tk. Both Immonen and Sandmair studies demonstrated that adenoviral-mediated HSV-tk delivery provides a superior survival advantage, when compared to that of retroviral-mediated HSV-tk delivery.

18

downregulate Bcl-2 and S-TRAIL[16], to induce apoptosis in glioma cells (93). Upon transduction of cultured glioma cells, increased caspase 3/7 activation and apoptosis were observed in cells transduced with viruses encoding anti-Bcl-2 and S-TRAIL, when compared to that observed for cells transduced with viruses coding for anti-Bcl-2 or S-TRAIL *per se*. Moreover, following intracranial implantation of lentivirally-transduced cells, reduced tumor growth was detected in animals injected with cells expressing the anti-Bcl-2 shRNA and S-TRAIL, when compared that observed in animals injected with cells expressing only S-TRAIL (93). Adenovirally-mediated delivery of calreticulin and melanoma-associated antigen 3 (MAGE-A3) genes was also shown to induce apoptosis and inhibit proliferation of cultured U87 GBM cells, and inhibit tumor growth following intratumoral injection in a mouse GBM xenograft (94).

1.3.5.3 Oncolytic viruses (OVs)

The limited efficacy of NRVs in several human clinical trials towards cancer, including GBM, opened a window for the usage of OVs. This type of carriers are capable of replicating in infected cancer cells and forming progeny that can spread throughout the tumor mass (80) (Fig. 5). Due to their virulence, OVs cause the lysis of infected cells and, therefore, they do not necessarily need to carry transgenes to cause cytotoxicity. Nevertheless, the clinical application of OVs bears a potential risk of high toxicity associated with their capacity to infect not only tumor cells but also healthy brain tissues, which can be attenuated by using tumor-specific promoters controlling the expression of the oncolytic genes (95).

Figure 5. Infection and replication of oncolytic viruses. Oncolytic (replication-competent) viruses can replicate in infected tumor cells and subsequently infect neighboring cells, while causing the lysis of infected cells when their replication machinery is no longer needed. Adapted from (96).

---

[16] Secreted tumor necrosis factor-related apoptosis-inducing ligand.

Several viruses have been investigated for therapeutic application as oncolytic agents. One of the most widely studied is the conditionally replicating herpes simplex virus (HSV) G207, a mutated HSV that expresses the HSV-tk gene and is capable of infecting rapidly dividing cells, which allows the combination (of virus) with pro-drugs like ganciclovir to further increase the oncolytic effect (97). A phase 1b trial[17] demonstrated that multi-dose administration of G207 into GBM, before or after tumor resection, is clinically safe and provides limited antitumoral activity (98). A different recombinant HSV engineered to target the human epidermal growth factor receptor 2 (HER2), frequently overexpressed in GBMs, was also shown to be safe and decrease tumor growth upon intratumoral administration in an animal model of GBM (99).

Viruses with capacity to infect both dividing and non-dividing cells, including adenoviruses, have also been tested in pre-clinical models and clinic trials for high grade gliomas. Preclinical studies in human malignant glioma xenografts involving ONYX-015, a modified oncolytic adenovirus capable of replication in p53-defective tumor cells (100) demonstrated that intratumoral viral delivery resulted in cell lysis and impaired tumor growth, although the response was independent of the p53 status[18]. A phase I clinical trial for recurrent high grade glioma revealed that the viral administration into the tumor cavity after surgical resection is safe and does not cause significant inflammatory response. In addition, increased survival was observed in patients receiving the highest doses of ONYX-015 (101).

In contrast to oncolytic HSVs and adenoviruses, replication-competent retroviruses (RCRs) do not possess cytolytic activity and depend on the incorporation of cytotoxic genes into the vector genome, to cause tumor cell death (102). One approach that has been successfully tested in pre-clinical studies involves a RCR vector engineered to efficiently deliver a modified cytosine deaminase (CD)-coding gene to glioma cells. The bacterial CD catalyzes the conversion of the pro-drug 5-fluorocytosine (5-FC) to the anticancer agent 5-fluorouracil (5-FU) within the tumor cells. Tai and colleagues reported a significant survival benefit in glioma-bearing animals injected with RCRs and further treated with single or multiple cycles of 5-FC, when compared to that observed for animals treated with saline vehicle control (103). Phase I/II testing is currently undergoing in recurrent high-grade glioma patients[19].

---

[17] Phase I clinical trials are designed to test the safety, tolerability, pharmacokinetics and pharmacodynamics of a drug in a small number of healthy patients. Phase 1b trials are usually conducted in patients who demonstrate some biomarker, surrogate, or possibly clinical outcome that could be considered for "proof of concept".
[18] Significant tumor growth delay was observed in p53 mutant (IGRG88) and p53 wild-type (IGRG93 and IGRG121) human xenografts treated at an advanced tumor stage.
[19] http://clinicaltrials.gov/show/NCT01156584.

Despite the potential of oncolytic virotherapy, the incapacity to reach distant tumor pockets after local delivery limits their efficacy. This relative inadequacy of viral spread may relate to several factors including large viral particle size and cell-to-cell barriers (104). The antitumor activity of OVs might also be significantly reduced by immune degradation as a result of infiltration of natural killer (NK) cells, macrophages and microglia (105).

1.3.5.4 Liposomes and lipid-based nanoparticles

Synthetic non-viral vectors present several advantages over viral carriers, including their reduced immunogenicity, capacity to carry larger amounts of genetic material and physicochemical versatility, including the potential for modification of their surface structures to allow targeting for specific tissues or cells (106, 107). Moreover, these type of vectors are usually easy to produce on a large scale and can be preserved.

Liposome-based carriers have been successfully tested for the delivery of therapeutic genes or nucleic acids to high grade gliomas in pre-clinical models (108, 109). One of the most popular approaches involves the intratumoral liposome-mediated delivery of genes coding for immunostimulatory proteins, such as interferon-β (IFN-β), in order to stimulate an antitumoral immune response (110-112). In this regard, studies from Yoshida and colleagues demonstrated that local administration of cationic liposomes containing the *IFN-β* gene in glioma-bearing mice induces NK and T-cell activation, resulting in a significant increase of animal survival (110, 111). These encouraging results paved the way for phase I-II clinical trials, in which five patients with recurrent malignant glioma were enrolled (113). Following tumor removal, complexes of cationic liposomes with the human *IFN-β* gene were injected into the tumor cavity; subsequent injections were also performed through an implanted cannula. Interestingly, therapy administration was well tolerated by all the patients and a considerable decrease in tumor volume (50%) was observed in two of them. However, due to the reduced number of patients involved in this study, no significant conclusions could be drawn. Phase III trials involving a larger number of patients should clarify whether an "immunogene" therapy approach will be clinically beneficial for the treatment of GBM. Cationic liposomes encapsulating the HSV-tk gene (combined with systemic ganciclovir) or a replication-incompetent Semliki Forest virus vector carrying the human interleukin-12 (*IL-12*) gene, have also shown some promise in clinical trials for GBM (64, 114).

Cationic liposomes were also used for delivery of siRNAs to glioma/GBM cells. Liposome-mediated delivery of anti-MGMT siRNAs enhanced the cytotoxicity of TMZ in

cultured GBM cells and in both subcutaneous in intracranial GBM mouse models[20] (109). Similarly, liposome-mediated delivery of anti-H-ferritin siRNAs into subcutaneously implanted mouse gliomas enhanced the cytotoxic effect of the alkylating agent BCNU (115).

Modified liposomes have also been tested for the delivery of therapeutic genes to glioma cells. Saw and colleagues prepared polyplexes by complexing nuclear factor kB (NF-kB) decoy oligonucleotides with a cell-penetrating peptide (CPP) composed of nine arginines (R9), and thereafter entrapped the polyplexes within R9-modified anionic liposomes, yielding a liposomal gene carrier with R9 peptides both on the surface and in the core of the particles (116). These nanocarriers were shown to be efficiently internalized by cultured U87 GBM and to promote oligonucleotide-mediated blocking of NF-kB transcription activity, which increased the cytotoxicity of the drug paclitaxel (116). Trans-activating transcriptional activator peptide (TATp)-modified liposomes were also shown to provide enhanced gene delivery to intracranial human brain tumor xenografts in nude mice (108).

In addition to liposomes, lipid-based nanocarriers were reported to be efficient in delivering nucleic acids to glioma cells. Jin and colleagues developed cationic solid lipid nanoparticles (SLN)[21], which were conjugated to pegylated anti-MET[22] siRNAs. The incubation of cultured U87 GBM cells with these carriers resulted in a decrease in both MET expression and cell proliferation (117). Importantly, in an orthotopic GBM xenograft tumor model, intravenous administration of the SLN nanoparticles specifically delivered the siRNAs to the tumor, which resulted in decreased tumor cell proliferation and tumorigenicity (117).

1.3.5.5 Polymer-based nanoparticles

Polymer-based nanoparticles have been extensively tested in animal models of cancer, including GBM. Zhan and colleagues developed a polyethylene glycol-polyethylenimine (PEG-PEI) gene carrier targeted for cancer cells by coupling a cyclic RGD sequence (cyclic arginine-glycine-aspartic acid-D-tyrosine-lysine) (118). This approach took advantage of the ability of the RGD peptide to bind to integrin αVβ3, a protein involved in invasion and angiogenesis that is overexpressed in GBM at the brain tumor border and vasculature. When complexed with a plasmid coding for the TRAIL and combined with PEG-

---

[20] When administered intratumorally.
[21] Nanoparticles were composed of cholesteryl oleate, glyceryl trioleate, L-α-dioleoylphosphatidylethanolamine (DOPE), 3β-[N-(N′, N′-dimethylaminoethane)-carbamoyl)-cholesterol (DC-Chol) and cholesterol (Chol), and were prepared by a modified emulsification-solvent evaporation protocol (Jin, 2011)
[22] MET, also known as hepatocyte growth factor receptor (HGFR), is a receptor with tyrosine kinase activity.

conjugated paclitaxel[23]-loaded polylactic acid micelles, the resulting targeted nanoparticles were found to prolong survival in human intracranial GBM xenografts (118). Similarly, Meng and colleagues used PEI conjugated to the hydrophobic molecule myristic acid (MA) to deliver TRAIL-coding plasmids to glioblastoma cells. In addition to the capacity to cross the BBB, these nanoparticles were shown to increase the survival of nude GBM-bearing mice, when compared to that of animals injected with nanoparticles lacking MA or a saline solution (119).

Targeted delivery systems based on the multifunctional carrier EHCO[24], a polymerizable surfactant with pH-sensitive amphiphilicity, demonstrated capacity to efficiently deliver siRNAs to target cells and promote endosomal release (120, 121). In this regard, Wang and colleagues developed a tumor-targeted delivery system by coupling the PEG-conjugated peptide bombesin to EHCO/siRNA nanoparticles. Upon systemic administration of targeted nanoparticle-formulated anti-HIF-1α siRNAs, a significant decrease in tumor growth was observed in GBM-bearing mice xenografts, when compared to that observed for animals treated with nontargeted nanoparticles or naked siRNAs (122).

Magnetic nanoparticles have also been tested for the delivery of nucleic acids to glioma cells. Veiseh and colleagues developed a nanovector construct comprised of a super paramagnetic iron oxide core coated with PEG-grafted chitosan and PEI, which was further functionalized with siRNA and a tumor-targeting peptide, chlorotoxin (CTX), to improve tumor specificity and enhance cellular internalization (123). The developed targeted nanovector was shown to specifically deliver anti-GFP[25] siRNAs to cultured GFP-expressing C6 rat glioma cells and facilitate endosomal release, which resulted in efficient knockdown of GFP. Importantly, this carrier was reported to enhance magnetic resonance imaging (MRI) contrast *in vitro*, which, in combination with its capacity to target tumor cells, reveals potential to be used in the MRI monitoring of glioma treatment *in vivo* (123).

Despite the encouraging results obtained in preclinical studies, polymer-based nanocarriers have yet to be tested in clinical trials for GBM, to fully demonstrate their potential as a relevant tool towards application in a therapeutic context.

---

[23] Paclitaxel is a mitotic inhibitor used in cancer chemotherapy.
[24] (1-aminoethyl)iminobis[N- (oleicylcysteinylhistinyl-1-aminoethyl)propionamide).
[25] Green fluorescent protein.

1.3.5.6 Neural and mesenchymal stem cells

Stem cells (SCs) have been extensively used as vehicles for the delivery of therapeutic genes to brain tumors due to their remarkable capacity to target tumor cells, when injected both *in loco* (124) and intra-arterially (125, 126). Although the molecular basis of tumor tropism of SCs is not yet fully understood, several *in vitro* studies provided evidence that tumor-secreted cytokines and growth factors, including VEGF and PDGF, act as chemoattractants that promote SC migration towards tumor cells (127, 128). Two types of SCs from distinct origins – neural and mesenchymal - have been preferentially used in pre-clinical high grade glioma models. Neural stem cells (NSCs) can be obtained from adult brains, fetal brains and embryonic SCs (129), while bone marrow and adipose tissue are excellent sources of mesenchymal stem cells (MSCs) (130, 131). Several *in vivo* studies demonstrated that SC-mediated gene delivery is able to induce tumor cell death and increase animal survival. Modified MSCs expressing immunostimulatory molecules, such as interleukin-2 (IL-2) and IFN-β, were shown to promote an antitumoral immune response and extend the survival of glioma-bearing rodents when administered intra-arterially (125, 126). Similarly, intratumoral MSC-based TRAIL gene delivery combined with the lipoxygenase inhibitor MK886 showed a greater therapeutic efficacy in glioma xenografted mice, when compared to that observed with single-agent treatment (132). A phase I clinical trial involving the post-resection local injection of genetically-modified NSCs expressing the bacterial CD combined with oral 5-FC[26] is ongoing for the treatment of recurrent grade glioma[27].

SCs have also been suggested as potential cell-based carriers for delivery of OVs, due to their exceptional migratory capacity and ability to act as immunosuppressors, which allows the therapeutic viruses to evade the host immuno system (104, 133). Sonabend and colleagues demonstrated that MSCs were very effective in delivering oncolytic adenoviruses to glioma-bearing mice, even when administered at sites distant to the tumor mass (134). Similarly positive results have been reported using viral-loaded NSCs to treat intracranial tumor-bearing mice (135).

Nevertheless, a few concerns are associated with the clinical application of NSCs. The genetic modification of SCs to express therapeutic genes could result in insertion of the

---

[26] Cytosine deaminase (CD) catalyzes the conversion of the pro-drug 5-fluorocytosine (5-FC) to the anticancer agent   5-fluorouracil (5-FU).
[27] www.clinicaltrials.gov/ct2/show/NCT01172964?term%C4%BDstem%20cell%E2%80%99%20AND%20cancer%20%20AND%20gene&rank%C4%BD6

gene into a critical locus, dysregulating the normal cell function and inducing cancer cell behavior (136, 137). Indeed, transformed NSCs have been suggested to be involved in the development of brain tumors (138). Another limitation concerns the number of SCs that can be obtained from each patient and the time involved in cell preparation to be successfully applied in the patient (137).

As illustrated in Figure 6, suicide gene therapy has been the most widely tested gene therapy strategy for high grade gliomas, including GBM.
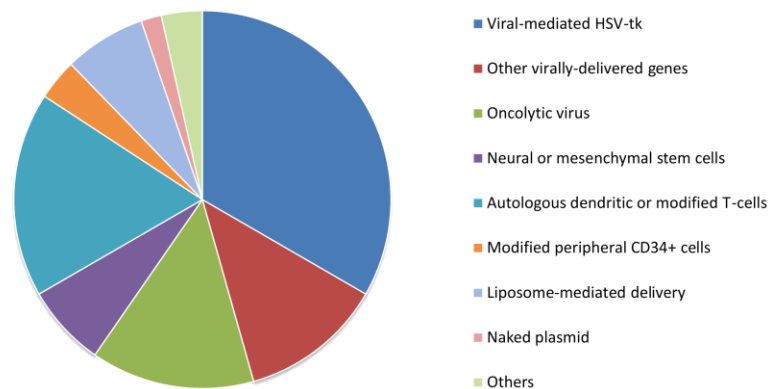
Figure 6. Distribution of the ongoing or completed clinical trials for high grade gliomas, including GBM, according to the applied gene therapy-based strategies. Autologous cells are patient cells removed for *ex vivo* manipulation. Following genetic modification, the cells are re-inserted in the patient, generally intratumorally. Data were obtained from (76) (http://www.abedia.com/wiley/index.html).

1.4 Tumor recurrence and the role of GBM stem-like cells

Despite the recent advances in cancer detection and therapy, GBM recurrence is nearly universal. In addition to the previously referred DNA repair mechanisms that confer protection against alkylating agents, infiltrating cancer cells that reside away from the main tumor mass may be responsible for tumor relapse, as well as radiation and chemotherapy resistance (139).

Another explanation for the extreme resistance and constant recurrence of this type of tumor relies on the existence of a specific niche of cancer cells (within the tumor) with stem-cell characteristics – generally known as GBM stem-like cells (GSCs) – which are not only capable of producing the various types of cells that constitute the bulk of the tumor, but are also extremely resistant to therapy (140). Indeed, cells with stem-cell properties have already

been isolated from GBM by several research groups (141, 142). Such cells display characteristics similar to those of normal NSCs found in different areas of the brain[28], including the capacity to self-renew, proliferate and differentiate into cells of various lineages (139). Although GSCs constitute a small fraction of the total cell population within GBMs (141, 142), they were shown to form tumors in animals upon transplantation (142). In addition to their capacity to promote tumor growth, a large number of studies suggest that GSCs provide increased chemoresistance (143, 144) and radioresistance (145) to the tumor population. Nevertheless, it remains controversial whether these cells originate from transformed NSCs or neural progenitor cell populations (138), or dedifferentiate from mature brain cells and reacquire characteristics of NSCs (140, 146). While the accumulated knowledge about GSCs suggest that these cells play an important role in the maintenance and resistance of the tumors, it has yet to be clarified whether they are involved in the genesis of GBM.

Despite the increased knowledge about the molecular mechanisms underlying GBM pathogenesis, the advances in tumor diagnostics and the establishment of more efficient and less aggressive surgical approaches, we are still far from reaching a significant and consistent improvement in patient life expectancy. The discovery of small RNA molecules - designated microRNAs (miRNAs) – that play an important role in the development and progression of several human cancers, revealed a wide and complex field of cellular regulation with potential for generating new therapeutic approaches. The biogenesis of miRNAs, their cellular functions and role in GBM pathology are discussed below.

2. MicroRNAs

2.1 Discovery of RNA-mediated gene silencing mechanisms

Gene expression is a multistep process by which the information from a gene is translated into the synthesis of a functional gene product. Along this complex (yet essential) biological process, regulators of gene transcription and translation operate at multiple levels in order to fine-tune the genome end products. In eukaryotic cells, post-transcriptional mechanisms - including mRNA translational repression and decay - play a key role in the regulation of gene expression and ultimately determine the expression levels of a considerable portion of the transcriptome (147, 148).

---

[28] Namely in the ventricular system and subcortical white matter.

The discovery of small RNA molecules with the capacity to regulate mRNA stability and translation (and consequently protein synthesis) has revealed an additional level of post-transcriptional gene control. In 1993, Ambros and colleagues discovered a gene, lin-4, that was involved in the development the worm *Caenorhabditis elegans* (*C. elegans*) and found that it coded for a small non-protein-coding RNA (149). Remarkable studies by Fire and Mello further showed that the injection of small double-stranded RNAs (dsRNA) in *C. elegans* resulted in a pronounced decrease of the endogenous mRNA transcript, thus providing evidence for the existence of RNA-mediated mechanisms of gene expression control (150). Since then, various small RNAs with distinct characteristics, including endogenous siRNAs (151) and Piwi-interacting RNAs (piRNAs) (152), have been described, their functions ranging from heterochromatin formation to mRNA destabilization and translational control (153). MiRNAs, an evolutionarily conserved class of small noncoding RNAs (ncRNAs) that regulate gene expression post-transcriptionally by base pairing to complementary sequences in the 3′ untranslated regions (UTRs) of target mRNAs, are part of this modulatory RNA network playing a pivotal role in cell fate. Functional studies indicate that miRNAs are involved in the regulation of almost every biological pathway (153), while bioinformatic predictions suggest that miRNAs may control approximately 30% of all protein-coding genes (154). Not surprisingly, changes in miRNA expression are also associated with several human pathologies, including cancer (155-157), thus highlighting the crucial role of these small RNA regulators in the global cellular function.

2.2 MiRNA biogenesis

As opposed to what was initially assumed, miRNA loci are predominantly located within intronic regions of protein-coding and noncoding genes and, to a smaller extent, in exons of long ncRNA transcripts (also designated intergenic regions) with autonomous transcription activity (158-160). Interestingly, miRNA-coding sequences are mostly found in the sense strand, which suggests the existence of an elegant and convenient mechanism for the coordinated expression of miRNAs and protein-coding or noncoding transcripts.

The synthesis of miRNAs from their initial chromosome encryption to the final mature form is a highly regulated stepwise process that takes place in the cell nucleus and cytoplasm (Fig. 7), and may interact with other important cellular functions, including splicing.

2.2.1 Canonical pathway

In the biologically predominant canonical pathway (Fig. 7), miRNAs are processed from 5' capped and 3' polyadenylated precursor molecules, designated primary miRNAs (pri-miRNAs), which are either transcribed from independent miRNA genes (exonic miRNAs) or are portions of introns of RNA polymerase II transcripts (intronic miRNAs) (153, 161). These long primary transcripts are subsequently cleaved by a microprocessor complex that includes the RNase III enzyme Drosha and the dsRNA-binding protein DGCR8 (also known as Pasha in invertebrates), to produce a 70-nucleotide (nt) hairpin-structured miRNA precursor (pre-miRNA). Growing evidence suggests the existence of a complex crosstalk between the production of pre-miRNAs, carried out by the microprocessor, and the pre-mRNA splicing reaction, carried out by the Spliceosome. Although it was initially assumed that intronic miRNAs are processed by Drosha from spliced introns (162), subsequent studies demonstrated that the production of pre-miRNAs can also occur from unspliced introns without affecting the normal splicing rate (159), thus indicating that the microprocessor and spliceosome may act in coordination to produce miRNAs and mRNAs from a single transcription unit (Fig. 8). The pre-miRNA is exported from the nucleus to the cytoplasm via the transporter exportin-5, in a GTP-dependent process, where it is cleaved by a multiprotein complex that includes the endonuclease Dicer and the RNA-binding protein TAR (TRBP), yielding a miRNA duplex of approximately 21 to 23 nucleotides, with 2-nucleotide overhangs at the 3′ ends.

2.2.2 Non-canonical pathway

In addition to the biologically prevalent canonical pathway, where miRNA precursor molecules are produced by the action of the Microprocessor complex, an alternative (non-conventional) pathway that produces miRNA precursors via splicing was discovered and characterized in invertebrates (163) (Fig. 7). Defined by Sibley and collaborators as small RNA molecules that are clustered at the outer edge of short introns, with unpaired flanking sequences immediately adjacent to the splice junctions (164), the mirtrons are splicing-produced short-hairpin introns that mimic the structural hallmarks of pre-miRNAs and therefore enter the miRNA-processing pathway. As in the canonical pathway, mirtrons are actively exported to the cytoplasm by the transporter exportin-5, where they are processed by the cellular machinery to produce miRNA duplexes. Although mammalian mirtrons have yet

to be identified in animal models, computational and *in vitro* approaches have identified 46 candidates, 3 of which show cross-species conservation (165).
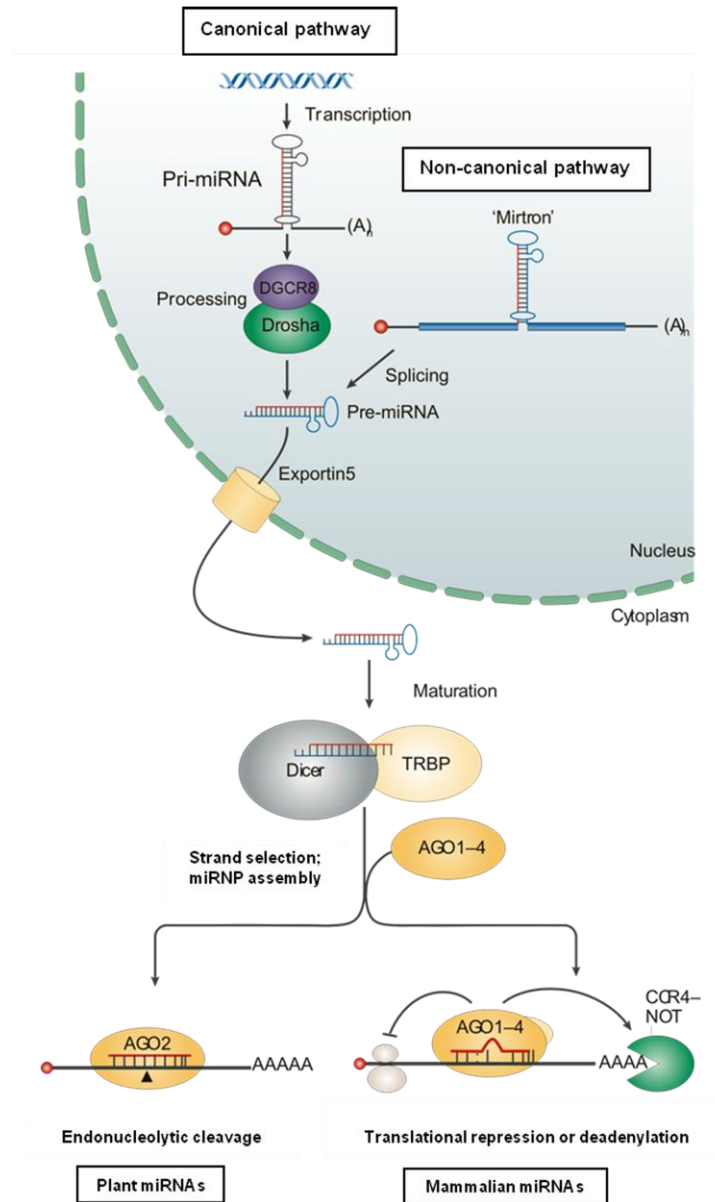
Figure 7. Mechanisms of miRNA biogenesis and miRNA-containing ribonucleoprotein complex (miRNP) assembly. The canonical pathway, involving the production of precursor miRNAs (pre-miRNAs) by Drosha-mediated cleavage of primary miRNA transcripts (pri-miRNA) and the recently discovered non-canonical pathway, involving the production of pre-miRNAs by splicing-mediated cleavage of short-hairpin introns (mirtrons). DGCR8: DiGeorge syndrome criticical region gene 8 protein; TRBP: RNA-binding protein TAR; Ago1-4: argonaute protein 1-4; CCR4-NOT: C-C chemokine receptor type 4-NOT. Adapted from (153).
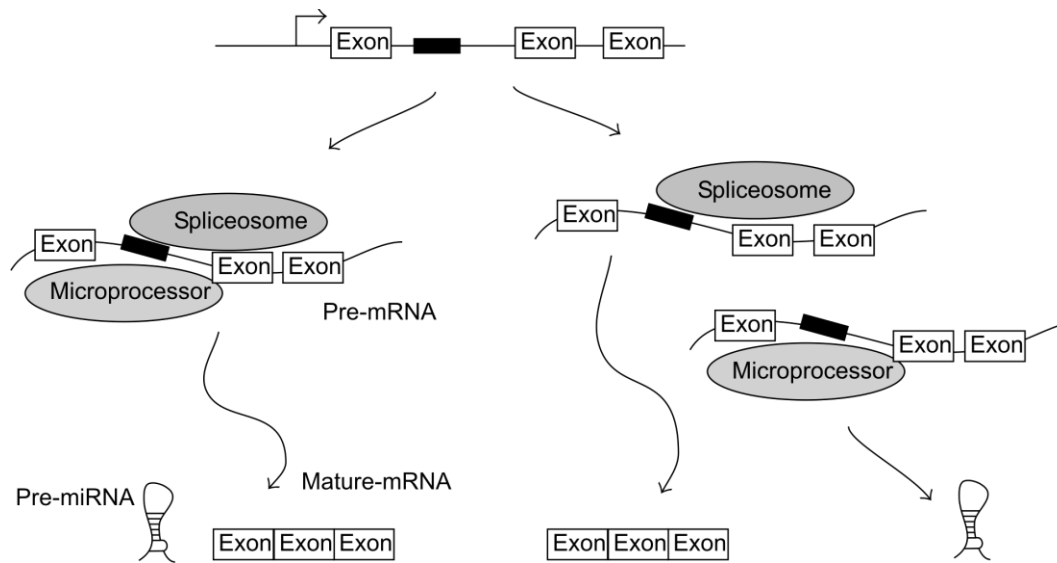
Figure 8. Possible models for production of intronic miRNAs. MiRNA and mRNA are both produced from one RNA transcript (left scheme), or each one is generated from an individual transcript (right scheme). Taken from (166).

2.2.3 MiRNA-containing ribonucleoprotein complexes (miRNP): assembly and function

Following the processing of the hairpin-containing pre-miRNA into a linear double stranded RNA molecule, effector miRNA-containing ribonucleoprotein complexes (miRNPs) are assembled through a dynamic (yet not fully understood) process, that involves recruitment of one of the four argonaute (Ago) proteins (167), the helicase gemin3, a glycine-tryptophan repeat–containing protein of 182 kDa (TNRC6, also known as GW182), as well as several other proteins (such as the CCR4-NOT deadenylase complex) which probably function as miRNP assembly or regulatory factors (153, 168).

The functional role of the miRNP complex in the miRNA-guided RNA silencing pathway is to recognize the miRNA guide in the miRNA-miRNA* duplex[29], pair it with its target mRNA and inhibit mRNA translation (168). The miRNA strand whose 5′ end is less stably bound to the opposite strand is generally selected as the guide (mature) strand, whereas the miRNA* strand is typically degraded (168, 169). This observation suggests that a helicase-like enzyme (possibly gemin3) samples the ends of the duplex multiple times to identify whose 5' end is less tightly paired, before unwinding the duplex miRNA (169, 170). The

---

[29] MiRNA* is the strand that has the same (or similar) sequence as the mature miRNA.

fragile X mental retardation protein (FMRP), which has been identified in mammalian miRNP complexes, may also play an important role in the interaction between the mature miRNA and its target mRNA. In this regard, Plante and colleagues proposed that FMRP mediates mRNA targeting through a strand exchange mechanism, in which the miRNA* of the duplex is swapped for the mRNA (171).

2.3 Suppression mechanisms of miRNA-mediated gene expression

The mechanisms by which miRNAs mediate gene silencing are dependent on the degree of complementarity between miRNAs and sequences on the 3' UTR of the target mRNA (170, 172, 173). Plant miRNAs generally show complete or near complete complementarity to sequences in target mRNAs, and trigger mRNA degradation via a mechanism similar to that operating in the RNA interference (RNAi) pathway. Upon assembly of the miRNP complex, Ago2, an argonaute protein with endonuclease activity, promotes the cleavage of the mRNA between the nucleotides pairing to residues 10 and 11 of the miRNA relative to the 5' end, as found also for siRNA-guided cleavage, while the miRNA remains intact (170, 173). The target mRNA is subsequently degraded via routine cellular pathways (174).

With very few exceptions, animal miRNAs regulate gene expression by imperfect base pairing with sequences of target mRNAs and further miRNP-mediated inhibition of translation and/or mRNA destabilization (170, 172). Functional studies, as well as computational approaches, have shown that perfect or near-perfect complementarity between the mRNA and the nucleotides 2–8 on the 5′ region of the miRNA, also known as the "seed" region, is determinant for target RNA recognition by the miRNA (174, 175). Insufficient 5' pairing can nevertheless be partially compensated by strong base-pairing between the 3′ region of the miRNA and the target mRNA (175, 176). While the seed sequence of the mature miRNA dictates which mRNAs it potentially interacts with, it is the protein components of the miRNP complex that execute the silencing of target mRNAs (177). In this regard, several studies have shown that the GW182 protein is essential for successful miRNP-mediated mRNA silencing, since argonaute-containing miRNPs fail to silence target mRNAs in the absence of GW182 (178, 179).

MiRNP complexes inhibit the production of protein by repressing mRNA translation at either initiation or post-initiation stages and/or promoting mRNA destabilization. These mechanisms are presented in Figure 9, and described below.

2.3.1 Inhibition of mRNA translation: initiation

The translation of an mRNA transcript into a polypeptide is a highly regulated process that encompasses three steps: initiation, elongation and termination. The initiation of translation of most cellular mRNAs is a multi-step mechanism that starts with the recognition of the mRNA 5′-end and its cap structure (7-methylguanosine, m7GpppN) by the eukaryotic initiation factor (eIF) eIF4E (180). Upon cap recognition, eIF4E (along with other eIFs) recruits the 40S small ribosomal subunit to identify the initiation codon and the 60S subunit is then attached to the small subunit to start mRNA translation. An alternative mechanism of translation initiation involves the cap-independent recruitment of ribosomes through interaction with structured regions in the 5′-UTR mRNA designated internal ribosome entry sites (IRES) (181). These structures are mostly present in viral mRNAs, although a few IRES-containing mRNAs have been described in mammalians (182). The current knowledge indicates that miRNAs repress the initiation of translation by interfering with key components of the initiation step machinery.

2.3.1.1 Interference with the 5' cap recognition

Several lines of evidence indicate that miRNPs repress the initiation of translation by interfering with the eIF4E-mediated 5' cap recognition, which prevents 40S subunit recruitment. Studies in cells and cell-free systems showed that miRNAs inhibit the translation of m7G-capped mRNAs, but not that of mRNAs containing IRES or a non-functional ApppN cap, through an Ago2-dependent mechanism (183-185). Similarly, an interesting study by Kiriakidou suggested that the cap-dependent repression of translation initiation resulted from the competition between Ago2 and eIF4E for cap binding (186). Nevertheless, functional and structural studies have since indicated that Ago2 does not significantly interact with the mRNA 5' end cap nor cap analogs (187, 188), thus contradicting the idea that Ago2 directly binds to the 5′ cap structure of target mRNAs and hinders the cap recognition by eIF4E. New mechanistic insights suggest that the CCR4-NOT deadenylase complex, recruited to the miRNP complexes by the Ago2-partner protein GW182 (189, 190), may be responsible for disrupting the interaction between 5' cap, eIF4E and the 40S ribosomal subunit (Fig. 9). CCR4-NOT was shown to repress cap-dependent translation in a deadenylation-independent manner (191), while the *in vitro* knockdown of several components of the this complex resulted in decreased GW182-mediated repression of poly(A)-depleted target mRNAs (189, 192). Nonetheless, the mechanisms by which the CCR4–NOT complex interacts with the 5'-

cap and the translational apparatus and prevents 40S ribosomal subunit recruitment have yet to be clarified.

2.3.1.2 Blocking of the assembly of functional ribosomes or mRNA circularization

MiRNP complexes inhibit translation initiation also by hampering the association between the 60S ribosomal subunit and the 40S initiation complex, thus preventing the formation of a complete (and active) ribosomal complex (193) (Fig. 9). Furthermore, it has been proposed that miRNP complexes repress translation initiation through GW182 binding to PABP, the poly(A)-binding protein attached to the 3' end of the mRNA that is involved in the circularization of the mRNA (194). By binding to PABP, GW182 blocks the interaction of this protein with the cap-binding initiation factor eIF4E (via eIF4G), thus preventing the circularization of the mRNA, a process that is essential for cap-dependent initiation of translation.

2.3.2 Inhibition of mRNA translation: post-initiation

Available evidence indicates that, in addition to the repression of translation initiation, miRNAs can repress mRNA translation at the post-initiation steps (Fig. 9). In order to detect at which step miRNAs inhibit their target mRNAs, a protocol of sucrose gradient sedimentation is usually performed. This approach takes advantage of the fact that mRNAs attached to different numbers of ribosomes sediment at different densities when run on a sucrose gradient. When the translation is inhibited at initiation, few or no ribosomes are attached to the silenced mRNA transcripts and therefore they do not sediment at the same sucrose density as the free ribosomes. However, when translation inhibition takes place at a step that is subsequent to initiation, the silenced mRNAs are associated with ribosomes and sediment in the polyribosome fractions (195). In this regard, three separate studies on the detection of miRNA-repressed mRNAs associated with actively translating polyribosome fractions provided experimental support to the mechanism of post-initiation inhibition of protein synthesis (196-198). Based on those studies, different mechanisms of post-initiation inhibition of mRNA translation were proposed, including the possibility that miRNAs might slow the process of elongation (196), promote nascent polypeptide degradation (197) or cause the ribosomes to detach from the mRNA during the process of translation ("drop-off"

mechanism) (198). Studies by Hendrickson and colleagues have since suggested that the post-initiation inhibition of mRNA translation might occur at an early stage of the elongation process, by stimulating ribosome "drop-off" preferentially near the start site, as opposed to the repression at a later stage of the elongation or termination steps (199). Nevertheless, the molecular details underlying these regulatory pathways remain unclear.
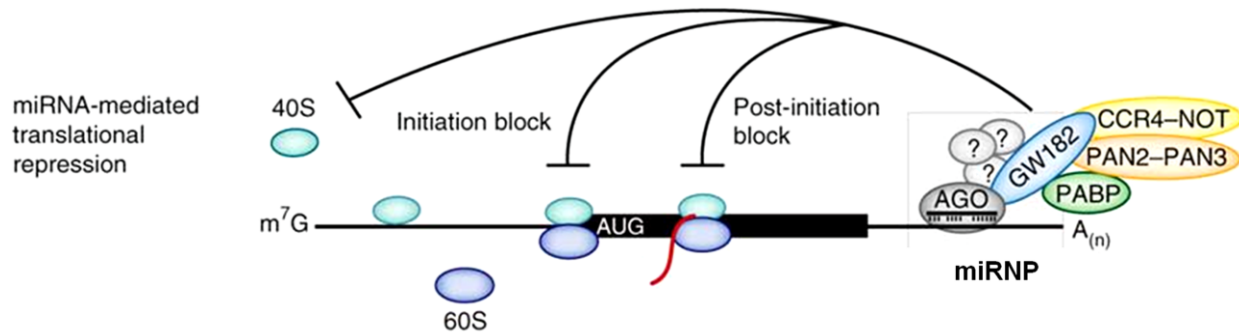
Figure 9. **Mechanisms of miRNA-mediated inhibition of protein translation in animals**. MiRNP-mediated translational repression can occur at either initiation or post-initiation steps. The miRNP complex inhibits translation initiation by either interfering with 5' cap (m7G) recognition and 40S small ribosomal subunit recruitment or antagonizing 60S subunit joining and preventing 80S ribosomal complex formation. Additionally, the miRNP complex inhibits translation at post-initiation steps by inhibiting ribosome elongation. AUG: initiation codon; AGO: argonaute; GW182: glycine-tryptophan repeat–containing protein of 182 KDa; PABP: poly(A)-binding protein; CCR4-NIT: C-C chemokine receptor type 4-NOT; PAN2-PAN3: PAB-dependent poly(A)-specific ribonuclease subunit 2/3. Adapted from (177).

2.3.3 Destabilization of mRNA

In eukaryotes, most mRNAs decay by a deadenylation-dependent pathway that is initiated with removal of the 3'-terminal poly(A) tail (148) (Fig. 10). Following deadenylation, the mRNA is subject to decay by one of two pathways. The mRNA body can be degraded by progressive 3′→5′ decay, a process that is catalysed by a large complex of exonucleases known as the exosome (200), or, alternatively, via removal of the 5'-cap by the decapping complex Dcp1-Dcp2, rendering the mRNA susceptible to 5′→3′ digestion by the exonuclease XRN1 (201).
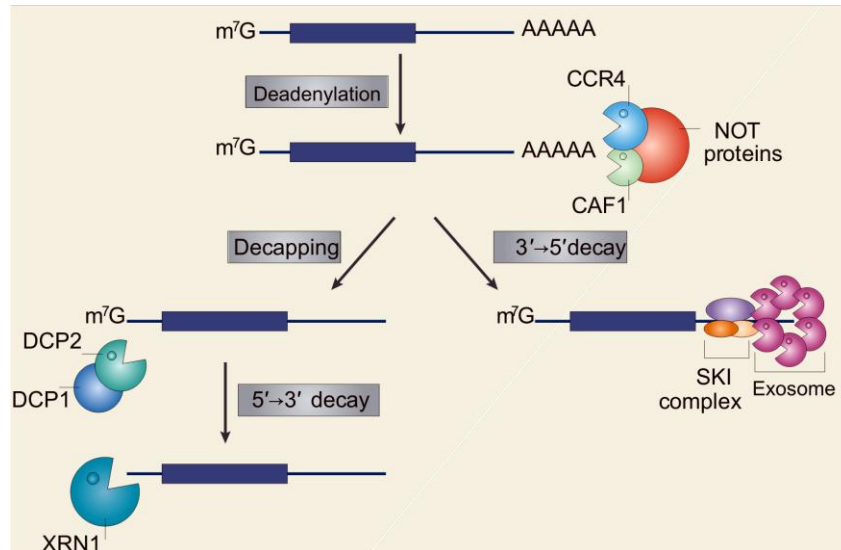
Figure 10. Mechanisms of mRNA degradation in eukaryotes. The initial step of mRNA degradation consists in the deadenylation of the poly(A) tail attached to the 3' end, which is carried out by the CCR4-CAF1-NOT1 complex and involves also the PARN2-PARN3 complex (not shown). The mRNA is further degraded by exonucleolytic digestion at both 3' and 5' ends. The mechanism of degradation that starts at the 3' end and runs towards the 5' end (3'→5') is carried out by a large complex of exonucleases designated exosome. Starting at the 5' end (5'→3'), the mRNA-decay pathway involves the removal of the cap structure by the decapping complex DCP1-DCP2 and subsequent exonucleolytic degradation by the exonuclease XRN1. Adapted from (202).

Early reports on the mechanisms of miRNA-mediated gene silencing indicated that miRNAs act primarily by repressing mRNA translation (without causing direct mRNA degradation), an idea that dominated the field in its early stages. Over the last few years, however, the balance of evidence has steadily been shifting, as high profile studies surveying a large number of miRNA targets strongly indicate that mRNA destabilization (and consequent mRNA degradation) might be a (if not the) key factor in the decrease of protein levels caused by miRNAs. Unanimously, these studies found that miRNA repression results in concomitant changes in mRNA and protein levels, with changes in mRNA levels (mRNA degradation) accounting for the majority, but not all, of the changes in protein abundance (195, 203, 204).

MiRNA-mediated mRNA decay is executed by the miRNP complexes through the recruitment of decay machinery components, leading to mRNA deadenylation (poly(A) tail removal) and 5'-terminal decapping (178, 205, 206) (Fig. 11). In this regard, growing evidence implies GW182 as a key component of these effector complexes that marks mRNA for decay (178). GW182 acts as an anchor for both CCR4–NOT and PAN2–PAN3 deadenylase complexes, which enhance mRNA decay by promoting poly(A) tail removal

35

(177, 189, 192), as well as for EDD/ubr5, an E3 ubiquitin ligase that associates with other silencing effectors (such as the DEAD box helicase RCK/p54) to accelerate mRNA decapping (207, 208).

The fact that GW182 regulates two distinct mRNA-silencing pathways (translational repression and deadenylation) by recruiting the same CCR4–NOT complex is a reflection of the highly complex nature of the miRNA-mediated gene silencing. However, what determines whether an mRNA follows the degradation or translational-repression pathway remains to be fully understood. The mechanism involved in the miRNA-mediated gene expression repression appears to differ for each miRNA–mRNA pair and is probably influenced by accessory proteins bound to the mRNA 3′ UTR region (which control the accessibility of the miRNAs to the target sequence) or structural mismatches of imperfect miRNA–mRNA duplexes (202, 209). Importantly, studies in zebrafish and drosophila melanogaster have shown that miRNA-mediated translational repression precedes mRNA decay (210, 211), which indicates that miRNAs may control protein synthesis in a stepwise mechanism that involves an initial deadenylation-independent inhibition of translation and subsequent decay of the target mRNAs.
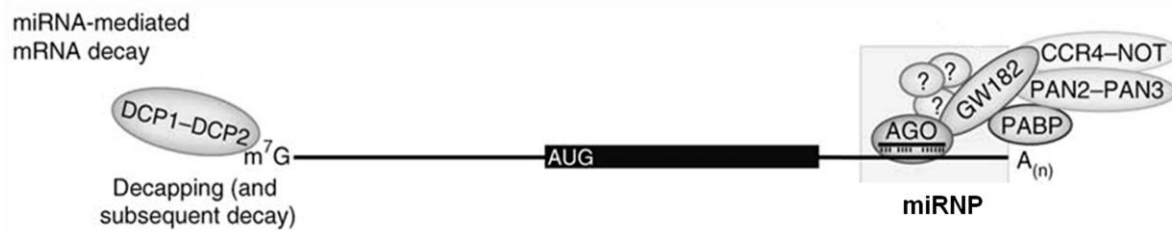
Figure 11. Mechanisms of miRNA-mediated mRNA decay in animals. In this pathway, the miRNP complex interacts with the two deadenylase complexes (CCR4–NOT and PAN2–PAN3) to facilitate deadenylation of the poly(A) tail (A(n)). Following deadenylation, the 5' end (m7G) is decapped by the action of the DCP1–DCP2 complex and the mRNA is subsequently degraded by the Xrn1 5′–3′ exonuclease. AGO: argonaute; GW182: glycine-tryptophan repeat–containing protein of 182 KDa; PABP: poly(A)-binding protein; CCR4-NIT: C-C chemokine receptor type 4-NOT; PAN2-PAN3: PAB-dependent poly(A)-specific ribonuclease subunit 2/3; DCP1-DCP2: mRNA-decapping enzyme 1/2. Adapted from (177).

2.3.4 Storage and decay of mRNA and subcellular compartments

2.3.4.1 P-bodies

The degradation of the miRNA-repressed mRNAs (or at least its final steps) is thought to occur in cytoplasmic foci called P-bodies, which are dynamic and reversible structures that

contain several components of the miRNP complexes, including argonaute and GW182 proteins, while ribosomal components (as well as others of the translational machinery) are not detected in these structures (153, 157, 202) (Fig. 12). Several observations support the idea that, in addition to the storage of repressed mRNAs, mRNA decay occurs in P-bodies. Firstly, most proteins that are involved in the 5′→3′ mRNA-decay pathway, including the CCR4-NOT deadenylase complex and the decapping effector DCP2, are localized in P-bodies (212). Secondly, miRNAs associated with their target mRNAs, as well as mRNA-decay intermediates are detected in P-bodies (213). Thirdly, the inhibition of mRNA degradation in the early steps of the decay process (by preventing deadenylation, for example) results in decreased size (or ultimately loss) of the P-bodies (213), whereas the inhibition of mRNA decay at later steps (after decapping) increases the abundance and size of P bodies (212, 213).

Although several P-body components play essential roles in the miRNA-mediated gene silencing mechanisms, miRNA repression is nevertheless observed in cells lacking detectable microscopic P-bodies, which indicates that P-body formation is a consequence (not the cause) of the mRNA decay activity (147). In this regard, it is currently recognized that P-body components are not confined to cytoplasmic foci, but are diffused throughout the cytoplasm in soluble protein complexes with inhibitory activity, which may aggregate to form the P-bodies (202, 214) (Fig. 12). Importantly, not all mRNAs that enter P-bodies are degraded, as it has been demonstrated that upon subjecting cells to specific stress conditions, repressed mRNAs can re-initiate translation (215).

2.3.4.1 Stress granules

Another type of subcellular foci in which repressed mRNAs and decay machinery are detected is the stress granules (SGs) (Fig. 12). These small aggregates were shown to assemble in response to different stress conditions and disperse after recovery (209). As opposed to the P-bodies, however, several components of the translational apparatus, including initiation factors (eIF3 and eIF4G) and the 40S ribosomal subunits are detected in these structures (216), which suggests that SGs might also be involved in the miRNA-mediated inhibition of translation.
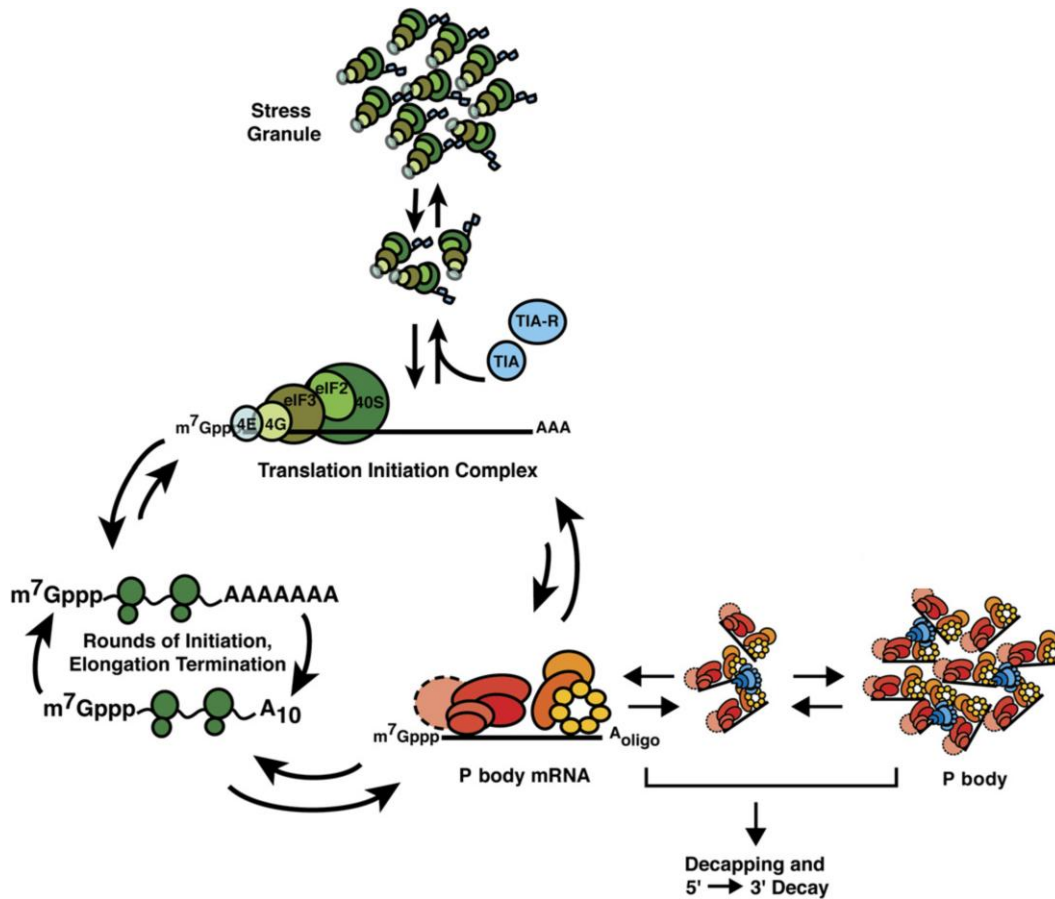
Figure 12. **MiRNA-mediated gene silencing and the subcellular compartments involved in the storage and degradation of the mRNAs**. Upon recognition and pairing between miRNA and target mRNA (P-body mRNA), miRNPs promote either mRNA translation inhibition or mRNA decay. MRNA decay occurs in diffuse cytoplasmic protein complexes that can aggregate to form microscopically-visible P-bodies. P-bodies are also considered storage structures for repressed mRNAs which, under certain stimuli, can be re-activated. Stress granules (SGs) are also very dynamic cytoplasmic foci that assemble under stress conditions. SGs may also be involved in the miRNA-mediated RNA translation inhibition. TIA: T-cell-restricted intracellular antigen (RNA binding protein); TIAR: TIA-related RNA-binding protein; eIF2/3: eukaryotic initiation factor 2/3; 4E/4G: eukaryotic initiation factor 4E/4G; m7Gppp: 7-methylguanosine. Adapted from (214).

Although considerable attention has been given to the miRNA activity in the cytoplasm, an interesting study by Hwang and colleagues showed that the mature miR-29b contains a hexanucleotide motif at the 3' terminal that works as a nuclear localization signal, targeting this miRNA into the nucleus (217). This observation suggests that, in addition to the canonical translation regulatory functions that are associated with the miRNAs, miR-29b (and other miRNAs with similar motifs) may play a role in nuclear processes, including transcription and/or splicing.

2.4. Functional roles of the miRNAs

As mentioned before, miRNAs emerged as important players in the highly complex world of gene regulation. A large number of studies involving transcriptomic, proteomic and bioinformatic approaches indicate that these evolutionarily conserved RNA molecules can regulate over 30% of all protein-coding genes and play a role in the most basic cellular processes - such as embryonic development, cell differentiation, metabolism, proliferation and cell death - in a wide range of invertebrate and vertebrate organisms (including humans) (154, 172, 218, 219). Widespread influence of miRNAs is also observed in (the regulation of) different physiological responses, including cardiovascular development (220), stem cell differentiation (221), immune response (222), cholesterol metabolism (223), insulin secretion (224) and anti-viral defense (225).

Rather than controlling protein production in a "loss (or gain)-of-function" type of mechanism (this usually occurring in protein-coding gene deletions/amplifications or mutations), most mammalian miRNAs function as subtle regulators of a wide range of cellular processes by fine-tuning the protein output. Indeed, several high-throughput studies indicate that each individual miRNA can regulate, though to a mild degree, hundreds of target genes (203, 204). Most miRNA targets contain only a single binding site, which might not be sufficient to confer strong repression (219). In this regard, it was proposed that miRNAs act synergistically to control cell (or tissue)-specific gene expression by reinforcing the expression of specific target genes while suppressing the expression of unwanted transcripts (157, 219). There is, nevertheless, another class of functional miRNAs - designated "switch" miRNAs - whose expression is associated with strong target repression due to the increased number of mRNA target binding sites for one or several miRNAs (157). In this case, small alterations in miRNA expression can lead to moderate changes in the levels of multiple proteins which, altogether, can account for large changes in cellular function. Abnormal expression of switch miRNAs has indeed been associated with impaired cellular functions, such as increased proliferation (226) and decreased apoptotic function (227), that may, in combination with other genetic alterations, result in human disease.

Since the miRNA milieu has a broad influence over diverse genetic and molecular pathways, it is not surprising that abnormal miRNA expression has been associated with several human diseases, including cardiovascular (228) and neurological (229) disorders, diabetes (230) and cancer (155). Since the main goal of the work presented in this thesis was to develop novel miRNA-based therapeutic approaches towards GBM, the next sections will

briefly address the current knowledge on the role of miRNAs in cancer, with particular emphasis in GBM.

2.5 Role of miRNAs in cancer

The transformation of a normal cell into a malignant clone is a gradual process that involves the accumulation of genomic, epigenetic and structural alterations. For almost three decades, it was assumed that these alterations affected protein-coding oncogenes and/or tumor suppressor genes (155). After the discovery, in the past decade, of a whole new class of ncRNAs with important regulatory activity, it became increasingly evident that alterations in both coding and noncoding genes could contribute to tumorigenesis.

The first indication that miRNA dysregulation could play a role in cancer was provided by Calin and colleagues, which demonstrated that two clustered miRNA genes, mir-15a and mir-16-1, were located in a region of the 13q14 locus that is commonly deleted in patients diagnosed with B-cell chronic lymphocytic leukemia (CLL) (231). Soon after, Croce and colleagues showed that approximately 50% of annotated human miRNAs are located in cancer-associated genomic regions (CAGRs), including fragile sites, minimal regions of loss of heterozygosity, minimal regions of amplification or common breakpoint regions (232). Altered expression of Dicer and Ago proteins were also implicated in the development of cancer (233, 234). Similarly, Kumar and colleagues demonstrated that global repression of miRNA maturation, through shRNA-mediated inhibition of several components of the miRNA processing machinery, promotes cellular transformation and tumorigenesis (235), thus supporting the idea that miRNAs might have a crucial function in cancer progression. Indeed, several genome-wide miRNA-profiling studies provided evidence that distinct miRNA expression profiles distinguish tumors from normal tissues (236, 237). Moreover, different miRNA signatures were also associated with poor patient prognosis in lung cancer and CLL (238, 239), indicating that miRNAs have the potential to be used as diagnostic and prognostic markers. Loss or gain or miRNA function and its role in the development of cancer will be addressed below.

2.5.1 MiRNAs as tumor suppressors

MiRNAs can act as tumor suppressors when their reduced expression or loss of function contributes to the development of a malignant cell phenotype (154) (Fig. 13).

Accumulated evidence suggests that the cellular miRNA milieu is mostly composed of tumor suppressor miRNAs: global downregulation of miRNAs was detected in tumors, when compared to normal tissues (236), and the repression of miRNA maturation in mammalian cells enhanced cellular transformation and tumorigenesis (235).

The loss of miR-15a and miR-16-1, due to chromosomal deletion of the locus 13q14 or germline mutation in their primary precursor, was associated with the development of the indolent form of CLL (231). Both miRNAs were found to regulate posttranscriptionally the expression of Bcl-2, an anti-apoptotic protein that is widely overexpressed in CLL (240), which supports the role of these miRNAs as tumor suppressors in CLL. Loss of miR-15a and miR-16-1 has also been observed in prostate cancer and multiple myeloma (241, 242). Similarly, members of the let-7 family of miRNAs were reported to map in genomic regions which are deleted in different human malignancies (232), and their downregulation is commonly observed in lung, breast and colon cancer (239, 243, 244). The tumor suppressor role of let-7 was clearly demonstrated in lung cancer, as concluded by the observation that downregulation of let-7 in lung tissues led to the constitutive overexpression of Ras and high-mobility group AT-hook 2 (HMGA2), oncoproteins that contribute to the pathogenesis of cancer (245-247). Reduced let-7 expression was also shown to enhance c-Myc signaling in Burkitt lymphoma (BL) cells (248), while let-7 overexpression induced apoptosis and cell cycle arrest in lung and colon cancer and in BL cell lines (243, 245, 248).

In addition to miR-15a/miR-16-1 and let-7, miR-29 family members (29a, 29b, and 29c) were shown to function as tumor suppressor miRNAs, their downregulation being associated with the development and progression of several human malignancies, including CLL, lung cancer, invasive breast cancer and hepatocellular carcinoma (238, 239, 244, 249). Interestingly, Fabbri and colleagues demonstrated that miR-29 can function as a tumor suppressor in lung cancer through interference with the methylation of tumor suppressor genes. By promoting the downregulation of the DNA methyltransferases 3A and B (DNMT3A and 3B), miR-29 induces re-expression of methylation-silenced tumor suppressor genes, such as the fragile histidine triad protein (FHIT) and the WW domain containing oxidoreductase (WWOX) (250).

It is currently recognized that the loss of miRNA function contributes to malignant transformation by enabling aberrant oncogenic signaling. The critical role of miRNAs in the control of oncogenic signaling is also reflected on the fact that a large number of miRNAs with tumor suppressor functions are coded in more than one genomic locus, which suggests the

existence of an evolutionarily conserved mechanism that preserves the function of an important miRNA in case of mutation or deletion of one locus (251).

2.5.2 MiRNAs as oncogenes

MiRNAs act as oncogenes when their increased expression or gain of function contributes to the development of a malignant cell phenotype (252) (Fig. 13).

One of the best-characterized oncogenic miRNAs is mir-17-92, a polycistronic cluster comprising six miRNAs (miR-17, miR-18a, miR-19a, miR-20a, miR-19b-1, and miR-92-1), that maps at 13q31.3, a region amplified in several types of lymphoma and solid tumors (253, 254). Expression profiling studies revealed widespread overexpression of these miRNAs in a large number of human hematopoietic malignancies and solid tumors, including breast, colon, lung, pancreatic, prostate and stomach cancers (237, 255). The members of the miR-17-92 cluster were shown to promote tumor proliferation and induce angiogenesis through the activation of c-Myc (253, 255, 256), which is frequently activated in cancer. Interestingly, O'Donnell and colleagues also reported that the transcription of the miR-17-92 cluster is directly transactivated by c-Myc (257). The miR-17-92 cluster was also shown to enhance proliferation by activating several members of the E2F family of transcription factors - E2F1, E2F2, E2F3 - which induce the expression of genes that drive cell cycle progression from G1 into S phase, and by inhibiting the cyclin-dependent kinase inhibitor 1A (CDKN1A, also known as p21), a potent negative regulator of the G1-S checkpoint (258). Similarly to what was observed for c-myc, both E2F1 and E2F3 can directly activate transcription of these miRNAs, establishing a negative feedback loop that reinforces the production of pro-oncogenic signals (255).

Strong evidence also suggests that miR-21 functions as an oncogene. Overexpression of this miRNA has been observed in numerous human malignancies, including colon, stomach, pancreas, prostate, lung, breast and liver cancer (237, 244, 259, 260), being associated in important cancer hallmarks, such as uncontrolled cell proliferation, decreased apoptose, invasion and migration (261). Since miR-21 was the main molecular target addressed in this thesis towards the development of therapeutic approaches for GBM, a specific section in this chapter will be devoted to the role of miR-21 in GBM pathogenesis.

Another miRNA with a clear role in the pathology of cancer is miR-10b. This miRNA is involved in the later stages of malignancy, by promoting the invasion of cancer cells into the surrounding stroma and metastasis to distant sites (262, 263). MiR-10b was found to be overexpressed in metastic samples of breast and hepatocellular carcinomas, when compared

with tumor samples from metastasis-free patients (264, 265), and patient samples from pancreatic adenocarcinomas (259) and glioblastomas (266), two types of extremely invasive/metastic cancer. It was proposed that miR-10b promotes invasion and metastasis by suppressing the translation of homeobox D10 (HOXD10), a transcriptional repressor known to inhibit the expression of several pro-metastatic genes, including the Ras homolog gene family member C (RHOC) (263). Moreover, Ma and colleagues suggested that miR-10b overexpression is induced by the metastasis-promoting transcription factor Twist in order to (indirectly) enhance Twist pro-metastic function, via miR-10b-mediated HOXD10 downregulation (263). In addition to translation suppression of HOXD10, an E-cadherin-related mechanism has been proposed to explain the role of miR-10b in breast cancer metastasis (267).
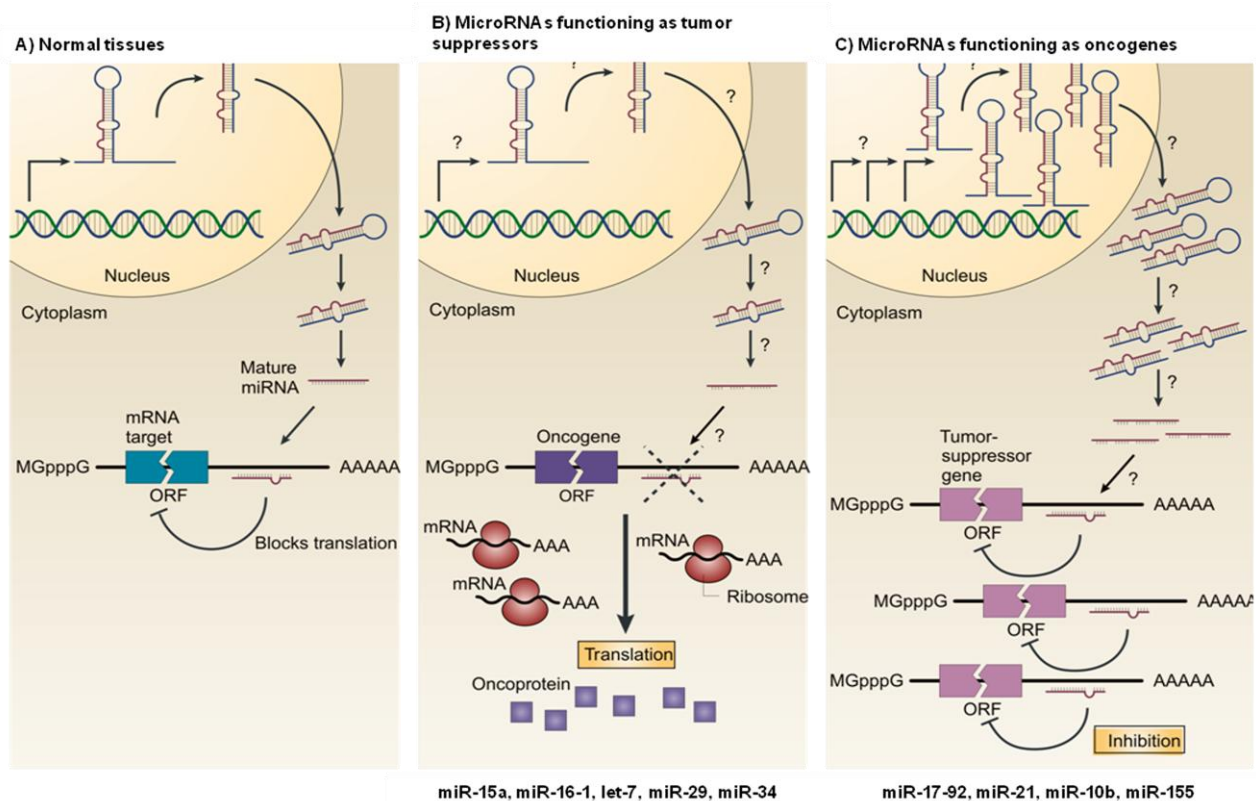
Figure 13. MicroRNAs as tumor suppressor and oncogenes. (**A**) In normal cells, miRNA transcription, processing and binding to complementary sequences in the target mRNA lead to the repression of their target genes, by either mRNA translation inhibition or mRNA degradation. (**B**) The reduced expression of a miRNA that functions as a tumor suppressor, as a result of chromosomal deletion or defects at any stage of miRNA biogenesis (indicated by question marks) ultimately leads to the increased expression of the miRNA-target oncoprotein (purple squares). The overexpression of several oncogenes results in the development of an oncogenic phenotype. (**C**) The increased expression of miRNAs, as a result of amplification of the miRNA gene or constitutive promoter activation (among others) (indicated by question marks), leads to the repression of miRNA-target tumor-suppressor genes (pink), which favors the development of an oncogenic phenotype. ORF: open reading frame; mGpppG: 7-methylguanosine. Adapted from (156).

2.5.3 Dual role of miRNAs

MiRNA function can vary according to the tissue and its transcriptome, including the miRNA targets expressed in that particular tissue (154). In addition to its well known oncogenic role, miR-17-5p, a member of the miR-17-92 cluster, was reported to be downregulated in breast cancer cells (268). Reduced levels of this miRNA enhanced the expression of the AIB1 (amplified in breast cancer 1) oncogene, while miR-17-5p overexpression resulted in decreased expression of AIB1 and decreased proliferation of breast cancer cells (268), thus suggesting that mir-17-5p can act as a tumor suppressor in this type of tumor. Deletion of the miR-17-92 genomic locus has also been described in 16.5% of ovarian cancers, 21.9% of breast cancers, and 20% of melanomas (255, 268). Although miR-21 is uniformly overexpressed in a wide variety of human tumors, miR-21 inhibition was associated with increased cell growth in cervical cancer cells (269). Similarly, the miR-221-222 cluster was shown to have a tumor suppressor role in erythroblastic cells by targeting the oncogene c-kit, which decreases the growth of erythroblastic leukaemia (270), while promoting tumor growth in breast cancer cells by repressing the tumor suppressors p27*, p57*, PTEN and TIMP3 (tissue inhibitor of metalloproteinases 3) (271). Therefore, as stated by Croce and collaborators, miRNAs should not be classified as oncogenes or tumor suppressors unless the tissue or cell type involved in their action is specified (154).

2.5.4 Mechanisms involved in the control of miRNA expression in cancer

Various genomic abnormalities were found to influence the activity of miRNAs, including deletions, amplifications or mutations involving miRNA loci, epigenetic silencing or dysregulation of transcription factors that target specific miRNAs (154, 155). Deletions, mutations and amplifications of miRNA genes, such as those described above for miRNAs with an oncogenic and tumor suppressor role, result from their location in unstable chromosome regions prone to deletion, amplification or even translocation (231, 238, 272).

2.5.4.1 Epigenetic alterations

In addition to structural genetic alterations, dysregulated miRNA expression in cancer can result from epigenetic changes, namely DNA methylation and histone acetylation.

DNA methylation is a mechanism of gene expression regulation by which cells "turn-off" selected genes. Methylation occurs at the cytosine residue of CpG dinucleotides, known as CpG islands, located at protein-coding and noncoding genes and throughout the genome. While the majority of gene-associated CpG islands are unmethylated in normal human cells, both hypomethylation and hypermethylation are commonly detected in tumors (273). Methylation of the CpG islands of tumor suppressors results in their silencing and contributes to malignant transformation (274). Similarly to what is observed for tumor suppressor-coding genes, promoter methylation was also found to repress several tumor suppressor miRNAs (275). Saito and colleagues reported that miR-127 is silenced by promoter methylation in bladder tumors, while treatment with hypomethylating agent azacitidine restored its expression (276). The downregulation of miR-34b and miR-34c, two direct transcriptional targets of the p53 tumor suppressor, was also found to be associated with hypermethylation of the neighboring CpG island in colorectal cancer, while 5-aza-2'-deoxycytidine (DAC) treatment rapidly restored miR-34b/c expression (277), which indicates that DNA demethylation can activate the expression of epigenetically-repressed miRNAs. DNA methylation can also control the expression of tumor suppressor intronic miRNAs by directly controlling their host genes (278). Conversely, DNA hypomethylation was also associated with increased expression of oncogenic miRNAs. Brueckner and colleagues demonstrated that increased let-7a-3 expression in some lung adenocarcinomas results from the hypomethylation of its promoter and is associated with enhanced tumor phenotypes (279).

Beside DNA methylation, another epigenetic mechanism that can affect miRNAs expression is histone acetylation. Acetylation removes the positive charge in histones, thereby decreasing their interaction with the negatively charged DNA. Consequently, the condensed chromatin is transformed into a more relaxed structure that is associated with greater levels of gene transcription. Histone acetylation is biologically reversed by histone deacetylases (HDAC). Several studies using HDAC inhibitors revealed rapid and extensive alteration of miRNA levels in breast, gastric and colorectal cancer cell lines (278, 280, 281), which indicates that histone acetylation plays a role in the regulation of miRNA expression.

2.5.4.2 Dysregulation of transcription factors

Dysregulation of miRNA expression can also result from increased or decreased transcription due to altered transcription factor activity (282).

Several studies demonstrated that the miR-34 family (miR-34a/b/c) is a direct transcriptional target of p53 that can mediate or fine-tune p53-related apoptotic and cell cycle programs (283, 284). Reduced miR-34 expression, commonly observed in different human malignancies (285) might thus result (at least in part) from decreased input of p53 signals, since mutations or deletions in the gene coding for p53 (TP53) are one of the most frequent alterations in human cancers (286). The transcription factor c-Myc was also shown to induce transactivation of the pro-oncogenic miR-17-92 cluster (255), and negatively regulate transcription of tumor suppressor miRNAs, such as let-7 (287) and miR-29 (288).

In addition to transcription factors, growth factors were also shown to induce alterations in the expression of miRNAs. Shao and colleagues demonstrated that PDGF-A and PDGF-B, two members of a vast family of angiogenic growth factors involved in the tumorigenesis of GBM (13, 289), regulate the expression of some of their known targets (e.g. cyclin D1) in glioblastoma and ovarian cancer cells by inducing the expression of miR-146b and repressing let-7d (290).

2.5.5 MiRNA profiling in cancer diagnosis and patient prognosis

In addition to their established role in the development of cancer, an increasing body of evidence suggests that miRNAs have potential to be clinically used as diagnostic and prognostic biomarkers, as well as to predict the therapeutic response (282) (Table 2).

A unique miRNA signature was associated with disease progression in CLL (238), while miR-155 overexpression and let-7a downregulation correlated with poor patient prognosis in lung cancer (239, 291). Low expression of miR-191 and high expression of miR-193b were also associated with poor melanoma-specific patient survival (292), whereas low expression of key components of miRNA processing such as Dicer and Drosha correlated with poor clinical outcome in ovarian cancer (293). Moreover, miRNA expression was shown to predict the therapeutic response to chemotherapy. Elevated serum levels of miR-21 correlated with poor overall survival[30] and gemcitabine resistance in pancreatic cancer (294, 295), while increased platinum-based chemotherapy resistence and decreased disease-free survival[31] were observed in non small-cell lung cancer (NSCLC) patients with high serum levels of this miRNA (296).

---

[30] Overall survival corresponds to the percentage of patients in a treatment group who are still alive for a certain period of time after they were diagnosed with or started treatment for a disease, such as cancer.
[31] Disease-free survival (DFS) corresponds to the length of time after cancer treatment that the patient survives without any signs or symptoms of that cancer.

46

Table 2. MicroRNAs associated with patient outcome in cancer

MicroRNA	Disease	Expression in poor outcome	Variable [a]	References
let-7a	non–small cell lung cancer	low	overall survival (OS) [b]	239, 291
miR-181a/b	CN-AML (<60 years)	low	disease-free survival (DFS) [c]	299
miR-181a	CLL	high	time to progression [d]	238
miR-21	colon adenocarcinoma	high	OS, DFS	297
miR-21	CLL	high	time to progression	238
miR-155	CLL	high	time to progression	238
miR-221/222	CLL	high	time to progression	238
miR-146	CLL	high	time to progression	238
miR-29-c	CLL	low	time to progression	238
miR-196-a	pancreas adenocarcinoma	high	OS	259
miR-191	AML	high	OS, DFS	298
miR-199a	AML	high	OS, DFS	298

[a] Clinical endpoint associated with the patient outcome.
[b] Percentage of patients in a treatment group who are still alive for a certain period of time after they were diagnosed with or started treatment for a disease, such as cancer.
[c] Length of time after cancer treatment that the patient survives without any signs or symptoms of that cancer.
[d] Interval of time after a disease is diagnosed (or treated) until the disease starts to get worse.
CLL, chronic lymphocytic leukemia; AML, acute myeloid leukemia; CN-AML, cytogenetically normal AML. Data obtained from (252).

2.6 Role of the oncogenic miR-21 in GBM

Over the last few years, several studies demonstrated that miRNA dysregulation contributes to the pathogenesis of GBM (300-302). Not surprisingly, the oncogenic miR-21 was found to modulate several signaling pathways involved in the control of cell cycle, proliferation, apoptosis and migration in GBM (Fig. 14). MiR-21 promotes tumor cell proliferation by inhibiting PDCD4 (programmed cell death protein 4), a tumor suppressor that represses protein translation by interacting with the initiation factors eIF4A and eIF4G (303), and prevents cell cycle progression via activation of the cyclin-dependent kinase 1 (Cdk1) inhibitor p21 (304). MiR-21 was also shown to target several components of p53, TGF-β and mitochondrial apoptotic networks in order to decrease apoptotic activation in GBM cells (305). Moreover, miR-21 enhances tumor cell migration by inhibiting the matrix metalloproteinase (MMP) regulators RECK (reversion-inducing-cysteine-rich protein with kazal motifs) and

TIMP3 (306). MMPs are a group of peptidases involved in degradation of the extracellular matrix, whose levels are significantly elevated in human gliomas and correlate with tumor invasiveness (300).

Genomic amplification of chromosome band 17q23.2, that includes the miR-21 locus, has been reported in neuroblastoma and breast, colon and lung cancer (155). In GBM, however, structural abnormalities have not been found (261), which indicates that gains in miR-21 function must result from epigenetic or transcriptional alterations. In this regard, accumulated evidence suggests that miR-21 can be induced by transcriptional and posttranscriptional mechanisms.

MiR-21 transcription is induced by interleukin 6 (IL-6) in myeloma cells, in a mechanism that requires Stat3 (signal transducer and activator of transcription 3) (307). Upon IL-6 stimulation, Stat3 is recruited to the miR-21 regulatory region where it binds to two conserved binding sites and induces the transcription of miR-21 (307). Increased expression of IL-6 and constitutive activation of Stat3 have already been reported for GBM, being associated with increased tumor cell proliferation (308, 309), which suggests that IL-6 and Stat3 can act cooperatively to induce miR-21 transcription in GBM. The transcription factor AP-1 (activator protein 1), an important regulator of cell proliferation, apoptosis and invasion, has also been shown to activate miR-21 transcription in human embryonic kidney cells through highly conserved AP-1-binding sites present in the miR-21 promoter, miPPR-21 (310). The androgen receptor (AR), a ligand-dependent transcription factor involved in the pathogenesis of prostate cancer, was also reported to bind to miPPR-21 upon androgen stimulation (311). Androgen-mediated miR-21 induction enhanced cellular proliferation of cultured prostate cancer cells (311). Additional studies have identified alternative regulators for this miRNA, including Ras (312) and the EGFR (313).

In addition to transcriptional regulation, post-transcriptional regulation of pri-miR-21 has been reported. Davis and colleagues demonstrated that TGF-β and BMP (bone morphogenic protein) signaling promotes a rapid increase in expression of mature miR-21 by inducing Drosha to accelerate the processing of primary transcripts of miR-21 into precursor miR-21 (314).
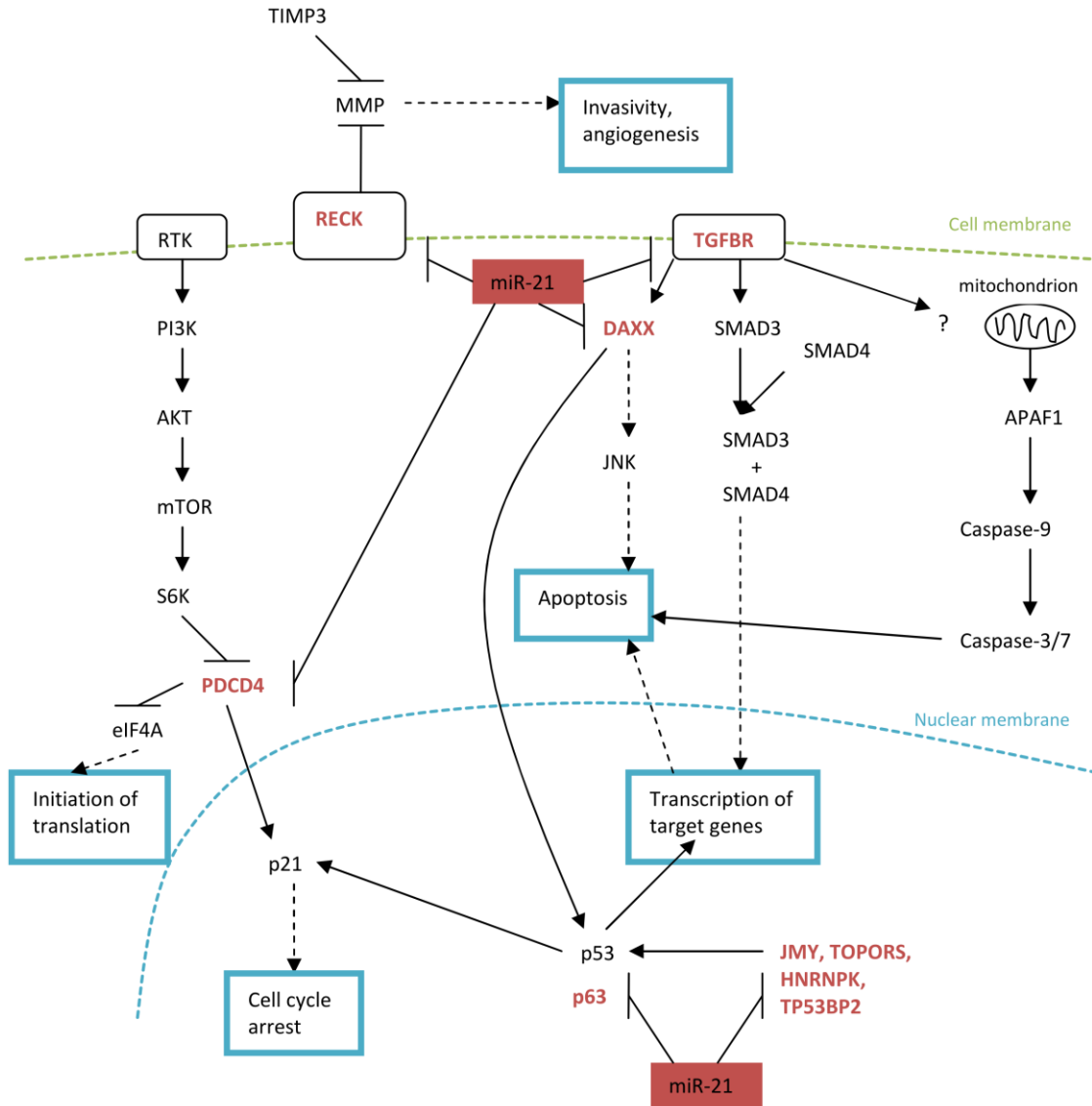
Figure 14. MiR-21-regulated signaling pathways in GBM. MiR-21 regulates invasion, apoptosis, cell cycle and protein translation in glioblastoma cells by inhibiting the translation of RECK (promoting invasion), TGFBR, DAXX, p63, JMY, TOPORS, HNRNPK, TP53BP2 (inhibiting apoptosis) and PDCD4 (inducing cell cycle progression and protein translation). TIMP3: tissue inhibitor of metalloproteinase 3; MMP: matrix metalloproteinase; RECK: reversion-inducing-cysteine-rich protein with kazal motifs; RTK: receptor tyrosine kinase; PI3K: phosphoinositide-3 kinase; Akt: protein kinase B; mTOR: mammalian target of rapamycin; S6K: ribosomal protein S6 kinase; PDCD4: programmed cell death protein 4; eIF4A: eukaryotic initiation factor-4A; TGFRβR: transforming growth factor beta receptor; DAXX: death-associated protein 6; JNK: c-Jun N-terminal kinase; SMAD3/4: Mothers against decapentaplegic homolog 3/4; APAF-1: apoptotic protease activating factor 1; JMY: junction-mediating and -regulatory protein; TOPORS: topoisomerase I binding ligase; HNRNPK: heterogeneous nuclear ribonucleoprotein K; TP53BP2: tumor suppressor p53-binding protein 2. Adapted from (300).

In addition to miR-21, overexpression of other oncogenic miRNAs and downregulation of tumor suppressor miRNAs was also suggested to contribute to the pathogenesis of GBM.

2.7 Other miRNAs that act as oncogenes in GBM

The cluster miR-221-222 was reported to promote tumor cell proliferation by repressing the cell cycle regulator p27Kip1 (cyclin-dependent kinase inhibitor 1B) (315, 316) (Fig. 15). This protein binds to cyclin-dependent protein kinases (CDKs) and prevents the phosphorylation of CDK substrates, which results in cell cycle arrest in the G1 phase. Indeed, high levels of miR-221-222 correlated with low levels of p27Kip1 in glioblastoma cell lines (315). While genomic amplification of the miR-221-222 locus has yet to be identified, bioinformatic analysis suggests that the cyclin-dependent kinase 4 (CDK4) is a possible activator of miR-221 (300). Inhibition of CDK4 was shown to enhance translation of p27Kip1 (317), which could result from the indirect decrease of miR-221-222 expression (and not from the direct action of CDK4).

MiR-26a, frequently amplified at the DNA level in human gliomas, was found to inhibit the expression of the tumor suppressor PTEN, which facilitates *de novo* tumor formation in a mouse glioma model and precluded loss of heterozygosity at the PTEN locus (318). Mir-26a was also shown to promote *in vivo* tumor growth independently of PTEN status, by cooperating with CDK4 and CENTG1[32] to target the RB1, PI3K/Akt, and JNK pathways (319).

Similarly, miR-10b was demonstrated to target several regulators of cell growth and survival in order to promote glioma growth (262). MiR-10b inhibits p16 and p21, cell-cycle inhibitors capable of inducing cell-cycle arrest and senescence in cancer cells, as well as the pro-apoptotic proteins Bim and TFAP2C (transcription factor AP-2 gamma) (320, 321). Interestingly, HOXD10, a validated miR-10b target involved in migration and invasion of breast carcinoma cells (263), was not affected by the increased expression of miR-10b in glioma. MiR-125b, miR-182, miR-196a, miR-296 and the cluster miR-17-92 are other miRNAs that have been proposed to play a pro-oncogenic role in this disease (302).

The downregulation of several miRNAs was also shown to play a role in GBM tumorigenesis.

---

[32] Arf-GAP with GTPase, ANK repeat and PH domain-containing protein 2.

2.8 MiRNAs that act as tumor suppressors in GBM

Godlewski and colleagues demonstrated that miR-128, a brain specific miRNA, was downregulated in GBM patient samples, when compared to the levels detected in normal brain (322) This miRNA directly targets E2F3a, a transcription factor that induces the expression of genes involved in cell cycle progression (323), and Bmi-1[33], a member of the polycomb repressor complex (PRC1) involved in epigenetic gene silencing by chromatin modifications (324) and stem cell renewal (322) (Fig. 15). In this regard, the inhibition of Bmi-1 in glioma cells was shown to block stem cell self-renewal and to repress cell cycle progression via decreased Akt activation and increased p21 expression (322), thus supporting the idea that miR-128 acts as a tumor suppressor in GBM by facilitating cell cycle arrest and inhibiting stem-cell renewal.

MiR-7 is another potential tumor suppressor in glioblastoma targeting critical cancer signaling pathways. Decreased levels of this miRNA are observed in GBM tissue, when compared to surrounding brain, as a consequence of impaired processing of its precursor (325). Kefas and colleagues demonstrated that miR-7 inhibits the pro-oncogenic AkT pathway by targeting EGFR or the insulin receptor substrate 2 (IRS-2), a molecule that activates the AkT pathway independently of EGFR (325) (Fig. 15).

Recently, two studies indicated that miRNA-34a could play a significant role in the regulation of GBM proliferation and GBM stem cell differentiation (326, 327). Reduced levels of miR-34a were observed in human gliomas, when compared to those determined in normal brain, and in mutant p53 gliomas as compared to wild-type p53 gliomas, which correlated with increased expression of the target oncogenes c-Met, Notch-1, Notch-2 and cyclin-dependent kinase 6 (CDK6) in glioma and stem cells (327). Transient expression of miR-34a strongly inhibited cell proliferation, cell cycle progression, cell survival and invasion (327) and, more importantly, induced GBM stem cell differentiation (326), while forced c-Met and Notch-1/2 expression partially rescued the effects of miR-34a on the cell cycle and cell death in gliomas, respectively (327). Moreover, transient expression of miR-34a in GBM cells strongly inhibited the *in vivo* growth of a glioma xenograft. Overall, these studies implicated miR-34a in the control of GBM stem cell differentiation, partly via regulation of Notch expression (302).

In addition to the above-referred miRNAs, let-7, miR-17, miR-146b, miR-153, miR-181, miR-184 and miR-326 were proposed to play a role as tumor suppressors in GBM.

---

[33] B lymphoma mouse Moloney leukemia virus insertion region 1.
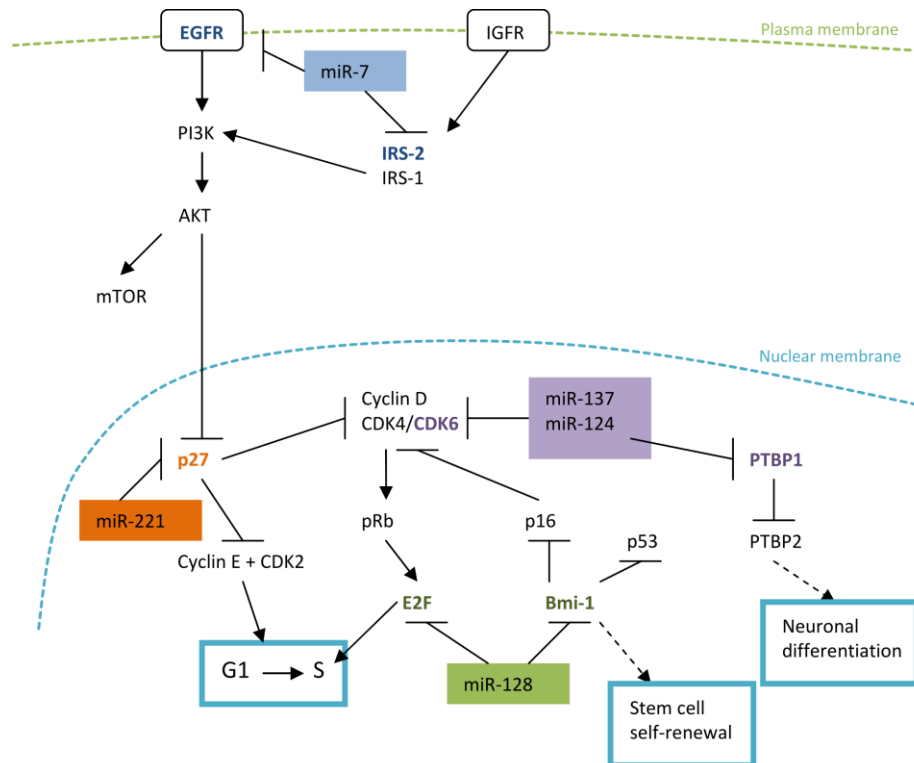
Figure 15. MiRNA-regulated signaling pathways in GBM. MiR-7 represses cell cycle progression by interfering with the Akt pathway via EGFR and IRS-2 inhibition. In contrast, the oncogenic miR-221 promotes cell cycle progression by inhibiting the translation of p27. Cell cycle arrest is also promoted by miR-128, through inhibition of E2F, as well as miR-137 and miR-124, through inhibition of CDK6. MiR-128 and miR-124 affect neuronal stem cells by targeting Bmi-1 and PTBP1, respectively. IGFR: insulin-like growth factor receptor; IRS-1/2: insulin receptor substrate 1/2; EGFR: epidermal growth factor receptor; PI3K: phosphoinositide-3 kinase; Akt: protein kinase B; mTOR: mammalian target of rapamycin; CDK2/4/6: cyclin-dependent kinase 2/4/6; pRB: retinoblastoma protein; Bmi-1: B lymphoma mouse Moloney leukemia virus insertion region 1;   PTBP1/2: polypyrimidine tract-binding protein 1/2. Adapted from (300).

2.9 MiRNAs as biomarkers for GBM diagnostics and patient outcome

In addition to its heterogeneity and aggressive and invasive growth, GBM lethality arises from the difficulty in obtaining an early diagnosis and the lack of specific biomarkers (with the exception of MGMT) that can predict the patient response to therapy and overall patient survival. With the accumulating evidence that different miRNA expression signatures not only distinguish tumors from normal tissues (236) but can also predict therapy response and patient outcome (239, 282, 291, 292), miRNA profiling studies involving samples from GBM patients tried to identify miRNAs that could be used as biomarkers for the early detection of this disease. In this regard, Roth and colleagues reported that miR-128 was upregulated and miR-342-3p was downregulated in the serum of 20 patients with GBM, when compared to those detected in age and sex-matched healthy controls (328). Increased levels

52

of miR-21 were also identified in the serum of GBM patients, when compared to those detected in the serum of healthy individuals (329, 330) while miR-15b and miR-21 were differentially overexpressed in cerebrospinal fluid (CSF) samples from patients with gliomas, compared to control healthy subjects or to subjects with various neurologic disorders (331).

MiRNA profiling studies also identified distinct miRNA signatures that correlate with clinical outcome in GBM (Table 3). Lakomy and colleagues reported that hypomethylation of the MGMT promoter and increased levels of miR-21, miR-181c, miR-195, and miR-196b were associated with poor survival in a study involving 38 GBM patients (332). In particular, the authors stated that the combination of miR-181c and miR-21 could be a very sensitive and specific test to identify patients at high risk of early progression after surgery (332). Similarly, Guan and colleagues reported that high miR-196a/b expression levels correlated with poor overall survival in a cohort of 39 GBM patients (333). Genome-wide miRNA profiling of 82 GBMs also demonstrated that miR-181d was inversely associated with overall patient survival, a clear survival advantage being observed in patients receiving standard TMZ therapy, when compared to those that have not been treated with the drug (334). The survival benefit observed in patients with increased miR-181d expression levels under treatment with TMZ was suggested to be mediated, in part, by posttranscriptional regulation of MGMT, a downstream target of miR-181d involved in the resistance to TMZ therapy (334).

Considering the promising findings arising from miRNA profiling studies, it is anticipated that miRNA profiling assays will be soon applied in clinics aiming at a better diagnostic of GBM and optimization of personalized treatment modalities towards a successful clinical outcome.

Table 3. MicroRNAs associated with patient outcome in GBM

MicroRNA	Expression in poor outcome	Variable [a]	References
miR-21, miR-181c	high	time to progression [b]	332
miR-195, miR-196b	high	time to progression [b]	332
miR-196a, b	high	time to progression [b]	333
miR-181d	low	overall survival (OS) [c]	334

[a] Clinical endpoint associated with the patient outcome.
[b] Interval of time after a disease is diagnosed (or treated) until the disease starts to get worse.
[c] Percentage of patients in a treatment group who are still alive for a certain period of time after they were diagnosed with or started treatment for a disease, such as cancer.

Although the examples presented above constitute a small subset of miRNAs implicated in cancer development, they emphasize that targeting aberrantly expressed miRNAs has potential to impact future cancer therapies (335). Strategies for manipulating the expression of miRNAs will be discussed below.

3. Therapeutic modulation of miRNAs

Two major challenges are associated with the manipulation of miRNA function. The first concerns the identification of molecules that can effectively inhibit or "mimic" mature miRNAs, in order to achieve losses or gains of miRNA function, respectively. The second challenge concerns the efficient delivery of these molecules to the specific targeted sites.

Nucleic acid-based strategies have long been used as tools to study gene function. The remarkable capacity of single-stranded or double-stranded (ds) DNA or RNA analogs to inhibit the activity of selected single-stranded genetic sequences was also explored in therapeutic approaches for several human gene-related diseases, including cancer. As mature miRNAs are short oligonucleotides, their inhibition can be achieved by base-pairing with complementary oligonucleotide sequences.

3.1 Inhibition of miRNA function

3.1.1 Antisense oligonucleotides (ASOs)

Multiple steps in the miRNA biogenesis pathway can be targeted with ASOs in order to repress miRNA production or function (336). Targeting the loop structure of the pre-miRNA was reported by Lee and colleagues (337), although this approach was not very effective, possibly due to the difficulty in accessing the loop region. Inhibition of Drosha and Dicer processing of pri-miRNAs and pre-miRNAs, respectively, was also achieved with morpholino ASOs in zebrafish (338). Although effective, this approach may have limited application in mammalian systems due to the slow turnover of the mature mammalian miRNAs[34] (339, 340), which restrains the timing of inhibition of miRNA activity.

Currently, ASOs complementary to the mature miRNA (also known as anti-miRNA oligonucleotides, AMOs), and designed to block its function in the miRNP silencing complex,

---

[34] The majority of mammalian mature miRNAs have a slow turnover. Their average half-life is approximately 5 days. However, miRNA turnover may vary under specific physiological conditions or different stimuli.

constitute the most effective technology for controlling miRNA expression experimentally and/or therapeutically (341).

The first studies involving AMOs used unmodified DNA oligonucleotides to inhibit 11 miRNAs in *Drosophila* embryos (342). Although a variety of developmental defects were observed in the embryos upon injection of the AMOs, as a result of the decreased expression of the targeted miRNAs, the authors suggested that unmodified oligonucleotides were not sufficiently effective in inhibiting miRNA activity due to their reduced affinity for the target miRNA (342, 343). Therefore, chemically-modified AMOs were developed to improve the efficacy of miRNA-targeting approaches. Among the tested modifications, the addition of chemical groups to the 2'-hydroxyl group[35] was particularly effective in increasing the binding affinity for RNA and protecting the AMOs from nuclease degradation (Table 4).

Studies with AMOs containing methylated hydroxyl groups[36] (2'-OMe) revealed increased resistance to nuclease cleavage and improved binding affinity to RNA compared to unmodified sequences (167, 343). When conjugated with a phosphorothioate backbone[37], intravenously-administered 2'-OMe-AMOs were also effective in inhibiting miRNA function in different animal tissues (344). The addition of methoxyethyl (2'-MOE) or fluorine (2'-F) groups further enhanced the activity of AMOs against the target miRNA, when compared to the simpler 2'-O-methyl modification (345). The strongest affinity for the target miRNA was nevertheless obtained with locked nucleic acid (LNA)-modified AMOs, which contain a methylene linker bridging the 2'-O-oxygen to the 4'-position which confers increased thermodynamic stability (346, 347).

Although 2' modifications were shown to improve affinity to target RNA, their anti-miRNA activity was not fully correlated with affinity (348), suggesting that other variables may also be important for effective miRNA inhibition.

---

[35] Chemical modification of the hydroxyl group at the C-2 carbon of the ribose.
[36] Delivery of the AMOs into cultured cells was performed by lipofection.
[37] In the absence of formulation, the phosphorothioate backbone modification is essential for *in vivo* delivery of AMOs to tissues, as the phosphorothioate promotes protein binding and delays plasma clearance.

Table 4. Summary of studies involving modified anti-miRNA oligonucleotides (AMOs)

Chemical modification	Setting	Reference(s)
2'-O-methyl	cultured cells	167, 343
2'-O-methyl with mixed phosphorothioate backbone	mouse	344
2'-O-methoxyethyl with phosphorothioate backbone	mouse	345
2'-O-methyl, 2'-O-methoxyethyl, 2'-O-fluoro, locked nucleic acid	cultured cells	346
locked nucleic acid	cultured cells	347
morpholino	zebrafish embryos	338

Delivery of AMOs into cultured cells was achieved by lipofection with commercially available cationic lipid formulations, whereas delivery into mouse embryos was achieved by direct injection into the embryos. Data presented in the table were obtained from (336).

3.1.2 Peptide nucleic acids (PNAs)

PNAs[38] are synthetic polymers similar to RNA and DNA that have been described as excellent candidates for antisense therapies (349). As opposed to the ribose and deoxyribose sugar backbone, PNAs contain a polyamide backbone composed of repeating N-(2-aminoethyl)-glycine units linked by peptide bonds (349). Since the backbone of PNA is electrostatically neutral (contains no charged phosphate groups), the binding between PNA/DNA and PNA/RNA strands is stronger than that between strands of DNA and/or RNA, due to the lack of electrostatic repulsion (350). PNAs are not easily recognized by either nucleases or proteases, making them resistant to enzyme degradation, and can be easily modified to increase miRNA targeting (351). Nevertheless, unmodified PNAs cannot readily cross cell membranes to enter the cytosol and, therefore, PNAs are usually coupled to targeting molecules, such as CPPs, to improve cytosolic delivery (352). Efficient PNA-mediated miRNA inhibition was already reported in *in vitro* (351) and *in vivo* studies[39] (353).

In addition to the normal AMOs, which contain only one binding site for the target miRNA, a different class of miRNA inhibitors containing multiple binding sites per molecule – designated miRNA sponges - have also been developed.

---

[38] PNAs can be also designated polyamide nucleic acids.
[39] PNAs were encapsulated in polymer nanoparticles.

3.1.3 MiRNA sponges

The concept of miRNA sponge was introduced by Ebert and coworkers (354). The authors reasoned that an mRNA-like transcript containing multiple complementary binding sites for an endogenous miRNA could bind the miRNA and block its activity. To achieve high levels of expression, they constructed plasmids encoding tandemly arrayed miRNA binding sites (MBS), driven by the CMV promoter (Fig. 16). Aiming to prevent cleavage of the transcript containing the MBS, the authors introduced central mismatches in the miRNA/trancript duplex at positions 9-12. Upon transient transfection into mammalian cells and transcription by the RNA polymerase II, the transcripts (miRNA sponges) were at least as effective as LNA-modified AMOs in inhibiting not only one miRNA but also multiple members of a miRNA family[40] (354). Based on the work of Ebert, Kluiver and colleagues developed a fast and flexible method to generate stably-expressed miRNA sponges containing 10 or more miRNA binding sites (355). Moreover, the authors reported that constructions containing multiple binding sites for two different miRNAs were efficient in inhibiting simultaneously both target miRNAs.

Interestingly, recent reports also suggested the existence of miRNA sponges in biological systems. Franco-Zorrilla and colleagues demonstrated that in *Arabidopsis*, the ncRNA IPS1 RNA serves as a sponge for miR-399 (356). In mammals, *PTENP1*, a pseudogene of PTEN[41] with a mutated start codon (therefore unable to produce protein), was shown to contain binding sites for five of the miRNAs with conserved binding sites in PTEN's 3'UTR: miR-26, -17-5p/20, -21, -19, and -214 (357, 358). The authors suggested that *PTENP1* regulates PTEN expression by acting as a decoy for miRNAs that bind to common sites in the 3'UTRs.

Fig. 16 MiRNA sponge construction. A miRNA sponge construction, developed by Ebert and coworkers, is represented in the figure. It contains multiple miRNA binding sites in the 3'UTR region and a destabilized GFP reporter gene (d2eGFP) driven by the cytomegalovirus (CMV) promoter, for transcription by the RNA polymerase II (Pol II). BGH poly(A): bovine growth hormone polyadenylation signal[42]. Adapted from (354).

---

[40] Members of the same miRNA family share the same seed sequence.
[41] Derived from retrotransposition.
[42] The bovine growth hormone polyadenylation signal is a specialized termination sequence for protein expression in eukaryotic cells.

3.1.4 Targeting miRNAs overexpressed in cancer

Since miRNA overexpression has been associated with several steps of the tumorigenic process, modulating their levels could provide therapeutic benefit. Indeed, encouraging results from *in vitro* and *in vivo* studies using AMO-based strategies have been already achieved.

Due to its considerable overexpression in a wide range of human tumors, miR-21 has been targeted in several anti-cancer AMO-based strategies. Knockdown of miR-21 in cultured hepatocellular cancer cells resulted in increased apoptosis and suppressed cell growth (260), while AMO-mediated miR-21 inhibition in androgen-independent prostate cancer cell lines (DU145 and PC-3) increased cell sensitivity to apoptosis and inhibited cell motility and invasion, without affecting tumor cell proliferation (359). Similarly, transfection of breast cancer cells with anti-miR-21 oligonucleotides suppressed both cell proliferation *in vitro* and tumor growth in a xenograft mouse model (360). Seike and colleagues reported that EGFR mutations are generally associated with increased miR-21 expression in nonsmoking lung cancer patients, and AMO-mediated miR-21 knockdown sensitized cancer cells to the EGFR-tyrosine kinase inhibitor AG1478 (313). In a separate study, the transgenic manipulation of miR-21 and the targeted delivery of anti-miR-21 oligonucleotides were shown to slow down tumor progression in a Ras-driven murine model of lung cancer (361).

In pancreatic cancer, two different studies in cultured cells demonstrated that oligonucleotide-mediated miR-221 silencing results in increased apoptotic activity, decreased tumor cell proliferation (362) and increased cytotoxicity of the anti-cancer agent benzyl isothiocyanate (363). Furthermore, 2'-O-Me phosphorothioate-modified anti-miR-221 oligonucleotides were shown to decrease proliferation of cultured hepatocellular cancer cells (364). When tested in a mouse model of disease, the administration of a cholesterol-modified isoform of anti-miR-221[43] not only improved pharmacokinetics and liver tissue distribution, compared to unmodified oligonucleotide, but also reduced miR-221 levels in the liver (within a week of intravenous administration), produced significant antitumor activity and increased animal survival (364). Similarly, the therapeutic silencing of miR-10b with cholesterol-modified AMOs (antagomirs) suppressed metastasis in a mouse mammary tumor model (365).

MiRNA sponges were also shown to be effective in inhibiting miRNA activity. Kluiver and colleagues demonstrated that the combined inhibition of miRNAs of the miR-17-92 cluster, using sponges containing binding sites for several elements of this family, was

---

[43] Conjugation of cholesterol to the 3′ end of a 2′-OMe-modified AMO decreases kidney clearance and improves the delivery to the liver.

significantly more effective in inhibiting the proliferation of cultured B-cell lymphoma cells, than individual miRNAs (355).

As mentioned previously, the miRNA milieu is mostly composed of miRNAs with tumor suppressor roles, and downregulation of specific miRNAs is generally observed in human cancer, being associated with increased tumorigenic potential. In addition to loss of miRNA function, gain of miRNA function might be therapeutically beneficial (Fig. 17). Strategies to restore miRNA expression will be addressed below.
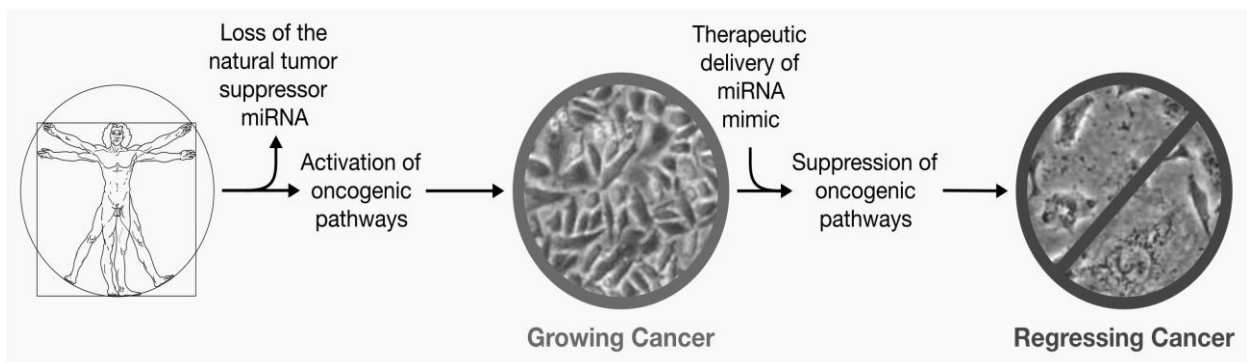
Figure 17. MiRNA replacement therapy. The loss of a miRNA with tumor suppressor role leads to hyperactivation of oncogenic pathways and tumorigenesis. Re-expressing a tumor suppressor miRNA may therefore suppress oncogenic pathways and cancer cell growth. Adapted from (366).

3.2 Overexpression of miRNAs

Two different strategies have been widely used to restore miRNA expression in cells: miRNA mimics and plasmid or virally-encoded miRNA constructs.

3.2.1 MiRNA mimics

MiRNA mimics are double-stranded RNA molecules similar to the endogenous Dicer product (miRNA:miRNA* duplex)[44], composed of a guided strand identical to the mature miRNA and a passenger strand that is partially or fully complementary to the guide strand (367). Due to their unfavorable physicochemical characteristics for *in vivo* administration,

---

[44] MiRNA mimics are also analogous in structure to siRNAs.

miRNA mimics can be chemically modified to increase protection from nuclease degradation, decrease innate immune system activation, reduce the incidence of off-target effects[45] and improve pharmacodynamics (368). The addition of methyl (2′-O-Me), methoxyethyl (2′-MOE) or fluorine (2'-F) groups (or their combination) to the ribose ring[46] enhances the stability of miRNA mimics (369, 370). Aromatic compounds, such as 3′-benzene-pyridine, can increase protection from nuclease degradation and enhance activity when added to the 3' end of miRNA mimics (371). The guided strand can also be modified to enhance the miRNA activity in the miRNP complex. The addition of 2′-OMe modifications at the 3′ end and the presence of a 2-nucleotide (nt) 3′ overhang assists with miRNP loading and degradation of the passenger strand (367, 372). It was also shown that the attachment of cholesterol to the 3'-end of the passenger enhances oligonucleotide permeability and targeting to the liver (367, 368).

Recently, a new class of miRNA mimics has also been described. As opposed to the traditional double-stranded miRNA mimics, Chorn and colleagues demonstrated that modified single-stranded miRNA mimics[47] also exhibit significant argonaute-mediated miRNA seed-based activity in cultured cells (373). However, the potency of single-stranded mimics was inferior to that achieved with double-stranded oligonucleotides, which suggested that additional modifications should be explored, aiming at improving the efficacy of these molecules (Chorn, 2012).

3.2.2 Plasmid or virally-encoded miRNA constructs

An alternative strategy for therapeutic miRNA replacement involves the expression of a shRNA or pri-miRNA mimic from a plasmid or viral construct (Fig. 18). When compared to the delivery of double-stranded miRNA mimics, this approach provides a more stable expression of the mature miRNA and allows the expression of multiple miRNAs from one transcript (374).

ShRNAs are structurally similar to pre-miRNAs, with a base paired stem, a small loop and a 3'-end UU overhang (375). Expression of shRNAs is usually driven by RNA polymerase III promoters, including the H1 and U6, as they are involved in the production of small cellular transcripts and use precise initiation and termination sites (375, 376). However, both promote high levels of shRNA expression, which can elicit toxicity (377). Indeed,

---

[45] Off-target effects result from the interaction between the miRNA mimic and unintended targets.
[46] Modifications are added to the hydroxyl group of the carbon 2 (C2).
[47] Strands are phosphorylated at the 5'-end and contain 2'-fluororibose modifications.

overexpression of shRNAs was already shown to saturate both exportin-5 and Ago2, which triggers a global dysfunction of the endogenous miRNA pathway (375, 378, 379).

As opposed to shRNAs, pri-miRNA mimics[48] are usually transcribed from low expression RNA polymerase II promoters, which can drive tissue-specific expression (377), and further processed by Drosha[49], thus reducing the risk of saturation of the endogenous miRNA pathway. In this regard, reduced *in vivo* toxicity was reported following miRNA re-expression via pri-miRNA mimics, when compared to that observed following miRNA re-expression via shRNAs (380, 381). Pri-miRNA mimics were nevertheless suggested to be less efficient in promoting the silencing of target mRNAs, when compared to matched shRNAs (380, 381).

A common hurdle to both shRNAs and pri-miRNA mimics is the existence of off-target effects associated with their application. As stated by Sybley and collaborators, complementary base pairing with as little as 8-nt homology is sufficient to cause translational repression of nontarget genes when multiple target matches are present within their 3′UTRs (377, 382). Furthermore, random strand selection by the miRNP silencing complex can result in combined activity of both guide and passenger strands, which leads to dysregulation of several mRNA transcripts (383). Therefore, careful design of shRNA or pri-miRNA mimics constructs should be considered in order to reduce the off-target effects associated with these technologies.

Figure 18. Pri-miRNA mimic and short-hairpin RNA structures. Pri-miRNA mimics are structurally identical to the endogenous pri-miRNAs. ShRNA structure is more simple and resembles pre-miRNAs. Adapted from (375).

3.2.3 Re-expressing miRNAs downregulated in cancer

MiR-34a plays a tumor suppressor role in a wide range of human cancers, its downregulation being associated with aberrant cell proliferation and malignant transformation

---

[48] Pri-miRNA mimics include typical pri-miRNA features, such as imperfect hairpin structures, bulged nucleotides, flanking sequences and larger loops.
[49] Drosha processing also restricts the progression of pri-miRNA transcripts in the endogenous miRNA pathway.

(154, 252). In several *in vitro* and *in vivo* studies, restoring miR-34a expression has shown to promote antitumor activity. Enforced expression of miR-34a in human cultured p53-mutant prostate cancer (PCa) cells induced cell-cycle arrest, apoptosis or senescence (384). The re-expression of miR-34a in CD44+[50] PCa cells also blocked tumor progression and metastasis following orthotopic tumor cell implantation in immunocompromised mice (384). Similarly, re-expression of miR-34a in human colon cancer cells (HCT116 and RKO) caused a significant inhibition of cell proliferation and induced senescence-like phenotypes in these cell lines (385). Importantly, intratumoral administration of complexes prepared by association of miR-34a and atelocollagen[51] suppressed tumor growth in subcutaneous mice xenograft tumors[52] (385). In a different study, reduced tumor cell proliferation, migration and invasion were observed in cultured breast cancer cells following exogenous expression of miR-34a (386).

Reduced expression and loss of function have also been reported for several members of the let-7 family in various human malignancies. The transient overexpression of let-7a and let-7f, two dominant isoforms of this family of miRNAs, in the A549 lung adenocarcinoma cell line, suppressed tumor cell proliferation (291). Similarly, overexpression of let-7 in A549 lung cancer and HepG2 liver cancer cell lines repressed cell cycle progression and cell division (226). Let-7 overexpression was also reported to induce apoptosis and cell cycle arrest in colon cancer and Burkitt's lymphoma (BL) cell lines (243, 248).

Decreased expression of members of the miR-29 family (miR-29a, b, c) were observed in various malignancies that contain aberrant DNA hypermethylation patterns, including lung cancer (250, 335). In this regard, the enforced expression of miR-29 in lung cancer cell lines led to reduced global DNA methylation, induced re-expression of methylation-silenced tumor suppressor genes, such as FHIT and WWOX, and inhibited tumor cell proliferation *in vitro* and tumor growth *in vivo* (250).

In CLL, the loss of miR-15a and miR-16-1 was associated with decreased apoptotic activity due to the overexpression of the anti-apoptotic protein Bcl-2, while mir-15a/miR-16-1 reconstitution increased apoptosis through repression of Bcl-2 mRNA translation (240). Furthermore, overexpression of miR-7, a miRNA involved in the repression of the pro-oncogenic Akt pathway, reduced the proliferation and invasiveness of different GBM cell lines and in one GBM stem cell line (325), while expression of miR-128 inhibited the proliferation of glioma cells by decreasing the levels of E2F3a (323).

---

[50] The adhesion molecule CD44 is a marker for prostate cancer stem cells.
[51] Atelocollagen is a highly purified, pepsin-treated type I collagen with physical properties identical to those of natural, unsolubilized collagen.
[52] Tumors were developed by subcutaneous injection of HCT116 or RKO cells.

Re-expression of miR-128 levels via lentivirally-mediated plasmid delivery resulted in reduced proliferation of the stably transfected cell lines, when compared to that observed for cells transfected with an empty plasmid (322). Moreover, following their implantation into the flanks of nude mice, miR-128-expressing cells formed tumors that were significantly smaller than those generated upon implantation of control cells[53].

The diagram in Figure 19 represents the different strategies developed for the modulation of miRNA expression.
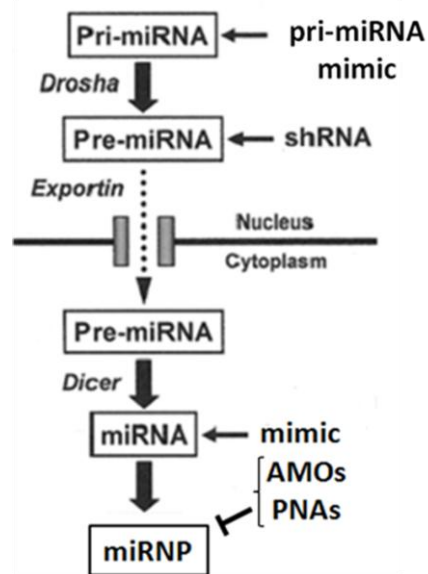
Figure 19. MiRNA pathway and the different types of constructs that can be used to modulate miRNA expression. Following nuclear transcription, primary miRNAs (pri-miRNA) are processed by Drosha into precursor miRNAs (pre-miRNA), which are then exported to the cytoplasm by exportin-5. Upon cleavage by Dicer, miRNA duplexes (miRNA) are incorporated in the ribonucleoprotein complexes (miRNP), where they are paired with their target miRNAs. At the right are indicated the strategies to silence or re-express mature miRNAs: virally-mediated nuclear expression of pri-miRNA mimics or shRNAs, or alternatively, cytoplasmic delivery of double-stranded miRNA mimics, anti-miRNA oligonucleotides (AMOs) and peptide nucleic acids (PNAs). Not represented in the figure are plasmid-mediated cytoplasmic expression of pri-miRNA mimics or shRNAs and miRNA sponges. Adapted from (378).

The majority of the above-described studies used commercially-available cationic lipid formulations (e.g. Lipofectamine 2000) to achieve nucleic acid internalization into cultured

---

[53] Cells transduced with an empty plasmid.

cells[54]. In preclinical studies, LNA-modified anti-miR-122 oligonucleotides were shown to promote efficient miR-122 repression in the liver, when administered intravenously in rodents and primates (387, 388). MiR-122 is a miRNA involved in the cholesterol biosynthesis in the liver, which was also shown to play a role in the cellular infection of the hepatitis C (HC) virus. By interacting with the 5'UTR region of the viral genome[55], miR-122 protects the 5'UTR from nucleolytic degradation, thereby promoting viral RNA stability and propagation (389, 390). A phase IIa clinical trial[56] involving this molecule for the treatment of HC has been finalized, a dose-dependent, prolonged antiviral activity being observed in treated HC patients[57]. If approved for commercialization, miravirsen will be the first miRNA-based drug on the market.

Although modified AMOs and miRNA mimics have been successfully tested for miRNA modulation in liver diseases, including hepatocellular cancer (364, 391), their widespread application to other non-hepatic diseases is restricted by the lack of tissue specificity. Moreover, with very few exceptions (392), oligonucleotides do not cross the BBB (393, 394), which limit their use to the treatment of brain tumors. Therefore, the successful *in vivo* nucleic acid delivery requires the development of carriers that can increase bioavailability, protect the nucleic acids from nuclease degradation and enhance their uptake by the target cells, while sparing the normal tissues. Delivering nucleic acids to GBM presents an additional challenge, related to the presence of the BBB, which restrains the movement of therapeutic molecules to the brain. In the next section, the different strategies for *in vivo* nucleic acid delivery will be addressed.

3.3 Delivery of nucleic acids to modulate miRNA function

The discovery of RNAi-mediated mechanisms of gene silencing and the development of suitable carriers for *in vitro* and *in vivo* delivery of siRNAs and shRNAs (378, 395), paved the way for establishing technical approaches that can be applied in miRNA-based therapies. Viral vectors, liposomes and nanoparticles have been successfully tested for siRNA/shRNA delivery in preclinical studies (396, 397), and, more recently, employed for delivery of AMOs or miRNA-expressing constructs in both cellular and animal models.

---

[54] This is currently considered the standard method/procedure for intracellular nucleic acid delivery into cultured cells.
[55] MiR-122 binds to two seed sites located in the 5' UTR of the virus genome.
[56] This 15-mer LNA-modified anti-miR-122 oligonucleotide is being tested by Santaris Pharma, under the designation of miravirsen. Phase IIa clinical trials involve patients (as opposed to phase I trials) and are designed to test the dose requirements for the therapy. Subsequent phase IIb trials are designed to evaluate the efficacy of the therapy.
[57] http://clinicaltrials.gov/show/NCT01200420.

3.3.1 Viral vectors

Modified adenoviruses and adeno-associated viruses (AAV) have been used for siRNA/shRNA delivery to the liver (398) and brain (395) with promising results. Due to their high transduction efficiency, viral vectors have been mostly used for delivering miRNA-expressing constructs to cancer cells, in miRNA-based therapeutics. The systemic administration of an AAV[58] encoding miR-26a, which is highly downregulated in hepatocellular cancer and induces cell cycle arrest by targeting the cyclins D2 and E2, resulted in inhibition of cancer cell proliferation, induction of tumor-specific apoptosis and significant tumor regression, without toxicity (399). Similarly, the intranasal administration of adenovirally-coded let-7 significantly reduced tumor burden in an orthotopic mouse model of NSCLC (400). Lentiviral vectors were also successfully used for the reestablishment of miRNA expression in tumors. In a xenograft prostate cancer mice model, the intratumoral injection of lentivirally-coded miR-15-16 led to growth arrest within 1 week of treatment and considerable volume regression thereafter, whereas no significant alterations in tumor growth were observed in animals treated with an empty viral vector (401).

Viral vectors have also been applied in miRNA-based therapeutic strategies towards GBM. Lee and colleagues took advantage of the abundant expression of the enzyme telomerase reverse transcriptase (hTERT[59]) in cancer cells and developed a multimodal GBM-targeting approach, combining hTERT-targeting ribozyme-controlled HSV-tk expression with overexpression of miR-145, a miRNA that is usually downregulated in GBM (402). For this purpose, the authors constructed adenoviral vectors that express hTERT.Rz.HSVtk and miR-145 under control of the CMV promoter, to ensure high expression of the transgene in the target cells. In a xenograft mice model, the intratumoral administration of the adenovirus harboring the HSV-tk expression cassette plus miR-145, combined with intraperitoneal injection of ganciclovir, resulted in increased animal survival, when compared to that observed with the administration of virus coding for HSV-tk or miR-145 *per se* (402). Adenoviruses encoding shRNAs targeting mature miRNAs have also been developed for GBM therapy. Wang and colleagues constructed an adenoviral vector expressing shRNAs that co-repress the expression of miR-221 and miR-222 (403). Upon transduction of cultured GBM cells, decreased levels of these miRNAs were detected, which were associated with

---

[58] Serotype 8 (AAV8).
[59] HTERT is a catalytic subunit of the enzyme telomerase. Telomerase, in addition with a RNA component that serves as a template for the telomere repeat, lengthens telomeres in DNA strands, thereby allowing senescent cells.

increased expression of their target p27kip1, cell cycle arrest in G1 phase and increased apoptosis (403).

MiRNAs have also been recently explored to control tissue tropism of oncolytic viruses. By inserting microRNA-target sequences into their genomes, viral replication and spread is inhibited in tissues expressing cognate microRNAs (404, 405). This strategy has also been applied in therapeutic approaches for GBM. Skalsky and colleagues designed a lentiviral vector expressing the HSV-tk gene under the regulation of miR-128. GBM cells transduced with this vector were selectively killed when cultured in the presence of ganciclovir, whereas reduced cell death was detected in differentiated neuronal SH-SY5Y cells transduced with the miR-128-regulated HSV-tk vector (406). Similarly, intratumorally-administered miRNA-sensitive oncolytic measles virus containing target sites for miR-7 in the 3′-UTR region of the viral genome[60] promoted tumor cell death in GBM xenografts, while sparing normal brain tissues (404).

3.3.2 Liposomes and lipid-based nanocarriers

Synthetic non-viral gene delivery vehicles, including liposomes and lipid-based nanovectors, have been predominantly tested for the delivery of miRNA-based nucleic acids into tumor cells (Table 5).

Cationic liposome-mediated delivery of a plasmid encoding miR-34a (T-VISA-miR-34a) to cultured breast cancer cells led to the downregulation of several miR-34a target genes and significantly suppressed breast cancer cell growth, migration and invasion (386). Furthermore, intravenous injection of T-VISA-miR-34a:liposomal complex nanoparticles significantly inhibited tumor growth, prolonged survival, and did not induce systemic toxicity in an orthotopic mouse model of breast cancer (386). Similarly, Pramanik and colleagues demonstrated that systemic intravenous delivery of liposome-formulated[61] plasmid-encoded miR-34a or miR-143-145 inhibited tumor growth in subcutaneous and orthotopic pancreas MiaPaca-2 xenografts (407). Chen and colleagues developed a LPH (liposome[62]-polycation-hyaluronic acid) nanoparticle formulation which was modified with the tumor-targeting GC4 single-chain antibody fragment (scFv) for systemic delivery of siRNAs and miRNAs into B16F10 melanoma lung metastasis in a syngeneic murine tumor model (408). Following intravenous administration of siRNA-formulated tumor-targeted LPH nanoparticles, a

---

[60] MiR-7 is highly downregulated in GBM.
[61] Lipid components of this formulation include the cationic amphiphile DOTAP and co-lipids cholesterol and DSPE-PEG-OMe (N-(Carbamoylmethoxypolyethylene glycol 2000)-distearoyl phosphatidylethanloamine).
[62] Lipid components of this formulation include DOTAP and cholesterol.

66

significant decrease in the protein levels of the targets c-Myc, MDM2 and VEGF and in tumor growth, were observed. On the other hand, targeted nanoparticle-mediated miR-34a delivery demonstrated a significant decrease in the expression of the protein survivin in the metastatic tumor and reduced tumor load in the lung. Importantly, when siRNAs and miR-34a were co-formulated in GC4-targeted nanoparticles, an increased antitumor effect was observed, as compared to that observed upon monotherapy administration (408).

A different lipid-based formulation was also employed for the delivery of miR-34a and let-7 to a Kras-driven NSCLC mouse model. Trang and colleagues used a neutral lipid emulsion (NLE)[63] that, when combined with synthetic miRNA mimics, forms nanoparticles in the nanometer diameter range and with a surface net charge close to zero (409). In this regard, following intravenous administration of the lipid-based nanoparticles, a significant reduction in tumor growth was observed for animals treated with nanoparticles containg miR-34a or let-7, when compared to that observed for animals treated with nanoparticles containing a control miRNA mimic (409).

3.3.3 Polymer-based nanoparticles

Polymer-based nanocarriers have also been used for delivery of miRNA-based nucleic acids, namely AMOs and miRNA mimics, to tumor cells (Table 5).

Polyurethanes are conventionally used in tissue engineering and gene delivery due to their biocompatibility and physicochemical properties (410, 411). When combined with PEI, cationic polyurethane (PU)-shortbranch PEI (PU-PEI) was shown to exhibit high transfection efficiency and low cytotoxicity *in vitro* and *in vivo* (411, 412). Using PU-PEI as a delivery vehicle, Yang and colleagues reported efficient delivery of miR-145[64] to CD133+ GBM cells[65], which resulted in a significant decrease in their tumorigenic potential and facilitated differentiation into CD133-negative cells (411). Moreover, PU-PEI-mediated miR-145 expression in CD133+ cells suppressed the expression of anti-apoptotic and drug-resistance genes, while increasing the cell sensitivity to radiation and TMZ. When administered intratumorally in an orthotopic GBM-CD133+ xenograft mouse model, nanoparticle-formulated miR145 significantly reduced tumorigenesis and improved animal survival when

---

[63] NLE consists of 1,2-dioleoyl-sn-glycero-3-phosphocholine (DSPC), squalene oil, polysorbate 20 and an antioxidant.
[64] MiR-145 is usually highly downregulated in GBM. In this study, the authors used a plasmid to express miR-145.
[65] CD133 is a marker for GBM stem-like cells.

combined with radiotherapy and TMZ, compared to that observed in animals treated with PU-PEI *per se* (411).

Poly(lactic-co-glycolic acid) (PLGA)-based nanoparticles have also been extensively used to enhance the delivery of therapeutic agents to target cells, due to their biocompatibility and biodegradability (413). In this regard, Babar and colleagues developed a delivery system by combining PLGA with PNAs targeting the oncogenic miR-155, and attached the CPP penetratin to the surface of the PLGA nanoparticles, in order to enhance cellular uptake (353). Following incubation of cultured lymphoma cells with the generated nanoparticles (ANTP-NP), a significant increase in particle internalization and a considerable reduction of the functional miR-155 levels were achieved, when compared to that observed for cells incubated with nanoparticles lacking penetratin or nanoparticles loaded with a scrambled control (353). Increased levels of SHIP1 (phosphatidylinositol-3,4,5-trisphosphate 5-phosphatase 1), a target of miR-155, were also obtained in cells incubated with ANTP-NP, when compared to that observed in cells exposed to nanoparticles loaded with a scrambled control. Moreover, upon intratumoral or systemic administration of ANTP-NP, a moderate (although significant) delay in tumor growth was detected in a subcutaneous xenograft mouse model of lymphoma (353).

Polyamidoamine (PAMAM) dendrimers[66] have also been tested for the delivery of antisense oligonucleotides to GBM cells. Due to the presence of positively charged amino groups on their surface, PAMAM dendrimers can easily interact with nucleic acids to form complexes through charge-based interactions and protect them from nuclease degradation, while exhibiting minimal toxicity (414, 415). Moreover, the open nature of the dendritic architecture enables the entrapment of drugs within their core through electrostatic, hydrophobic and hydrogen bond interactions (416). Ren and colleagues used PAMAM dendrimers as a carrier to co-deliver anti-miR-21 oligonucleotides and the drug 5-FU to human GBM cells and reported a significant increase of apoptosis and enhanced cytotoxicity of 5-FU, associated with a decrease in the invasive capacity of U251 GBM cells (415).

---

[66] Dendrimers are repetitively branched molecules.

Table 5. Summary of the studies involving lipid- and polymer-based carriers for delivery of anti-miRNA oligonucleotides or miRNA mimics to cancer cells

Carrier	Target miRNA	Outcome [a]	Reference
cationic amphiphile DOTAP and colipid cholesterol (CHOL)	miR-34a	intravenous injection of liposome-based nanoparticles containing miR-34a significantly inhibited tumor growth and prolonged animal survival in an orthotopic mouse model of breast cancer	386
cationic amphiphile DOTAP and colipids CHOL and DSPE-PEG-OMe	miR-34a, miR-143-145	intravenous administration of liposome-formulated plasmid-encoded miR-34a or miR-143-145 inhibited tumor growth in subcutaneous and orthotopic pancreas xenografts	407
Neutral lipid emulsion [b]	miR-34a, let-7	intravenous administration of the lipid-based nanoparticles containing miR-34a or let-7 resulted in a significant reduction in lung tumor growth	409
cationic polyurethane-shortbranch polyethyleneimine	miR-145	reduced GBM tumorigenesis and improved animal survival, when combined with radiotherapy and temozolomide	411
poly(lactic-co-glycolic acid)	miR-155	moderate delay in tumor growth following intratumoral or systemic nanoparticle administration in a subcutaneous xenograft mouse model of lymphoma	353
Polyamidoamine	miR-21	significant increase of apoptosis and enhanced cytotoxicity of 5-fluorouracil, associated with a decrease in the invasive capacity of U251 human GBM cells	415

[a] Cellular effect of the miRNA modulation.
[b] NLE consists of 1,2-dioleoyl-sn-glycero-3-phosphocholine (DSPC), squalene oil, polysorbate 20 and an antioxidant.
DOTAP: 1,2-dioleoyl-3-dimethylammonium-propane; DSPE-PEG-OMe: N-(Carbamoylmethoxypolyethylene glycol 2000)-distearoyl phosphatidylethanloamine.

4. Concluding remarks

MiRNAs are a class of subtle gene regulators that, by targeting oncogenes and tumor suppressors, have the ability to modulate key cellular processes that define the cell phenotype. Abnormal expression of these small molecules was shown to play a causal role in different steps of tumorigenesis, from initiation and development to metastatic progression. MiRNA-based therapeutic strategies have been successfully tested in *in vitro* and pre-clinical studies for several human malignancies, which emphasize the potential of miRNAs as therapeutic targets for cancer treatment. Considering the extreme lethality of GBM and the lack of efficient treatment modalities towards this disease, miRNAs may constitute important molecular targets for the development of alternative or complementary therapeutic strategies for GBM.

Chapter 2

Objectives

Objectives

The main goal of the Work performed in the context of this thesis consisted in the development and application of a miRNA-based gene therapy approach for the treatment of glioblastoma (GBM), involving nucleic acid delivery to tumor cells via targeted lipid-based nanoparticles.

To achieve this purpose the following specific aims were proposed:

- Identification of abnormally expressed miRNAs in human patients samples and mouse models of GBM, and evaluation of their potential as therapeutic targets through modulation of the expression levels. Analysis of the ensuing cellular and molecular alterations in order to validate this potential.

- Development and physicochemical characterization of stable nucleic acid lipid particles (SNALPs) targeted to brain tumor cells by the tumor-specific peptide chlorotoxin to restore or silence the dysregulated miRNAs, and evaluation of their efficiency as a therapeutical tool, both *in vitro* and *in vivo*.

- Evaluation of the effect of the angiogenic growth factor PDGF-B on the expression of oncogenic and tumor suppressor miRNAs in order to elucidate its role in GBM tumorigenesis.

Chapter 3

MicroRNA-21 silencing enhances the cytotoxic effect of the antiangiogenic drug sunitinib in glioblastoma
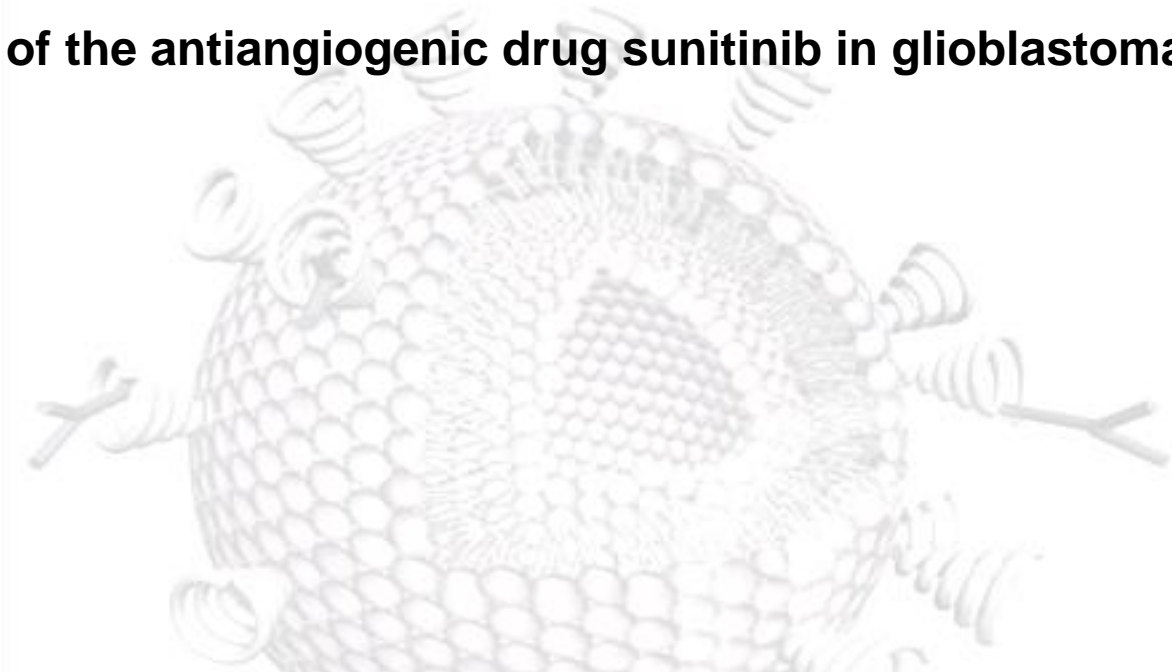
Pedro M. Costa, Ana L. Cardoso, Clévio Nóbrega, Luís F. Pereira de Almeida, Jeffrey N. Bruce, Peter Canoll, Maria C. Pedroso de Lima. "MicroRNA-21 silencing enhances the cytotoxic effect of the antiangiogenic drug sunitinib in glioblastoma".

1. Abstract

Highly malignant glioblastoma (GBM) is characterized by high genetic heterogeneity and infiltrative brain invasion patterns, and aberrant miRNA expression has been associated with hallmark malignant properties of glioblastoma. The lack of effective GBM treatment options prompted us to investigate whether miRNAs would constitute promising therapeutic targets towards the generation of a gene therapy approach with clinical significance for this disease.

Here, we show that microRNA-21 (miR-21) is upregulated and microRNA-128 (miR-128) is downregulated in mouse and human glioblastoma samples, a finding that is corroborated by analysis of a large set of human GBM data from The Cancer Genome Atlas. Moreover, we demonstrate that oligonucleotide-mediated miR-21 silencing in U87 human GBM cells resulted in increased levels of the tumor suppressors PTEN and PDCD4, caspase 3/7 activation and decreased tumor cell proliferation. Cell exposure to pifithrin, an inhibitor of p53 transcriptional activity, reduced the caspase activity associated with decreased miR-21 expression. Finally, we demonstrate for the first time that miR-21 silencing enhances the anti-tumoral effect of the tyrosine kinase inhibitor sunitinib, whereas no therapeutic benefit is observed when coupling miR-21 silencing with the first line drug temozolomide.

Overall, our results provide evidence that miR-21 is uniformly overexpressed in glioblastoma and constitutes a highly promising target for multimodal therapeutic approaches towards GBM.

2. Introduction

GBM is the most common and aggressive type of glioma, a class of tumors arising from glial cells. Despite the increasing knowledge about this malignancy at genetic and molecular levels, and the considerable advances in cancer therapy, patient outcome has slowly improved over the past decade. Standard treatment for GBM includes surgical resection of the tumor, when possible, followed by single-agent adjuvant therapy with temozolomide and radiotherapy (24). However, these procedures lack effective long-term impact on disease control and patient survival, and clinical recurrence is nearly universal (24, 25, 417). Hence, there is an urgent need to explore new treatment options that can prove to be effective for brain tumors, as well as to better understand the molecular and cellular alterations that occur in GBM.

The discovery of miRNAs, a class of small non-coding RNAs that regulate gene expression through imperfect pairing with the target mRNAs (418, 195), has revealed an additional level of fine tuning of the genome, that integrates with transcriptional and other regulatory mechanisms to expand the complexity of eukaryotic gene expression. MiRNAs regulate post-transcriptionally the expression of over 30% of protein-coding genes (170) and *in silico* data indicate that each miRNA can control hundreds of gene targets, including oncogenes and tumor suppressors, underscoring the influence of miRNAs in key cellular processes that define cell phenotype (170, 156). Accumulated evidence has shown that miRNAs are differentially expressed in normal tissues and cancers, and aberrant miRNA expression is associated with tumor development and progression (237, 238), including GBMpathogenesis (266, 419).

In the present work, we analyzed the expression of miR-128, miR-21 and miR-221 in human GBM samples and in mouse GBM models, as well as in several GBM cell lines. Our results demonstrate that miR-21 is upregulated and miR-128 is downregulated in GBM tissue samples and cell lines screened, a finding that is corroborated by analysis of a large set of human GBM data from The Cancer Genome Atlas (TCGA) Research Network. Furthermore, we identified a group of miRNAs, including the cluster miR-221/222 and oncogenic miR-106a/miR-20a, whose alterations may be correlated with different molecular subtypes of GBM described in the literature (12).

The classic genetic alterations that occur in GBM are found in pathways governing cellular proliferation and survival, including EGFR and PTEN-regulated pathways, as well as invasion and angiogenesis (4). However, the therapeutic intervention with inhibitory agents targeting EGFR and other transduction pathways has yet to demonstrate a clear survival

benefit for patients (420, 421). Due to their small size and pivotal roles in the cell, certain microRNAs may be of direct therapeutic utility, as single agents or in combinations with other regimens (422). Studies performed by Silber and colleagues revealed that overexpression of miR-124 and miR-137, which are found to be downregulated in human GBM samples, induce GBM cell cycle arrest and differentiation of brain tumor stem cells (423). Similarly, overexpression of miR-128 has been shown to reduce tumor cell proliferation, both in glioma cell lines and a glioma-bearing animal model (322).

Here, we tested a therapeutic strategy for GBM that combines gene therapy through silencing of miR-21, found to be overexpressed in this type of brain tumor, with sunitinib, an inhibitor of PDGF and VEGF receptors (424) that is being currently evaluated in clinical trials for GBM. Our results demonstrate that lipoplex-mediated miR-21 silencing in U87 human and F98 rat glioma cells significantly enhances cell sensitivity to the cytotoxic effect of sunitinib, which may represent an attractive and effective therapeutic approach towards GBM.

3. Results

3.1 MiR-21 is overexpressed and miR-128 is downregulated in human and mouse glioblastoma samples and glioblastoma cell lines

We have recently developed retrovirally-induced mouse GBM models, characterized by the overexpression of the oncogenic ligand PDGF-B and conditional deletion of tumor suppressor genes ($PTEN^{-/-}$ and $PTEN^{-/-}p53^{-/-}$), which display molecular and histopathological features that closely resemble human GBM (425). Real-time PCR (qPCR) quantification of miR-128, miR-21 and miR-221 expression in RNA extracts from six brain tumors (of each genotype) and three control samples, obtained from double-floxed mouse brains following animal injection with a control vector (no PDGF), revealed that miR-21 was highly overexpressed in all tumor samples when compared to control mouse brain, whereas miR-221 was moderately overexpressed in all samples from PTEN-floxed (3.15 ± 2.59) and double-floxed (4.99 ± 3.27) tumor samples (both values representing the relative miRNA expression value to control) (Fig. 1A). MiR-128 was slightly downregulated in 83% of the double-floxed mouse tumors (0.70 ± 0.97), whereas slightly increased levels of miR-128 were observed in 67% of PTEN-floxed mouse tumors (1.63 ± 1.09, p>0.05), when compared to those observed in samples from control mouse brain (Fig. 1A).

MiRNA expression levels, evaluated in mouse GBM cell lines derived from the retrovirally-induced double-floxed and PTEN-floxed mouse models (Fig. 1B), were consistent with the values observed in the tumor models, despite a significant decrease in miR-128 levels being observed in both double-floxed and PTEN-floxed mouse cells (0.033 ± 0.022 and 0.078 ± 0.0589, respectively). Increased expression of miR-21 and decreased miR-128 expression were also observed in the F98 rat glioma cell line, when compared to that observed in primary rat astrocytes or P19 embryonic carcinoma cells (Supplementary Results, Fig. 1A, B), previously demonstrated to express low levels of miR-21 (426).

In order to evaluate whether the results observed for the mouse GBM models would replicate in the human disease, we measured the expression of miR-128, miR-21 and miR-221 in RNA extracts from 22 human GBM samples and from the widely used U87 human GBM cell line. Two different brain tissues (epileptic and tumor-adjacent brain tissue) and total RNA extracted from human brain (see Materials and Methods section) were used as references. Similarly to the results obtained in the mouse models and in accordance with published data (266, 322, 426), miR-21 overexpression and miR-128 downregulation were observed in U87 cells (Fig. 1C). More importantly, miR-21 was significantly overexpressed in 80% of the human tumors when compared to control epileptic tissue (7.05 ± 6.07; $p<0.01$), whereas miR-128 was downregulated in all tumor samples (0.07 ± 0.08) (Fig. 1D). However, as opposed to our results in the mouse models and U87 cells, as well as to those previously reported (266, 427), miR-221 was found to be downregulated in 91% of the tumors (Fig. 1D). For comparison, the miRNA expression levels in U87 cells and human tumor samples relative to tumor-adjacent brain tissue and total RNA from human brain are presented in Supplementary Results (Fig. 1C, D).

Aiming at increasing the biological significance of our results, we analyzed the miRNA expression in a large number of human GBM samples from the Cancer Genome Atlas (TCGA), a publicly available repository that has accumulated comparative genomic hybridization, gene expression, and miRNA expression analyses for approximately 200 human GBM samples (11). The analysis of a specific subset of GBMs from this set of samples (Supplementary Data, Table S1) revealed that miR-21 was significantly overexpressed and miR-128 was downregulated in 98% of the tumors (185/188) when compared to control normal samples (Fig. 1E). Remarkably, miR-221 was found to be downregulated in 48% (90/188) of the tumors (0.57 ± 0.59), thus corroborating our experimental data from the studies on the human tumor samples.
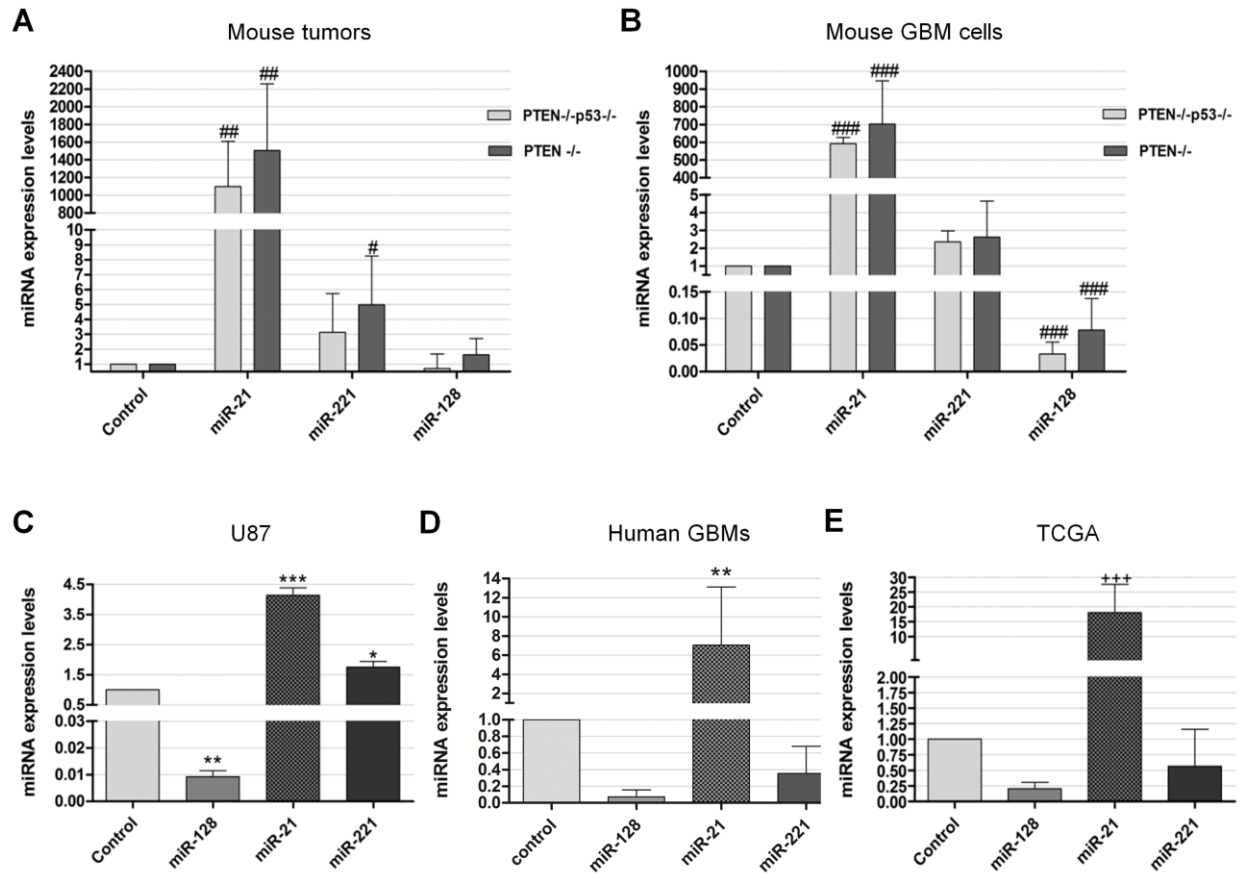
Figure 1. MiRNA expression levels in mouse and human glioblastoma tissue samples and cell lines. MiR-21, miR-128 and miR-221 expression levels in (**A**) double-floxed (PTEN$^{-/-}$p53$^{-/-}$) and PTEN-floxed (PTEN$^{-/-}$) mouse tumor samples (n=6) and (**B**) double-floxed (PTEN$^{-/-}$p53$^{-/-}$) and PTEN-floxed (PTEN$^{-/-}$) mouse GBM cells, compared to control sample (n=7), obtained from double-floxed mouse brains following animal injection with a control vector (no PDGF). MiR-21, miR-128 and miR-221 expression levels in human (**C**) U87 cells and (**D**) tumor samples from the Tissue Bank (n=22), compared to control epileptic brain tissue (n=4). (**E**) MiR-21, miR-128 and miR-221 expression levels obtained from the analysis of the TCGA data on 188 human glioblastomas. * p<0.05, ** p<0.01, *** p <0.001 compared to control epileptic tissue. $^\#$ p<0.05, $^{\#\#}$ p<0.01, $^{\#\#\#}$ p <0.001 compared to control mouse brain. $^{+++}$p<0.001 compared to normal human brain.

MiR-21 overexpression in the double-floxed mouse model was also evident from FISH experiments performed in formalin-fixed paraffin embedded (FFPE) tissue sections. Figure 2 displays typical images obtained from these experiments showing miR-21 staining in two different GBM samples (Fig. 2A, B), whereas residual staining was detected in control brains (Fig. 2D, E) or using a control scrambled probe (Fig. 1C, F). Similarly, analysis of tissue distribution of miR-21, assessed by FISH in FFPE human tumor sections, showed an increase in miR-21 staining when compared to that using a control scrambled probe (Fig. 2G, H, I).
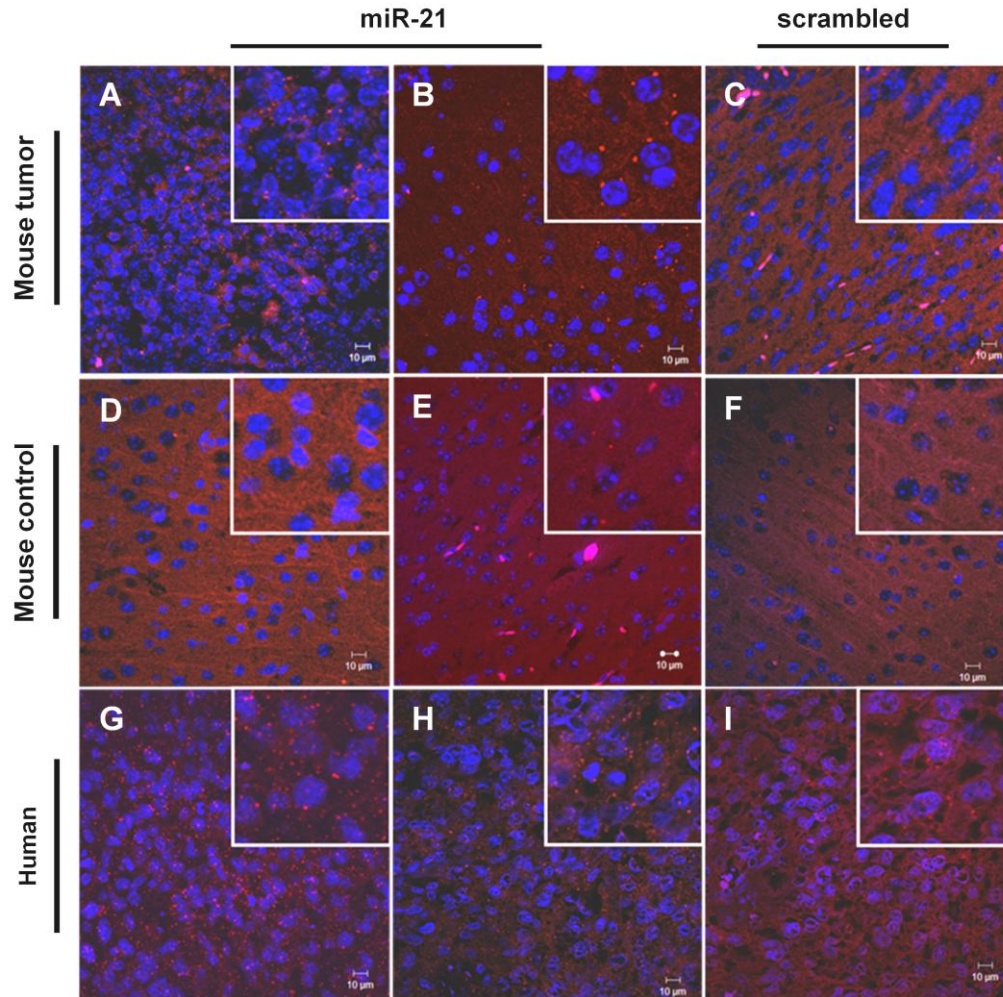
Figure 2. FISH staining in mouse and human GBM tissue samples. FISH staining in (**A, B, C**) double-floxed mouse GBM sections and (**D, E, F**) control mouse brain tissue (n=2) stained with (**A, B, D, E**) miR-21-specific or (**C, F**) scrambled LNA probe. Nuclear staining was obtained using DNA-binding Hoechst 33342. MiR-21 staining (red dots) is observed in the GBM sections, surrounding the cell nucleus (blue), whereas residual staining is observed in control brain sections. Human GBM sections (n=2) stained with (**G, H**) miR-21-specific or (**I**) non-coding (scrambled) LNA probe. MiR-21 staining (red dots) is predominantly cytoplasmic, surrounding the cell nucleus (blue). Control experiments targeting the endogenous U6snRNA (positive control) and without LNA probe (negative control) were performed in parallel (not shown). Images were obtained by confocal microscopy with a 40x EC Plan-Neofluar. Scale corresponds to 10 μm.

3.2 MiR-106a, miR-130b, miR-20a, miR-221, miR-222, miR-155 and let-7i dysregulation correlates with different subtypes of GBM

Recent analysis of the set of gliomas available from TCGA has shown that they can be divided into four different subtypes (classical, mesenchymal, neural and proneural) that reflect the common signaling abnormalities found in these tumors (12). As miR-21 and miR-

128 dysregulation constitutes a common molecular alteration among the four GBM subtypes (Fig. 3 and Supplementary Table S1), we sought to identify miRNAs whose dysregulation might correlate with the different subtypes of GBM. Considering those miRNAs whose expression is altered in at least 45% of the tumors (Fig. 3A), excluding uniformly altered miRNAs (>90% tumors with alterations in miRNA levels), and employing a significance threshold of 0.05 and a 5% FDR to correct for multiple comparisons (Supplementary Data, Table S2), we identified a small group of miRNAs whose alterations are associated with specific GBM subtypes. Our findings, presented in Figure 3B, suggest that concurrent alterations in miR-106a, miR-130b, miR-20a, miR-221 and miR-222 are predominant in the proneural subtype of GBM, whereas alterations occurring only in miR-155, miR-221 and miR-222 are predominant in the neural group. Furthermore, alterations in miR-106a, miR-130b, miR-20a and let-7i concomitant with the absence of alterations in miR-221/222 are predominant in the classical subtype of glioblastoma. This characterization is potentially very useful as a molecular classification tool.
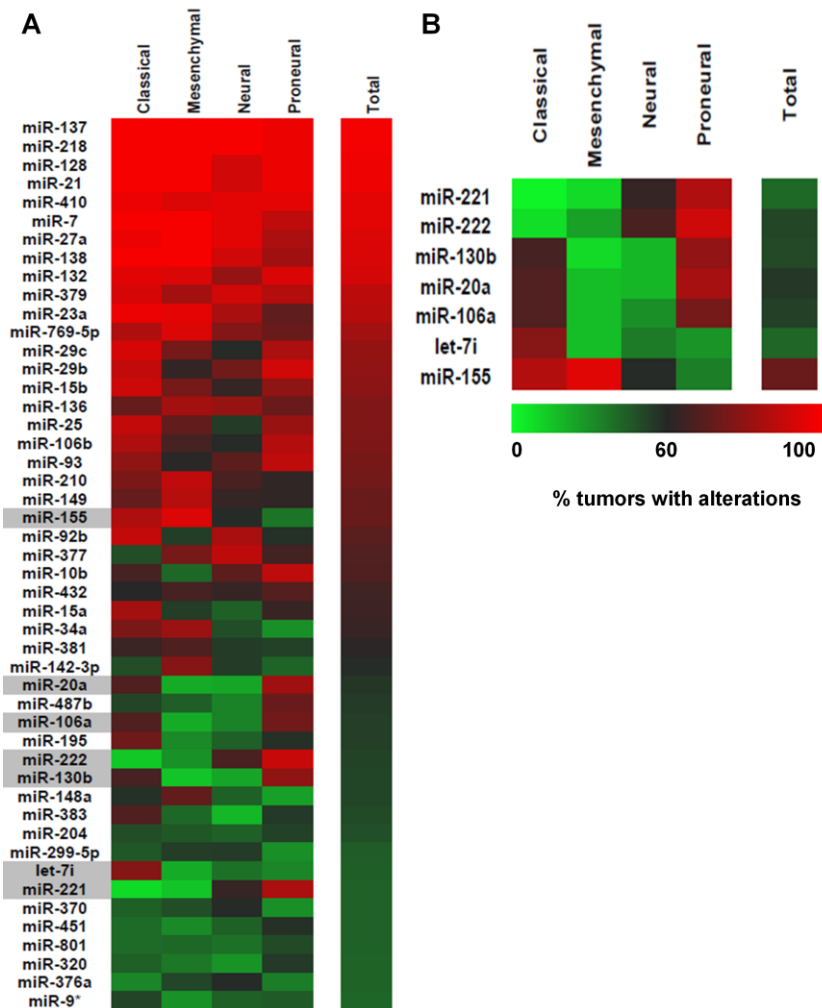
Figure 3. Analysis of TCGA data on 188 human GBMS. (**A**) Heat-map representation of the miRNAs dysregulated in at least 45% (85/188) of the tumors (n=188), displayed as percentage of tumors with alterations in each of the four GBM subtypes (classical, mesenchymal, neural, proneural). Highlighted in grey are the miRNAs represented in (B). (**B**) MiRNAs whose dysegulation is associated with specific GBM subtypes, by applying a significance threshold of 0.05 and a FDR of 5% (0.05). Statistical analysis was performed as described in Materials and Methods.

3.3 Liposomal delivery system (DLS)-based lipoplexes efficiently deliver anti-miR-21 oligonucleotides to glioma cells

Accumulated evidence from in vitro and in vivo studies strongly suggests a key role for miR-21 in tumorigenesis (261, 428). In this context, our findings of invariant overexpression of miR-21 in GBM cells prompted us to examine whether silencing of miR-21 in GBM cells, through delivery of anti-miR-21 oligonucleotides, would result in an antitumoral effect.

In this regard, we have recently shown that DLS liposomes enhance intracellular delivery of single-stranded antisense oligonucleotides, while improving release from endocytic vesicles (429). Therefore, our initial studies addressed the capacity of DLS liposomes to deliver anti-miR-21 oligonucleotides to GBM cells. Using flow cytometry, extensive lipoplex-cell association was observed 4 hours after cell transfection with lipoplexes (~87% transfected cells), as illustrated by the huge increase (~ 42-fold) in the fluorescence intensity of the transfected cells (Fig. 4B), when compared to that of untreated cells (control) (Fig. 4A). Internalization of the lipoplexes carrying FAM-labeled anti-miR-21 oligonucleotides was also monitored in U87 cells, by confocal microscopy. The results presented in Supplementary Results Figure 2 reveal that 4 hours after lipoplex-mediated delivery of FAM-labeled oligonucleotides, green fluorescent particles were found in a large extent in the cytoplasm of transfected U87 cells (Supplementary Figure 2C), whereas no fluorescence was observed in untreated control cells (Supplementary Figure 2A). A similar observation was made when F98 glioma cells were incubated with lipoplexes carrying FAM-labeled anti-miR-21 oligonucleotides (Supplementary Results, Fig. 2B, D). In contrast, the delivery of a similar amount of naked FAM-labeled oligonucleotides did not allow detection of green fluorescence within the cells (data not show).

3.4 MiR-21 silencing increases PTEN and PDCD4 expression in U87 human GBM cells

Following the demonstration of the feasibility of DLS-based lipoplexes to mediate efficient delivery of oligonucleotides into GBM cells, we evaluated the effect of intracellularly-delivered anti-miR-21 oligonucleotides on the levels of miR-21 and mRNA of its target genes. The transfection of U87 cells with anti-miR-21 oligonucleotides (50 nM) resulted in a significant decrease in miR-21 levels (0.0065 ± 0.007), which was further enhanced when cells were transfected with 100 nM anti-miR-21 oligonucleotides (0.0015 ± 0.0007), as compared to those obtained upon transfection with a non-coding (scrambled) oligonucleotide sequence (Fig. 4C). Parallel experiments demonstrated that miR-21 silencing did not significantly affect the levels of other miRNAs (Supplementary Figure 3). We further evaluated the effect of miR-21 silencing on the expression of the tumor suppressors PDCD4 and PTEN, which have been previously identified as miR-21 targets (260, 428, 430). As shown in Figure 4D, a moderate, even though not significant, increase in PTEN mRNA levels was observed in cells transfected with 50 or 100 nM anti-miR-21 oligonucleotides, when compared to those observed in cells transfected with a scrambled sequence (~20 and 15% increase, respectively), whereas no significant changes were observed in PDCD4 mRNA levels. Nevertheless, a considerable increase in PTEN (~34%, p>0.05) and PDCD4 (~33%, p<0.05) protein expression was observed in U87 cells transfected with anti-miR-21 oligonucleotides, when compared to that observed in cells transfected with a scrambled sequence, as shown in Figure 4E and F.
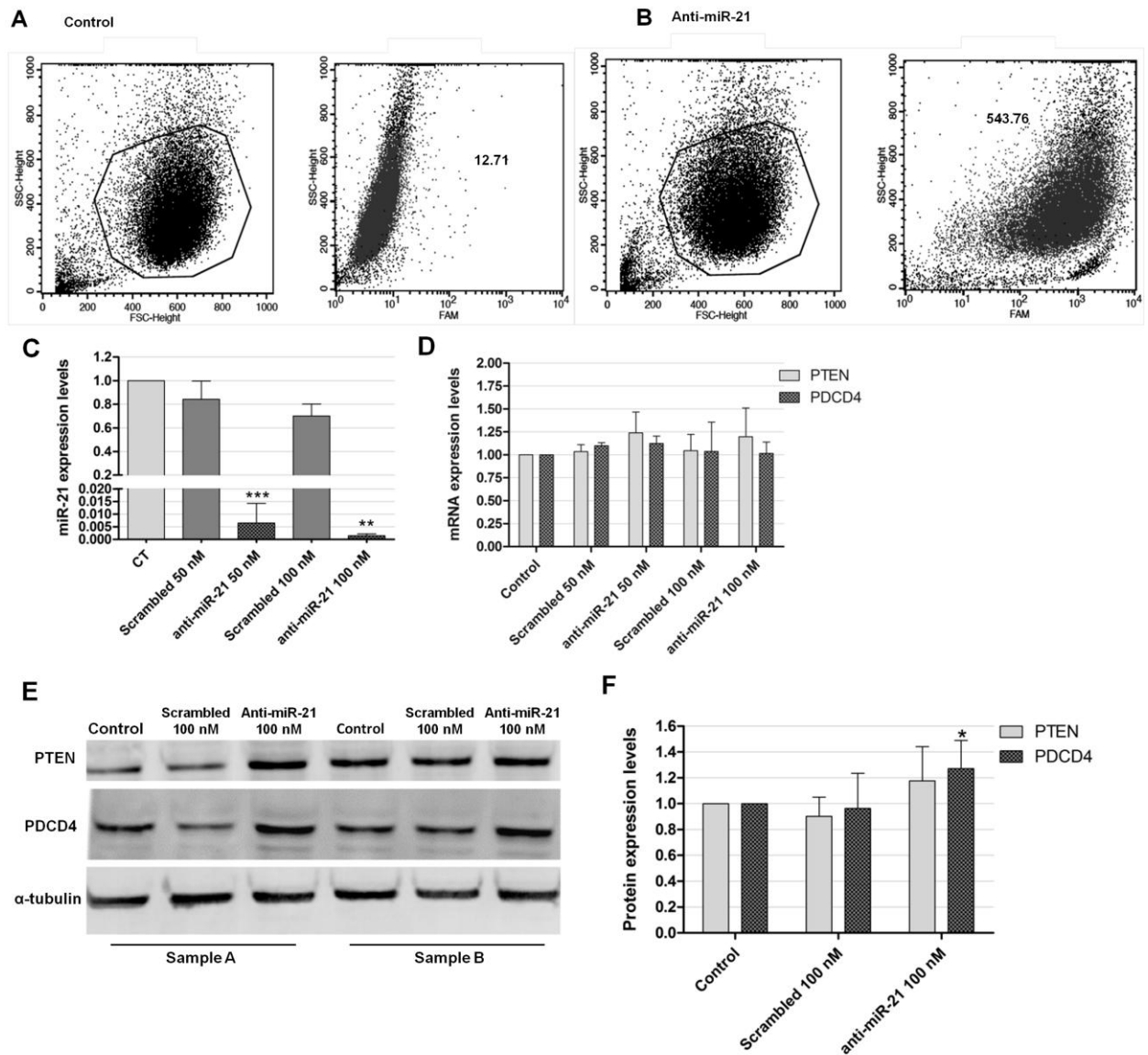
Figure 4. Lipoplex-mediated delivery of anti-miR-21 oligonucleotides in U87 human GBM cells and miR-21, PTEN and PDCD4 expression after oligonucleotide-mediated miR-21 silencing.. For the assessment of lipoplex-cell association, U87 cells were incubated with lipoplexes for 4 hours, rinsed with PBS and prepared for flow cytometry analysis (as described in Supplementary Materials and Methods). Viable cells were gated based on morphological features, including cell volume (given by the forward scatter, FSC) and cell complexity (given by the side scatter, SSC) (left plots in (A) and (B)). Fluorescent intensity plots of U87 cells (**A**) untreated or (**B**) transfected with lipoplexes at a final concentration of 100 nM anti-miR-21 oligonucleotides are shown in the right plots in (A) and (B). Mean fluorescence values (geometric mean) are indicated for each plot. (**C**) miR-21 and (**D**) PTEN and PDCD4 mRNA expression levels in U87 cells 48 hours after transfection with anti-miR-21 or scrambled oligonucleotides (n=3), at a final oligonucleotide concentration of 50 or 100 nM. MiR-21 expression levels, normalized to the reference U6snRNA, as well as PTEN and PDCD4 expression levels, normalized to the reference HPRT1, are presented as relative expression values to control untreated cells. (**E**) Representative gel showing PTEN and PDCD4 protein levels in U87 cells 48 hours after transfection with anti-miR-21 or scrambled oligonucleotides (n=3) at a final oligonucleotide

concentration of 100 nM. (**F**) Quantification of PTEN and PDCD4 bands observed in (E), corrected for individual α-tubulin signal intensity. Results are presented as PTEN and PDCD4 expression levels relative to control. [*] p<0.05, [**] p<0.01, [***] p<0.001 compared to cells transfected with a similar amount of scrambled oligonucleotides.

3.5 MiR-21 silencing increases apoptotic activity in U87 GBM cells

MiR-21 has been previously shown to target several components of important apoptotic pathways, including the p53-dependent apoptotic pathway (305). For this reason, we evaluated whether a decrease in the levels of this miRNA would have any effect on the activity of the tumor suppressor p53. Western blot quantification of p53 using two different antibodies failed to detect the protein in U87 cells (data not shown). The fact that U87 cells express wild-type p53, an isoform with extremely short half-life (431), may explain the absence of detection of this protein. Therefore, we assessed p53 activity indirectly, by measuring the levels of p21/WARF1, a cyclin-dependent kinase inhibitor that is a direct transactivation target of p53 (432). In this regard, a moderate increase (~20%) in the levels of p21 was observed in cells transfected with anti-miR-21 oligonucleotides, when compared to that observed in cells transfected with scrambled oligonucleotides (Figure 5A, B; p>0.05).

Moreover, we investigated whether miR-21 silencing would increase the apoptotic activity in U87 GBM cells, by determining the activity of the effector caspases 3 and 7, crucial components of the apoptotic cell death. As shown in Figure 5C, transfection of U87 cells with 100 nM anti-miR-21 oligonucleotides resulted in a two-fold increase in caspase 3/7 activity (p>0.05), compared to that observed for cells transfected with a scrambled sequence. More importantly, silencing of miR-21 followed by cell exposure to 15 µM of the tyrosine kinase inhibitor sunitinib resulted in a dramatic increase in caspase 3/7 activity (8.15 ± 3.773), when compared to that observed for cells exposed to sunitinib, either *per se* (1.171 ± 0.1539, p<0.001) or in combination with transfection mediated by scrambled oligonucleotides (2.62 ± 0.800, p<0.01).In contrast, miR-21 silencing followed by treatment of U87 cells with 100 µM of the alkylating drug temozolomide, currently used in the clinic as frontline therapy, did not result in significant enhancement of cell apoptotic activity.

3.6 Pifithrin-α-mediated p53 inhibition reduced the caspase activation associated with decreased miR-21 expression levels

To evaluate whether the increase in apoptosis observed for U87 cells following miR-21 silencing could be mediated by p53, a transient inhibition of p53 function was induced in

88

both untreated and anti-miR-21 transfected U87 cells (wild-type p53), using pifithrin-α, a DNA binding inhibitor of p53 transcriptional activity (433, 434). In accordance with previously reported studies (435, 436), reduced signs of toxicity were detected when U87 cells were incubated with 10 µM of pifithrin- α for up to 48 h, while a marked decrease in viability could be observed immediately after cell treatment with 30 µM or higher concentrations of the drug (Fig. 5D). As demonstrated in Figure 5E, a small, but significant, decrease in the levels of caspase 3/7 activity was observed in cells transfected with anti-miR-21 oligonucleotides and further incubated with 10 µM of pifithrin-α (2.645 ± 0.54), when compared to that of cells transfected with anti-miR-21 oligonucleotides without drug treatment (4.41 ± 0.99, p<0.05).
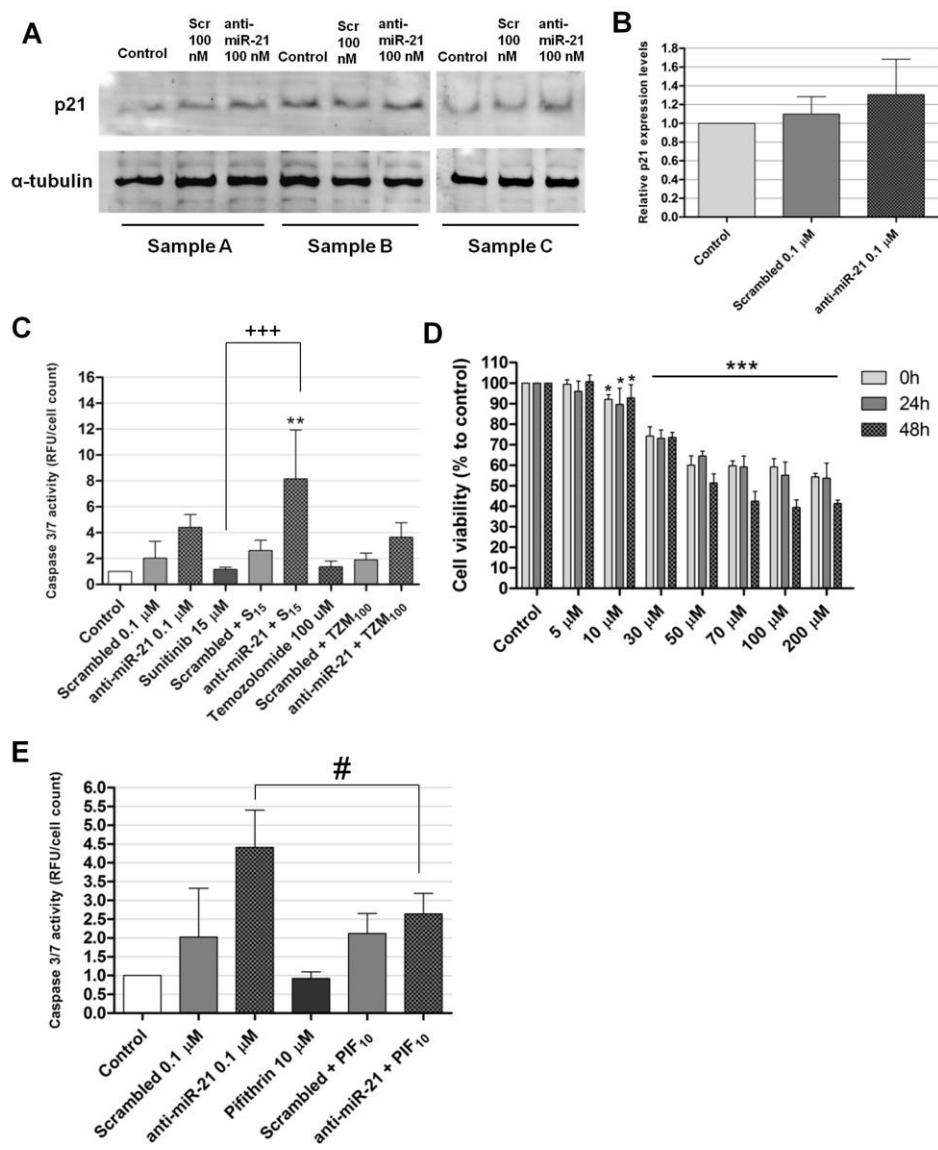
Figure 5. Western blot detection of p21 and caspase activation in U87 human GBM cells. (**C**) Caspase 3/7 activity in U87 cells transfected with anti-miR-21 or scrambled oligonucleotides (0.1 µM), either *per se* or in com(**A**) Representative gel showing p21 levels in U87 cells 48 hours after transfection with anti-miR-21 or scrambled (Scr) oligonucleotides (n=3) at a final oligonucleotide concentration of 100 nM. (**B**) Quantification of p21 bands observed in (A), corrected for individual α-tubulin signal intensity.bination with exposure to 15 µM sunitinib or 100 µM temozolomide (n=3). Twenty-four hours after transfection, cells were exposed to 15 µM sunitinib or 100 µM temozolomide for 24 hours, rinsed with PBS, after which cells were either prepared for caspase detection (cells incubated with sunitinib) or further cultured for 24 hours and then prepared for caspase detection (cells incubated with temozolomide). Results, presented as relative fluorescence units (RFU) with respect to control untreated cells, were normalized for the number of cells in each condition. Scrambled/anti-miR-21 + S_{15}/TZM_{100}: cells transfected with scrambled or anti-miR-21 oligonucleotides and further incubated with 15 µM sunitinib or 100 µM temozolomide. [**] $p < 0.01$ compared to cells transfected with scrambled oligonucleotides and further incubated with 15 µM sunitinib. [***] $p < 0.001$ compared to cells exposed to 15 µM sunitinib. [#] $p < 0.01$ compared to cells transfected with scrambled oligonucleotides (One-way ANOVA with Benferroni's posthoc test). (**D**) Cell viability, evaluated by the Alamar Blue assay, immediately (0), 24 hours (24h) or 48 hours (48h) after incubation with pifithrin-α. [*] $p < 0.05$, [***] $p < 0.001$ compared to untreated cells. (**E**) Caspase 3/7 activity in U87 cells transfected with anti-miR-21 or scrambled oligonucleotides (0.1 µM), either *per se* or in combination with exposure to 10 µM pifithrin-α (n=3). Four hours after transfection, cells were incubated with 10 µM pifithrin-α for 24 hours, and further incubated for 24 hours in fresh DMEM medium. Caspase activity was assessed as described in Materials and Methods. Results, presented as relative fluorescence units (RFU) with respect to control untreated cells, were normalized for the number of cells in each condition. Scrambled/anti-miR-21 + PIF_{100}: cells transfected with scrambled or anti-miR-21 oligonucleotides and further incubated with 10 µM pifithrin-α. [#] $p < 0.01$ compared to cells transfected with anti-miR-21 oligonucleotides.

3.7 Lipoplex-mediated miR-21 silencing enhances the cytotoxic effect of sunitinib in U87 and F98 glioma cells

To evaluate whether the caspase activation associated with decreased miR-21 expression in U87 cells would correlate with changes in cell proliferation, cell viability was measured after transfection with anti-miR-21 oligonucleotides, either per se or in combination with sunitinib or temozolomide. Initial experiments were performed by exposing U87 cells to different concentrations of sunitinib or temozolomide for 24 hours (Fig. 6A, B), in order to determine the optimal concentration of drug to be used in the assay. A moderate decrease in cell viability was observed when U87 cells were transfected with anti-miR-21 oligonucleotides (78.2 ± 10.8), as compared to that observed for cells transfected with a scrambled sequence (95.4 ± 1.2, p>0.05) (Fig. 6D).

Remarkably, a significant decrease in the percentage of viable cells was observed when cells were transfected with anti-miR-21 oligonucleotides and further exposed to

sunitinib (56.52 ± 14.48), as compared to that observed upon exposure to sunitinib, either per se (78.20 ± 10.78, p<0.001) or in combination with the transfection of scrambled oligonucleotides (80.26 ± 7.78, p<0.01). Conversely, lipoplex-mediated miR-21 silencing in U87 cells did not improve significantly the reduction in cell viability associated with exposure to temozolomide (Fig. 6E).

A significant decrease in the percentage of viable cells was also observed when F98 rat glioma cells were transfected with anti-miR-21 oligonucleotides and further exposed to sunitinib (54.95 ± 9.611), as compared to that observed upon exposure to sunitinib, either per se (83.16 ± 3.317, p<0.001) or in combination with the transfection of scrambled oligonucleotides (69.6 ± 8.109, p<0.05) (Fig. 6F). Similarly to what was observed with the U87 cells, lipoplex-mediated miR-21 silencing of F98 cells did not improve significantly the reduction in cell viability associated with exposure to temozolomide (data not shown).
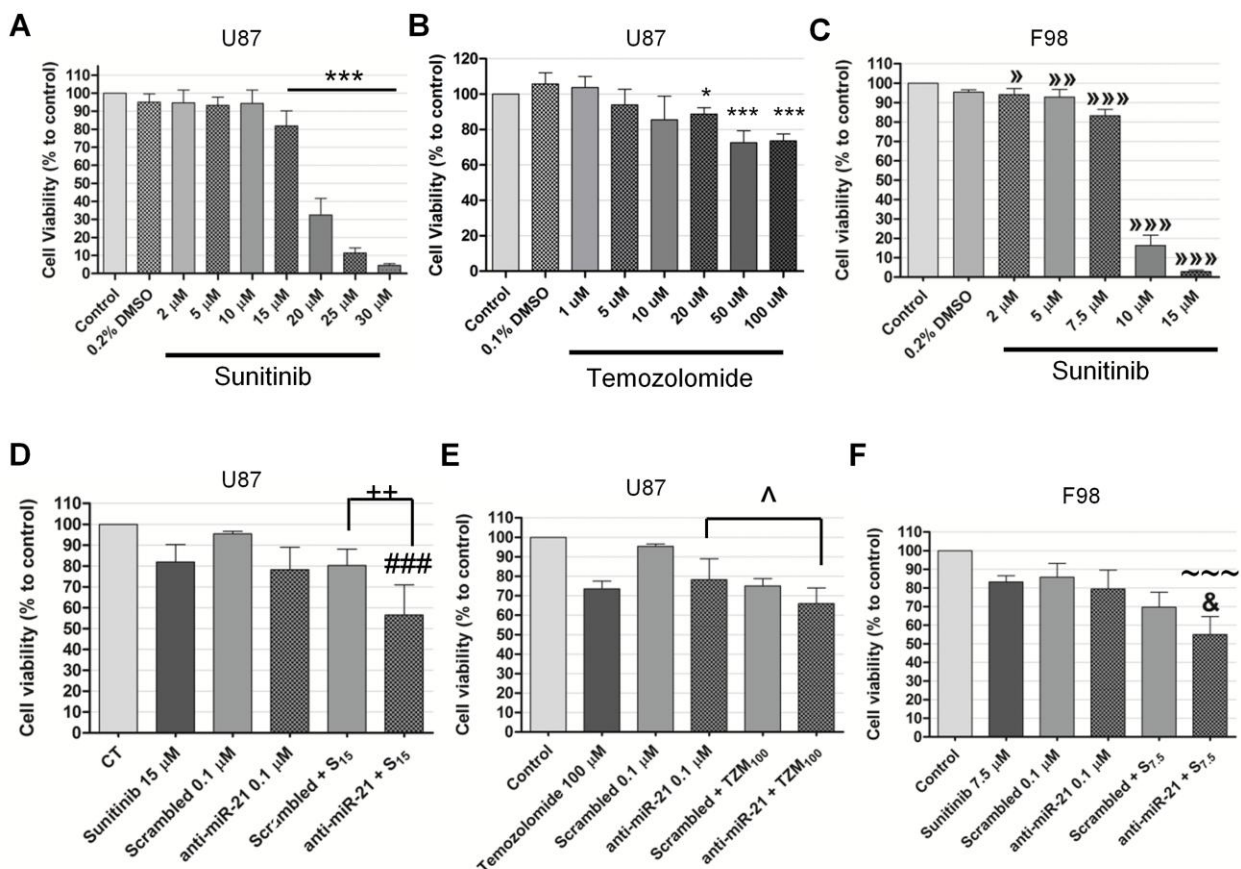

Figure 6. Cell viability after incubation with sunitinib or temozolomide, either per se or in combination with the transfection of anti-miR-21 or scrambled oligonucleotides. Twenty four hours before any experiment, U87 and F98 cells were plated onto 24-well plates at a density of 3.5×10^4

and 3×10^4 cells/well (respectively). Cells were transfected for 4 hours with anti-miR-21 or scrambled oligonucleotides, rinsed with PBS, cultured for 24 hours in fresh DMEM and then exposed to sunitinib or temozolomide for 24 hours. Cell viability was evaluated by the Alamar Blue assay (as described in Materials and Methods) immediately (sunitinib) or 24 hours (temozolomide) after incubation with the drug. Cell viability in (**A**, **B**) U87 and (**C**) F98 glioma cells after incubation with different concentrations of (**A, C**) sunitinib or (**B**) temozolomide for 24 hours. Cell viability in (**D**, **E**) U87 and (**F**) F98 cells after incubation with sunitinib (**D**, **F**) or temozolomide (**E**), either per se or in combination with the transfection of anti-miR-21 or scrambled oligonucleotides. Scrambled/anti-miR-21 + $S_{7.5}$/S_{15}/TZM_{100}: cells transfected with scrambled or anti-miR-21 oligonucleotides and further incubated with 7.5 or 15 μM sunitinib or 100 μM temozolomide. * $p<0.05$, *** $p<0.001$ compared to control untreated U87 cells. » $p<0.05$, »» $p<0.01$, »»» $p<0.001$ compared to control untreated F98 cells. ++ $p<0.01$ compared to U87 cells transfected with scrambled oligonucleotides and further incubated with 15 μM sunitinib. ### $p<0.001$ compared to U87 cells exposed to 15 μM sunitinib. ^ $p<0.05$ compared to U87 cells transfected with anti-miR-21 oligonucleotides. & $p<0.05$ compared to F98 cells transfected with scrambled oligonucleotides and further incubated with 7.5 μM sunitinib. ~~~ $p<0.001$ compared to F98 cells transfected with anti-miR-21 oligonucleotides or incubated with 7.5 μM sunitinib.

3.8 Sunitinib exposure decreases NF-kB activation in U87 GBM cells

A study by Perkins and colleagues has shown that the p53-inhibitor pifithrin-α may indirectly enhance NF-kB signaling in tumor cells (437). Moreover, several reports have demonstrated the existence of reciprocal regulation between p53 and NF-kB (431, 438). The observation of increased p53 activity and sunitinib cytotoxicity in cells with decreased miR-21 levels prompted us to test whether miR-21 silencing and/or sunitinib exposure would have any effect on NF-kB, a transcription factor whose activity has been linked to inflammation and cancer (439). In response to cellular stimuli, the p65/RelA subunit of NF-kB is translocated to the nucleus, where it binds specific DNA motifs and initiates transcription.

The nuclear expression of p65/RelA was assessed in U87 cells transfected with scrambled or anti-miR-21 oligonucleotides, and compared to that of untransfected cells. As shown in Figure 7A and B, no significant decrease in p65 expression was observed in U87 cells transfected with anti-miR-21 oligonucleotides, when compared to that observed for cells transfected with scrambled oligonucleotides. Importantly, p65 expression was reduced by approximately 32% in U87 cells exposed to sunitinib, when compared to normal untreated cells ($p<0.05$). Decreased p65 expression was also observed in U87 cells transfected with anti-miR-21 oligonucleotides and further exposed to sunitinib, when compared to that observed for untreated cells or cells transfected with scrambled oligonucleotides and further exposed to sunitinib (~10 and 5%, respectively; $p>0.05$).
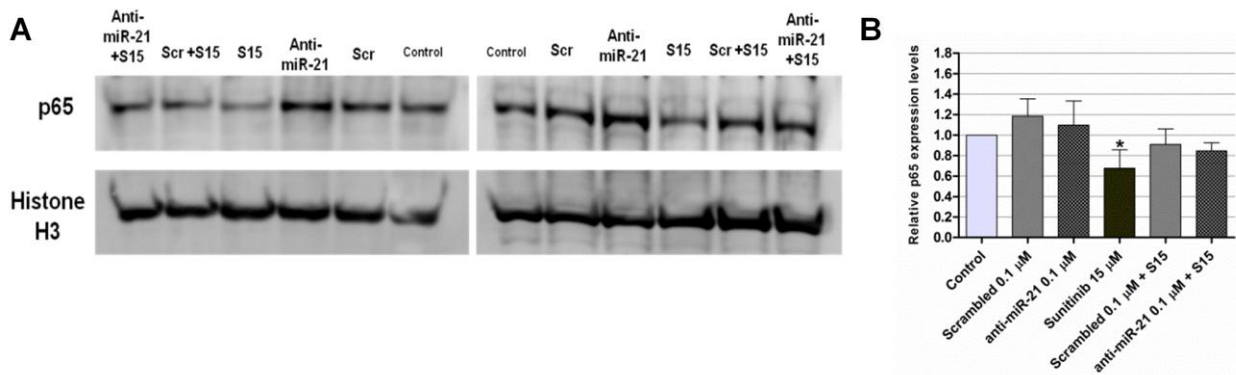
Figure 7. Western blot detection of NF-kB (p65 subunit) in U87 GBM cells. Twenty-four hours after cell transfection with scrambled (Scr) or anti-miR-21 oligonucleotides, at a final concentration of 100 nM, cells were exposed to 15 μM sunitinib for 24 hours, rinsed with PBS, after which nuclear extracts were prepared. (**A**) Representative gel showing p65 levels in U87 cells 48 hours after transfection with anti-miR-21 or scrambled (Scr) oligonucleotides (n=3) at a final oligonucleotide concentration of 100 nM, either *per se* or in combination with exposure to 15 μM sunitinib (S15). (**B**) Quantification of p65 bands observed in (A), corrected for individual histone H3 signal intensity. [*] $p < 0.05$, compared to control untreated U87 cells.

3.9 Lentivirally-mediated miR-21 silencing does not significantly affect the sensibility of U87 cells towards sunitinib

Aiming at evaluating whether a permanent decrease of miR-21 expression in U87 GBM cells could sensitize these cells towards sunitinib, we developed a lentivirally-modified U87 cell line expressing a short hairpin against the mature form of miR-21, as well as GFP (U87-anti-miR-21). Lentivirally-modified U87 cells expressing only GFP were used as a control (U87-GFP). Viral transduction of U87 cells was very efficient, as concluded by the observation of approximately 85% (U87-anti-miR-21) and 90% (U87-GFP) of cells expressing GFP (data not shown).

As shown in Figure 8A, miR-21 expression levels were significantly reduced in U87-anti-miR-21 cells (0.426 ± 0.184, p<0.001), as compared to those observed in U87-GFP cells expressing GFP (0.858 ± 0.05) or parental (nontransduced) U87 cells. Parallel experiments demonstrated that miR-21 silencing did not significantly affect the levels of miR-128 (Fig. 8A), thus indicating that the observed reduction in miR-21 levels is sequence-specific. Furthermore, U87-anti-miR-21 cells displayed decreased proliferation rate, when compared to that of U87-GFP and parental U87 cells (Fig. 8B). A small, although not significant, decrease in cell viability was observed in U87-anti-miR-21 cells following incubation with 15 μM sunitinib for 24 hours (72.68 ± 7.85), as compared to that observed in U87-GFP cells

expressing GFP (79.64 ± 7.03) (Fig. 8C). A smaller decrease was observed when cells were incubated with 20 µM sunitinib (~3%), whereas no differences were observed when cells were incubated with 10 µM sunitinib.
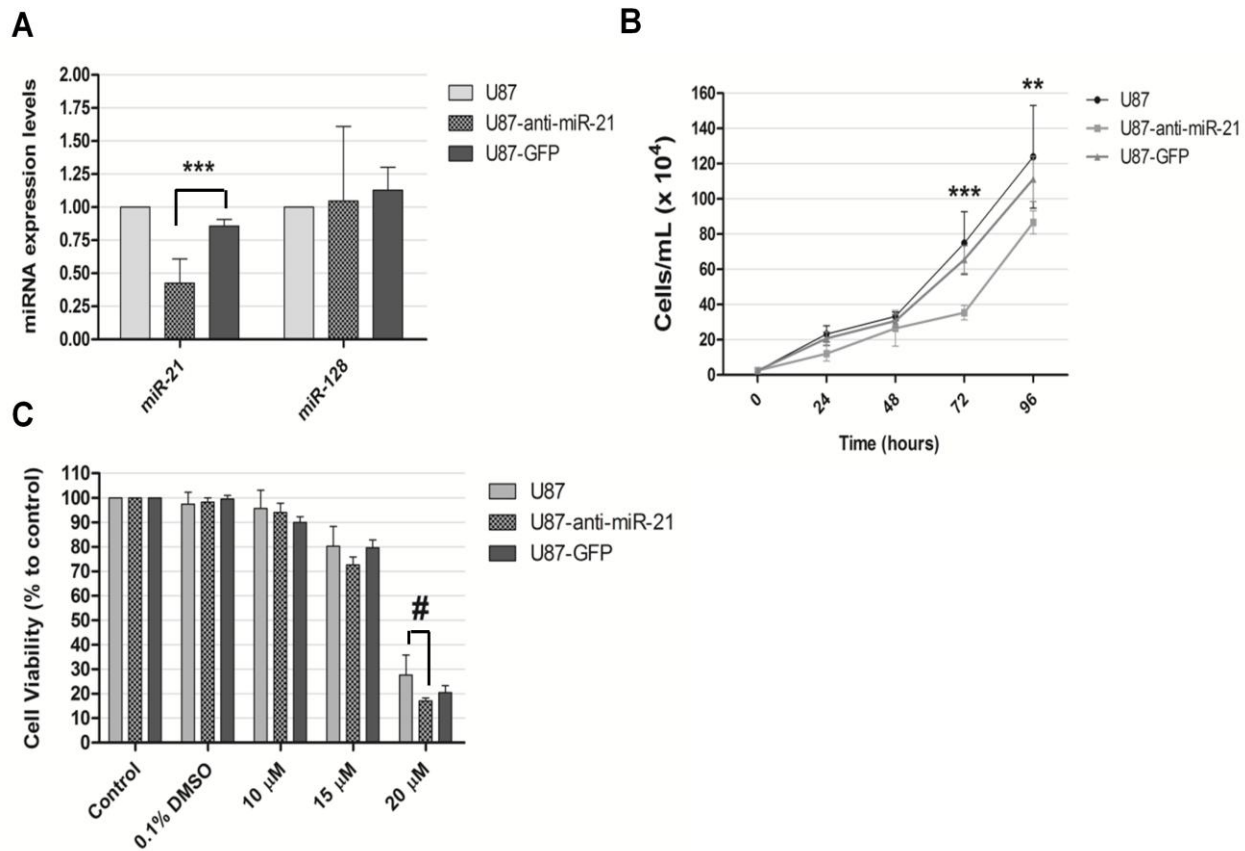
Figure 8. Evaluation of miR-21 expression, proliferation and viability in U87, U87-anti-miR-21 and U87-GFP GBM cells after incubation with sunitinib. Modified U87 cell lines, expressing either an anti-miR-21 short hairpin (U87-anti-miR-21) or a GFP-coding short hairpin (U87-GFP), were developed as described in the Materials and Methods section. (**A**) miR-21 and miR-128 expression in U87-anti-miR-21 and U87-GFP cells, normalized to the reference U6snRNA. Results are presented as relative expression values to control U87 cells. Two-way ANOVA combined with the Bonferroni's posthoc test was used for statistical analysis. *** $p < 0.001$ compared to U87-GFP cells. (**B**) U87, U87-anti-miR-21 and U87-GFP cells were plated onto 48-well plates at a density of 2.5×10^4 cells/well. At defined time points, cells were washed with PBS, trypsinized and ressuspended in culture medium. The number of viable cells was determined by Trypan blue exclusion. Two-way ANOVA combined with the Bonferroni's posthoc test was used for statistical analysis. ** $p < 0.01$, *** $p < 0.001$ compared to U87-GFP cells. (**C**) Twenty-four hours before incubation with sunitinib, cells were plated onto 24-well plates at a concentration of 5×10^4 cells/well. Cells were exposed to different concentrations of sunitinib for 24 hours, and further grown for 24 h in fresh culture medium, after which the cell viability was evaluated by the Alamar Blue assay (as described in Materials and Methods). Two-way ANOVA combined with the Bonferroni's posthoc test was used for statistical analysis. # $p < 0.001$ compared to U87 cells.

4. Discussion

Over the last decade, accumulated evidence has shown that miRNAs play an important role in relevant molecular and cellular mechanisms governing GBM tumorigenesis, including cell proliferation, invasion and stem cell renewal (306, 322, 422). Due to their small size and influence in a broad range of biological processes, miRNAs are very attractive therapeutic targets for GBM. In the present study, we demonstrate that combination of a liposome-based gene therapy approach targeting miR-21, uniformly overexpressed in the different subtypes of glioblastoma, with sunitinib, an inhibitor of tyrosine kinase receptors that include PDGFR and VEGFR, enhances the cytotoxic effect of this drug in U87 human and F98 glioma cells.

Alterations in miRNA signaling have been associated with several aspects of carcinogenesis, including tumor invasion and metastasis and patient outcome (440, 441). Here, by demonstrating that miR-21 is overexpressed and miR-128 is downregulated in mouse GBM models and in a large number of human GBM samples (Fig. 1), our results not only support those from previously reported studies (266, 426, 427), but also underline the universal character of these alterations in the global GBM profile.

Recently, an interesting study from the TCGA Research Network divided GBMs into four clinically relevant subtypes characterized by abnormalities in PDGFRA, IDH1, EGFR and NF1 (12); among the two main subtypes identified, the "classical" GBMs predominantly harbor EGFR amplification and rearrangement, while the "proneural" GBMs are predominantly driven by PDGF signaling (12). By identifying a small group of miRNAs whose alterations are associated with the different GBM subclasses, we extended the molecular characterization of this group of tumors to non-coding RNAs (ncRNAs). The results here presented suggest that alterations in the expression of the miR-221/222 cluster occur predominantly in the proneural and neural subtypes (Fig. 3B and Supplementary Table S1), whereas alterations in let-7i are predominant in the classical group; alterations in the oncogenic miR-20a and miR-106a are common to both subtypes (Fig. 3B). However, as none of the miRNAs analyzed is strictly altered in a unique GBM subtype (under the defined exclusion criteria), our data does not implicate such miRNAs as additional direct biomarkers but rather complementary molecular markers that may help in the correct identification of the different GBM subclasses.

The biological effects of miR-21 are most likely associated to the simultaneous repression of multiple tumor suppressor genes, including TPM1, PDCD4 and PTEN (260, 442, 443), as well as of several invasion/metastasis suppressors (428). Here, and in

accordance with previous studies (442, 444), we provide evidence that oligonucleotide-mediated miR-21 silencing increases the expression levels of the tumor suppressors PTEN and PDCD4 (Fig. 4). PTEN is a frequently disrupted tumor suppressor in glioma and capable of restricting growth and survival signals by limiting the activity of the phosphoinositide-3-kinase (PI3K) pathway, a signaling cascade that controls cell proliferation, growth, differentiation and survival (445, 446). PDCD4 is also frequently lost in glioma (447) and has been shown to regulate important cellular processes affecting cell phenotype, including protein translation (303), promoter activation (448) and cell cycle regulation (304). The observation of increased levels of the PDCD4 protein (and not mRNA) following miR-21 silencing suggest that miR-21 regulates PDCD4 expression in U87 GBM cells by inhibiting its translation, rather than promoting PDCD4 mRNA degradation. A similar mechanism has previously been reported by Chen and colleagues (449).

MiR-21 has also been shown to target multiple components of important apoptosis-related pathways including p53, TGF-β and mitochondrial apoptosis (305). Knockdown of miR-21 in cultured GBM cells and glioma-bearing mice has been previously shown to trigger caspase activation and lead to increased apoptotic cell death and decreased tumor cell viability (426, 450). In this regard, our results also reveal an increase in caspase 3/7 activation following miR-21 silencing in U87 cells, thus confirming an anti-apoptotic role of miR-21 in human GBM cells. The observation of increased p21 expression in U87 cells with decreased miR-21 levels, as well as reduced caspase activation following miR-21 silencing in cells with repressed p53 transcriptional activity, strongly suggests that miR-21 silencing increases p53 activity in U87 GBM cells (Fig. 5).

The increased expression of the tumor suppressors and the activation of caspases observed following miR-21 silencing may not only explain the reduction observed in the proliferation of U87 cells, but also render the cells susceptible to drugs targeting other signaling pathways governing GBM tumorigenesis. In this regard, several in vitro studies have already shown that miR-21 modulation potentiates the cytotoxic effect of anti-neoplastic drugs. The co-delivery of anti-miR-21 oligonucleotides significantly improved the cytotoxicity of fluorouracil (5-FU) in U251 human GBM cells, while increasing apoptosis and decreasing tumor cell migration (451). MiR-21 inhibition was also shown to enhance the chemo-sensitivity of human GBM cells to taxol, independent of PTEN status (452).

Here, we are the first to demonstrate that lipoplex-mediated miR-21 silencing enhances significantly the cytotoxic effect of sunitinib in both U87 human and F98 rat glioma cells (Fig. 6). Sunitinib is currently approved by the FDA for the treatment of gastro-intestinal

stromal tumors (GIST) and renal cell carcinoma and several phase II clinical trials are underway for GBM (33). Moreover, we demonstrate that sunitinib decreases the nuclear expression of p65, the gene regulatory subunit of the NF-kB transcription factor, which suggests that sunitinib decreases the activation of the oncogenic NF-kB pathway in U87 GBM cells (Fig. 7).

The oncogenic NF-kB and the tumor suppressor p53 have reciprocal activities and functions. P53 can regulate the levels of NF-kB to promote apoptosis and cell death, whereas NF-kB-mediated negative regulation of p53 can contribute to tumorigenesis (438). In this regard, the simultaneous induction of p53-related activity and repression of NF-kB, achieved by the silencing of miR-21 concomitant with sunitinib exposure, may explain the synergistic cytotoxic effect observed with the simultaneous application of both strategies. In this context, the results obtained in this study reveal a miRNA-based therapeutic approach with potential to complement a primary drug-based therapy, which may prove to be of great importance for clinical application, particularly considering the drug resistance and toxic side-effects usually associated with the use of chemotherapy. Experiments in an animal model of GBM are currently in progress in our laboratory to address the in vivo efficacy of the generated combined therapeutic approach, and will constitute a separate study.

The results obtained in this study also indicate that a permanent decrease in miR-21 levels, achieved by lentiviral transduction of U87 cells, does not significantly improve the sensitivity of U87 cells towards sunitinib, as opposed to what was achieved with the transient oligonucleotide-based approach (Fig. 8). In this regard, the moderate decrease in the levels of miR-21 obtained in cells transduced with lentivirus (~2-fold), when compared to the pronounced decrease in the levels of miR-21 in oligonucleotide-transfected cells (~150-fold), may help explain the observed differences. Experiments involving an optimized lentiviral vector, able to produce a more efficient anti-miR-21 shRNA, may clarify whether the sensitivity of U87 cells towards sunitinib relates with the expression levels of miR-21.

In summary, the observation of an invariable overexpression of miR-21 in GBM associated with the highly promising results achieved in lipoplex-mediated miR-21-antagonism studies suggests that miR-21 is an ideal candidate for a multimodal therapeutic approach, combining miRNA-based gene therapy with antiangiogenic activity towards GBM.

5. Materials and Methods

Materials

Sunitinib malate (Sutent®) was kindly offered by Pfizer (Basel, Switzerland) and temozolomide (Temodar®, Merck) was acquired from Sigma (Munich, Germany). Stock solutions were prepared in DMSO (Sigma, Germany) and stored at -20ºC or 4ºC (respectively). The miRZip anti-miR-21 construct was acquired from System Biosciences (Mountain View, CA, USA). The locked nucleic acid (LNA)-modified anti-miR-21 oligonucleotides and a non-coding (scrambled) sequence, as well as digoxigenin (DIG)-labeled LNA detection probes for miR-21, scrambled and U6snRNA, were accquired from Exiqon (Vedbaek, Denmark). All sequences are displayed in Supplementary Data, Table S3. All other reagents were obtained from Sigma unless stated otherwise.

Human and mouse tissue samples

Human GBM samples and non-neoplastic brain tissue were obtained from the Bartoli Brain Tumor Bank at the Columbia University Medical Center (CUMC), and were used in accordance with the policies of the CUMC review board. Briefly, tissue samples were flash frozen in liquid nitrogen immediately after surgical resection, and further stored at -80ºC. Neoplastic tissue samples were obtained from viable areas of tumor, while trying to avoid necrotic areas. Non-neoplastic brain tissue samples were derived from the temporal lobes of patients surgically treated for temporal lobe epilepsy. Tissue adjacent to the tumors was also obtained from post-mortem specimens. Commercially available total RNA from adult human brain was acquired from Clontech (Mountain View, CA, USA) (Catalog No: 636530, Lot number: 9022522A).

Mouse GBM samples were obtained from established GBM models developed by injection of the retroviral vector PDGF-IRES-CRE in the subcortical white matter of double-floxed (PTEN$^{-/-}$p53$^{-/-}$) or PTEN-floxed (PTEN$^{-/-}$) mice, as described previously (20). Control samples were obtained from brains of double-floxed mice injected with Cre-only retrovirus (no PDGF).

Cell lines and culturing conditions

Mouse GBM cell lines, derived from brain tumors of double-floxed (PTEN$^{-/-}$p53$^{-/-}$) or PTEN-floxed mice, were maintained in culture as described previously (425). The F98 rat glioma cell line was a kind offer from Dr. Hélène Elleaume (European Synchrotron Radiation Facility, Grenoble, France) and the U87 human glioblastoma cell line was obtained from the American Type Culture Collection (Manassas, VA, USA). Cells were maintained in DMEM (Invitrogen, Carlsbad, CA, USA), supplemented with 10% heat-inactivated fetal bovine serum (FBS) (Gibco, Paisley, Scotland), 100 U/ml penicillin (Sigma), 100 µg/ml streptomycin (Sigma) and cultured at 37°C under a humidified atmosphere containing 5% CO$_2$. Undifferentiated P19 embryonal carcinoma cell line was a kind gift from Dr. Richard Cerione (Cornell University, NY, USA), and was maintained in α-MEM (Gibco); supplements and growth conditions were similar to those used for glioma cells. Primary rat cortical astrocyte cultures were prepared from the cerebral cortices of newborn pups according to established protocols (453).

For all the experiments, cell plating densities are indicated in Supplementary Material, as well as in Figure legends.

Lentiviral production and cellular transdution

Lentiviruses encoding the anti-miR-21 shRNA and GFP or a control shGFP were produced in 293T cells with a four-plasmid system, as previously described (454, 455). The lentiviral particles were produced and resuspended in phosphate-buffered saline (PBS) containing 1% bovine serum albumin. The viral particle content of batches was determined by assaying HIV-1 p24 antigen (RETROtek, Gentaur, Paris, France). The stocks were stored at -80ºC until use.

For the lentiviral transduction of U87 cells, cells were plated onto 6-well plates at a final concentration of 1.6 x 10^5 cells/well. Twenty-four hours after plating, 10 ng of virus coding for either anti-miR-21 shRNA or control shGFP were added per 1x10^5 cells; 8 µg of polybrene (hexadimethrine bromide) were also added to each well, in order to increase the efficiency of infection. Cell culture medium was replaced 6 hours after infection, and cells were further grown for 48 hours, after which were plated onto 10-cm dishes. Infected cells were selected by growing cells culture medium containing 1 ug/mL of puromycin.

Lipoplex preparation and cell transfection

For transfection of anti-miR-21 oligonucleotides, lipoplexes were prepared with DLS liposomes, as described previously (429, 456). DLS liposomes were prepared by mixing 1 mg of dioctadecylamidoglycylspermidine (DOGS) (Promega, Madison, WI) and 1 mg of dioleoyl phosphatidylethanolamine (DOPE) (Sigma, Munich) in 40 µl of 90% ethanol, followed by the addition of 360 µl of sterile H_2O; the mixture was further incubated for 30 min to allow liposome formation. The final lipid concentration was 5mg/ml (2.5mg of DOGS and 2.5mg of DOPE). Lipoplexes were prepared by gently mixing 12 µg of oligonucleotides with 125 µg of lipid in a final volume of 125 µl, followed by incubation for 30 min at room temperature. DLS lipoplexes were prepared fresh for every experiment. Lipoplexes were added to cells, maintained in OptiMEM (Gibco), at a final concentration of 50 or 100 nM oligonucleotides/well. After a 4-hour incubation period, cells were washed with PBS and further cultured in fresh DMEM medium for 48 hours.

RNA extraction in tissue samples and cDNA synthesis

Total RNA from human and mouse tissue samples was extracted using the miRNeasy Mini kit (Qiagen, Valencia, CA, USA) following the manufacter's instructions. After RNA quantification, cDNA conversion was performed using the TaqMan MicroRNA Reverse Transcription Kit (Applied Biosystems, Foster City, CA, USA) and miRNA-specific primers. For each sample, cDNA was produced from 10 ng of total RNA in an TC-PLUS SAT/02 thermocycler (VWR, Radnor, PA, USA), by applying the following protocol: 30 min at 16°C, 30 min at 42°C and 5 min at 85°C. The cDNA was further diluted 1:20 with RNase-free water prior to quantification by qPCR. RNA extraction for cultured cells and cDNA synthesis are described in Supplementary Material.

QPCR quantification of miRNA expression in tissue samples

MiRNA quantification in human and mouse tissue samples was performed in an ABI Prism 7300 real-time PCR System (Applied Biosystems) using 96-well microtitre plates and the TaqMan® Universal PCR Master Mix (Applied Biosystems). The primers for the target miRNAs (miR-128, miR-21 and miR-221) and the reference RNA (U6snRNA) were also acquired from Applied Biosystems (457). A master mix was prepared for each primer set, containing a fixed volume of TaqMan master mix and the appropriate amount of each primer

to yield a final concentration of 150 nM. For each reaction, performed in duplicate, 17.67 µl of master mix were added to 1.33 µl of template cDNA. The reaction conditions consisted of enzyme activation at 95°C for 10 min followed by 40 cycles at 95°C for 15 s (denaturation) and 60 s at 60°C (annealing and elongation). Threshold values for threshold cycle determination (Ct) were generated automatically by the SDS Optical System software. Relative miRNA levels were determined following the Pfaffl method for relative miRNA quantification in the presence of target and reference genes with different amplification efficiencies (458). The amplification efficiency for each target or reference gene was determined according to the formula: $E=10^{(-1/S)}$, where S is the slope of the standard curve obtained for each gene.

MiRNA and mRNA quantification in cultured cells is described in Supplementary Material.

Western blot analysis

Total protein extracts were prepared from cultured U87 cells, homogeneized at 4ºC in RIPA lysis buffer (50 mM Tris pH 8.0, 150 mM NaCl, 50 mM EDTA, 0.5% sodium deoxycholate, 1% Triton X-100) containing a protease inhibitor cocktail (Sigma), 2 mM DTT and 0.1 mM PMSF. The concentration of protein lysates was determined using the Bio-Rad Dc protein assay (Bio-Rad) and 25 µg of total protein were resuspended in loading buffer (20% glycerol, 10% SDS, 0.1% bromophenol blue), incubated for 5 min at 95ºC and loaded onto a 10% polyacrylamide gel for electrophoretic separation. After electrophoresis, the proteins were blotted onto a PVDF membrane, blocked in 5% nonfat milk for 1 hour, incubated overnight at 4ºC with an anti-PTEN (#9552, Cell Signaling; 1:1000), anti-PDCD4 (clone D29C6, Cell signaling; 1:1000), anti-p53 (clone Pab240, Millipore; 1:500 and clone 1C12, Cell signaling; 1:1000) and anti-p21 (Ab7960, Abcam; 1:200) antibody, and with the appropriate alkaline phosphatase labeled-secondary antibody (1:20000) (Amersham, Uppsala, Sweden) for 2 hours at room temperature. Equal protein loading was verified by reprobing the membrane with an anti-α-tubulin antibody (1:10000) (Sigma) and with the same secondary antibody. After antibody incubation, the blots were washed several times with TBS-T (Bio-Rad), incubated with the enzyme substrate ECF (Amersham Biosciences, UK) for 5 min at room temperature and then submitted to fluorescence detection at 570 nm using a VersaDoc Imaging System Model 3000 (Bio-Rad). The analysis of band intensity was performed using the Quantity One software (Bio-Rad).

NF-kB activation analysis

In order to detect NF-kB activation, the nuclear translocation of the regulatory subunit p65/RelA was evaluated by Western blotting. The protocol for extraction of nuclear and cytoplasmic fractions, described in Supplementary Material, was adapted from the protocol described by Ferreira and colleagues (459). Ten micrograms of nuclear protein were separated on a 10% polyacrylamide gel. After electrophoresis, the proteins were blotted onto a PVDF membrane, blocked in 5% nonfat milk for 1 hour, incubated overnight at 4ºC with an anti-N (#9552, Cell Signaling; 1:1000), anti-PDCD4 (clone D29C6, Cell signaling; 1:1000), anti-p53 (clone Pab240, Millipore; 1:500 and clone 1C12, Cell signaling; 1:1000) and anti-p21 (Ab7960, Abcam; 1:200) antibody, and with the appropriate alkaline phosphatase labeled-secondary antibody (1:20000) (Amersham, Uppsala, Sweden) for 2 hours at room temperature.

Fluorescence *in situ* hybridization (FISH) in tissue sections

FISH was performed in human and mouse FFPE tissue sections as described by Pena and colleagues (460), with a few modifications. The detailed protocol is supplied in Supplementary Material.

Cell viability

Cell viability was evaluated by a modified Alamar Blue assay (461). Briefly, 10% (v/v) resazurin dye in complete DMEM medium was added to each well and cells were incubated at 37°C until the development of a pink coloration. Two hundred microliters of supernatant were collected from each well, transferred to clear 96-well plates and the absorbance at 570 (reduced form) and 600 nm (oxidized form) was measured in a microplate reader (SpectraMax Plus 384, Molecular Devices). Cell viability was calculated as percentage of control cells using the equation: (A_{570} − A_{600}) of treated cells × 100 / (A_{570} − A_{600}) of control cells.

Apoptosis assay

Caspase-3/7 activity was assessed using the SensoLyte homogenous AMC caspase-3/7 assay (AnaSpec, San Jose, CA, USA). Briefly, 48 hours after lipoplex-mediated

oligonucleotide transfection, 24 hours after temozolomide incubation or immediately after exposure to sunitinib, cells were collected and lysed, according to the manufacter's instructions. Cell supernatant and caspase substrate (Ac-DEVD-AMC) were mixed, according to the manufacturer's recommendation, and further incubated in a black 96-well plate for 40 min at room temperature (under shaking). The production of the AMC fluorophore, released as a result of caspase action on the substrate, was measured for a period of 8 hours, using a microplate reader (SpectraMax Plus 384, Molecular Devices) at excitation/emission of 354/442 nm. Results, presented as relative fluorescence units (RFU) to control untreated cells, were normalized for the number of cells in each condition.

Confocal microscopy and flow cytometry studies

In order to assess the extent of cellular internalization of the DLS-based lipoplexes, confocal microscopy and flow cytometry studies in proliferating cells were performed. The detailed protocols are described in Supplementary Material.

Analysis of the TCGA GBM data

The TCGA miRNA expression data was obtained from the public access Data Portal (http://tcga-data.nci.nih.gov/tcga/) through the Data Browser tool. Expression values were obtained in a logarithmic scale (log 2 tumor/normal ratio) and further converted into tumor/normal ratio (a threshold value of 1 was used to identify dysregulated miRNAs in tumor samples). Tumor IDs and derived data values are given in Supplementary Data, Table S1. Multiple comparison analysis was performed using the commercially available Microsoft Excel and P values were adjusted by controlling the false discovery rate (FDR) (462). Changes were considered significant ($p<0.05$) if the FDR was smaller than 0.05 (Supplementary Data, Table S2).

Statistical analysis

All data are presented as means ± standard deviation of at least three independent experiments, each performed in triplicate, unless stated otherwise. One way analysis of variance (ANOVA) combined with the Tukey posthoc test was used for multiple comparisons in cell culture experiments (unless stated otherwise) and considered significant when $p< 0.05$. Statistical differences are presented at probability levels of $p< 0.05$, $p< 0.01$ and $p<$

0.001. Calculations were performed with standard statistical software (Prism 5, GraphPad, San Diego, CA, USA).

6. Supplementary Figures
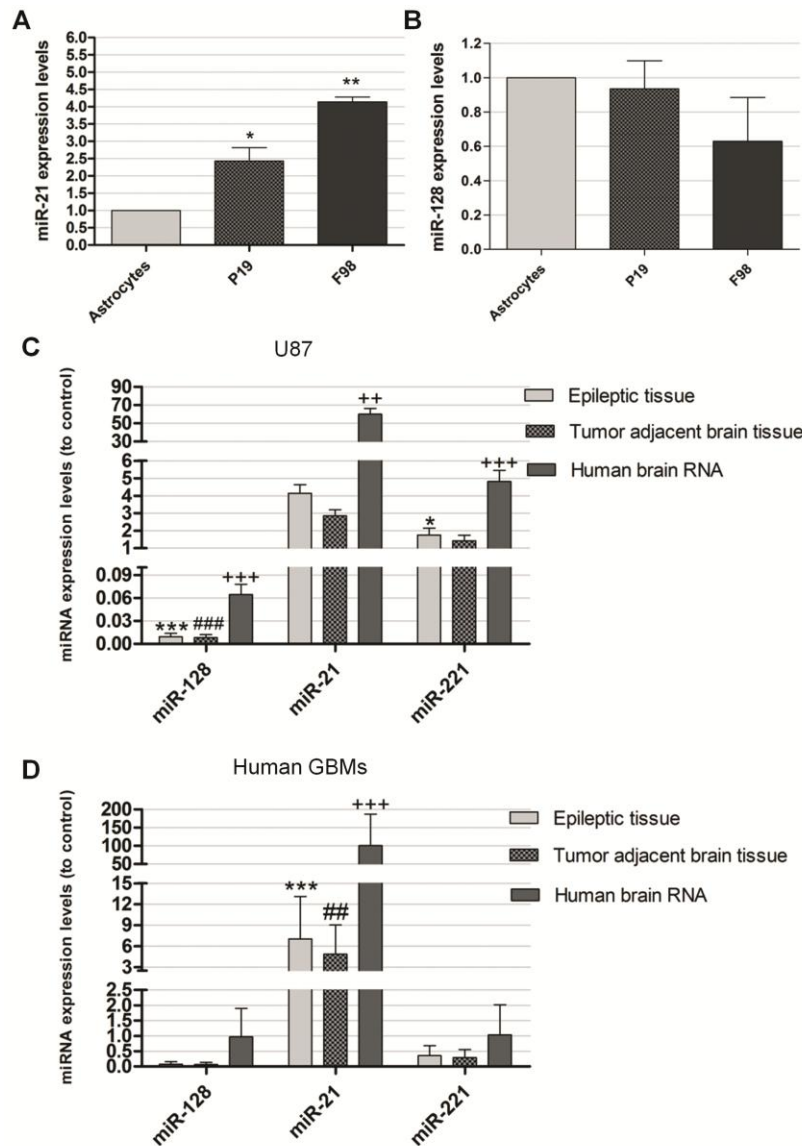
Supplementary Figure 1. MiRNA expression levels in human (U87) and rat (F98) GBM/glioma cell lines and human GBM tissue samples. (**A**) miR-21 and (**B**) miR-128 expression levels in F98 rat glioma and P19 human embryonic carcinoma cells (n=3), compared to control rat primary astrocytes (n=3). P19 cells were used as a control in this study as they were shown to express low levels of miR-21 (Chan et al., 2005). * p<0.05, ** p<0.01, compared to control rat astrocytes. (**C**) MiRNA expression levels in U87 GBM cells (n=3), compared to three different controls: epileptic brain tissue, tumor-adjacent brain tissue and total RNA from human brain. (**D**) MiRNA expression levels in human GBM tumor samples (n=22) compared to three different controls: epileptic brain tissue, tumor-adjacent brain

tissue and total RNA from human brain. * p<0.05, *** p<0.001 compared to control epileptic tissue (n=4). $^{\#\#}$ p<0.01, $^{\#\#\#}$ p<0.001 compared to tumor adjacent brain tissue (n=3). $^{++}$p<0.01, $^{+++}$p<0.001 compared to total RNA from human brain.
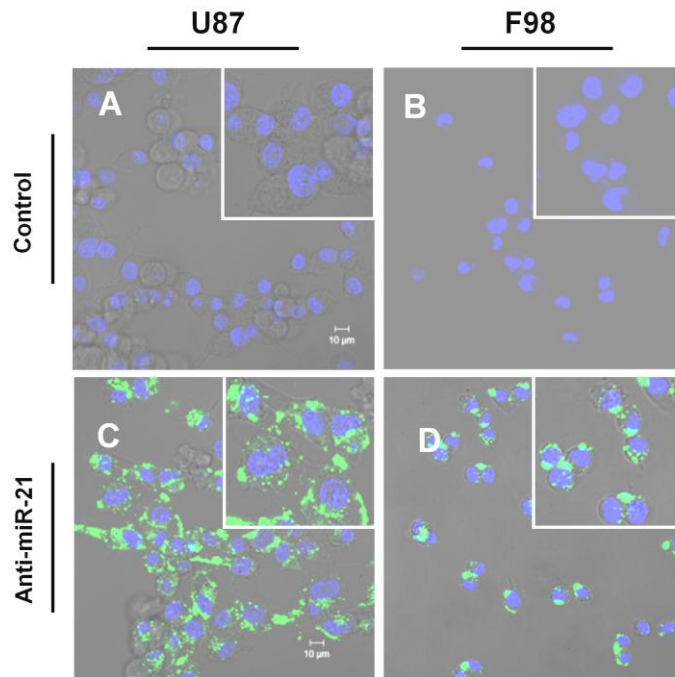
Supplementary Figure 2. Lipoplex-mediated delivery of anti-miR-21 oligonucleotides in U87 human and F98 rat GBM/glioma cells. For the assessment of cellular internalization, U87 and F98 cells were transfected with lipoplexes for 4 hours, rinsed twice with PBS, stained with DNA-specific Hoescht 33342 (blue) and then observed by confocal microscopy. The panel shows representative images at 40× magnification of (**A**, **C**) U87 GBM or (**B**, **D**) F98 glioma cells, either (**A**, **B**) untreated or (**C**, **D**) transfected with lipoplexes at a final concentration of 100 nM anti-miR-21 oligonucleotides. Results are representative of two independent experiments.
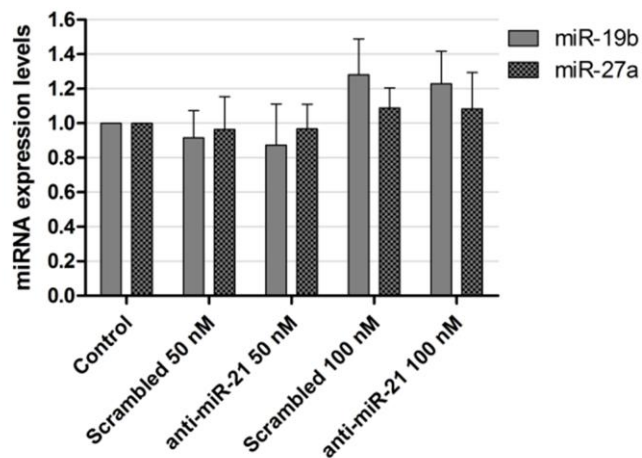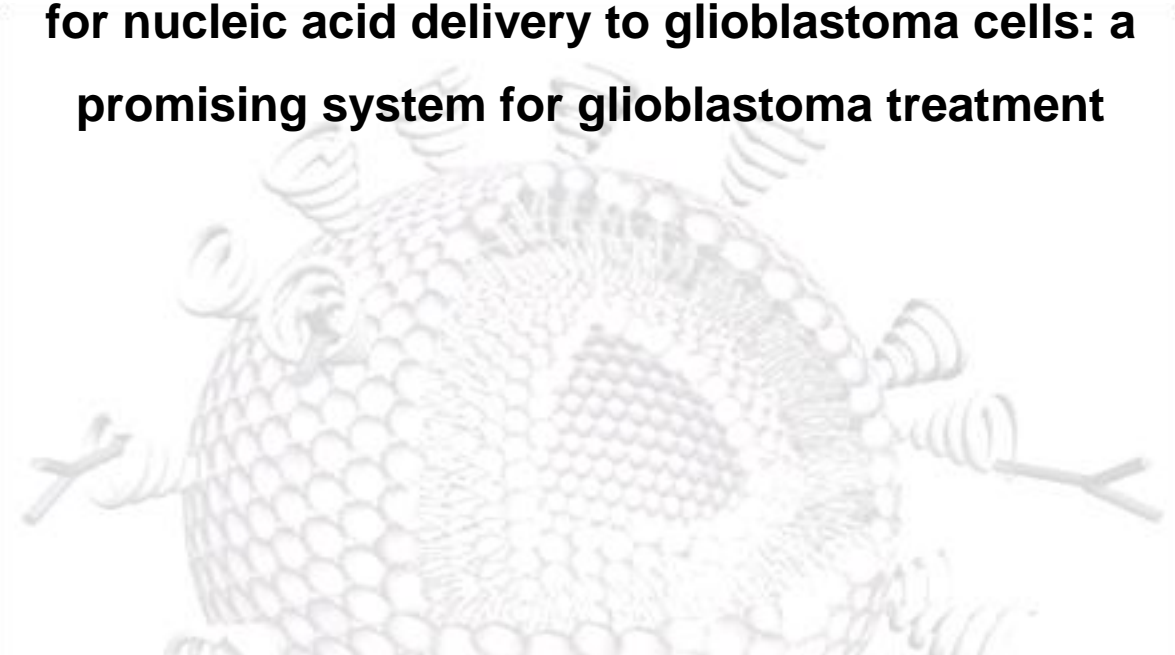
Supplementary Figure 3. MiR-19b and miR-27a expression levels in control and transfected U87 cells. MiR-19b and miR-27a expression levels in U87 cells 48 hours after transfection with anti-miR-21

or scrambled oligonucleotides (n=3), at a final oligonucleotide concentration of 50 or 100 nM. MiRNA expression levels, normalized to the reference U6snRNA, are presented as relative expression values to control untreated cells.

Chapter 4

Tumor-targeted chlorotoxin-coupled nanoparticles for nucleic acid delivery to glioblastoma cells: a promising system for glioblastoma treatment

1. Abstract

The present work aimed at the development and application of a lipid-based nanocarrier for targeted delivery of nucleic acids to glioblastoma (GBM). For this purpose, chlorotoxin (CTX), a peptide reported to bind selectively to glioma cells while showing no affinity for non-neoplastic cells, was covalently coupled to liposomes encapsulating antisense oligonucleotides (asOs) or siRNAs. The resulting targeted nanoparticles, designated chlorotoxin-coupled stable nucleic acid lipid particles, exhibited excellent features for *in vivo* application, namely small size (below 180 nm) and neutral surface charge. Cellular association and internalization studies revealed that attachment of CTX onto the liposomal surface enhanced particle internalization into glioma cells, whereas no significant internalization was observed in non-cancer cells. Moreover, nanoparticle-mediated miR-21 silencing in U87 human GBM and GL261 mouse glioma cells resulted in increased levels of the tumor suppressors PTEN and PDCD4, caspase 3/7 activation and decreased tumor cell proliferation.

Preliminary *in vivo* studies revealed that CTX enhances particle internalization into established intracranial tumors.

Overall, our results indicate that the developed targeted nanoparticles represent a valuable tool for targeted nucleic acid delivery to cancer cells. Combined with a drug-based therapy, nanoparticle-mediated miR-21 silencing constitutes a promising multimodal therapeutic approach towards GBM.

2. Introduction

GBM is the most common and lethal primary brain tumor in humans (4). Despite the ongoing research efforts, current treatment options for GBM are largely unsatisfactory and the prognosis is usually poor, with a 9-12 month median survival time (following diagnosis) that has not improved significantly over the last decade (25, 417). It is therefore important to develop new therapeutical strategies that could encompass both high specificity for tumor cells and complete tumor eradication.

Driven by the tremendous advances in molecular biology, gene therapy constitutes an attractive approach for modulation of the cell genetic background. Regulators of gene transcription and translation operate at multiple levels in order to fine-tune the genome end products. MicroRNAs (miRNAs) are elements of this complex modulatory network that play a pivotal role in cell fate. Dysregulation of several miRNAs (such as miR-21) has indeed been associated with development and progression of several cancers, including GBM (237, 300). Therefore, these small post-transcriptional regulators constitute novel and highly promising targets for anti-tumoral strategies.

Due to their unique characteristics (low size, low immunogenicity, high target affinity), ASOs constitute an important tool for the manipulation of miRNA function in biological systems. In this regard, recent studies (including those reported in our previous manuscript) have shown that miRNA modulation in glioblastoma cells results in decreased tumor cell migration and proliferation, as well as increased cytotoxic effect of anti-neoplastic drugs (463-465). Nevertheless, the successful therapeutic application of oligonucleotide-based therapies to brain cancer requires novel strategies to overcome the barriers imposed by this complex organ. The presence of the blood brain barrier, which restricts entry of therapeutic molecules into the brain (393), and the possible degradation of nucleic acids by nucleases present in the blood constitute major obstacles associated with nucleic acid delivery *in vivo*. It is therefore crucial that oligonucleotides are properly delivered by vehicles that are not only reliable and effective in overcoming cellular and physiological barriers, but are also highly target specific.

Carrier systems, such as viruses or liposomes, have been developed to ensure protection and improvement of nucleic acid delivery into target cells (466-468). Recently, a new class of nucleic acid lipid particles, designated stable nucleic acid lipid particles (SNALPs), were shown (by us and other groups) to be very efficient in delivering siRNAs, both *in vitro* and *in vivo* (469-471). Targeted therapy using peptides coupled to liposomal systems towards overexpressed tumoral receptors enables tumor-specific delivery, while minimizing side effects to normal cells. In this regard, CTX, a scorpion-derived peptide, was

reported as a specific marker for gliomas (472) and is currently used as a targeting agent in imaging studies (as well as in delivery of RNAi therapeutics) (123, 473). Moreover, CTX was reported to bind to MMP-2, a metalloproteinase that is specifically upregulated in gliomas and related cancers, but poorly expressed in brain and normal tissues (474).

In this work, we employed CTX as a ligand to design targeted SNALPs for the delivery of asOs and siRNAs to GBM. Our results show that CTX-coupled SNALPs are more effective (both *in vitro* and *in vivo*) in mediating nucleic acid delivery to tumor cells than their nontargeted counterpart. Moreover, we demonstrate that SNALP-mediated miR-21 silencing in GBM/glioma cells increases the expression of the tumor suppressors PTEN and PDCD4, enhances caspase 3/7 activity, and, importantly, enhances the cytotoxic effect of the anti-angiogenic drug sunitinib.

3. Results

3.1 Preparation and physicochemical characterization of targeted (CTX-coupled) and nontargeted SNALPs

We have previously developed a lipid formulation composed of DODAP/DSPC/Chol/C16 mPEG2000 Ceramide (25:22:45:8, mol %), which was shown to efficiently encapsulate both siRNAs and ASOs (471). Here, LNA-modified ASOs or siRNAs were encapsulated into this lipid formulation. Aiming at achieving specific tumor-targeting and increasing intracellular delivery, the ligand CTX was attached to the liposomal surface by postinsertion of CTX-coupled DSPE-PEG2000 (in a micellar form) into preformed liposomes. In this regard, when liposomes, encapsulating anti-miR-21 oligonucleotides or siRNAs, were incubated with 4 mol % of micelles, values of 5.393 ± 2.826 and 4.967 ± 3.044 nmol CTX/µmol total lipid, respectively, were obtained. As shown in Table 1, the postinsertion step did not interfere with the loading of the encapsulated nucleic acids, since high encapsulation yields were obtained for anti-miR-21 oligonucleotides and siRNA in both targeted (89.30 ± 19.78% and 87.52 ± 11.10%, respectively) and NT (82.17% ± 15.81 and 85.54% ± 17.12) formulations.

Moreover, the SNALPs exhibited a net surface charge close to neutrality, with lower values of zeta potential for NT formulations (encapsulating siRNAs or anti-miR-21 oligonucleotides) as compared with CTX-coupled formulations (Table 1). The presence of

positively-charged lysine residues (from CTX) on the surface of the nanoparticles may explain the differences observed in the zeta potential values between targeted and NT SNALPs.

The developed formulations also revealed capacity to protect the nucleic acid molecules from nuclease degradation, since in the absence of the detergent C12E8, the intercalation of the probe SYBR safe with the encapsulated anti-miR-21 oligonucleotides/siRNAs was reduced by approximately 87 and 92%, respectively.

Results obtained from photon correlation spectroscopy revealed that all formulations exhibited a size under 180 nm, nanoparticles encapsulating siRNAs being generally smaller than those encapsulating anti-miR-21 oligonucleotides, with a narrow distribution (PD index<0.3) (Table 1). The insertion of protein conjugates onto the liposome surface resulted in a small increase of liposomal size: NT liposomes encapsulating anti-miR-21 oligonucleotides or siRNAs exhibited 163.8 ± 24.97 and 130.4 ± 12.56 nm, respectively, whereas CTX-coupled liposomes encapsulating anti-miR-21 oligonucleotides or siRNAs exhibited 178.1 ± 21.04 and 144.4 ± 20.62 nm, respectively. Nevertheless, particle aggregation (and consequent increase in size) was observed for CTX-coupled SNALPs three months after their preparation, whereas particle aggregation was observed to a lesser extent in the NT formulations (data not shown), thus indicating that the presence of CTX may decrease the stability of the formulation over time.

Table 1. Physicochemical characterization of CTX-coupled and NT liposomes encapsulating anti-miR-21 oligonucleotides (anti-miR-21) or anti-survivin siRNAs[a,b].

	CTX-coupled SNALPs				NT SNALPs			
	Size (nm)	PD index[c]	Encapsulation efficiency (%)	Zeta potential (mV)	Size (nm)	PD index	Encapsulation efficiency (%)	Zeta potential (mV)
anti-miR-21	178.1 ± 21.04	0.298 ± 0.1060	89.30 ± 19.78	3.782 ± 1.879	163.8 ± 24.97	0.219 ± 0.1266	82.17 ± 15.81	8.255 ± 2.075
siRNAs	144.4 ± 20.62	0.214 ± 0.1095	87.52 ± 11.10	4.122 ± 2.118	130.4 ± 12.56	0.143 ± 0.052	85.54 ± 17.12	7.652 ± 1.779

[a] Experiments were performed as described in Materials and Methods.

[b] Values are the mean ± SD of at least 3 independent experiments.

[c] Polydispersity index.

3.2 Evaluation of cellular association of SNALPs by flow cytometry

The extent of cellular association of CTX-coupled and NT liposomes encapsulating FAM-labeled anti-miR-21 oligonucleotides was evaluated, by flow cytometry, in the U87 human GBM cell line. Extensive association was observed 4 hours after cell exposure (at 37°C) to CTX-coupled liposomes encapsulating 0.5 µM of oligonucleotides, which was further enhanced when cells were exposed to 1 µM of targeted SNALPs (~75% fluorescent cells, 9.585 ± 4.187 fold increase in fluorescence intensity), when compared to that observed in cells exposed to 1 µM of oligonucleotides encapsulated in NT liposomes (~5% fluorescent cells, 1.564 ± 0.448) (Fig. 1a, b). Similar results were obtained when GL261 mouse glioma cells were incubated with CTX-coupled or NT liposomes encapsulating 0.5 or 1 µM of oligonucleotides (Fig. 1c, d). In contrast, following cell incubation with SNALPs at 4°C (Fig. 1b) or with 1 µM of oligonucleotides, either *per se* or encapsulated in liposomes associated with a smaller amount of CTX (1 mol % of micelles instead of 4 mol %) (data not shown), no significant cellular association was detected.

In order to demonstrate that cellular association of CTX-coupled SNALPs was mediated by specific interaction with cellular receptors, U87 cells were pre-incubated with 20 µM of free CTX to block the CTX receptors. A moderate decrease in cellular association (reflected in the decrease in fluorescence intensity) was observed when cells were exposed to free CTX prior to the addition of CTX-coupled liposomes encapsulating 1 µM of oligonucleotides (7.385 ± 1.941), when compared to that detected in cells exposed to 1 µM of targeted SNALPs (11.25 ± 2.975). Reduced extent of association was also observed in cells exposed to BSA-coupled liposomes encapsulating 0.5 or 1 µM of oligonucleotides (Fig. 1e).

Aiming at evaluating whether CTX-coupled SNALPs would specifically target tumor cells, experiments were performed to determine the extent of their association with the nonmalignant cell line HEK293T (human embryonic kidney). As demonstrated in Figure 1f and g, a significant decrease in the extent of cellular association was observed following incubation with CTX-coupled SNALPs, when compared to that determined in U87 GBM cells exposed to similar amounts of targeted SNALP-formulated oligonucleotides. Similar results were obtained from parallel experiments performed with primary cultures of mouse astrocytes (Supplementary Figure 1).
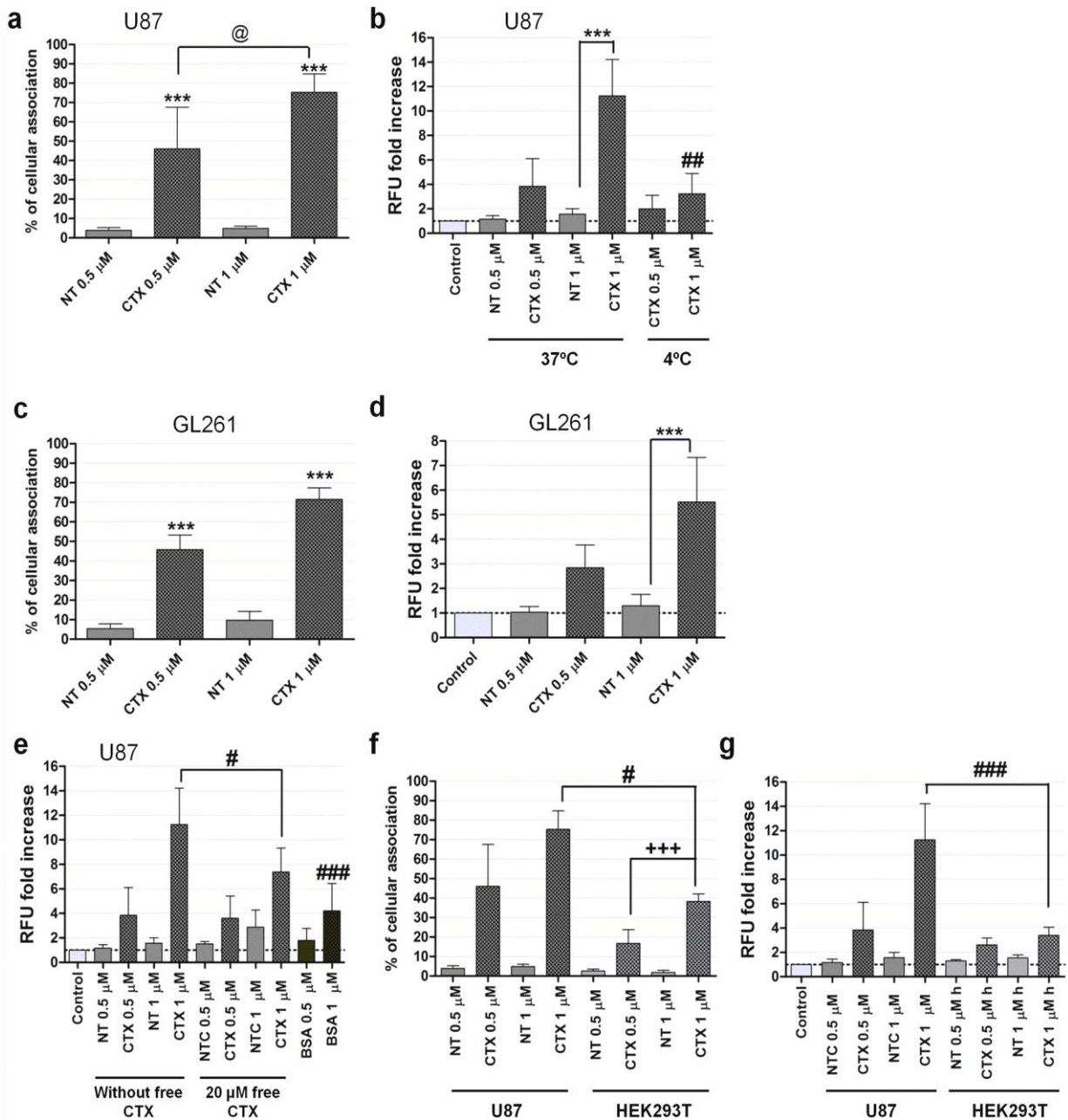
Figure 1. Association of SNALPs with U87 human GBM, GL261 mouse glioma and HEK293T human embryonic kidney cells. Cells were incubated with CTX-coupled (CTX) or nontargeted (NT) liposomes encapsulating FAM-labeled anti-miR-21 oligonucleotides (for 4 hours), rinsed with PBS and prepared for flow cytometry analysis (as described in Materials and Methods). The extent of cell association was assessed only in viable cells, these being gated on the basis of morphological features (including cell volume and complexity). (**a**, **c**) Cellular association and (**b**, **d**) fluorescence intensity plots of (**a**, **b**) U87 and (**c**, **d**) GL261 cells incubated with SNALPs at 4 (U87) and 37ºC (U87, GL261). (**e**) Fluorescence intensity plot of U87 cells exposed to CTX-coupled or NT SNALPs either *per se* (without free CTX) or following pre-incubation with 20 μM of free CTX (20 μM free CTX), or incubated with BSA-coupled liposomes (BSA). (**f**) Cellular association and (**g**) fluorescence intensity plots of U87

and HEK293T cells incubated with CTX-coupled or NT SNALPs at 37ºC. The percentage of cellular association in a, c and f was normalized to control cells (untreated). Relative fluorescence units (RFU) to control cells (untreated) are indicated for b, d, e and g. Values are presented as means ± standard deviation (n=3). *** p<0.001 compared to cells exposed to a similar amount of NT SNALP-formulated oligonucleotides. $^{@}$ p<0.05 compared to cells exposed to 0.5 µM of CTX-coupled SNALP-formulated oligonucleotides. $^{##}$ p<0.01, $^{###}$ p<0.001 compared to U87 cells exposed to 1 µM of CTX-coupled SNALP-formulated oligonucleotides.

3.3 Evaluation of cellular internalization by confocal microscopy

In order to confirm the results obtained on targeting specificity of CTX-coupled SNALPs by flow cytometry, cell internalization studies were performed using confocal microscopy.

The results shown in Figure 2 reveal that following incubation of U87 cells, at 37ºC, with rhodamine-labeled CTX-coupled liposomes encapsulating FAM-labeled anti-miR-21 oligonucleotides, intensive red (lipid) and moderate green (oligonucleotide) fluorescence was detected throughout the cell cytoplasm (Fig. 2b, d), whereas residual fluorescence was detected in the cytoplasm of cells exposed to NT liposomes (Fig. 2a, c).

A similar pattern of internalization was observed in GL261 mouse and F98 rat glioma cells exposed to liposomes encapsulating FAM-labeled oligonucleotides (Supplementary Figure 2), while only residual fluorescence was detected in mouse primary astrocytes (Fig. 2e, f) or HEK293T cells (Fig. 2g, h) incubated under the same conditions. Moreover, reduced internalization was observed upon cell incubation with CTX-coupled liposomes at 4ºC (Fig. 3c, f) or pre-saturation of the CTX receptor with excess of free CTX (20 µM) (Fig. 3b, e), when compared to that observed in cells exposed to CTX-coupled liposomes at 37ºC (Fig. 3a, d).

Although aggregation has been observed for CTX-coupled SNALPs three months after their preparation, these were shown to be effective in delivering anti-miR-21 oligonucleotides to U87 cells (Supplementary Figure 3). Cellular association and internalization studies of liposomes encapsulating siRNAs also revealed enhanced particle uptake in cells exposed to increased concentrations of siRNAs encapsulated in CTX-coupled liposomes, when compared to their NT counterpart (Supplementary Figure 4).

116
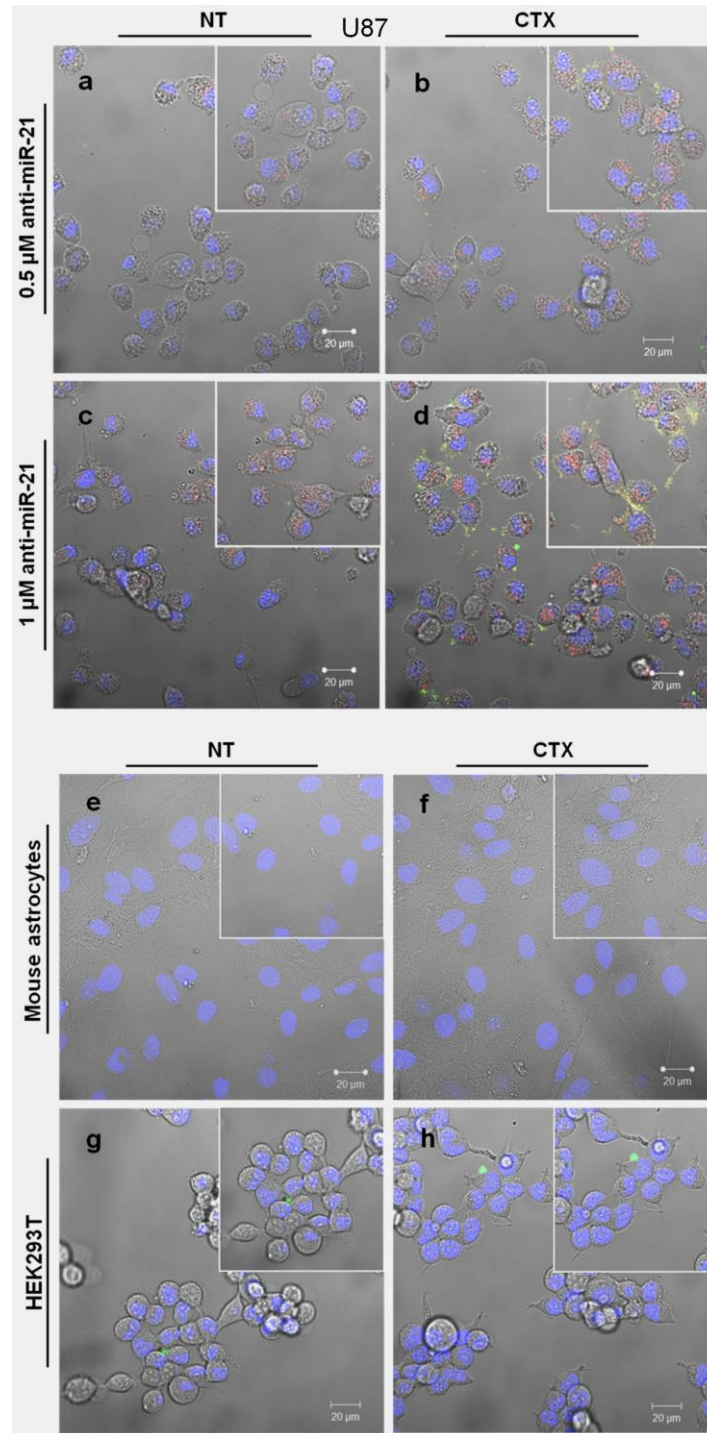
Figure 2. SNALP internalization in U87 GBM cells, HEK293T human embryonic kidney cells and mouse primary astrocytes. Cells were incubated with CTX-coupled (CTX) or nontargeted (NT) liposomes encapsulating FAM-labeled anti-miR-21 oligonucleotides (for 4 hours at 37ºC), rinsed twice with PBS, stained with DNA-specific Hoechst 33342 (blue) and then observed by confocal microscopy. The panel shows representative images at 40× magnification of (**a**, **b**, **c**, **d**) U87 cells incubated with either rhodamine-labeled (**a**, **c**) NT or (**b**, **d**) CTX-coupled liposomes at a final oligonucleotide concentration of (**a**, **b**) 0.5 or (**c**, **d**) 1 µM. The yellow dots are most likely due to the cellular co-

localization of lipid and nucleic acid. Representative images of (**e**, **f**) mouse astrocytes and (**g**, **h**) HEK293T cells incubated with 1 µM of SNALP-formulated oligonucleotides. Results are representative of two independent experiments. Scale corresponds to 20 µm.
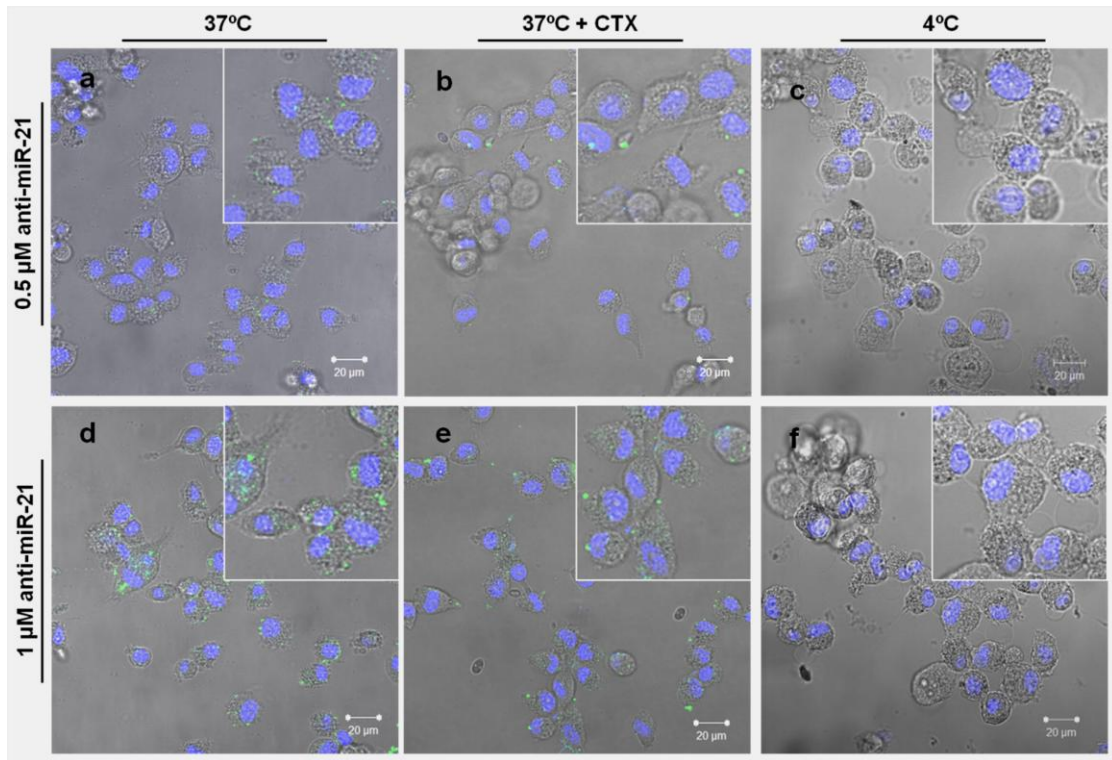
Figure 3. SNALP internalization in U87 GBM cells and effect of cell pre-incubation with free CTX. Cells were incubated with CTX-coupled liposomes encapsulating FAM-labeled anti-miR-21 oligonucleotides (for 4 hours), rinsed twice with PBS, stained with DNA-specific Hoechst 33342 (blue) and then observed by confocal microscopy. The panel shows representative images at 40× magnification of U87 cells exposed to targeted SNALP-formulated oligonucleotides at 37ºC (**a**, **d**) either *per se* (37ºC) or (**b**, **e**) following pre-incubation with 20 µM of free CTX for 1 hour (37ºC + CTX). (**c**, **f**) Cells exposed to targeted SNALP-formulated oligonucleotides at 4ºC. Results are representative of two independent experiments. Scale corresponds to 20 µm.

3.4 MiR-21 silencing mediated by CTX-coupled SNALPs and its effect on the expression of the target proteins PTEN and PDCD4

Having shown that CTX-coupled SNALPs efficiently deliver oligonucleotides to GBM/glioma cells, we evaluated whether intracellularly-delivered anti-miR-21 oligonucleotides could modulate the expression of mature miR-21. As illustrated in Figure 4a and b, incubation of U87 and GL261 cells with 0.25 µM of SNALP-formulated anti-miR-21 oligonucleotides resulted in a significant decrease in miR-21 levels (0.1697 ± 0.2117 and 0.2111 ± 0.0909, respectively), which was further enhanced with increasing concentrations of

anti-miR-21 oligonucleotides (0.5 and 1 µM). Parallel experiments demonstrated that cell exposure to NT liposomes encapsulating anti-miR-21 oligonucleotides did not significantly affect the levels of miR-21 (data not shown).

MiR-21 silencing was also reflected on the expression of two of its targets, the tumor suppressors PDCD4 and PTEN (260, 430). As shown in Figure 4c, a moderate increase in PTEN mRNA levels was observed in both U87 (~15%, $p > 0.05$) and GL261 (25%, $p < 0.05$) cells incubated with 1 µM anti-miR-21 oligonucleotides, as compared to those observed when cells were exposed to a similar amount of scrambled oligonucleotides. Although no significant changes were observed in U87 cells, a small increase in PDCD4 mRNA was obtained in GL261 cells under the same experimental conditions (~20%, $p > 0.05$). More importantly, a considerable and significant increase in PDCD4 protein expression was observed in both U87 (25%, $p < 0.05$) and GL261 (30%, $p < 0.01$) cells incubated with 1 µM of anti-miR-21 oligonucleotides, when compared to that observed in cells transfected with a scrambled sequence (Fig. 4d, e).

119
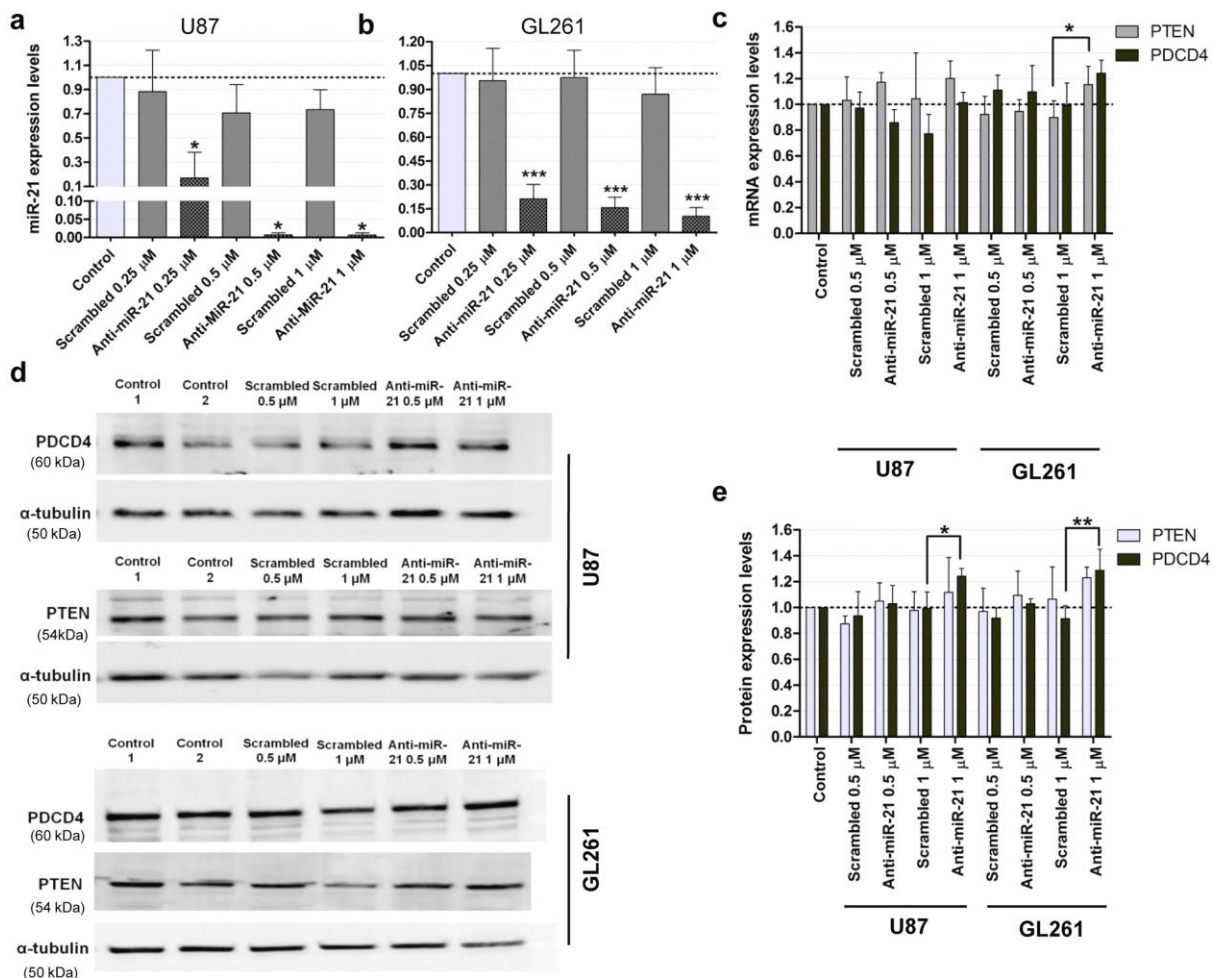
Figure 4. MiR-21 and PTEN/PDCD4 expression in U87 GBM and GL261 glioma cells following incubation with CTX-coupled liposomes encapsulating anti-miR-21 oligonucleotides. (**a**, **b**) MiR-21 and (**c**) PTEN/PDCD4 mRNA expression levels in (**a**) U87 and (**b**) GL261 cells, 48 hours after cell incubation with CTX-coupled liposomes encapsulating anti-miR-21 or scrambled oligonucleotides (n=3). MiR-21 expression levels, normalized to the reference snord44 (human) or snord110 (mouse), and PTEN and PDCD4 expression levels, normalized to the reference HPRT1, are presented as relative expression values to control untreated cells. (**d**) Representative gel showing PTEN and PDCD4 protein levels in U87 (upper panel) and GL261 (lower panel) cells 48 hours after cell incubation with CTX-coupled liposomes encapsulating anti-miR-21 or scrambled oligonucleotides (n=3). (**e**) Quantification of PTEN and PDCD4 bands observed in d, corrected for individual α-tubulin signal intensity. Results are presented as PTEN and PDCD4 expression levels relative to control. Values are presented as means ± standard deviation (n=3). * p<0.05, ** p<0.01, *** p<0.001 to cells incubated with a similar amount of CTX-coupled liposomes encapsulating scrambled oligonucleotides.

Similarly to what was observed with the intracellularly delivered anti-miR-21 oligonucleotides, CTX-coupled liposome-mediated anti-survivin-siRNA delivery resulted in decreased levels of survivin mRNA (Supplementary Figure 4).

3.5 Evaluation of caspase activation and apoptosis in tumor cell lines with reduced miR-21 expression

Since an inverse correlation between the expression of the anti-apoptotic miR-21 and the pro-apoptotic tumor suppressors PTEN and PDCD4 was observed in U87 GBM and GL261 glioma cells, we sought to determine the biological effect of miR-21 silencing on these cells. For this purpose, we investigated whether miR-21 silencing mediated by CTX-coupled SNALPs would affect the activity of the effector caspases 3 and 7, crucial components of the apoptotic cell death.

As shown in Figure 5a, incubation of U87 and GL261 cells with 1 µM of SNALP-formulated anti-miR-21 oligonucleotides resulted in a two-fold increase (~1.76 and 1.66, respectively) in caspase 3/7 activity (p>0.05), as compared to that observed upon incubation to SNALP-formulated scrambled oligonucleotides. More importantly, silencing of miR-21 followed by cell exposure to 15 (U87) and 5 (GL261) µM of the tyrosine kinase inhibitor sunitinib resulted in a considerable increase in caspase 3/7 activity (5.33 ± 2.263 and 4.847 ± 1.941, respectively), when compared to that observed for cells exposed to sunitinib, either *per se* (1.643 ± 0.696 and 2.084 ± 0.836) or in combination scrambled oligonucleotides (2.141 ± 1.133, p<0.01 and 2.909 ± 0.807, p>0.05).

120

Furthermore, an increase in the percentage of late apoptotic (p>0.05) and necrotic cells (p<0.05) was observed in U87 cells incubated with 1 µM of SNALP-formulated anti-miR-21 oligonucleotides (Fig. 5b, d), compared to that observed for cells incubated to 1 µM of SNALP-formulated scrambled oligonucleotides (Fig. 5b, c). The presence of sunitinib, a fluorescently active molecule, interfered with the cytometric detection of FAM-labeled annexin V (a specific marker for cells undergoing apoptotic cell death) and propidium iodide (a probe that intercalates with DNA in cells with compromised cell membrane) and, therefore, no information could be obtained about apoptotic cell death in the presence of sunitinib.

3.6 Evaluation of tumor cell death following miR-21 silencing

We further evaluated whether the increase in tumor suppressor expression and caspase activity observed following SNALP-mediated miR-21 silencing would correlate with changes in tumor cell proliferation.

Initial experiments were performed by exposing GL261 cells to different concentrations of sunitinib for 24 hours (Supplementary Figure 5), in order to determine the optimal concentration of drug to be used in the assay. As demonstrated in Figure 5e, a small decrease in cell viability was observed when U87 cells were incubated with 1 µM of SNALP-formulated anti-miR-21 oligonucleotides (82.12 ± 5.663), as compared to that observed for cells incubated with the same formulation encapsulating 1 µM of scrambled oligonucleotides (86.31 ± 6.701, p>0.05). Remarkably, a considerable decrease in the percentage of viable cells was observed when cells were exposed to 1 µM of anti-miR-21 oligonucleotides and further exposed to sunitinib (70.25 ± 12.29), when compared to that observed upon exposure to sunitinib, either *per se* (80.23 ± 8.081, p>0.05) or in combination with 1 µM of scrambled oligonucleotides (78.49 ± 8.051, p<0.05).

A significant decrease in the percentage of viable cells was also observed when GL261 cells were incubated with 1 µM of anti-miR-21 oligonucleotides and further exposed to sunitinib when compared to that observed upon exposure to sunitinib *per se* (~8% decrease, Fig. 5e).
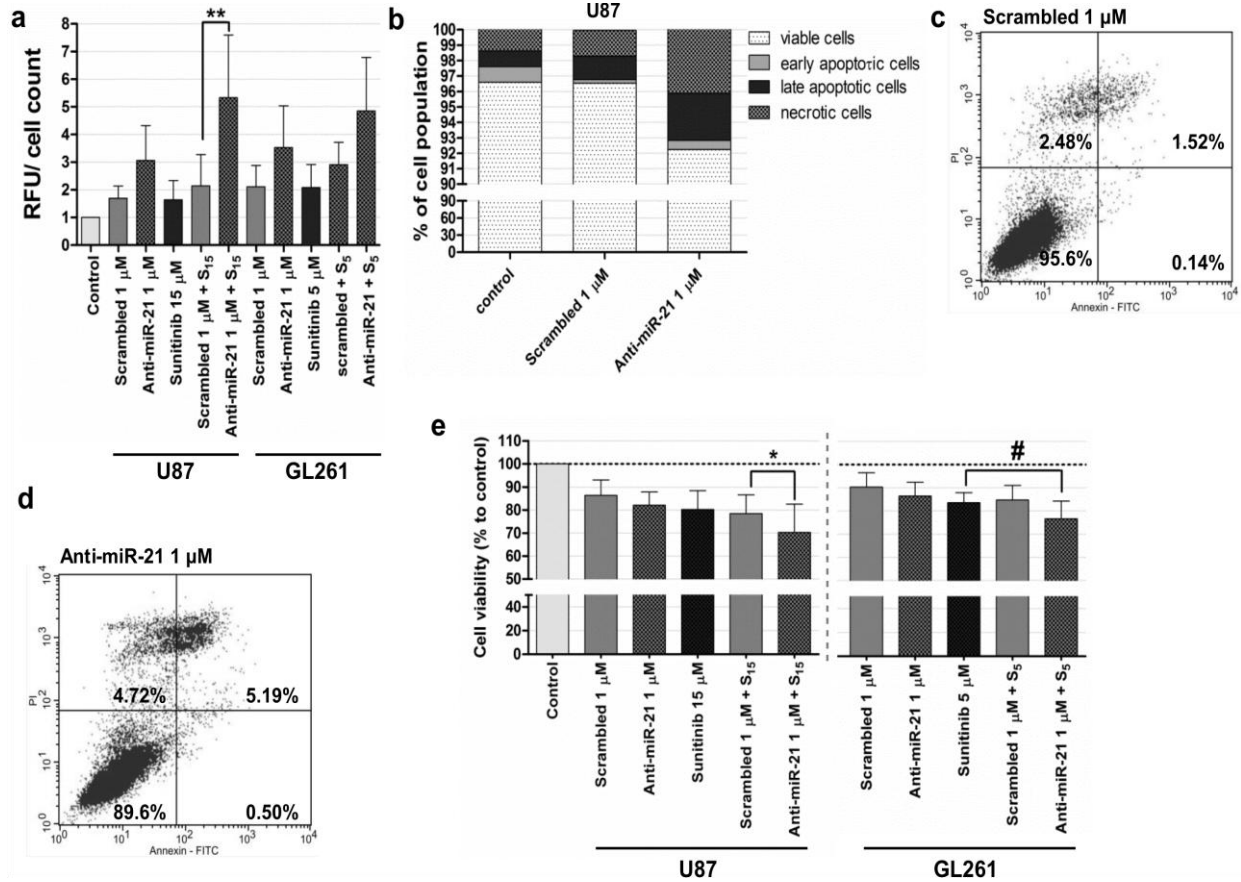
Figure 5. Evaluation of caspase activation, apoptosis and tumor cell proliferation in U87 GBM and GL261 glioma cells. Cells were incubated with CTX-coupled liposomes encapsulating anti-miR-21 or scrambled oligonucleotides for 4 hours, washed with PBS and further incubated for 24 hours with fresh medium. Cells were subsequently exposed to 15 (U87) or 5 µM (GL261) of sunitinib for 24 hours, rinsed with PBS, after which caspase/cell death detection and cell viability assays were performed. (**a**) Caspase 3/7 activity in U87 and GL261 cells incubated with 1 µM of SNALP-formulated anti-miR-21 or scrambled oligonucleotides, either *per se* or in combination with sunitinib. Results, presented as relative fluorescence units (RFU) with respect to control untreated cells, were normalized for the number of cells in each condition. (**b**) Cell death detection in U87 cells exposed to 1 µM of SNALP-formulated anti-miR-21 or scrambled oligonucleotides. For each condition (control, scrambled/anti-miR-21 1 µM), results are presented as percentage of viable, early/late apoptotic and necrotic cells. Representative cell death plots for U87 cells incubated with SNALP-formulated (**c**) scrambled and (**d**) anti-miR-21 oligonucleotides. The percentage of viable (lower left), early apoptotic (lower right), late apoptotic (upper right) and necrotic (upper left) cells in the cell population is indicated in the plots. (**e**) Cell viability, evaluated by the Alamar Blue assay (as described in Materials and Methods) immediately after cell incubation with sunitinib. Values are presented as means ± standard deviation (n=3). Scrambled/anti-miR-21 1 µM + $S_{15/5}$: cells transfected with scrambled or anti-miR-21 oligonucleotides and further incubated with 15 or 5 µM sunitinib. [**] p<0.01 compared to cells incubated with SNALP-formulated scrambled oligonucleotides and further treated with 15 µM sunitinib.

3.7 Characterization of the glioma mouse model and intravenous injection of SNALP-formulated siRNAs

Following the demonstration of the efficacy of CTX-coupled SNALPs to deliver LNA-modified ASOs (and siRNAs) to glioma cells, studies were addressed to investigate whether the developed nanoparticles would be efficient in delivering their encapsulated contents to intracranial tumors when administered via systemic route. For this purpose, we employed a previously developed (and characterized) mouse glioma model that displays molecular and histopathological features of human GBM (475). The stereotactic injection of 1.25×10^5 GL261 cells resulted in the formation of tumors, microscopically visible after 10 days, with an average tumor size of 75.47 ± 18.89 mm^3 twenty-days after tumor implantation (Fig. 6a, b).

Intravenous administration of SNALP-formulated siRNAs (through the tail vein) was performed 14 days after tumor cell implantation (Fig. 6c), so that the tumor could reach a volume which would allow achieving a therapeutic effect with potential clinical impact. As shown in Figure 6d, increased fluorescence intensity was detected in tumors of animals injected with CTX-coupled SNALPs (9.182 ± 2.896), when compared to that detected in tumors of animals injected with NT SNALPs (5.739 ± 2.224, $p < 0.05$) or saline solution. Increased fluorescence was also detected in the liver of animals injected with CTX-coupled or NT SNALPs, when compared to that detected in animals injected with PBS (Fig. 6e).
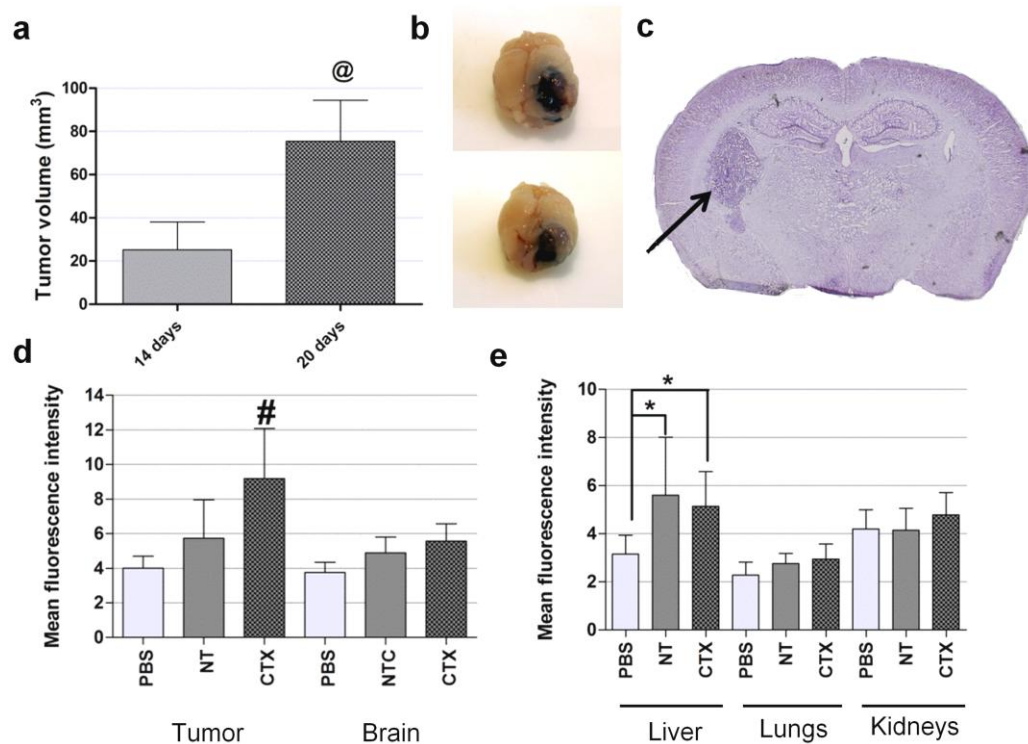
Figure 6. Tumor characterization and biodistribution analysis of systemically-administered liposome-formulated FAM-labeled siRNAs. Following tumor implantation, animals (n=3) were sacrificed at defined time points (10, 14 and 20 days), the brains were removed and fixed in 4% PFA, frozen and further processed for histological evaluation, as described in Materials and Methods. (**a**) Average tumor volume (calculated as described in Materials and Methods) on the day of animal sacrifice. Unpaired t-test with Welch's correction was used to calculate the statistical significance. (**b**) Representative photographs of GL261 tumors 20 days after implantation and (**c**) representative image of a 20 µm-thick tumor section (14 days after tumor implantation), stained with cresyl violet and observed under a light microscope. The scale corresponds to 5000 µm. Flow cytometry analysis (fluorescence intensity plots) of (**d**) tumor, brain and (**e**) liver, kidney and lung homogenates from animals injected intravenously with CTX-coupled/NT liposomes encapsulating FAM-labeled siRNAs or saline solution (PBS). The protocol for intravenous administration and tissue processing is described in Materials and Methods, as well as in Supplementary Material. The extent of cellular association was assessed only in viable cells, these being gated on the basis of morphological features (including cell volume and complexity). Relative fluorescence units (RFU) are indicated for d and e. Values are presented as means ± standard deviation. [@] $p < 0.05$ compared to the tumor volume of animals sacrificed 14 days after tumor implantation. [#] $p < 0.05$ compared to animals injected with a similar amount of NT SNALP-formulated siRNAs. * $p < 0.05$ compared to animals injected with PBS.

4. Discussion

Despite the potential of nucleic acid-based strategies to generate highly specific and biocompatible drugs, these molecules have intrinsic limitations that restrain their *in vivo* administration, namely poor pharmacokinetics, fast blood clearance and inability to target specific tissues or cells. Non-viral vectors, namely cationic liposomes, were developed to improve both nucleic acid protection and the biodistribution profile, while enhancing uptake by the target cells. Despite being extensively utilized in vitro and in vivo, clinical application of cationic liposomes is limited by their large size and impaired ability to reach tissues beyond the vasculature, unless directly injected into the tissue (476). Advances in lipid chemistry and liposome preparation enabled the development of a new class of lipid-based carriers, designated stable nucleic acid lipid particles (SNALPs), which was found to be very efficient for in vivo delivery of siRNAs and ASOs (471, 477, 478).

In this work, we generated tumor-targeted stabilized liposomes encapsulating either LNA-modified anti-miR-21 oligonucleotides or siRNAs, and evaluated their biological activity in different glioma cell lines. In accordance with previously reported studies (477, 479), high encapsulation yields were obtained for both ASOs and siRNA (Table 1), which can be attributed to the inclusion in the formulation of DODAP, an ionizable lipid that is positively charged at pH 4 and was shown to improve nucleic acid entrapment (477). Moreover, the developed liposome formulation exhibited a net surface charge close to neutrality (Table 1),

which is extremely important for successful *in vivo* application, as it reduces their ability to interact with serum proteins involved in the early clearance from the blood stream (480), thus increasing particle bioavailability.

The attachment of CTX onto the liposomal surface, performed at 39°C in order to avoid peptide denaturation and consequent decrease in biological activity, resulted in low yields of peptide-conjugate insertion (onto the liposomal surface). However, the obtained values are in agreement with those reported in studies involving transferrin-targeted liposomes (471), which may be due to the similar temperature used in the postinsertion step and the similar amount of CerC16 mPEG incorporated in the preformed liposomes (8 mol %). Increased particle size was also observed following CTX attachment onto the surface of liposomes encapsulating ASOs or siRNAs. Nevertheless, all formulations exhibited sizes below 180 nm and homogeneous particle size distribution (Table 1).

Taken together, our observations indicate that CTX-coupled SNALPs display optimal physicochemical properties for an *in vivo* application, including high encapsulation efficiency, low size, electrical neutrality and high protection against enzymatic degradation.

The stability of the generated nanoparticles was also reflected in their capacity to interact with the target cells. Cellular association and internalization studies demonstrated that the attachment of CTX to the liposomal surface (at 4 mol %) strongly enhanced uptake of the targeted SNALPs in U87 GBM and GL261 glioma cells, when compared to their nontargeted counterpart (Figs. 1 and 2). The gradual increase in association and internalization of targeted liposomes encapsulating 0.5 and 1 µM of anti-miR-21 oligonucleotides and the decreased association observed for SNALPs coupled to a smaller amount of CTX (1 mol %), suggests that the extent of cellular uptake was also dependent on the concentration of CTX. Furthermore, a moderate decrease in cellular association and internalization was observed in cells either incubated with 20 µM of free CTX (to saturate the CTX receptor) prior to the addition of CTX-coupled SNALPs, or exposed to BSA-coupled SNALPs (Fig. 1), thus suggesting that the cellular uptake was peptide-specific, although unspecific binding may also be responsible for the internalization of a small fraction of the nanoparticles.

Cellular association of CTX-coupled SNALPs was strongly inhibited when incubations were performed at 4°C (Figs. 1 and 3), which indicates that an energy-dependent process, most likely receptor-mediated endocytosis is involved in the uptake of the targeted nanoparticles. Importantly, reduced extent of cellular association was observed in non-cancer HEK293T human kidney cells and mouse astrocytes (Figs. 1 and 2), which indicates that the

125

interaction of CTX-coupled liposomes with the target cells was mostly tumor cell-specific. This observation may be of great relevance for clinical application, as it strongly indicates that the developed CTX-coupled formulation is internalized by tumor cells while sparing normal tissues, thus reducing the toxicity associated with its systemic administration.

Increased cellular association and internalization, as well as a significant decrease in the mRNA levels of survivin, were also obtained in cells exposed to CTX-coupled liposomes encapsulating anti-survivin siRNAs, when compared to their targeted counterpart (Supplementary Figure 4), which provides evidence that the targeted nanoparticles are very efficient in delivering not only LNA-modified ASOs but also siRNAs to GBM/glioma cells.

While cellular association and internalization studies demonstrated that CTX enhances tumor cell uptake of liposomes encapsulating anti-miR-21 oligonucleotides or siRNAs, it is important to demonstrate that increased nanoparticle internalization results in alterations in the cell's biological functions. Several reports suggested that the incorporation of high percentages of CerC16-PEG2000 in stabilized liposomes may result in the loss of activity of the encapsulated siRNAs or antisense oligonucleotides (469, 481, 482). The steric barrier imposed by PEG inhibits the interaction of liposomes with the endosomal membrane, which is essential for endosomal membrane destabilization and the subsequent release of the entrapped nucleic acids. In this regard, our results indicate that incorporation of 8 mol% of CerC16-PEG2000 in the developed formulation allows liposomal size stability without compromising the release of anti-miR-21 oligonucleotides into the cell cytoplasm, where the miRNA processing machinery is located.

In accordance with previous studies (30, 31), we demonstrate that targeted liposome-mediated anti-miR-21 delivery efficiently reduces miR-21 expression levels, thus increasing the expression of the tumor suppressor PTEN and PDCD4 (Fig. 4), whose loss of expression (frequently observed in glioma) results in dysregulation of important signaling pathways that control cell proliferation, growth, differentiation and survival (304, 445, 448). In contrast, cell incubation with NT liposomes encapsulating anti-muR-21 oligonucleotides did not significantly affect the levels of miR-21, which indicates that the presence of CTX in the formulation is crucial to achieve a biological effect.

The increased tumor suppressor expression and caspase 3/7 activity detected in U87 and GL261 cells with decreasing miR-21 levels not only provides evidence that CTX-coupled SNALPs are biologically active, but may also render the cells susceptible to drugs targeting other signaling pathways governing GBM tumorigenesis. In this regard, several *in vitro* studies (including our own) have already shown that miR-21 modulation potentiates the

126

cytotoxic effect of anti-neoplastic drugs (451, 452, 463), which may be of great importance to overcome treatment resistance, one of the major unsolved problems in clinical oncology. The observation of increased cytotoxic effect of sunitinib, a drug currently being tested in several phase II clinical trials for GBM (33), following miR-21 silencing in U87 GBM and GL261 glioma cells via the generated CTX-coupled SNALPs (Fig. 5), not only confirms the results obtained in our previously published studies, but enforces the huge potential of combining targeted liposome-mediated miR-21 silencing and anti-angiogenic therapy, which may translate into meaningful therapeutics that benefit cancer patients.

Due to limitations inherent to *in vitro* models, the results from cell culture experiments should be validated in a reliable animal model of disease. Several reports have shown that the efficacy of *in vivo* tumor internalization of liposomes may be independent of the presence of a targeting ligand. Studies by Moreira and colleagues (483) revealed that while antagonist G-targeted liposomes enhanced *in vitro* uptake, their tumor accumulation was similar to that observed for the NT liposomes. Similarly, Bartlett et al. demonstrated that transferrin-targeted and nontargeted siRNA nanoparticles exhibited similar biodistribution and tumor accumulation, with increased biological activity (reduction in tumor luciferase activity by 50%) being observed for the targeted formulation (484). In opposition, our results from experiments on the intravenous administration of SNALP-formulated siRNAs indicated that CTX enhances the tumor internalization of the nanoparticles, when compared to their nontargeted counterpart (Fig. 6). Further studies involving SNALP-mediated anti-miR-21 intravenous administration, either *per se* or in combination with sunitinib, should ascertain the biological effect and tumor cell-killing potential of both targeted and nontargeted formulations.

Increased uptake of both CTX-coupled and NT SNALPs was also detected in the liver of animals following intravenous injection, when compared to that detected in animals injected with PBS (Fig. 6), thus suggesting that nonspecific particle retention occurs in organs involved in blood clearance (liver). This observation was not surprising since several studies involving stabilized lipid-based nanoparticles (containing nucleic acids) have already shown that these particles generally accumulate in firstpass organs, namely the liver, spleen and lungs (470, 479, 485).

Overall, the results presented in this study demonstrate that the developed CTX-coupled SNALPs not only exhibit adequate physicochemical properties for intravenous administration, but also enhance the delivery of anti-miR-21 oligonucleotides to different glioma cell lines and intracranial tumors, while revealing reduced affinity for non-cancer cells.

Moreover, the molecular and cellular alterations that resulted from SNALP-mediated miR-21 silencing, including increased tumor-suppressor expression and caspase activity, as well as increased cytotoxic activity of sunitinib, indicate that a multimodal SNALP-mediated therapeutic approach, combining miRNA silencing with anti-angiogenic chemotherapy deserves to be explored in pre-clinical and clinical applications.

5. Materials and methods

Materials

Sunitinib malate (Sutent®) was kindly offered by Pfizer (Basel, Switzerland). The lipids 1,2-dioleoyl-3-dimethylammonium-propane (DODAP), 1,2-distearoyl-sn-glycero-3-phosphocholine (DSPC), N-palmitoyl-sphingosine-1-(succinyl(methoxypolyethylene glycol) 2000) (C16 PEG2000 Ceramide), 1,2-distearoyl-sn-glycero-3-phospatidylethanolamine-N-(maleimide (polyethylene glycol)-2000) ammonium salt (DSPE-PEG-MAL), L-α-phosphoethanolamine-N-(lissamine rhodamine B sulfonyl) (Rho-PE) and 1,2-dipalmitoyl-*sn*-glycero-3-phosphoethanolamine-N-(7-nitro-2-1,3-benzoxadiazol-4-yl) ammonium salt (NBD-PE) were acquired from Avanti Polar Lipids (Alabaster, AL, USA).

The locked nucleic acid (LNA)-modified anti-miR-21, FAM-labeled anti-miR-21 and noncoding (scrambled) oligonucleotides were acquired from Exiqon (Vedbaek, Denmark). The anti-survivin siRNA (486) was obtained from Dharmacon (Lafayette, CO, USA). All sequences are displayed in Supplementary Table S1. The 36 aminoacid peptide chlorotoxin (MCMPCFTTDHQMARKCDDCCGGKGRGKCYGPQCLCR) (487) was synthesized by Genecust (Dudelange, Luxembourg). All other reagents were obtained from Sigma unless stated otherwise.

Cell lines and culturing conditions

The F98 rat and GL261 mouse glioma cell lines were kindly donated by Dr. Hélène Elleaume (European Synchrotron Radiation Facility, Grenoble, France) and Dr. Perez-Castillo (Universidad Autónoma de Madrid, Madrid, Spain), respectively; the U87 human GBM cell line was a kind gift from Dr. Peter Canoll (Columbia University, New York, USA). HEK293T human embryonic kidney cells were obtained from the American Type Culture Collection (Manassas, VA, USA). Cells were maintained in DMEM containing 4.5 g/L glicose (Invitrogen,

Carlsbad, CA, USA) supplemented with 10% heat-inactivated FBS (Gibco, Paisley, Scotland), 100 U/mL penicillin (Sigma), 100 µg/mL streptomycin (Sigma), 10 mM HEPES and cultured at 37°C under a humidified atmosphere containing 5% CO_2. Primary mouse cortical astrocyte cultures were prepared from the cerebral cortices of newborn pups according to established protocols (453). Cell plating densities that are not included in the Materials and Methods section are indicated in Supplementary Material.

Preparation of liposomes encapsulating LNA-modified antisense oligonucleotides or siRNAs

The preparation of liposomes encapsulating ASOs or siRNAs was performed as described previously (469, 471), with a few modifications. Thirteen micromoles of a lipid mixture composed of DODAP:CHOL:DSPC:CerC16-PEG2000 (25:45:22:8, % molar ratio to total lipid) in 200 µL of absolute ethanol were slowly added, under strong vortex, to 0.086 µmol of anti-miR-21, 0.116 µmol of scrambled oligonucleotides or 0.041 µmol of anti-survivin siRNAs in 300 µL of 20 mM citrate buffer (pH 4), previously heated at 60ºC. The final charge ratio of the preparation was 2:1 (cationic lipid:ASOs). The resulting particles were extruded 21 times through 100-nm-diameter polycarbonate membranes, using a LiposoFast basic extruder (Avestin, Toronto, Canada). The removal of ethanol and nonencapsulated ASOs or siRNAs was carried out by running extruded nanoparticles through a Sepharose CL-4B column equilibrated with HEPES buffered saline (HBS) (20 mM HEPES, 145 mM NaCl, pH 7.4). Subsequently, the total lipid concentration was assessed by cholesterol quantification, using the Liebermann-Burchard test (488). Briefly, 150 µL of Liebermann-Burchard reagent were added to 5 µL of sample (in a 96-well plate) followed by incubation at 37ºC for 30 min. Absorbance was measured at 625 nm in a spectrophotometer and the concentration was determined from a standard curve for cholesterol content.

Preparation and purification of targeted SNALPs

CTX-coupled (targeted) SNALPs were prepared by the postinsertion method (471, 489). Briefly, CTX was modified with the addition of thiol groups upon reaction with freshly prepared 2-iminothiolane hydrochloride (2-IT, in HBS pH 8), at a molar ratio of 1:10 (CTX:2-IT). The reaction occurred under gentle stirring for 1 h, in the dark at room temperature (RT). Thiolated CTX was then coupled to DSPE-PEG-MAL micelles, prepared in MES buffer pH 6.5

(471), by a thioesther linkage (1:1, protein:DSPE-PEG-MAL molar ratio). The coupling reaction was performed overnight (at RT), in the dark with gentle stirring. For the nontargeted SNALPs (NT), postinsertion was performed with plain micelles (without conjugated ligand), which were prepared by adding HBS (pH 8.0) to the DSPE-PEG-MAL micelles. The neutralization of free maleimide groups in the micelles was carried out upon incubation with β-mercaptoethanol at a maleimide:β-mercaptoethanol molar ratio of 1:5, under stirring for 30 min (at RT). The insertion of CTX-DSPE-PEG-MAL conjugates or plain DSPE-PEG-MAL micelles onto the preformed liposomes, at 1 or 4 mol % (relative to the total lipid concentration), was performed upon incubation in a water bath at 39°C for 16 h (in the dark).

Targeted and NT SNALPs were purified by size exclusion chromatography on a Sepharose CL-4B column, using HBS (pH 7.4) as running buffer to remove nonconjugated micelles and chemical reagents used during SNALPs preparation.

Characterization of the SNALPs

The final total lipid concentration was assessed by cholesterol quantification (using the Liebermann-Burchard test), as described above. The quantification of encapsulated ASOs/siRNAs was performed with the DNA-intercalating probe SYBR® Safe (Life Technologies, USA), in the presence of the detergent octaethylene glycol monododecyl ether (C12E8) (Sigma). The encapsulation efficiency was calculated from the formula ((asO/total lipid) final molar ratio/(asO/total lipid) initial molar ratio) × 100. The extent of nucleic acid protection resulting from the encapsulation of the ASOs/siRNAs into the liposomes was determined by evaluating the ability of the SYBR® Safe probe to intercalate into the ASOs/siRNAs in the absence of C12E8. The amount of CTX associated with the SNALPs determined using with the BCA Protein Assay Kit (Pierce, Rochford, IL, USA) from a CTX standard curve (at 562 nm), in a microplate reader (SpectraMax Plus 384, Molecular devices). The insertion efficiency was calculated from the formula ((CTX/total lipid) final molar ratio/(CTX/total lipid) initial molar ratio) × 100. SNALPs size distribution was assessed by photon correlation spectroscopy, using an N5 submicrometer particle size analyzer (Beckman Coulter, Miami, FL, USA). Measurements were made at a 90° angle and at 20°C. Zeta potential measurements of targeted and NT SNALPs were performed at RT, using a Zetasizer Nano ZS™ (Malvern Instruments, UK).

Assessment of cellular association by flow cytometry

To evaluate the extent of cellular association of the SNALPs, cells were plated onto 48-well plates at densities of 5.5×10^4 (HEK293T), 5×10^4 (U87) and 4.5×10^4 cells/well (GL261, mouse astrocytes). Twenty-four hours after plating, cells were incubated with targeted (CTX-coupled or bovine serum albumin (BSA)-coupled) or NT liposomes encapsulating FAM-labeled anti-miR-21 oligonucleotides, for 4 h at 4 or 37°C. Subsequently, cells were washed twice with cold phosphate buffer saline (PBS, pH 7.4), detached by exposure to trypsin (5 min, 37ºC) and further washed twice with PBS. Cells were then ressuspended in 350 µL of cold PBS and immediately analyzed in a FACS Calibur flow cytometer (BD, Biosciences). FAM fluorescence was evaluated in the FL-1 channel and a total of 20,000 events were collected (unless otherwise stated). The data were analyzed by Cell Quest software (BD).

Assessment of cellular association by confocal microscopy

To assess the extent of cellular internalization of the SNALPs, cells were plated onto ibiTreat 8-well slides (Ibidi, Munich, Germany) at densities of 3.5×10^4 (HEK293T), 3×10^4 (U87, GL261, F98) and 2.5×10^4 cells/well (mouse astrocytes). Twenty-four hours after plating, cells were incubated with CTX-coupled or NT liposomes encapsulating FAM-labeled anti-miR-21 oligonucleotides, for 4 hours at 4 or 37°C. Cells were rinsed twice with PBS, stained with the DNA binding dye Hoechst 33342 (Molecular Probes, Oregon, USA) (1 µg/mL) for 5 min (in the dark), rinsed twice with PBS and maintained in this saline solution for image acquisition. Confocal images were acquired in a point scanning confocal microscope Zeiss LSM 510 Meta (Zeiss, Germany), as described in Supplementary Material.

Cell transfection with anti-survivin or scrambled siRNAs

For transfection with siRNAs, complexes of siRNAs with Lipofectamine RNAiMax (Invitrogen) were prepared, following the manufacturer's instructions, and added to cells, maintained in OptiMEM medium (Gibco), at a final concentration of 50 or 100 nM siRNA. After incubation for 4 hours, cells were washed with PBS and further cultured in fresh DMEM medium for 48 hours.

RNA extraction and cDNA synthesis

RNA extraction and cDNA synthesis for miRNA and mRNA quantification were performed as described previously (463). The detailed protocol is provided in Supplementary Material.

QPCR quantification of miRNA expression

MiRNA quantification was performed in an iQ5 thermocycler using 96-well microtitre plates and the SYBR® Green Master Mix (Exiqon). The primers for miR-21 and references snord110 (mouse) and snord44 (human) were also acquired from Exiqon. For each primer set, a master mix was prepared containing a fixed volume of SYBR Green master mix and the appropriate amount of each primer. For each reaction, performed in duplicate, 6 µL of master mix were added to 4 µL of template cDNA. Reaction conditions consisted of enzyme activation and well-factor determination at 95°C for 10 min, followed by 40 cycles at 95°C for 10 s (denaturation) and 60 s at 60°C (annealing and elongation). The melting curve protocol started immediately after and consisted of 1 min heating at 55°C followed by eighty 10 s steps, with 0.5°C increases in temperature at each step. Threshold values for threshold cycle determination (Ct) were generated automatically by the iQ5 Optical System Software. Relative miRNA levels were determined following the Pfaffl method for relative miRNA quantification in the presence of target and reference genes with different amplification efficiencies (458). The protocol for qPCR quantification of mRNA is provided in Supplementary Material.

Western blot analysis

The preparation of protein extracts and protein quantification were performed as described previously (463) and in Supplementary Material. Twenty-five micrograms of total protein were resuspended in loading buffer (20% glycerol, 10% SDS, 0.1% bromophenol blue), incubated for 5 min at 95ºC and loaded onto a 10% polyacrylamide gel for electrophoretic separation. After electrophoresis the proteins were blotted onto a PVDF membrane, which was blocked in 5% nonfat milk and further incubated with an anti-PTEN or anti-PDCD4 (1:1000) (Cell Signaling, Beverly, MA, USA) overnight at 4ºC, and with the appropriate alkaline phosphatase-labeled secondary antibody (1:20000) (Amersham,

Uppsala, Sweden) for 2 h at room temperature. Equal protein loading was shown by reprobing the membrane with an anti-α-tubulin antibody (1:10000) (Sigma) and with the same secondary antibody. The blots were washed several times with TBS/T (25 mM Tris-HCl, 150 mM NaCl, 0.1% Tween-20), incubated with ECF (alkaline phosphatase substrate) for 5 min (at RT) and then submitted to fluorescence detection at 570 nm using a VersaDoc Imaging System Model 3000 (Bio-Rad). For each membrane, the band intensity was analyzed using the ImageJ software (490).

Evaluation of caspase 3/7 activity

Caspase-3/7 activity was assessed using the SensoLyte homogenous AMC caspase-3/7 assay (AnaSpec, San Jose, CA, USA), as described previously (463). The detailed protocol is provided in Supplementary Material.

Evaluation of apoptotic cell death

The detection of apoptosis was performed in U87 cells using the FITC Annexin V Apoptosis Detection Kit II (BD Pharmingen, San Diego, CA, USA). Briefly, 48 hours after SNALP-mediated oligonucleotide transfection or immediately after exposure to sunitinib, cells were detached using trypsin, washed twice with cold PBS and resuspended in 1X Binding Buffer at a concentration of 1×10^6 cells/mL. From this suspension, 1×10^5 cells were transferred to 5 mL polystyrene tubes, followed by the addition 5 μL of FITC Annexin V and 5 μL PI and cells were then incubated for 15 min (at RT), in the dark. Four-hundred microliters of 1X Binding Buffer were added to each tube and the samples were immediately analyzed in a FACS Calibur flow cytometer. FITC fluorescence was evaluated in the FL-1 channel, PI was evaluated in the FL-3 and a total of 20,000 events were collected. The data was analyzed by Cell Quest software.

Evaluation of cell viability

Cell viability was evaluated by a modified Alamar blue assay, as described previously (491). The detailed protocol is provided in Supplementary Material.

Establishment of an orthotopic glioma mouse model and histological analysis

Primary tumors were induced in the right hemisphere of adult male C57BL/6 mice, obtained from Charles River Laboratories (Wilmington, MA, USA) as described by Aguilar-Morante et al. (475), with a few modifications. Briefly, eight-week-old mice anesthetized by intraperitoneal administration of Ketamine/Xylazine (100 and 10 mg/Kg, respectively) were injected stereotactically with 1.25×10^5 GL261 glioma cells into the right hemisphere (stereotactic coordinates relative to bregma: -1.06 mm anterior, 3 mm lateral, 3 mm deep) using a Hamilton syringe with a 33-gauge needle (3 µL at 0.2 µL/minute). Following surgery, animals were monitored daily and sacrificed as soon as they displayed neurological deficits or lost >20% of their body weight.

For determination of the tumor growth rate, animals were sacrificed at 11, 14 or 20 days after tumor implantation by intracardiac perfusion with 15 mL ice cold PBS, followed by 15 mL cold 4% paraformaldehyde (PFA) prior to tissue harvesting. Brains were collected into polystyrene tubes and fixed overnight at 4ºC in 4% PFA, placed in 25% sucrose for additional 48 hours and frozen (after drying) at -80ºC. Sequential cryosections (20 µm) were obtained by microtome sectioning and processed for cresyl violet staining (as described in Supplementary Material). Tumor volume was calculated from cresyl violet-stained sections using the software 3D Doctor (Able Software, Lexington, MA, USA). All the procedures with animals were carried out in accordance with the International Recommendations For The Use Of Animals In Scientific Research (normative 86/609 from the European Communities Council).

Systemic administration of SNALP-formulated siRNAs and biodistribution analysis

Fourteen-days after tumor implantation, mice were randomly assigned to target (injected with CTX-coupled and nontargeted SNALPs) or control (injected with PBS) groups (n=3). SNALP-formulated FAM-labeled siRNAs (2.5 mg/kg) were administered via standard intravenous injection into the lateral tail vein. Four-hours after injection, animals were sacrificed by intracardiac perfusion with 30 mL of ice-cold PBS and brain, lungs, liver and kidneys were harvested into polystyrene tubes containing PBS supplemented with 2% FBS. The brains were then dissected to separate tumor from healthy tissue. Tissues were homogenized for flow cytometry analysis, as described in Supplementary Material. FAM detection was performed by incubating approximately 1×10^6 cells with an anti-FAM antibody

(Sigma, clone FL-D6, 1:100), for 2 hours at 4ºC, followed by cell incubation with an Alexa488-conjugated anti-mouse secondary antibody (1:200; Molecular Probes, Life technologies, USA), for 1 hour at RT. All samples were immediately analyzed in a FACS Calibur flow cytometer; Alexa488 fluorescence was evaluated in the FL-1 channel and a total of 30,000 events were collected. The data were analyzed by Cell Quest software.

Statistical analysis

All data are presented as means ± standard deviation of at least three independent experiments, each performed in triplicate (unless stated otherwise). One way analysis of variance (ANOVA) combined with the Tukey posthoc test was used for multiple comparisons (unless stated otherwise) and considered significant when $p < 0.05$. Statistical differences are presented at probability levels of $p < 0.05$, $p < 0.01$ and $p < 0.001$. Calculations were performed with Prism 5 (GraphPad, San Diego, CA, USA).

6. Supplementary Figures
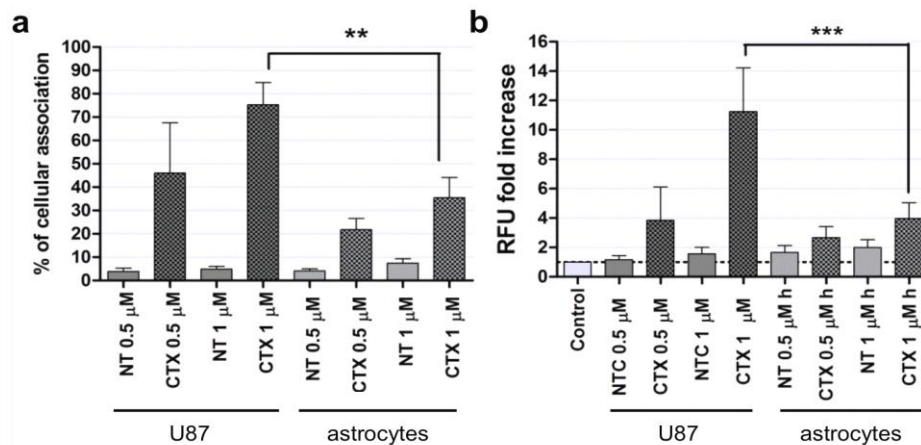
Supplementary Figure 1. Association of SNALPs with U87 GBM cells and mouse primary astrocytes. Cells were incubated, for 4 hours at 37ºC, with CTX-coupled (CTX) or nontargeted (NT) liposomes encapsulating FAM-labeled anti-miR-21 oligonucleotides. After incubation, cells were rinsed with PBS and prepared for flow cytometry analysis, as described in Materials and Methods. The extent of cellular association was assessed only in viable cells, these being gated on the basis of morphological features (including cell volume and complexity). (**a**) Cellular association and (**b**) fluorescence intensity plots of cells incubated with 0.5 or 1 μM of SNALP-formulated anti-miR-21 oligonucleotides. The percentage of cellular association in a was normalized to control cells (untreated). Relative fluorescence units (RFU) to control cells (untreated) are indicated in b. Values are presented as means ± standard deviation (n=2). ** $p < 0.01$, *** $p < 0.001$ compared to U87 cells incubated with a similar amount of CTX-coupled liposomes encapsulating anti-miR-21 oligonucleotides.
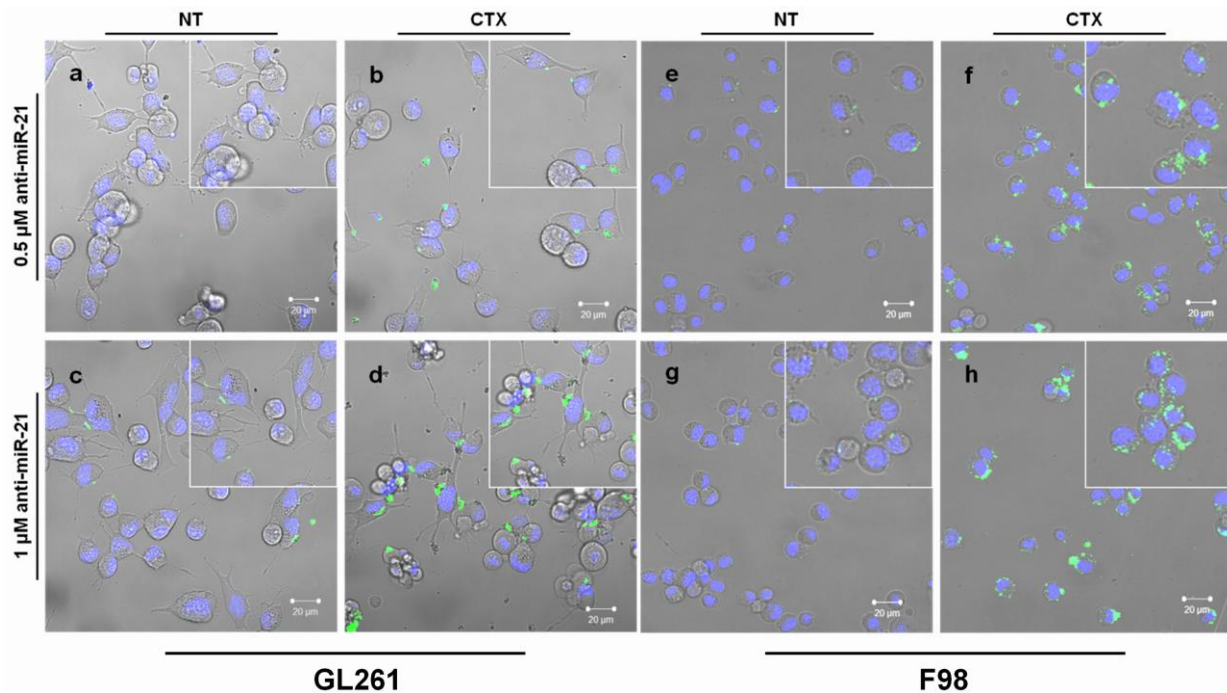
Supplementary Figure 2. Internalization of SNALPs in GL261 mouse and F98 rat glioma cells. Cells were incubated, for 4 hours at 37ºC, with CTX-coupled (CTX) or nontargeted (NT) liposomes encapsulating FAM-labeled anti-miR-21 oligonucleotides. After incubation, cells were rinsed twice with PBS, stained with DNA-specific Hoechst 33342 (blue) and then observed by confocal microscopy. The panel shows representative images at 40× magnification of (**a**, **b**, **c**, **d**) GL261 or (**e**, **f**, **g**, **h**) F98 cells incubated with SNALP-formulated oligonucleotides at a final oligonucleotide concentration of (**a**, **b**, **e**, **f**) 0.5 or (**c**, **d**, **g**, **h**) 1 µM. Results are representative of two independent experiments. Scale corresponds to 20 µm.
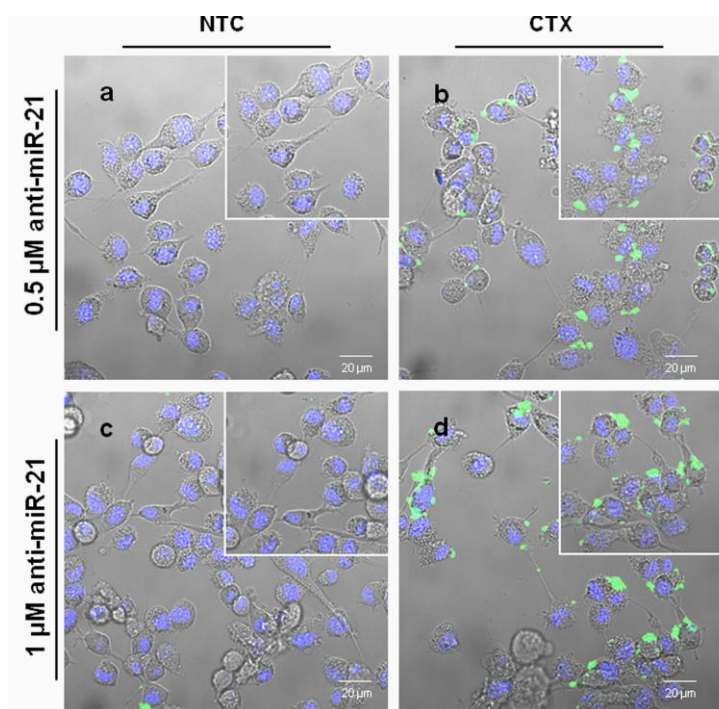
Supplementary Figure 3. Tumor cell internalization of SNALPs three months after their preparation. CTX-coupled (CTX) or nontargeted (NT) liposomes encapsulating FAM-labeled anti-miR-21 oligonucleotides were prepared and stored at 4ºC for three months. After this storage period, U87 GBM cells incubated with the SNALPs for 4 hours (at 37ºC), rinsed twice with PBS, stained with DNA-specific Hoechst 33342 (blue) and then observed by confocal microscopy. The panel shows representative images at 40× magnification of U87 cells incubated with either (**a**, **c**) NT or (**b**, **d**) CTX-coupled SNALPs at a final oligonucleotide concentration of (**a**, **b**) 0.5 or (**c**, **d**) 1 µM. Results are representative of two independent experiments. Scale corresponds to 20 µm.
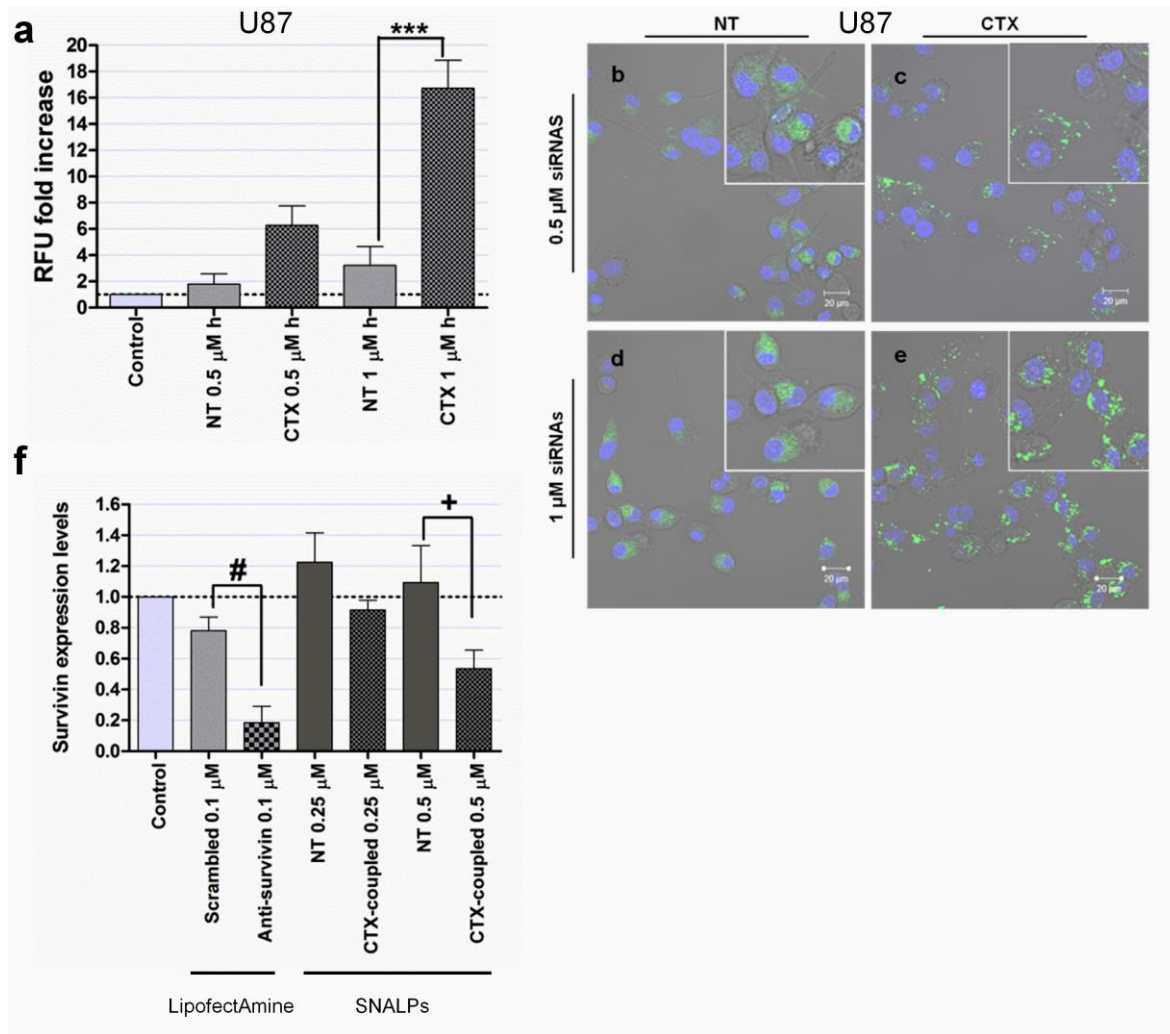
Supplementary Figure 4. **Association and internalization of liposomes encapsulating anti-survivin siRNAs in survivin-expressing U87 glioma cells, and effect on survivin mRNA expression**. Cells were incubated, for 4 hours at 37ºC, with NBD-labeled CTX-coupled (CTX) or nontargeted (NT) liposomes encapsulating anti-survivin siRNAs. Cells were then rinsed twice with PBS and prepared for flow cytometry analysis or stained with DNA-specific Hoechst 33342 (blue) for confocal microscopy analysis. (**a**) Fluorescence intensity plot of cells incubated with 0.5 or 1 µM of

SNALP-formulated anti-survivin siRNAs. Relative fluorescence units (RFU) to control cells (untreated) are indicated for each plot. (**b**, **c**, **d**, **e**) Representative images at 40× magnification of U87 cells incubated with (**b**, **d**) NT or (**c**, **e**) CTX-coupled liposomes at a final siRNA concentration of (**b**, **c**) 0.5 and (**d**, **e**) 1 µM. Results are representative of two independent experiments. (**f**) Survivin mRNA expression levels in U87 cells, 48 hours after cell incubation with NT or CTX-coupled liposomes encapsulating anti-survivin or scrambled siRNAs, at a final siRNA concentration of 0.25 or 0.5 µM (n=2). Cells transfected with lipoplexes (prepared with siRNAs and Lipofectamine as described in Materials and Methods) were used as positive control. Survivin expression levels, normalized to the reference HPRT1, are presented as relative expression values to control untreated cells. Values are presented as means ± standard deviation (n=3). *** $p<0.001$ compared to cells incubated with a similar amount of NT SNALP-formulated siRNAs. $^{#}$ $p<0.05$ compared to cells incubated with a similar amount of scrambled siRNAs. $^{+}$ $p<0.05$ compared to cells incubated with a similar amount of NT SNALP-formulated siRNAs. Scale corresponds to 20 µm.
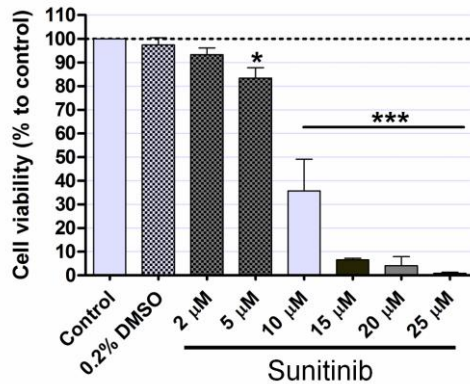
Supplementary Figure 5. Effect of sunitinib in the viability of GL261 glioma cells. Cell viability was evaluated by the Alamar Blue assay (as described in Materials and Methods) 24 hours after incubation with sunitinib. Values are presented as means ± standard deviation (n=3). * $p<0.05$, *** $p<0.001$ compared to cells exposed to cell culture medium containing 0.2% DMSO.

Chapter 5

PDGF-B-mediated downregulation of miR-21: new insights into PDGF signaling in glioblastoma

1. Abstract

Glioblastoma (GBM) is a highly heterogeneous type of tumor characterized by genomic and signaling abnormalities affecting pathways involved in control of cell fate, including tumor suppressor- and growth factor-regulated pathways. Aberrant miRNA expression has been observed in GBM, being associated with impaired cellular functions resulting in malignant transformation, proliferation and invasion.

Here, we demonstrate for the first time that platelet-derived growth factor-B (PDGF-B), a potent angiogenic growth factor involved in GBM development and progression, promotes downregulation of pro-oncogenic (miR-21) and anti-oncogenic (miR-128) miRNAs, as well as upregulation/downregulation of several miRNAs involved in GBM pathology. Retrovirally-mediated overexpression of PDGF-B in U87 human GBM cells or their prolonged exposure, as well as that of F98 rat glioma cells to this ligand, resulted in decreased miR-21 and miR-128 levels, which was associated with increased cell proliferation. Furthermore, siRNA-mediated PDGF-B silencing led to increased levels of miR-21 and miR-128, while miRNA modulation through overexpression of miR-21 did not alter the levels of PDGF-B. Finally, we demonstrate that modulation of tumor suppressors PTEN and p53 in U87 cells does not affect the decrease in miR-21 levels associated with PDGF-B overexpression.

Overall, our findings suggest that, besides its role in inducing GBM tumorigenesis, PDGF-B may enhance tumor proliferation by modulating the expression of oncomiRs and tumor suppressor miRNAs in U87 human GBM cells.

2. Introduction

The human GBM represents the most common and lethal type of glioma (2). Despite recent improvement in imaging and surgical techniques, allowing more accurate diagnosis and treatment, current therapeutic options for GBM lack effective long-term impact on disease control and patient survival, and clinical recurrence is nearly universal (25, 417). This clearly emphasizes the need for new and effective therapeutic strategies, as well as a better understanding of the molecular and cellular alterations that occur in GBM.

The discovery of miRNAs, a new class of small noncoding RNAs that regulate gene expression, has revealed an additional level of fine tuning of the genome. MiRNAs have been found to regulate post-transcriptionally the expression of over 30% of protein-coding genes (170) through imperfect pairing with the target mRNAs (195, 418) and bioinformatic data indicate that each miRNA can control hundreds of gene targets, underscoring the potential influence of miRNAs in almost every genetic pathway (156, 170). Accumulated evidence has shown that miRNA dysregulation is associated with cancer development and progression (237, 238, 244), including GBM pathogenesis (266, 300, 423). Studies from Holland and colleagues showed that miR-26a is amplified in high-grade gliomas and facilitates gliomagenesis *in vivo* (318). Godlweski and colleagues demonstrated that expression of miR-128, a highly downregulated miRNA in GBM, reduced significantly glioma cell proliferation *in vitro* and glioma xenograft growth *in vivo* (322). Nevertheless, the causes of the widespread disruption of miRNA expression in cancer cells are not completely understood and, most probably, various abnormalities in each tumor could contribute to the global miRNA-expression profile (155).

Relevant molecular alterations that govern GBM progression have already been identified, including mutation/deletion of p53 and PTEN and amplification/overexpression of the epidermal growth factor receptor (EGFR) (4, 492). PDGF, a vast family of angiogenic growth factors, has also been proposed to play a role in glioblastoma development and progression. Alterations in PDGF signaling, including overexpression of PDGF-A and -B ligands or their receptors (PDGFR-α and -ß), are commonly observed in high-grade gliomas (12, 13, 493); *in vitro* studies have also shown that PDGF directly stimulates the migration and proliferation of glial progenitors (494, 495). Moreover, retrovirally-mediated expression of PDGF-B in adult white matter, subventricular zone and brainstem progenitors induces tumors that closely resemble human GBM (289, 496-498), thus emphasizing the importance of PDGF signaling in brain tumors.

Emerging evidence suggested that PDGF signaling modulates miRNAs in several biological processes. Davis and colleagues demonstrated that miR-221 is transcriptionally induced upon PDGF treatment in primary vascular smooth muscle cells (vSMC), leading to downregulation of the targets c-Kit and p27^{Kip1} and consequent induction of cell proliferation (314). Recent studies identified a group of miRNAs whose expression is altered shortly after PDGF stimulation and revealed that the EGFR expression and function are repressed by PDGF-induced miR-146b (290).

Here, we demonstrate that PDGF-B overexpression modulates miRNA expression in human U87 GBM cells. Prolonged exposure of human and rat GBM cells to PDGF-B promotes miR-21 and miR-128 downregulation, this effect being specific for this ligand (PDGF-B), as concluded from the observation of increased levels of these miRNAs upon siRNA-mediated PDGF-B silencing. On the other hand, transient miR-21 overexpression does not significantly affect PDGF-B mRNA levels. Moreover, we demonstrate that PDGF-B-related miR-21 downregulation is not affected by the modulation of tumor suppressors PTEN and p53.

3. Results

3.1 MiR-21 and miR-221 are significantly downregulated in U87 cells overexpressing PDGF-B

We have recently demonstrated that the pro-oncogenic miR-21 is overexpressed and the anti-oncogenic miR-128 is highly downregulated in several human GBMs, which was corroborated by the analysis of miRNA expression data in approximately 200 human GBM samples from The Cancer Genome Atlas (TCGA) (11) (Chapter 3). Similarly, significant miR-21 overexpression and miR-128 downregulation were observed in the widely used U87 human GBM cell line (Fig. 1A, B).

Although a large number of *in vitro* and *in vivo* studies have demonstrated that PDGF-B is an important mediator in GBM development and progression (498, 499, 500), its influence on miRNA expression in tumor cells remains to be clarified. In order to address the potential involvement of PDGF-B in miRNA expression in GBM, we measured the expression levels of miR-128, miR-21 and miR-221 in retrovirally-modified U87 cells overexpressing PDGF-B (U87-PDGF), which were compared to those in control U87 cells transduced with a noncoding retroviral vector (no PDGF-B), or control epileptic tissue. Our results from qPCR

144

experiments revealed that PDGF-B mRNA levels are significantly higher in U87-PDGF cells (~10-fold) than in parental U87 cells (Figure 1C, $p < 0.001$). Moreover, U87-PDGF cells displayed altered morphology and increased proliferation rate, compared to parental U87 cells (Supplementary Results, Fig. 1).

Surprisingly, miR-21 was significantly downregulated in U87-PDGF cells compared to parental U87 cells (~58-fold decrease, $p < 0.001$) or control epileptic tissue, as shown in Figure 1A. Similarly, a considerable reduction in miR-21 staining, as assessed by FISH, was observed in cultured U87-PDGF cells (Fig. 1F) when compared to control U87 cells (Fig. 1D), thus supporting our findings of miR-21 downregulation in U87 cells overexpressing PDGF-B.

Our observation of miR-221 downregulation in U87-PDGF cells compared to parental U87 cells suggests that PDGF-B-related miRNA downregulation is not miR-21 specific (Fig. 1B). On the other hand, the robust downregulation of miR-128 in parental U87 cells was slightly reduced in U87-PDGF cells (Fig. 1B).

3.2 Culturing U87 human and F98 rat glioma cells in PDGF-B-enriched medium promotes downregulation of miR-21 and miR-128 expression levels

In order to mimic the autocrine production of PDGF-B by U87-PDGF cells, parental U87 cells were grown in medium supplemented with PDGF-B (30 ng/ml) for 60 days and miR-128, miR-21 and miR-221 levels were subsequently assessed. As shown in Figure 1, miR-21 (Fig. 1A) and miR-221 (Fig. 1B) levels were significantly reduced in U87 cells under these conditions, when compared to those observed when the cells were maintained in PDGF-B-depleted medium or control epileptic tissue ($p < 0.001$), whereas miR-128 levels were not considerably changed (Fig. 1B). Furthermore, the decrease in miR-21 and miR-221 expression levels was clearly time-dependent, a significant reduction in the miR-21 and miR-221 levels being observed when culturing cells in PDGF-B for long periods of time (Fig. 1H, I).

Interestingly, when PDGF-B-enriched medium was replaced by normal culture medium and cells were grown for one week, a slight recovery in miR-21 and miR-221 levels was observed (Fig. 1H, I, $p < 0.05$); this effect was further enhanced by culturing U87 cells in normal medium for 30 days (not shown), suggesting that PDGF-B-related miRNA modulation may constitute a reversible and time-dependent mechanism affected by the presence of this ligand in the extracellular environment.
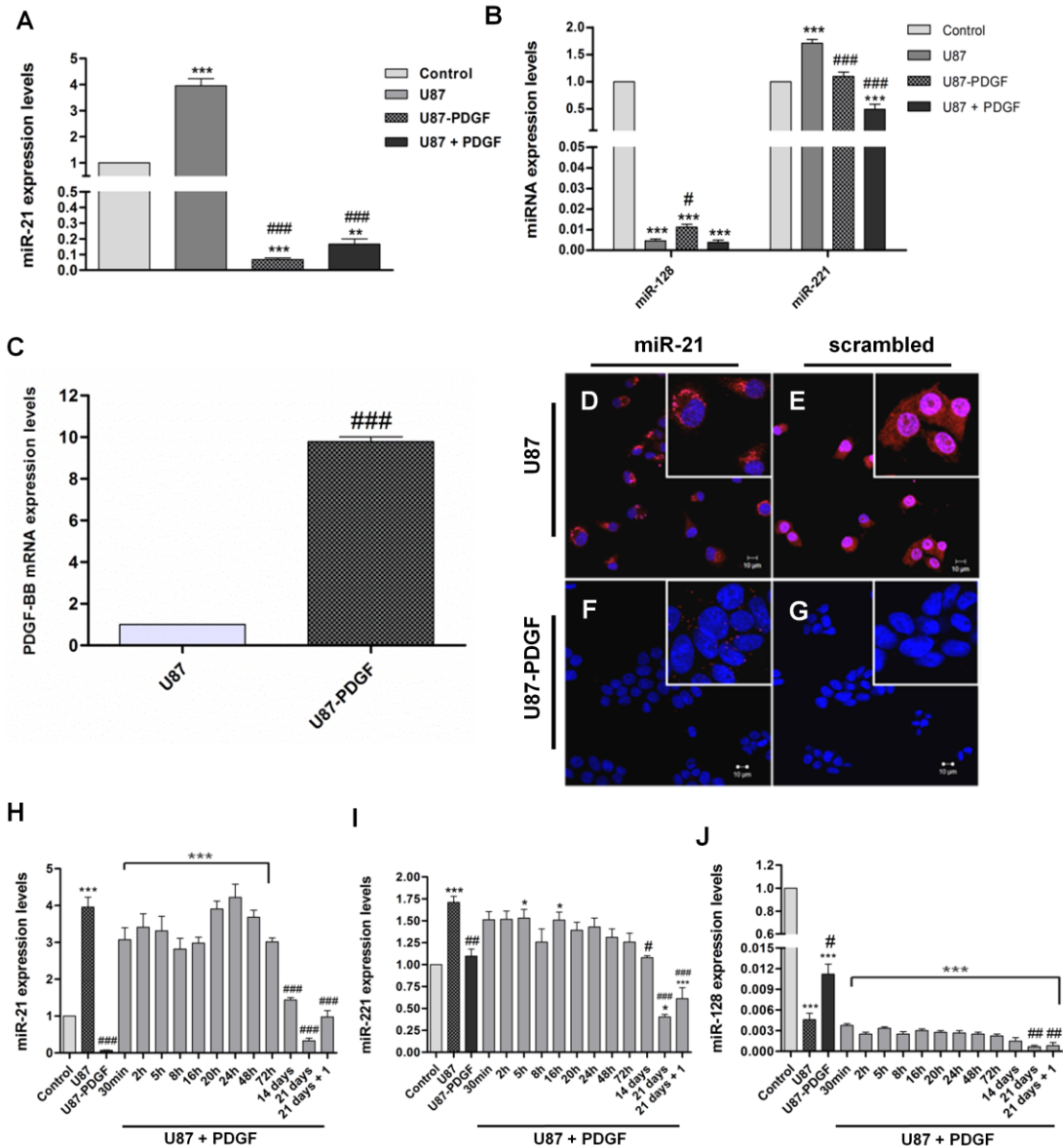
Figure 1. PDGF-B-related modulation of miRNA expression levels in U87 and U87-PDGF human GBM cells. (**A**) MiR-21 and (**B**) miR-128/miR-221 expression levels in parental U87 cells, PDGF-B-overexpressing U87 cells (U87-PDGF) and U87 cells cultured in the presence of 30 ng/ml PDGF-B for 60 days (U87 + PDGF), compared to control epileptic tissue. (**C**) PDGF-B mRNA levels in U87 and U87-PDGF. FISH staining in cultured (**D, E**) U87 and (**F, G**) U87-PDGF cells. Cells were stained with (**D, F**) miR-21 or (**E, G**) non-coding (scrambled) probes. Nuclear staining was accomplished using the cell-permeable DNA stain Hoescht 33342 (Blue). MiR-21 staining (red dots) is observed in U87 cells, predominantly in the cytoplasm, whereas only residual staining is detected in U87-PDGF cells. Images were obtained by confocal microscopy with a 40x EC Plan-Neofluar. Scale corresponds to 10 μm. (**H**) MiR-21, (**I**) miR-221 and (**J**) miR-128 expression levels after culturing parental U87 cells in medium supplemented with PDGF-B (30 ng/ml) for different time periods; 21 days + 1: cells cultured for 21 days in PDGF-B enriched medium followed by 7 days of culture in normal medium (PDGF-B-depleted medium). * p<0.05, ** p<0.01, *** p<0.001 compared to control epileptic tissue. $^{#}$ p<0.05, $^{##}$ p<0.01, $^{###}$ p<0.001 compared to parental U87 cells.

146

Based on our results on miRNA downregulation promoted by PDGF-B in human GBM cells, we tried to clarify whether this effect would be cell-specific or could also be observed in glioma cells from a different origin. For this purpose, F98 rat glioma cells were cultured in medium supplemented with PDGF-B (30 or 50 ng/ml) for different periods of time and subsequently assessed for the effect on miR-128 and miR-21 expression levels, when compared to untreated cells. As shown in Figure 2A, a considerable decrease in miR-21 (p<0.001) and miR-128 levels (p>0.05) was observed when the cells were cultured for 60 days in medium containing 30 ng/ml PDGF-B, which was enhanced when the cells were further cultured for 30 days in 50 ng/ml PDGF-B. Similarly to what was observed for U87 cells, miR-21 and miR-128 expression levels did not change significantly upon culturing F98 cells in PDGF-B-enriched medium for short periods of time (Figure 2B, C). A significant decrease in miR-21 levels (p<0.05) was also observed in GL261 mouse glioma cells cultured for 30 days in medium containing 50 ng/ml PDGF-B (Figure 2D), when compared to untreated cells.
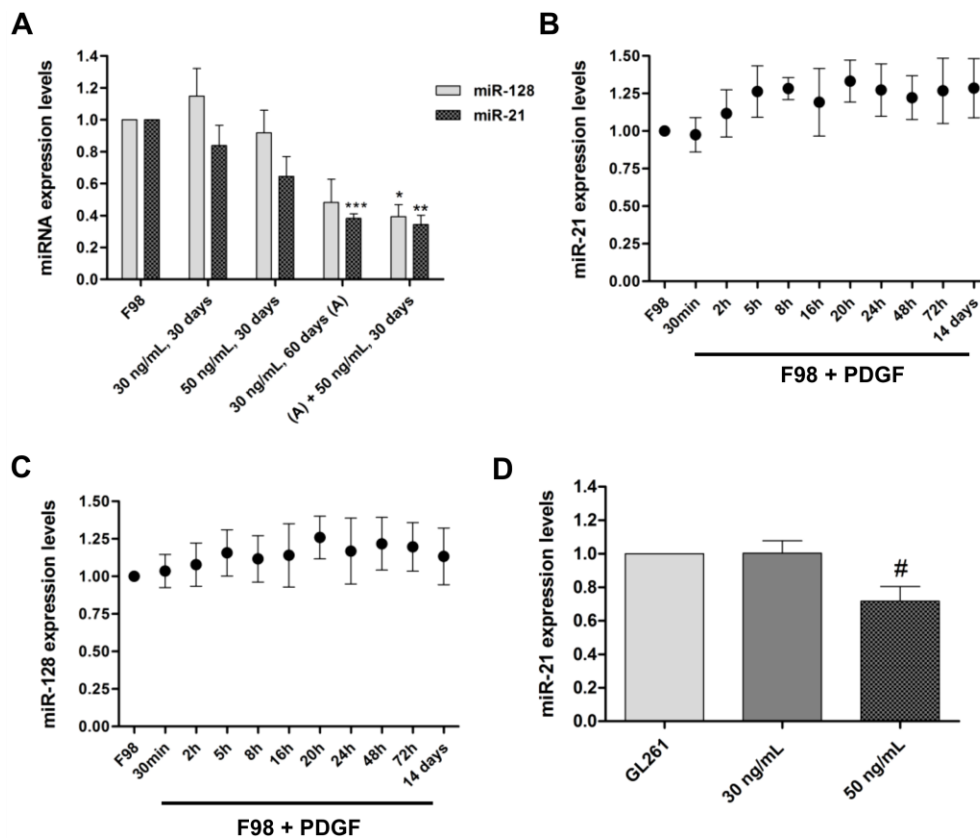
Figure 2. PDGF-B-related modulation of miRNA expression levels in F98 rat and GL261 mouse glioma cells. (**A**) MiR-21 and miR-128 expression levels in F98 cells cultured in PDGF-B-depleted

medium (control) or cultured in medium supplemented with PDGF-B (30 or 50 ng/ml) for different time periods; (A) + 50 ng/ml, 30 days: cells cultured for 60 days in PDGF-B-enriched medium (30 ng/ml), followed by a further incubation of 30 days in medium containing a higher concentration of PDGF-B (50 ng/ml). (**B**) MiR-21 and (**C**) miR-128 expression levels in F98 cells cultured in medium supplemented with PDGF-B (30 ng/ml) for different time periods, compared to those obtained in F98 cells cultured in PDGF-B-depleted medium. 14 days: cells cultured for 14 days in PDGF-B- enriched medium. (**D**) MiR-21 expression levels in GL261 glioma cells cultured in PDGF-B-depleted medium (control) or cultured in medium supplemented with PDGF-B (30 or 50 ng/ml) for 30 days. * p<0.05, ** p<0.01, *** p<0.001 compared to control F98 cells; $^{#}$ p<0.05 compared to control GL261 cells.

Overall, our results suggest that PDGF-B promotes a time-dependent downregulation of miRNAs in glioma cells.

3.3 SiRNA-mediated PDGF-B silencing increases miR-21 and miR-128 expression levels in U87-PDGF cells

As our results demonstrated that PDGF-B promotes the downregulation of miRNAs in human and rat glioma cells, we evaluated the effect of modulating the autocrine production of PDGF-B in U87-PDGF cells, via siRNA-mediated PDGF-B mRNA silencing, on miR-128 and miR-21 expression levels. As shown in Figure 3A, cell transfection with a PDGF-B-specific siRNA sequence (50 nM) resulted in a pronounced, although not significant, decrease in PDGF-B mRNA levels, as compared to those obtained upon transfection with a noncoding siRNA sequence (~ 28%, p>0.05); no further decrease was observed when U87-PDGF cells were transfected with 100 nM siRNAs (data not shown). Nonetheless, miR-21 levels were significantly upregulated in U87-PDGF cells transfected with anti-PDGF-B siRNAs (10.33 ± 0.73), compared to those transfected with a noncoding sequence (1.606 ± 0.537, p<0.01); although not significant, miR-128 upregulation was also observed under these conditions (Fig. 3B).

These results suggesting that PDGF-B mRNA knockdown in U87-PDGF cells induced the upregulation of miR-21 and miR-128 levels prompted us to test whether PDGF-B mRNA silencing in cells expressing lower levels of this growth factor would also promote such considerable miR-21 upregulation. As observed in Figure 3C, transfection of parental U87 cells with anti-PDGF-B siRNAs also resulted in PDGF-B mRNA downregulation, although no significant increase in miR-21 and miR-128 levels was observed, when compared to those obtained in cells transfected with a noncoding siRNA (Fig. 3D).
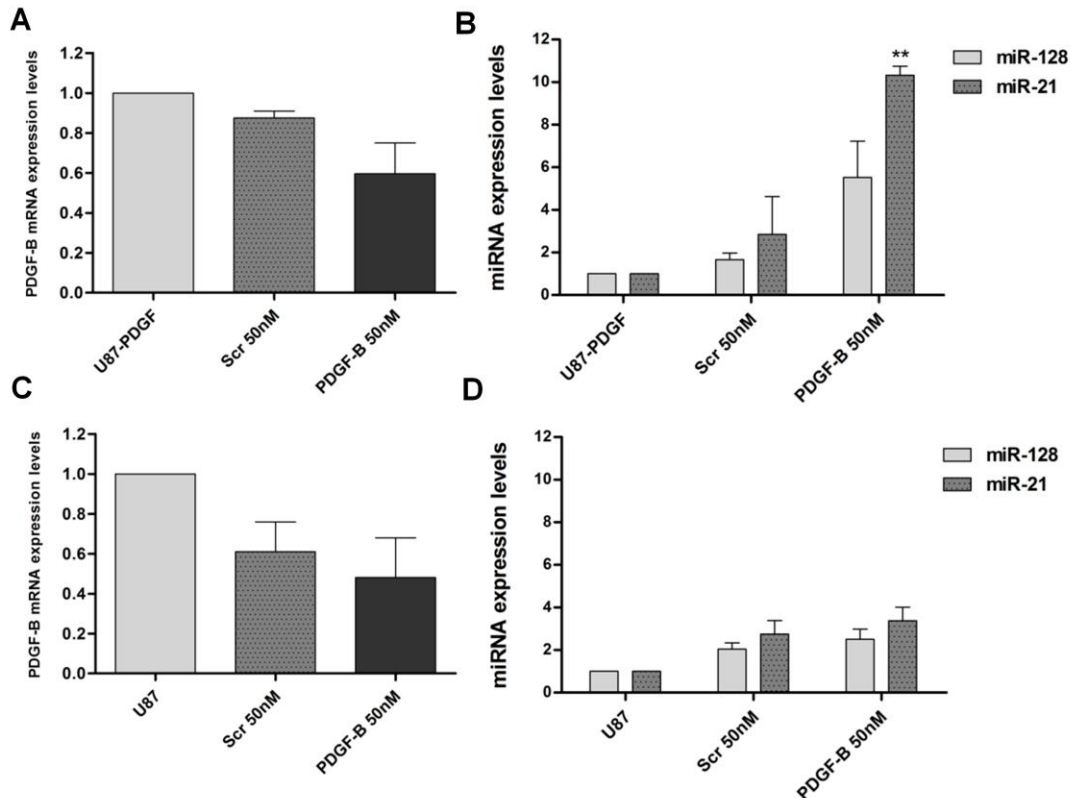
Figure 3. MiR-21 and miR-128 expression levels following siRNA-mediated PDGF-B mRNA silencing. For siRNA transfection, 24 hours before any experiment U87 and U87-PDGF cells were plated on 12-well plates at a density of $7x10^4$ and $6x10^4$ cells/well (respectively) and total RNA was extracted 24 hours after transfection. PDGF-B mRNA expression levels in (**A**) U87-PDGF and (**C**) parental U87 cells after transfection with 50 nM anti-PDGF-B siRNA (PDGF-B 50 nM) or a non-coding sequence (Scr 50 nM). MiR-21 and miR-128 expression levels in (**B**) U87-PDGF and (**D**) U87 cells after siRNA transfection. ** $p<0.01$ compared to untreated U87-PDGF cells.

3.4 Plasmid-induced miR-21 upregulation in U87-PDGF cells does not significantly alter PDGF-B mRNA levels

Based on our findings of the modulating effect of PDGF-B on miRNA expression in GBM cells and since miRNAs regulate gene expression post-transcriptionally through imperfect pairing with the 3' UTR of their target mRNAs (170, 501), we sought to identify possible interactions between miR-21/miR-128 and the PDGF-B mRNA. Although bioinformatic analysis using mirWalk (502) and other tools that predict miRNA targets has not revealed any conserved sites at 3' UTR of the human PDGF-B mRNA for either of these miRNAs (Supplementary Data, Table S1), we examined whether a transient upregulation of miR-21 in human GBM cells would have any effect on PDGF-B mRNA expression and cell

proliferation. As shown in Figure 4A, transfection of U87-PDGF cells with the plasmid pcDNA3.1-miR-21 resulted in a significant increase in miR-21 levels (10.18 ± 3.12), when compared to those observed with the noncoding plasmid pCMV-PL (1.6 ± 0.54, p<0.01). An increase in miR-21 levels was also obtained upon transfection of U87 cells (Fig. 4C), although such increase was not so pronounced, as these cells express higher basal levels of miR-21. As observed, in both cell lines, miR-21 upregulation did not affect significantly the levels of PDGF-B mRNA (Fig. 4B, D). Moreover, no significant changes in viability were observed in U87-PDGF cells transfected with miR-21-coding pcDNA3.1-miR-21, when compared to that observed in cells transfected with control pCMV-PL, whereas a small, although significant, increase in viability was observed in U87 cells transfected with the same formulations (~9%, p<0.05) (Supplementary Results, Fig. 2A).
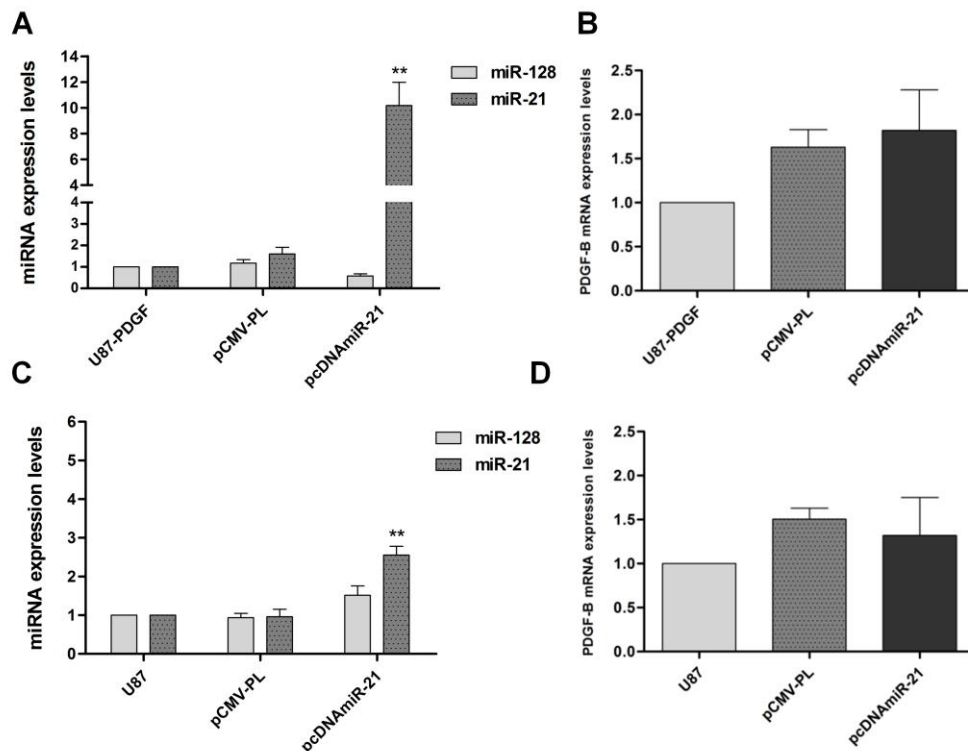
Figure 4. MiR-21 and miR-128 expression levels following plasmid-mediated miR-21 overexpression. For plasmid transfection of U87 and U87-PDGF cells, 24 hours before any experiment cells were plated onto 6-well plates at a density of 1×10^5 and 8×10^4 cells/well (respectively) and total RNA was extracted 48 hours after transfection. MiR-21 and miR-128 expression levels in (**A**) U87-PDGF and (**C**) U87 cells after transfection with the human miR-21-coding plasmid pcDNA3.1-miR-21 (pcDNAmiR-21) or non-coding plasmid (pCMV-PL). PDGF-B mRNA levels in (**B**) U87-PDGF and (**D**) U87 cells after transfection. ** p<0.01, *** p<0.001 compared to untreated U87-PDGF cells.

150

3.5 PDGF-B overexpression promotes the upregulation and downregulation of several miRNAs in U87 GBM cells

As our results demonstrated that PDGF-B-overexpression promotes ligand-specific downregulation of the pro-oncogenic miR-21 and the anti-oncogenic miR-128 in glioma cells, which was associated with increased cell proliferation (Supplementary Results, Fig. 1), we evaluated whether PDGF-B would modulate the expression of other miRNAs involved in GBM pathology that could contribute to a more tumorigenic phenotype. As shown in Figure 5 and Supplementary Table S2, several miRNAs, including the anti-oncogenic let-7b, miR-130a and miR-29b, were found to be downregulated in U87-PDGF cells, when compared to parental U87 cells, whereas the pro-oncogenic miR-17, miR-20a, miR-10b and the anti-oncogenic miR-101 were upregulated under the same conditions. Furthermore, miR-188-5p and miR-623, were considerably overexpressed in U87-PDGF cells, compared to control U87 cells. Although no role in GBM has been reported for these miRNAs, increased expression of miR-188 has been associated with enhanced cellular proliferation in ovarian cancer (503).

miRNA expression to control U87 cells (log scale)
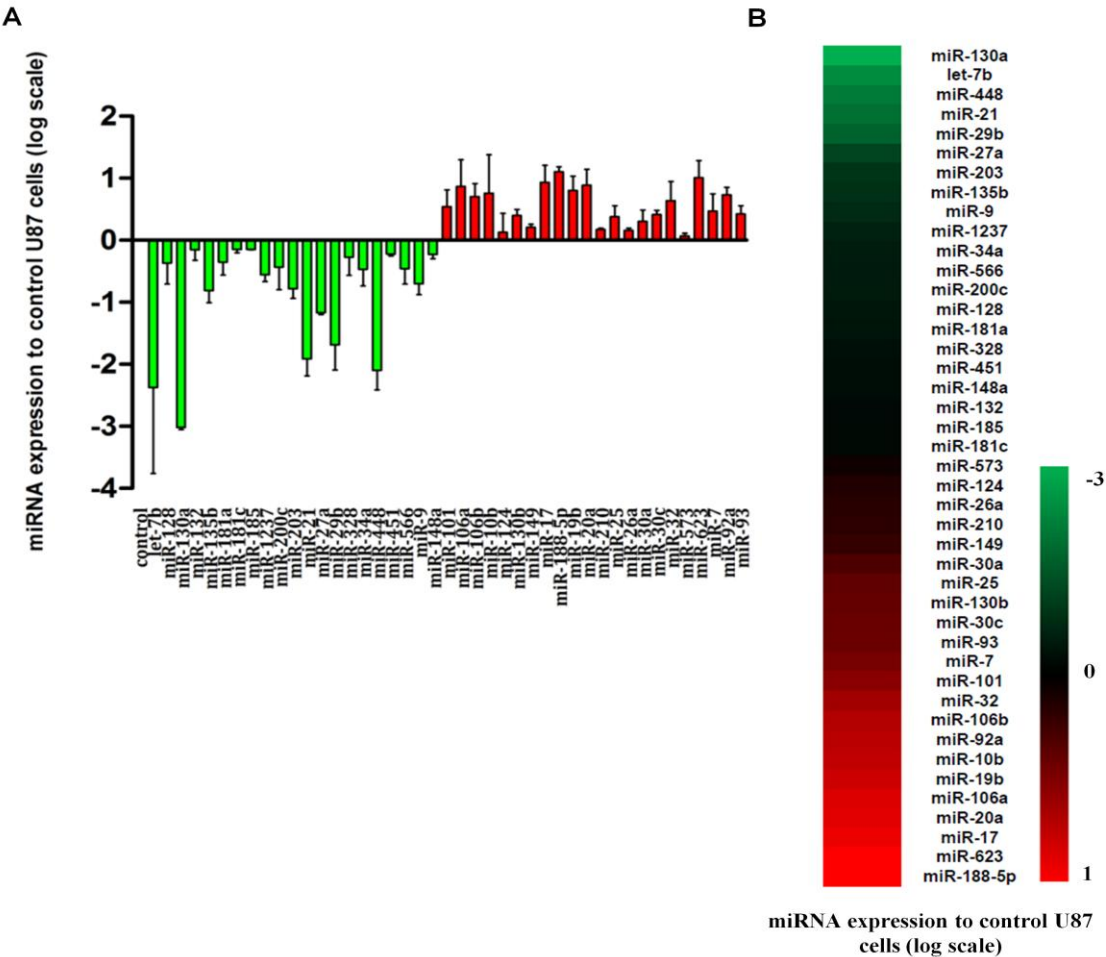
Figure 5. QPCR quantification of 44 miRNAs in U87-PDGF cells, using pre-designed miRNA PCR plates. (**A**) Column graphic and (**B**) heatmap representation of the relative miRNA expression levels in PDGF-B-overexpressing U87 cells (U87-PDGF), compared to parental U87 cells (n=3). Ct values were obtained for each sample (threshold=40 cycles) and normalized to references U6snRNA, snord44 and snord49A; the GeNorm module was used to determine the most stable reference gene (snord44). Relative miRNA expression values were calculated using the qBase^{Plus} software, and statistical significance was assessed using one-way ANOVA combined with Benferroni's posthoc test (Supplementary Data, Table S2). MiR-367 was not detected in both U87 and U87-PDGF cells and therefore is not represented in the chart.

3.6 PDGF-driven mouse tumor models overexpress miR-21

The observation of a reduction in the levels of the oncogenic miR-21 in U87-PDGF cells (compared to control epileptic tissue), as opposed to what has been published regarding the expression of this miRNA in glioblastoma, prompted us to evaluate if such reduction would also be observed in a PDGF-driven animal model. In this regard, we have recently developed a retrovirally-induced mouse GBM model characterized by the deletion of the tumor suppressors PTEN and p53 and overexpression of PDGF-B (PDGF$^+$PTEN$^{-/-}$p53$^{-/-}$), which displays molecular and histopathological features that closely resemble human GBM (425). A similar GBM model with deleted PTEN and functional p53 (PDGF$^+$PTEN$^{-/-}$) was also established and characterized.

The expression levels of miR-128, miR-21 and miR-221 were measured by qPCR in primary cultures prepared from tumors of both models and compared to those of control samples, obtained from double-floxed (PTEN$^{-/-}$p53$^{-/-}$) mouse brains following animal injection with a control vector (no PDGF). As shown in Figure 6, miR-221 was overexpressed (Fig. 6A) and miR-128 was highly downregulated (Fig. 6B) in both primary cultures, without significant differences between double-floxed and PTEN-floxed samples.

As opposed to what was observed in U87-PDGF cells, miR-21 was found to be highly and differentially overexpressed in both PDGF-driven primary cultures when compared to control, with an average fold change of 592.3 ± 35.14 in double-floxed samples (p<0.001) and 703.3 ± 243.8 in PTEN-floxed samples (p<0.001) (Fig. 6C). As U87-PDGF cells express wild-type PTEN and p53, we ascertained whether the status of these tumor suppressors could explain such considerable differences in miR-21 levels.
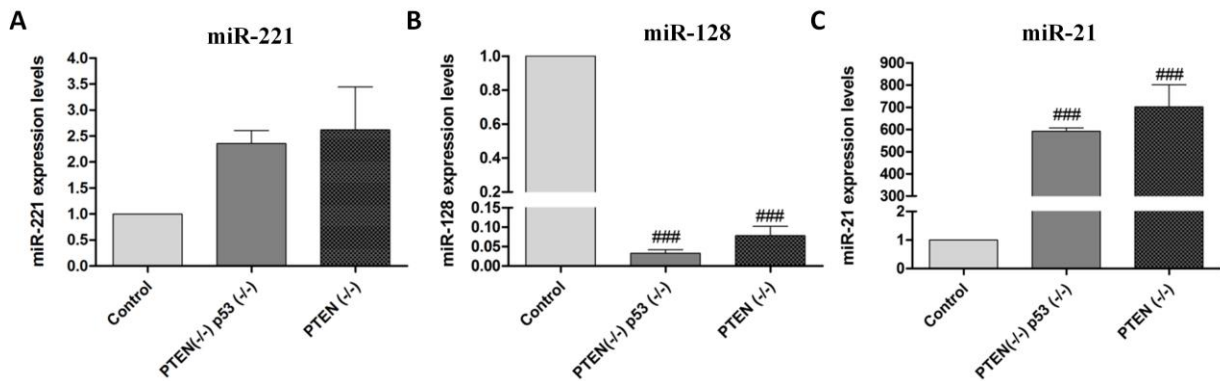
Figure 6. MiRNA expression levels in primary cultures established from PDGF-B-driven mouse GBM tumor models. (**A**) miR-221 (**B**) miR-128 and (**C**) miR-21 expression levels in PDGF-B-overexpressing double-floxed (PTEN$^{-/-}$p53$^{-/-}$) or PTEN-floxed (PTEN$^{-/-}$) primary cultures (n=3) prepared from mouse tumors (as described in Materials and Methods), compared to double-floxed (PTEN$^{-/-}$p53$^{-/-}$) mouse brains following animal injection with a control vector (no PDGF) (n=4). [###] p<0.001 compared to control mouse brain.

3.7 PTEN and p53 modulation does not significantly affect miR-21 levels in PDGF-B-overexpressing U87 cells

The modulation of tumor suppressors PTEN and p53 in U87-PDGF cells was achieved via siRNA-mediated PTEN silencing and/or pifithrin-α-mediated inhibition of p53.

As shown in Figure 7, cell transfection with a PTEN-specific siRNA sequence (50 nM) resulted in a small decrease in PTEN mRNA (0.90 ± 0.164, Fig. 7A) and protein levels (0.802 ± 0.181, Fig. 7B, C), as compared to those obtained upon transfection with a noncoding siRNA sequence. A more pronounced decrease in both mRNA (0.805 ± 0.243, Fig. 7A) and protein levels (0.657 ± 0.175, Fig. 7B, C) (p<0.05) was observed when U87-PDGF cells were transfected with 100 nM PTEN-specific siRNAs, resulting in a small, although not significant, decrease in miR-21 expression levels (0.77±0.45, Fig. 7D); such effect was, nevertheless, proportional to the degree of siRNA-mediated PTEN inhibition obtained.

Modulation of p53 was achieved by using pifithrin-α, a specific DNA binding inhibitor of p53 transcriptional activity. Several studies performed in different cell types using pifithrin-α have not reported toxicity when the drug was applied at a range of concentrations up to 30 μM (434, 504, 505). Similarly, no signs of toxicity were observed when U87-PDGF cells were treated with 10 μM of pifithrin- α, while a marked decrease in cell viability could be observed in cells treated with 30 μM or higher concentrations of the drug (Supplementary Results, Fig.

2B). In agreement with the results obtained in the abovementioned PTEN-silencing experiments, miR-21 expression levels did not significantly change in U87-PDGF cells exposed to 10 μM of pifithrin-α either *per se* (0.925 ± 0.064) or in combination with siRNA-mediated PTEN silencing (0.71 ± 0.184), as compared to those obtained upon transfection with a PTEN-specific siRNAs without drug (0.77±0.45) (Figure 7D). These results suggest that PTEN and p53 modulation do not significantly affect the decrease in miR-21 levels associated with PDGF-B overexpression in U87 cells. However, the limited efficiency of siRNA-mediated PTEN silencing should be considered when analyzing these findings.
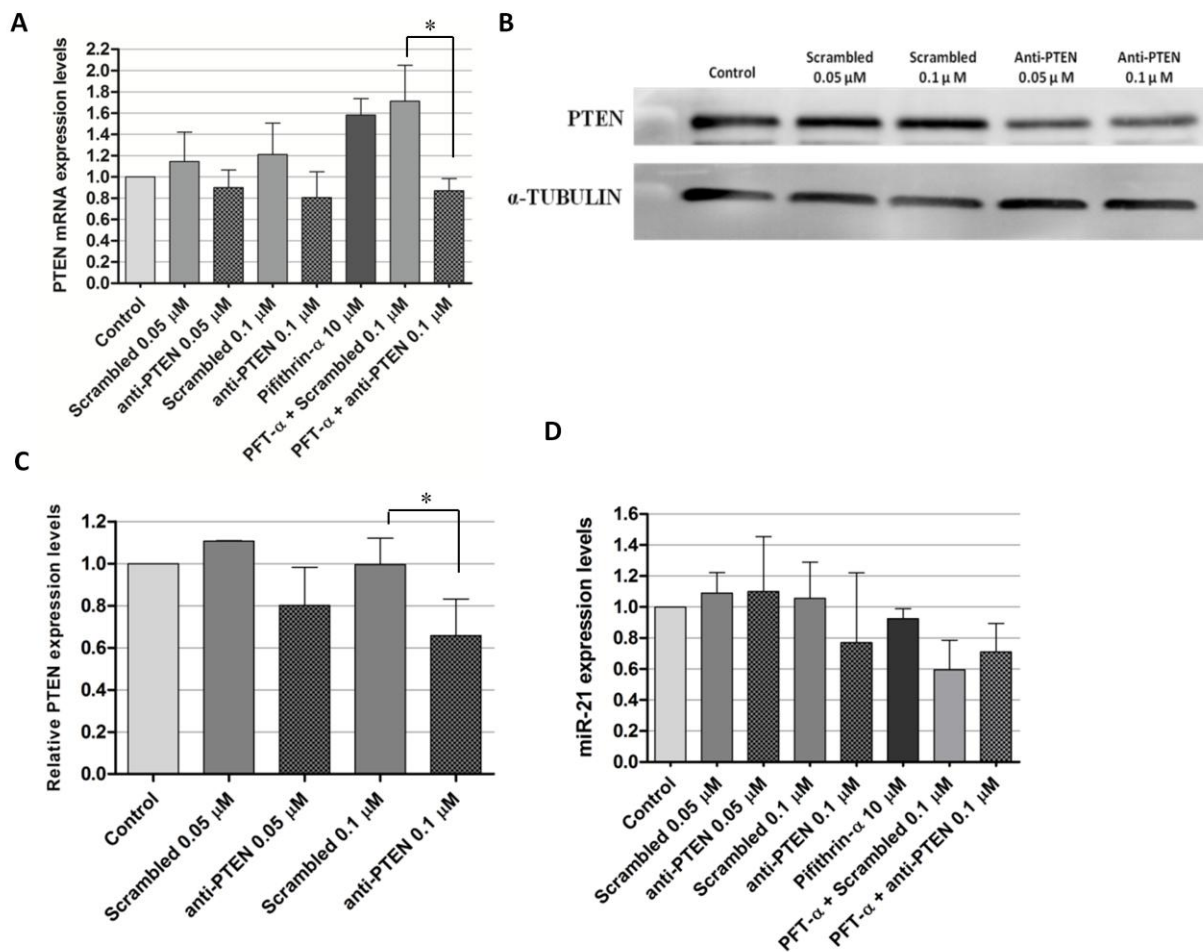
Figure 7. Modulation of PTEN and p53 in U87-PDGF cells. For siRNA transfection and/or pifithrin-α incubation, 24 hours before any experiment U87-PDGF cells were plated onto 12-well plates at a density of $6x10^4$ cells/well (RNA quantification) or 6-well plates at $1.1x10^5$ cells/well (protein quantification). Complexes, prepared as described in Materials and Methods, were added to the cells at a final concentration of 0.05 or 0.1 μM and medium was replaced by fresh DMEM after 4 hours. Twenty-four hours after transfection, cells were exposed to 10 μM pifithrin-α for a period of 24 hours, which was followed by the extraction of RNA and protein. (**A**) PTEN mRNA levels after transfection

154

with anti-PTEN siRNAs (0.05/0.1 µM) or a noncoding sequence (Scrambled), either *per se* or in combination with exposure to 10 µM pifithrin-α. (**B**) Representative gel showing PTEN protein levels 48 hours after transfection with anti-PTEN or scrambled siRNAs (n=3). (**C**) Quantification of PTEN silencing observed in (B), corrected for individual α-tubulin signal intensity. Results are presented as PTEN expression levels relative to control. (**D**) MiR-21 expression levels after transfection with anti-PTEN siRNAs (0.05/0.1 µM) or a noncoding sequence (Scrambled), either *per se* or in combination with exposure to 10 µM pifithrin-α.[*] $p < 0.05$ compared to the indicated condition.

4. Discussion

Several lines of evidence have shown that PDGF signaling plays an important role in the development and progression of high-grade gliomas (13, 289, 497, 498). The results obtained in the present study show that PDGF modulates the expression of several oncomiRs and tumor-suppressor miRNAs in human GBM cells, which may constitute a mechanism for the enhancement of PDGF-driven GBM tumorigenesis.

MiRNA dysregulation has shown to be an important hallmark in the oncogenic process. Different miRNA signatures distinguish normal and neoplastic tissues, as well as tumors of various differentiation states (236); alterations in miRNA signaling have also been associated with several aspects of carcinogenesis, including tumor invasion and metastasis and patient outcome (263, 440, 441, 506). Nevertheless, the underlying mechanisms of miRNA dysregulation in human cancer are still partially unknown.

PDGF, a widely-studied pro-oncogenic growth factor, has been shown to modulate cellular responses in different biological processes, including proliferation and migration of smooth muscle cells and osteogenesis, through miRNA induction/repression (314, 507, 508). Interestingly, PDGF has been recently shown to modulate EGFR expression and function in GBM and ovarian cancer cells by enhancing miR-146b expression (290). Conversely, here we demonstrate that prolonged exposure of GBM cells to PDGF-B promotes ligand-specific downregulation of oncogenic miR-21 and anti-oncogenic miR-128 (Fig. 1, 2); this was associated with increased cell proliferation as retrovirally-modified U87 cells overexpressing PDGF-B (U87-PDGF) display increased proliferation rate, compared to parental U87 cells. Furthermore, our results provide evidence that miR-21 and miR-128 dysregulation in GBM cells is specifically modulated by PDGF-B (Fig. 3), while miRNA modulation does not have any effect on PDGF-B mRNA levels (Fig. 4), thus suggesting that PDGF-B-mediated miRNA downregulation is a one-way mechanism of gene regulation.

Several studies, including our recent data (Chapter 3), have demonstrated that miR-21 is highly overexpressed in a number of human malignancies, including GBM (266, 509, 510), which is associated with tumor development and proliferation. Surprisingly, here we observed a significant reduction in miR-21 levels which may be associated with the increased cell proliferation and tumorigenic potential in PDGF-overexpressing U87 cells. In this regard, we tried to clarify two main questions, the first one being related to the ability of PDGF-B to modulate the expression of other miRNAs that, by balancing the effect of decreased miR-21 expression, would contribute to a more tumorigenic phenotype.

Interestingly, several members of the miR-106b family, a pro-oncogenic microRNA family with seed region homology that includes the oncogenic polycistrons miR-17-92 and miR-106-363 (258), were found to be modulated following PDGF-B exposure (Fig. 5). Mir-17, miR-19b, miR-20a and miR-92a, encoded by the polycistronic miR-17-92 cluster, miR-106a and miR-106b, as well as miR-10b, were upregulated in U87-PDGF cells, compared to control U87 cells. The miR-17-92 cluster is frequently overexpressed in human cancers and functions pleiotropically during both normal development and malignant transformation to promote proliferation, increase angiogenesis and sustain cell survival (253, 511-513); increased levels of miR-17 and miR-106b also were observed in GBM stem cell-containing CD133$^+$ cell populations and miR-17 inhibition reduced neurosphere formation and stimulated cell differentiation (514). MiR-106a, erraticaly expressed in human GBM (515, 516), is part of the miR-106-363 cluster, whose oncogenic potential has been demonstrated in leukemias and other cancer types (517). Nevertheless, high levels of miR-17, miR-106a and miR-20a have been correlated with increased survival in glioma patients (515). Studies by Gabriely and colleagues revealed that survival of GBM patients expressing high levels of miR-10 family members (miR-10a/b) is significantly reduced in comparison to patients with low miR-10 levels (262).

On the other hand, let-7b, miR-29b and miR-130a were downregulated following PDGF-B-overexpression (Fig. 5). Let-7b was shown to have an anti-tumorigenic effect on GBM cells as its expression reduced not only the in vitro proliferation and migration of GBM cells, but also the size of the tumors produced after transplantation into nude mice (518). Similarly, by targeting podoplanin, a protein related to cellular invasion in astrocytic tumors, miR-29b was shown to inhibit invasion, apoptosis and proliferation of GBM. MiR-130a, expressed at low levels in lung cancer cell lines, was able to reduce TRAIL resistance in NSCLC cells through the c-Jun-mediated downregulation of miR-221 and miR-222 (519).

Based on the aforementioned evidence, it is reasonable to assume that PDGF-B drives U87-PDGF cells towards a more tumorigenic phenotype not by reducing miR-21 expression levels but by promoting the upregulation of several oncomiRs and downregulation of tumor suppressor miRNAs. Nevertheless, the mechanisms by which PDGF-B regulates the expression of each miRNA remain unclear and their clarification will be crucial to understand why miR-21 needs to be downregulated in this tumorigenic phenotype. It would be equally important to quantify the global miRNA levels in both U87 and U87-PDGF cells, as relevant studies have associated a reduction in global miRNA levels with increased tumorigenic potential (235, 236, 520).

The second main question we addressed focused the mechanisms by which PDGF-B promoted miR-21 downregulation in U87 cells. As opposed to human U87-PDGF cells, miR-21 was highly overexpressed in PDGF-driven, PTEN/p53-null and PTEN-null mouse GBM cells (Fig. 6). Considering that U87-PDGF cells express wild-type PTEN and p53, we transiently modulated the expression of both tumor suppressors in U87-PDGF cells, although no significant changes in miR-21 expression levels have been detected (Fig. 7). These observations suggest that the effect of PDGF-B on miRNA expression varies according to the type of target cell and genetic background. However, since we were not able to completely silence PTEN and p53 in U87-PDGF cells, at least partially due to the reduced number of cells that internalizes the fluorescently-labeled siRNAs, future studies should involve the development of PTEN/p53-null U87-PDGF cells to fully elucidate the role of these tumor suppressors in PDGF-related miRNA modulation.

Studies from Hata's group may provide a clue to clarify the mechanisms by which PDGF-B promotes miR-21 downregulation in U87-PDGF cells. TGF-β and BMP were shown to trigger vSMC differentiation to a more contractile phenotype by SMAD-mediated increase in miR-21 expression (314). Moreover, by inducing miR-24, PDGF-B was shown to reduce the expression of SMAD proteins and decrease BMP and TGF-β signaling, thus promoting a synthetic phenotype in vSMCs (521). Therefore, by antagonizing TGF-β, PDGF-B was able to modulate the levels of miR-21 in vSMCs. It is possible that such a mechanism can also be occurring in U87-PDGF cells. Another explanation for the observed reduction in miR-21 levels relies on the existence of miRNA "sponge" modulators (522), which include both mRNAs and noncoding RNAs. Depending on their expression levels and on the total number of functional miRNA-binding sites, "sponge" modulators can decrease the number of free miRNA molecules available to repress other functional targets (522). Therefore, it is reasonable to assume that by activating several signaling pathways, including Ras and ERK1/2 (523),

PDGF-B could be modulating a network of genes that would ultimately result in the overexpression of a miR-21 "sponge" and consequent decrease in miR-21 levels.

In summary, our findings provide new insights into the PDGF signaling in brain tumors and implicate ncRNAs in the PDGF-mediated regulation of tumorigenesis, which can be of great importance for the development of targeted anticancer therapies towards the highly heterogeneous GBM.

5. Materials and Methods

Materials

Pifithrin-α was acquired from Sigma (Munich, Germany) and stock solutions were prepared in DMSO (Sigma) and used within a 3-day period. The anti-PDGF-B siRNA and a noncoding sequence were acquired from Ambion (Austin, TX, USA). The anti-PTEN siRNA and a noncoding sequence were kindly donated by GenePharma (Shangai, China). The plasmids pcDNA3.1-miR-21 and pCMV-PL were obtained from Addgene (Cambridge, MA, USA). The locked nucleic acid (LNA)-modified anti-miR-21 oligonucleotides and a noncoding (scrambled) sequence were acquired from Exiqon (Vedbaek, Denmark). Digoxigenin (DIG)-labeled LNA detection probes for miR-21, scrambled control and U6snRNA were also acquired from Exiqon. All sequences are displayed in Supplementary Data, Table S3. Custom-designed miRNA PCR plates (Pick&Mix miRNA PCR panels) were acquired from Exiqon. Total RNA from adult human brain was acquired from Clontech (Mountain View, CA, USA). All other reagents were obtained from Sigma unless stated otherwise.

Cell lines and culturing conditions

Double-floxed (PTEN$^{-/-}$p53$^{-/-}$) (MGPP1) and PTEN-floxed (PTEN$^{-/-}$) mouse GBM cell lines overexpressing PDGF-B (PDGF-B$^{+/+}$) were derived from established mouse GBM models and maintained in culture, as described previously (425). F98 rat glioma cell line was kindly donated by Dr. Hélène Elleaume (European Synchrotron Radiation Facility, Grenoble, France). GL261 mouse glioma cell line was kindly donated by Dr. Perez-Castillo (Universidad Autónoma de Madrid, Madrid, Spain). U87 human GBM cell line was obtained from the American Type Culture Collection (Manassas, VA, USA). Glioma cell lines were maintained in DMEM (Invitrogen, Carlsbad, CA, USA), supplemented with 10% heat-inactivated FBS (Gibco, Paisley, Scotland), 100 U/ml penicillin (Sigma), 100 µg/ml streptomycin (Sigma) and

cultured at 37°C under a humidified atmosphere containing 5% CO_2. Undifferentiated P19 embryonal carcinoma cell line, kindly donated by Dr. Richard Cerione (Cornell University, NY, USA), was maintained in alpha minimum essential medium (α-MEM) (Gibco); supplements and growth conditions were similar to those used for glioma cells. Primary rat cortical astrocyte cultures were prepared from the cerebral cortices of newborn pups according to established protocols (453). Cell plating densities for all our experiments are indicated in Supplementary Methods.

Cell line production and PDGF concentration measurement

A modified U87 cell line overexpressing PDGF-B (U87-PDGF) was derived from U87 cells after infection with a previously described PDGF-B retrovirus (289). Briefly, a 0.8 kb fragment encoding PDGF-B-hemagglutinin (HA) was ligated into the MCS1 region of the retroviral vector PQ-MCS1-IRES-eGFP. U87 cells infected with the same retroviral vector but without the PDGF-B-HA construct were used as a control. Cell lines were maintained in culture as described above for glioma cells. Cells plated onto 10 cm culture dishes at a 90% confluency were incubated for 48 hours in serum-free basal media. PDGF-B determination was performed in the conditioned media via ELISA (R&D Systems, Minneapolis, MN, USA). Parental U87 conditioned media had undetectable levels of PDGF-B, while U87-PDGF conditioned media had a mean concentration of 353 ng/ml. We have previously shown that the U87 cell line does not secrete significant levels of PDGF-A (289).

Cell transfection

For siRNA and plasmid transfection, complexes with siRNAs and Lipofectamine RNAiMax or DNA with Lipofectamine 2000 (respectively) (Invitrogen) were prepared following the manufacturer's instructions and added to cells, maintained in OptiMEM medium (Gibco), at a final concentration of 50/100 nM siRNA or 1 μg plasmid/100.000 cells. After 4 hour incubation, cells were washed with PBS and further cultured in fresh DMEM medium for 24 (anti-PDGF-B siRNA transfection) or 48 hours (anti-PTEN siRNA or plasmid transfection), before RNA extraction. Anti-miR-21 oligonucleotide transfection followed a similar procedure but lipoplexes were prepared with DLS liposomes, as described by Trabulo and colleagues (429). This formulation has already shown great efficacy in delivering single-stranded oligonucleotides into cultured cells.

Cell viability

Cell viability was evaluated by a modified Alamar blue assay, as described previously (466). Briefly, 1 ml of 10% (v/v) Alamar blue dye in complete DMEM medium was added to each well and cells were incubated at 37°C until the development of a pink coloration. Two hundred microliters of supernatant were collected from each well, transferred to 96-well plates and the absorbance at 570 and 600 nm was measured in a microplate reader (SpectraMaz Plus 384, Molecular devices). Cell viability was calculated as percentage of control cells using the formula: $(A_{570} − A_{600})$ of treated cells × 100 ∕ $(A_{570} − A_{600})$ of control cells.

RNA extraction and cDNA synthesis in cultured cells

Total RNA from cultured cells was extracted using the miRCURY RNA extraction kit (Exiqon). After RNA quantification, different transcription protocols were performed depending on the type of RNA to be determined by qPCR.

For miRNA quantification, cDNA conversion was performed using the Universal cDNA synthesis Kit (Exiqon). For each sample, cDNA was produced from 25 ng of total RNA (10 ng for the miRNA PCR panel assay) in an iQ5 thermocycler, by applying the following protocol: 60 min at 42°C and 5 min at 95°C. The cDNA was further diluted 1:60 (1:100 for the miRNA PCR panel assay) with RNase-free water prior to quantification by qPCR.

For mRNA quantification, cDNA conversion was performed using the iScript™ cDNA synthesis Kit (Bio-Rad). For each sample, cDNA was produced from 1 μg of total RNA in an iQ5 thermocycler, by applying the following protocol: 5 min at 25°C, 30 min at 42°C and 5 min at 85°C. The cDNA was further diluted 1:3 with RNase-free water prior to quantification by qPCR.

QPCR quantification of miRNA expression

MiRNA quantification in cultured cells was performed in an iQ5 thermocycler using 96-well microtitre plates and the SYBR® Green Master Mix (Exiqon). The primers for the target miRNAs (miR-128, miR-21 and miR-221) and the references U6snRNA, snord44 and snord110 were also acquired from Exiqon. A master mix was prepared for each primer set, containing a fixed volume of SYBR Green master mix and the appropriate amount of each primer to yield a final concentration of 150 nM. For each reaction, performed in duplicate, 12

μl of master mix were added to 8 μl of template cDNA. Reaction conditions consisted of enzyme activation and well-factor determination at 95°C for 10 min followed by 40 cycles at 95°C for 10 s (denaturation) and 60 s at 60°C (annealing and elongation). The melting curve protocol started immediately after and consisted of 1 min heating at 55°C followed by eighty 10 s steps, with 0.5°C increases in temperature at each step. Threshold values for threshold cycle determination (Ct) were generated automatically by the iQ5 Optical System Software. Relative miRNA levels were determined following the Pfaffl method for relative miRNA quantification in the presence of target and reference genes with different amplification efficiencies (458). The amplification efficiency for each target or reference gene was determined according to the formula: $E=10^{(-1/S)}$, where S is the slope of the standard curve obtained for each gene.

QPCR quantification of mRNA expression

MRNA quantification in cultured cells was performed in an iQ5 thermocycler using 96-well microtitre plates and the iQ™ SYBR® Green Supermix Kit (Bio-Rad). The primers for the target genes (PDGF-BB, PTEN) and the reference gene (HPRT1) were pre-designed by Qiagen. A master mix was prepared for each primer set, containing a fixed volume of SYBR Green master mix, water and the appropriate amount of each primer to yield a final concentration of 150 nM. For each reaction, performed in duplicate, 20 μl of master mix were added to 5 μl of template cDNA. The reaction conditions consisted of enzyme activation and well-factor determination at 95°C for 1 min and 30 s followed by 40 cycles at 95°C for 10 s (denaturation), 30 s at 55°C (annealing) and 30 s at 72°C (elongation). The melting curve protocol consisted of 1 min heating at 55°C followed by eighty 10 s steps, with 0.5°C increases in temperature at each step. The percentage of PDGF-BB knockdown was determined following the Pfaffl method for relative mRNA quantification in the presence of target and reference genes with different amplification efficiencies (458).

MiRNA PCR panels

MiRNA quantification using the 96-well miRNA PCR plates (Exiqon) was performed in an iQ5 thermocycler using the SYBR® Green Master Mix (Exiqon). The primers for the target miRNAs and the references are displayed in Supplementary Table S2. A master mix was prepared for each sample, containing equal volumes (1:1) of SYBR Green master mix and

diluted cDNA. For each reaction, performed in duplicate, 10 µl of master mix were added per well. Reaction conditions and melting curve protocol were similar to those described for qPCR quantification of miRNA expression. Threshold values for threshold cycle determination (Ct) were generated automatically by the iQ5 Optical System Software. The GeNorm module (524) was used to determine the most stable reference gene. Relative miRNA levels calculation and statistical analysis were performed using the software qBase[Plus] software (Biogazelle, Gent, Belgium).

Western blot analysis

Total protein extracts were prepared from cultured U87-PDGF cells homogeneized at 4º C in lysis buffer (50 mM Tris pH 8.0, 150 mM NaCl, 50 mM EDTA, 0.5% sodium deoxycholate, 1% Triton X-100) containing a protease inhibitor cocktail (Sigma), 2 mM DTT and 0.1 mM PMSF. Protein content was determined using the Bio-Rad Dc protein assay (Bio-Rad) and 30 µg of total protein were resuspended in loading buffer (20% glycerol, 10% SDS, 0.1% bromophenol blue), incubated for 5 min at 95 ºC and loaded onto a 10% polyacrylamide gel. After electrophoresis the proteins were blotted onto a PVDF membrane according to standard protocols. After blocking in 5% nonfat milk, the membrane was incubated with an anti-PTEN antibody (1:1000) (Cell Signaling, Beverly, MA, USA) overnight at 4 ºC, and with the appropriate alkaline phosphatase-labelled secondary antibody (1:20000) (Amersham, Uppsala, Sweden) for 2 h at room temperature. Equal protein loading was shown by reprobing the membrane with an anti-α-tubulin antibody (1:10000) (Sigma) and with the same secondary antibody. The blots were washed several times with saline buffer (TBS/T- 25 mM Tris-HCl, 150 mM NaCl, 0.1% Tween-20), incubated with ECF (alkaline phosphatase substrate; 20 µl of ECF/cm^2 of membrane) for 5 min at room temperature and then submitted to fluorescence detection at 570 nm using a VersaDoc Imaging System Model 3000 (Bio-Rad). For each membrane, the analysis of band intensity was performed using the Quantity One software (Bio-Rad).

Fluorescence *in situ* hybridization (FISH) in cultured cells

FISH analysis was performed in cultured adherent cells as described by Pena and colleagues (460), with some modifications incorporated from the protocol of Lu and colleagues (525). The detailed protocol is described in Supplementary Methods.

Statistical analysis

All data are presented as means ± standard deviation of at least three independent experiments, each performed in triplicate, unless stated otherwise. One way analysis of variance (ANOVA) combined with the Tukey posthoc test was used for multiple comparisons in cell culture experiments and considered significant when $P < 0.05$. Statistical differences are presented at probability levels of $p < 0.05$, $p < 0.01$ and $p < 0.001$. Calculations were performed with standard statistical software (Prism 5, GraphPad, San Diego, CA, USA).

6. Supplementary Figures
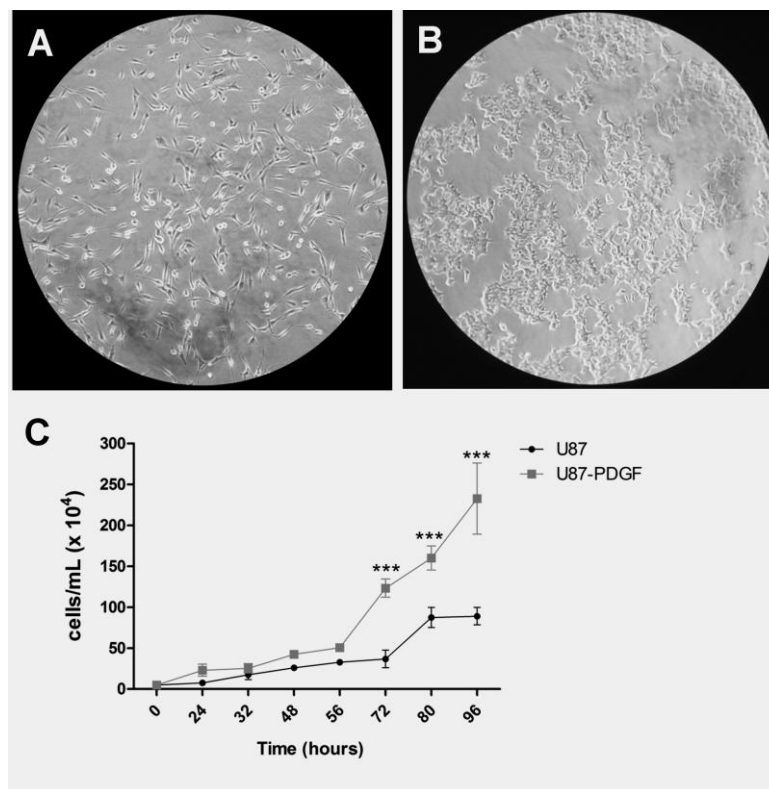
Supplementary Figure 1. Morphology and proliferation of cultured U87 and U87-PDGF human glioblastoma cells. Cultured (**A**) U87 and (**B)** U87-PDGF GBM cells, 48 hours after platting onto cell culture flasks. Images were obtained by light microscopy with a 10x ampliation. (**C)** U87 and U87-PDGF cells were plated onto 48-well plates at a density of 2.5×10^4 cells/well. At defined time points, cells were washed with PBS, trypsinized and ressuspended in culture medium. The number of viable cells was determined by Trypan blue exclusion. *** $p < 0.001$ compared to U87-PDGF cells.
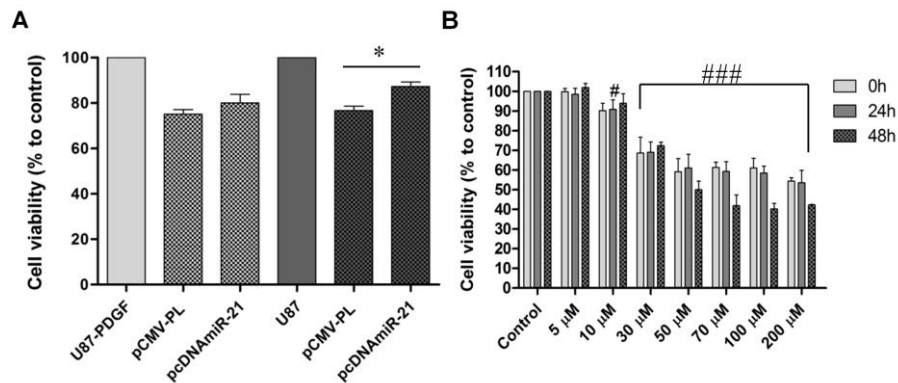
Supplementary Figure 2. Cell viability after incubation with the miR-21-encoding plasmid pcDNAmiR-21 or the p53 inhibitor pifithrin-α. For plasmid transfection of U87 and U87-PDGF cells, 24 hours before any experiment cells were plated onto 6-well plates at a density of 1×10^5 and 8×10^4 cells/well (respectively). (**A**) U87-PDGF and U87 cells incubated for 4 hours with the plasmid coding for the human miR-21 (pcDNA3.1-miR-21) or non-coding plasmid (pCMV-PL), followed by replacement with fresh medium. Forty-eight hours after medium replacement, cell viability was evaluated using the Alamar blue assay, as described in Materials and Methods. ** p<0.01 compared to imatinib-treated cells. For incubation with pifithrin-α, 24 hours before any experiment U87-PDGF cells were plated onto 24-well plates at a density of 4×10^4 cells/well. (**B**) U87-PDGF cells incubated for 24 hours with different concentrations of pifithrin-α, followed by replacement with fresh medium. Cell viability was evaluated using the Alamar blue assay after medium replacement (0h) and further incubation for 24 (24h) and 48 hours (48h). Control experiments with the vehicle DMSO did not affect cell viability (not shown). # p<0.05, ### p<0.001 compared to control U87-PDGF cells.

Chapter 6

Concluding remarks and future perspectives

Concluding remarks and future perspectives

The major remarks from the results presented in this Thesis and their implications in the field of gene therapy for glioblastoma (GBM) are summarized below.

- MiR-21 was shown to be upregulated and miR-128 was shown to be downregulated in tissue samples from mouse GBM models and in a large number of human GBM samples. Importantly, overexpression of miR-21 and reduced expression of miR-128 were found to occur in the four different subtypes of GBM (classical, pro-neural, neural and mesenchymal), which emphasizes the widespread character of these alterations in the global GBM profile.

- Abnormal expression of a group of miRNAs (miR-106a, miR-130b, miR-155, miR-20a, miR-221/222, let-7i) was found to be associated with the different GBM subtypes. Alterations in the expression of the miR-221/222 cluster occur predominantly in the proneural and neural subtypes, whereas alterations in let-7i are predominant in the classical group; alterations in the oncogenic miR-20a and miR-106a are common to both subtypes. In addition to other miRNA signatures that were reported to correlate with treatment response and overall survival in GBM patients, these findings hold great promise in clinics, as complementary molecular markers that may help in the correct identification of the different GBM subclasses.

- LNA-modified oligonucleotide-mediated miR-21 silencing increased the expression of the tumor suppressors PTEN and PDCD4 and the p53-related cell cycle regulator p21. Moreover, increased caspase 3/7 activation was observed in GBM cells following repression of miR-21 expression, which indicates that miR-21 has a significant anti-apoptotic role in GBM.

- MiR-21 silencing enhanced the cytotoxic effect of the tyrosine kinase inhibitor sunitinib, a drug currently being tested in clinical trials for GBM, whereas no therapeutic benefit was observed upon combination of miR-21 silencing with the first line drug temozolomide. Moreover, sunitinib was shown to repress the signaling of the pro-oncogenic transcription factor NF-kB, which, in association with the increased expression of tumor suppressors PTEN and PDCD4 and p53-related p21, contributed

to the decreased tumor cell viability resulting from the combination of miR-21 silencing with this drug.

- Stable nucleic acid lipid particle (SNALPs), targeted to glioma cells by covalent coupling of the tumor-specific peptide chlorotoxin (CTX), were shown to display optimal physicochemical properties for *in vivo* application, including high encapsulation efficiency, low size, electrical neutrality and high protection against enzymatic degradation.
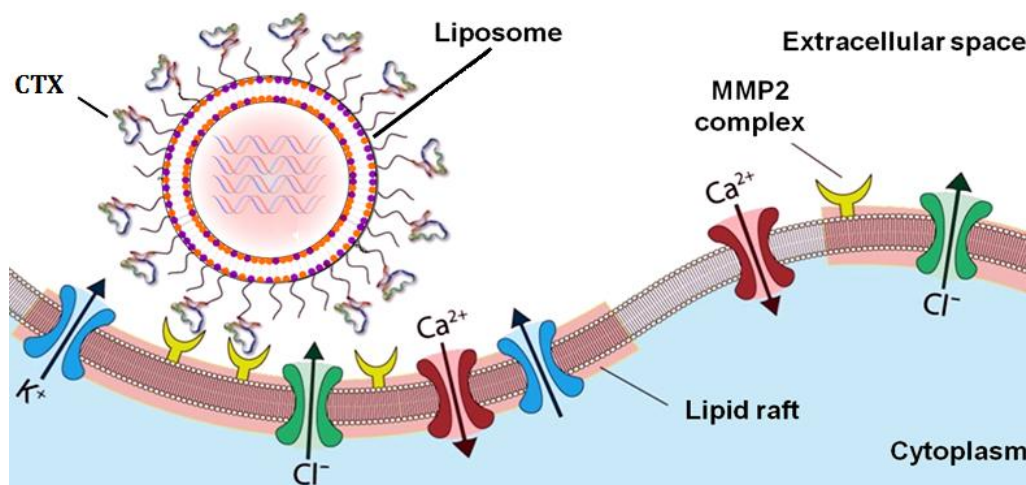
Figure 20. **SNALPs targeted to tumor cells by attachment of the peptide CTX**. CTX was reported to bind to a multiprotein complex that includes the matrix metalloproteinase MMP-2, in cholesterol-rich areas of the cell membrane known as lipid rafts. Upon binding to their receptor, the nanoparticles are internalized via receptor-mediated endocytosis. Adapted from Veiseh and Gunn, 2009 (http://www.ncbi.nlm.nih.gov/pmc/articles/PMC2692352/pdf/nihms-109549.pdf).

- Targeted (CTX-coupled) SNALPs were able to efficiently deliver anti-miR-21 oligonucleotides to cultured GBM cells, which resulted in a decreased expression of miR-21, increased expression of the tumor suppressors PTEN and PDCD4, caspase 3/7 activation and enhanced cytotoxic effect of sunitinib.

- No significant CTX-coupled SNALP internalization was observed in astrocytes and human embryonic kidney cells, which indicates that delivery of encapsulated nucleic

168

acids via targeted SNALPs is restricted to non-cancer cells, therefore minimizing the side effects that are generally associated with the current anti-tumoral approaches.

- Targeted SNALPs were shown to efficiently deliver antisense oligonucleotides and siRNAs to GBM cells, which indicates that these nanoparticles are highly versatile and can deliver different types of oligonucleotides to target cells.

- Increased FAM-labeled siRNA internalization into implanted intracranial tumors was observed upon intravenous administration of the targeted SNALPs, which suggests that SNALPs efficiently deliver nucleic acids to established brain tumors. Future experiments should evaluate whether the intravenous administration of the targeted SNALPs concomitant with oral sunitinib will promote an anti-tumor activity similar to that observed in cultured GBM cells upon incubation with targeted SNALPs followed by exposure to sunitinib.

- PDGF-B, an angiogenic growth factor which has been implicated in the development and progression of GBM, was shown to enhance tumorigenesis of U87 human GBM cells by promoting the upregulation of several oncomiRs (including members of the miR-106b family) and downregulation of tumor suppressor miRNAs (including let-7b). Nevertheless, the mechanisms by which this growth factor regulates miRNA expression need to be investigated.

Overall, the results presented in this Thesis demonstrate the great potential of the multimodal miRNA-based gene therapy, combining tumor-targeted SNALP-mediated miR-21 silencing with the multiple tyrosine kinase inhibitor sunitinib, which therefore deserves to be explored in preclinical studies, aiming at its successful clinical application towards GBM. Considering the elevated expression of miR-21 in other human malignancies and the reported affinity of chlorotoxin towards cancer cells, it is expected that the developed targeted nanosystem will constitute a valuable tool to be applied as an alternative or complementary therapeutic approach for other types of cancer.

References

1. Ware, ML, Berger, MS, and Binder, DK (2003). Molecular biology of glioma tumorigenesis. *Histol Histopathol* **18**: 207-216.
2. Furnari, FB, Fenton, T, Bachoo, RM, Mukasa, A, Stommel, JM, Stegh, A*, et al.* (2007). Malignant astrocytic glioma: genetics, biology, and paths to treatment. *Genes Dev* **21**: 2683-2710.
3. Wen, PY, and Kesari, S (2008). Malignant gliomas in adults. *N Engl J Med* **359**: 492-507.
4. Ohgaki, H, and Kleihues, P (2007). Genetic pathways to primary and secondary glioblastoma. *Am J Pathol* **170**: 1445-1453.
5. Nieto-Sampedro, M, Valle-Argos, B, Gomez-Nicola, D, Fernandez-Mayoralas, A, and Nieto-Diaz, M (2011). Inhibitors of Glioma Growth that Reveal the Tumour to the Immune System. *Clin Med Insights Oncol* **5**: 265-314.
6. Schwartzbaum, JA, Fisher, JL, Aldape, KD, and Wrensch, M (2006). Epidemiology and molecular pathology of glioma. *Nat Clin Pract Neurol* **2**: 494-503; quiz 491 p following 516.
7. Kunkle, B, Yoo, C, and Roy, D (2012). Discovering gene-environment interactions in Glioblastoma through a comprehensive data integration bioinformatics method. *Neurotoxicology* **35C**: 1-14.
8. Kesari, S (2011). Understanding glioblastoma tumor biology: the potential to improve current diagnosis and treatments. *Semin Oncol* **38 Suppl 4**: S2-10.
9. Bonavia, R, Inda, MM, Cavenee, WK, and Furnari, FB (2011). Heterogeneity maintenance in glioblastoma: a social network. *Cancer Res* **71**: 4055-4060.
10. Nowell, PC (1976). The clonal evolution of tumor cell populations. *Science* **194**: 23-28.
11. The Cancer Genome Atlas Research Network (2008). Comprehensive genomic characterization defines human glioblastoma genes and core pathways. *Nature* **455**: 1061-1068.
12. Verhaak, RG, Hoadley, KA, Purdom, E, Wang, V, Qi, Y, Wilkerson, MD*, et al.* (2010). Integrated genomic analysis identifies clinically relevant subtypes of glioblastoma characterized by abnormalities in PDGFRA, IDH1, EGFR, and NF1. *Cancer Cell* **17**: 98-110.
13. Brennan, C, Momota, H, Hambardzumyan, D, Ozawa, T, Tandon, A, Pedraza, A*, et al.* (2009). Glioblastoma subclasses can be defined by activity among signal transduction pathways and associated genomic alterations. *PLoS One* **4**: e7752.
14. Dunn, GP, Rinne, ML, Wykosky, J, Genovese, G, Quayle, SN, Dunn, IF*, et al.* (2012). Emerging insights into the molecular and cellular basis of glioblastoma. *Genes Dev* **26**: 756-784.
15. Quelle, DE, Zindy, F, Ashmun, RA, and Sherr, CJ (1995). Alternative reading frames of the INK4a tumor suppressor gene encode two unrelated proteins capable of inducing cell cycle arrest. *Cell* **83**: 993-1000.
16. Sherr, CJ (2006). Autophagy by ARF: a short story. *Mol Cell* **22**: 436-437.
17. Bolos, V, Grego-Bessa, J, and de la Pompa, JL (2007). Notch signaling in development and cancer. *Endocr Rev* **28**: 339-363.
18. Merchant, AA, and Matsui, W (2010). Targeting Hedgehog - a cancer stem cell pathway. *Clin Cancer Res* **16**: 3130-3140.
19. Lokker, NA, Sullivan, CM, Hollenbach, SJ, Israel, MA, and Giese, NA (2002). Platelet-derived growth factor (PDGF) autocrine signaling regulates survival and mitogenic pathways in glioblastoma cells: evidence that the novel PDGF-C and PDGF-D ligands may play a role in the development of brain tumors. *Cancer Res* **62**: 3729-3735.
20. Zhao, S, Lin, Y, Xu, W, Jiang, W, Zha, Z, Wang, P*, et al.* (2009). Glioma-derived mutations in IDH1 dominantly inhibit IDH1 catalytic activity and induce HIF-1alpha. *Science* **324**: 261-265.
21. Cichowski, K, and Jacks, T (2001). NF1 tumor suppressor gene function: narrowing the GAP. *Cell* **104**: 593-604.
22. Feldkamp, MM, Angelov, L, and Guha, A (1999). Neurofibromatosis type 1 peripheral nerve tumors: aberrant activation of the Ras pathway. *Surg Neurol* **51**: 211-218.
23. Hegi, ME, Diserens, AC, Gorlia, T, Hamou, MF, de Tribolet, N, Weller, M*, et al.* (2005). MGMT gene silencing and benefit from temozolomide in glioblastoma. *N Engl J Med* **352**: 997-1003.
24. Stupp, R, Mason, WP, van den Bent, MJ, Weller, M, Fisher, B, Taphoorn, MJ*, et al.* (2005). Radiotherapy plus concomitant and adjuvant temozolomide for glioblastoma. *N Engl J Med* **352**: 987-996.
25. Stupp, R, Hegi, ME, Mason, WP, van den Bent, MJ, Taphoorn, MJ, Janzer, RC*, et al.* (2009). Effects of radiotherapy with concomitant and adjuvant temozolomide versus radiotherapy alone on survival in glioblastoma in a randomised phase III study: 5-year analysis of the EORTC-NCIC trial. *Lancet Oncol* **10**: 459-466.

26. Kaina, B, Christmann, M, Naumann, S, and Roos, WP (2007). MGMT: key node in the battle against genotoxicity, carcinogenicity and apoptosis induced by alkylating agents. *DNA Repair (Amst)* **6**: 1079-1099.

27. Cahill, DP, Levine, KK, Betensky, RA, Codd, PJ, Romany, CA, Reavie, LB*, et al.* (2007). Loss of the mismatch repair protein MSH6 in human glioblastomas is associated with tumor progression during temozolomide treatment. *Clin Cancer Res* **13**: 2038-2045.

28. Agnihotri, S, Gajadhar, AS, Ternamian, C, Gorlia, T, Diefes, KL, Mischel, PS*, et al.* (2012). Alkylpurine-DNA-N-glycosylase confers resistance to temozolomide in xenograft models of glioblastoma multiforme and is associated with poor survival in patients. *J Clin Invest* **122**: 253-266.

29. Anton, K, Baehring, JM, and Mayer, T (2012). Glioblastoma multiforme: overview of current treatment and future perspectives. *Hematol Oncol Clin North Am* **26**: 825-853.

30. Perry, JR, Rizek, P, Cashman, R, Morrison, M, and Morrison, T (2008). Temozolomide rechallenge in recurrent malignant glioma by using a continuous temozolomide schedule: the "rescue" approach. *Cancer* **113**: 2152-2157.

31. Jain, RK, di Tomaso, E, Duda, DG, Loeffler, JS, Sorensen, AG, and Batchelor, TT (2007). Angiogenesis in brain tumours. *Nat Rev Neurosci* **8**: 610-622.

32. Batchelor, TT, Sorensen, AG, di Tomaso, E, Zhang, WT, Duda, DG, Cohen, KS*, et al.* (2007). AZD2171, a pan-VEGF receptor tyrosine kinase inhibitor, normalizes tumor vasculature and alleviates edema in glioblastoma patients. *Cancer Cell* **11**: 83-95.

33. Neyns, B, Sadones, J, Chaskis, C, Dujardin, M, Everaert, H, Lv, S*, et al.* (2011). Phase II study of sunitinib malate in patients with recurrent high-grade glioma. *J Neurooncol* **103**: 491-501.

34. Desjardins, A, Reardon, DA, Coan, A, Marcello, J, Herndon, JE, 2nd, Bailey, L*, et al.* (2012). Bevacizumab and daily temozolomide for recurrent glioblastoma. *Cancer* **118**: 1302-1312.

35. Vredenburgh, JJ, Desjardins, A, Herndon, JE, 2nd, Dowell, JM, Reardon, DA, Quinn, JA*, et al.* (2007). Phase II trial of bevacizumab and irinotecan in recurrent malignant glioma. *Clin Cancer Res* **13**: 1253-1259.

36. Fraum, TJ, Kreisl, TN, Sul, J, Fine, HA, and Iwamoto, FM (2011). Ischemic stroke and intracranial hemorrhage in glioma patients on antiangiogenic therapy. *J Neurooncol* **105**: 281-289.

37. Gerstner, ER, and Batchelor, TT (2012). Antiangiogenic therapy for glioblastoma. *Cancer J* **18**: 45-50.

38. Soda, Y, Marumoto, T, Friedmann-Morvinski, D, Soda, M, Liu, F, Michiue, H*, et al.* (2011). Transdifferentiation of glioblastoma cells into vascular endothelial cells. *Proc Natl Acad Sci USA* **108**: 4274-4280.

39. Clarke, J, Butowski, N, and Chang, S (2010). Recent advances in therapy for glioblastoma. *Arch Neurol* **67**: 279-283.

40. Chang, SM, Wen, P, Cloughesy, T, Greenberg, H, Schiff, D, Conrad, C*, et al.* (2005). Phase II study of CCI-779 in patients with recurrent glioblastoma multiforme. *Invest New Drugs* **23**: 357-361.

41. Galanis, E, Buckner, JC, Maurer, MJ, Kreisberg, JI, Ballman, K, Boni, J*, et al.* (2005). Phase II trial of temsirolimus (CCI-779) in recurrent glioblastoma multiforme: a North Central Cancer Treatment Group Study. *J Clin Oncol* **23**: 5294-5304.

42. Abounader, R (2009). Interactions between PTEN and receptor tyrosine kinase pathways and their implications for glioma therapy. *Expert Rev Anticancer Ther* **9**: 235-245.

43. Cheng, CK, Fan, QW, and Weiss, WA (2009). PI3K signaling in glioma--animal models and therapeutic challenges. *Brain Pathol* **19**: 112-120.

44. Deeken, JF, and Loscher, W (2007). The blood-brain barrier and cancer: transporters, treatment, and Trojan horses. *Clin Cancer Res* **13**: 1663-1674.

45. Qin, DX, Zheng, R, Tang, J, Li, JX, and Hu, YH (1990). Influence of radiation on the blood-brain barrier and optimum time of chemotherapy. *Int J Radiat Oncol Biol Phys* **19**: 1507-1510.

46. Schlageter, KE, Molnar, P, Lapin, GD, and Groothuis, DR (1999). Microvessel organization and structure in experimental brain tumors: microvessel populations with distinctive structural and functional properties. *Microvasc Res* **58**: 312-328.

47. Rapoport, SI (2001). Advances in osmotic opening of the blood-brain barrier to enhance CNS chemotherapy. *Expert Opin Investig Drugs* **10**: 1809-1818.

48. Jahnke, K, Kraemer, DF, Knight, KR, Fortin, D, Bell, S, Doolittle, ND*, et al.* (2008). Intraarterial chemotherapy and osmotic blood-brain barrier disruption for patients with embryonal and germ cell tumors of the central nervous system. *Cancer* **112**: 581-588.

49. Liu, HL, Hua, MY, Chen, PY, Chu, PC, Pan, CH, Yang, HW*, et al.* (2010). Blood-brain barrier disruption with focused ultrasound enhances delivery of chemotherapeutic drugs for glioblastoma treatment. *Radiology* **255**: 415-425.

50. McDannold, N, Arvanitis, CD, Vykhodtseva, N, and Livingstone, MS (2012). Temporary disruption of the blood-brain barrier by use of ultrasound and microbubbles: safety and efficacy evaluation in rhesus macaques. *Cancer Res* **72**: 3652-3663.

51. Buonerba, C, Di Lorenzo, G, Marinelli, A, Federico, P, Palmieri, G, Imbimbo, M*, et al.* (2011). A comprehensive outlook on intracerebral therapy of malignant gliomas. *Crit Rev Oncol Hematol* **80**: 54-68.

52. Westphal, M, Hilt, DC, Bortey, E, Delavault, P, Olivares, R, Warnke, PC*, et al.* (2003). A phase 3 trial of local chemotherapy with biodegradable carmustine (BCNU) wafers (Gliadel wafers) in patients with primary malignant glioma. *Neuro Oncol* **5**: 79-88.

53. Affronti, ML, Heery, CR, Herndon, JE, 2nd, Rich, JN, Reardon, DA, Desjardins, A*, et al.* (2009). Overall survival of newly diagnosed glioblastoma patients receiving carmustine wafers followed by radiation and concurrent temozolomide plus rotational multiagent chemotherapy. *Cancer* **115**: 3501-3511.

54. Sabel, M, and Giese, A (2008). Safety profile of carmustine wafers in malignant glioma: a review of controlled trials and a decade of clinical experience. *Curr Med Res Opin* **24**: 3239-3257.

55. Allard, E, Passirani, C, and Benoit, JP (2009). Convection-enhanced delivery of nanocarriers for the treatment of brain tumors. *Biomaterials* **30**: 2302-2318.

56. Sampson, JH, Akabani, G, Archer, GE, Berger, MS, Coleman, RE, Friedman, AH*, et al.* (2008). Intracerebral infusion of an EGFR-targeted toxin in recurrent malignant brain tumors. *Neuro Oncol* **10**: 320-329.

57. Yamashita, Y, Krauze, MT, Kawaguchi, T, Noble, CO, Drummond, DC, Park, JW*, et al.* (2007). Convection-enhanced delivery of a topoisomerase I inhibitor (nanoliposomal topotecan) and a topoisomerase II inhibitor (pegylated liposomal doxorubicin) in intracranial brain tumor xenografts. *Neuro Oncol* **9**: 20-28.

58. Krauze, MT, Forsayeth, J, Yin, D, and Bankiewicz, KS (2009). Convection-enhanced delivery of liposomes to primate brain. *Methods Enzymol* **465**: 349-362.

59. Saito, R, Krauze, MT, Noble, CO, Tamas, M, Drummond, DC, Kirpotin, DB*, et al.* (2006). Tissue affinity of the infusate affects the distribution volume during convection-enhanced delivery into rodent brains: implications for local drug delivery. *J Neurosci Methods* **154**: 225-232.

60. Marupudi, NI, Han, JE, Li, KW, Renard, VM, Tyler, BM, and Brem, H (2007). Paclitaxel: a review of adverse toxicities and novel delivery strategies. *Expert Opin Drug Saf* **6**: 609-621.

61. Sawyer, AJ, Saucier-Sawyer, JK, Booth, CJ, Liu, J, Patel, T, Piepmeier, JM*, et al.* (2011). Convection-enhanced delivery of camptothecin-loaded polymer nanoparticles for treatment of intracranial tumors. *Drug Deliv Transl Res* **1**: 34-42.

62. Chastagner, PB, Labussière, M., Pinel, S., Bernier, V., Fouyssac, F., Plénat, F. (2005). Comparison of doxorubicin and its non-pegylated liposomal form as radiosensitizer in high grade glioma xenografts. *Journal of Clinical Oncology, 2005 ASCO Annual Meeting Proceedings* **23**: 1542.

63. Jiang, X, Xin, H, Sha, X, Gu, J, Jiang, Y, Law, K*, et al.* (2011). PEGylated poly(trimethylene carbonate) nanoparticles loaded with paclitaxel for the treatment of advanced glioma: in vitro and in vivo evaluation. *Int J Pharm* **420**: 385-394.

64. Voges, J, Reszka, R, Gossmann, A, Dittmar, C, Richter, R, Garlip, G*, et al.* (2003). Imaging-guided convection-enhanced delivery and gene therapy of glioblastoma. *Ann Neurol* **54**: 479-487.

65. Ananda, S, Nowak, AK, Cher, L, Dowling, A, Brown, C, Simes, J*, et al.* (2011). Phase 2 trial of temozolomide and pegylated liposomal doxorubicin in the treatment of patients with glioblastoma multiforme following concurrent radiotherapy and chemotherapy. *J Clin Neurosci* **18**: 1444-1448.

66. Parney, IF, Farr-Jones, MA, Chang, LJ, and Petruk, KC (2000). Human glioma immunobiology in vitro: implications for immunogene therapy. *Neurosurgery* **46**: 1169-1177.

67. Zuber, P, Kuppner, MC, and De Tribolet, N (1988). Transforming growth factor-beta 2 down-regulates HLA-DR antigen expression on human malignant glioma cells. *Eur J Immunol* **18**: 1623-1626.

68. Wintterle, S, Schreiner, B, Mitsdoerffer, M, Schneider, D, Chen, L, Meyermann, R*, et al.* (2003). Expression of the B7-related molecule B7-H1 by glioma cells: a potential mechanism of immune paralysis. *Cancer Res* **63**: 7462-7467.

69. Heimberger, AB, Hlatky, R, Suki, D, Yang, D, Weinberg, J, Gilbert, M*, et al.* (2005). Prognostic effect of epidermal growth factor receptor and EGFRvIII in glioblastoma multiforme patients. *Clin Cancer Res* **11**: 1462-1466.

70. Heimberger, AB, and Sampson, JH (2009). The PEPvIII-KLH (CDX-110) vaccine in glioblastoma multiforme patients. *Expert Opin Biol Ther* **9**: 1087-1098.

71. Chang, CN, Huang, YC, Yang, DM, Kikuta, K, Wei, KJ, Kubota, T*, et al.* (2011). A phase I/II clinical trial investigating the adverse and therapeutic effects of a postoperative autologous dendritic cell tumor vaccine in patients with malignant glioma. *J Clin Neurosci* **18**: 1048-1054.

72. Izumoto, S, Tsuboi, A, Oka, Y, Suzuki, T, Hashiba, T, Kagawa, N*, et al.* (2008). Phase II clinical trial of Wilms tumor 1 peptide vaccination for patients with recurrent glioblastoma multiforme. *J Neurosurg* **108**: 963-971.

73. Phuphanich, S, Wheeler, CJ, Rudnick, JD, Mazer, M, Wang, H, Nuno, MA*, et al.* (2012). Phase I trial of a multi-epitope-pulsed dendritic cell vaccine for patients with newly diagnosed glioblastoma. *Cancer Immunol Immunother* **62**: 125-135.

74. Crane, CA, Han, SJ, Ahn, B, Oehlke, J, Kivett, V, Fedoroff, A*, et al.* (2012). Individual patient-specific immunity against high-grade glioma after vaccination with autologous tumor derived peptides bound to the 96 KD chaperone protein. *Clin Cancer Res* **19**: 205-214.

75. Maes, W, and Van Gool, SW (2011). Experimental immunotherapy for malignant glioma: lessons from two decades of research in the GL261 model. *Cancer Immunol Immunother* **60**: 153-160.

76. Wiley, J. and Sons (2012). Gene therapy clinical trials worlwide. vol. 2013. Journal of Gene Medicine.

77. Caruso, G, Caffo, M, Raudino, G, Alafaci, C, Salpietro, FM, and Tomasello, F (2010). Antisense oligonucleotides as innovative therapeutic strategy in the treatment of high-grade gliomas. *Recent Pat CNS Drug Discov* **5**: 53-69.

78. Schlingensiepen, KH, Schlingensiepen, R, Steinbrecher, A, Hau, P, Bogdahn, U, Fischer-Blass, B*, et al.* (2006). Targeted tumor therapy with the TGF-beta 2 antisense compound AP 12009. *Cytokine Growth Factor Rev* **17**: 129-139.

79. Hau, P, Jachimczak, P, and Bogdahn, U (2009). Treatment of malignant gliomas with TGF-beta2 antisense oligonucleotides. *Expert Rev Anticancer Ther* **9**: 1663-1674.

80. Fulci, G, and Chiocca, EA (2007). The status of gene therapy for brain tumors. *Expert Opin Biol Ther* **7**: 197-208.

81. Aghi, M, and Chiocca, EA (2006). Gene therapy for glioblastoma. *Neurosurg Focus* **20**: E18.

82. Hamel, W, Magnelli, L, Chiarugi, VP, and Israel, MA (1996). Herpes simplex virus thymidine kinase/ganciclovir-mediated apoptotic death of bystander cells. *Cancer Res* **56**: 2697-2702.

83. Mesnil, M, and Yamasaki, H (2000). Bystander effect in herpes simplex virus-thymidine kinase/ganciclovir cancer gene therapy: role of gap-junctional intercellular communication. *Cancer Res* **60**: 3989-3999.

84. Immonen, A, Vapalahti, M, Tyynela, K, Hurskainen, H, Sandmair, A, Vanninen, R*, et al.* (2004). AdvHSV-tk gene therapy with intravenous ganciclovir improves survival in human malignant glioma: a randomised, controlled study. *Mol Ther* **10**: 967-972.

85. Mitchell, P (2010). Ark's gene therapy stumbles at the finish line. *Nat Biotechnol* **28**: 183-184.

86. Rainov, NG (2000). A phase III clinical evaluation of herpes simplex virus type 1 thymidine kinase and ganciclovir gene therapy as an adjuvant to surgical resection and radiation in adults with previously untreated glioblastoma multiforme. *Hum Gene Ther* **11**: 2389-2401.

87. Sandmair, AM, Loimas, S, Puranen, P, Immonen, A, Kossila, M, Puranen, M*, et al.* (2000). Thymidine kinase gene therapy for human malignant glioma, using replication-deficient retroviruses or adenoviruses. *Hum Gene Ther* **11**: 2197-2205.

88. Lorberboum-Galski, H (2011). Human toxin-based recombinant immunotoxins/chimeric proteins as a drug delivery system for targeted treatment of human diseases. *Expert Opin Drug Deliv* **8**: 605-621.

89. Candolfi, M, Xiong, W, Yagiz, K, Liu, C, Muhammad, AK, Puntel, M*, et al.* (2010). Gene therapy-mediated delivery of targeted cytotoxins for glioma therapeutics. *Proc Natl Acad Sci USA* **107**: 20021-20026.

90. Assi, H, Candolfi, M, Baker, G, Mineharu, Y, Lowenstein, PR, and Castro, MG (2012). Gene therapy for brain tumors: basic developments and clinical implementation. *Neurosci Lett* **527**: 71-77.

91. Kunwar, S, Prados, MD, Chang, SM, Berger, MS, Lang, FF, Piepmeier, JM*, et al.* (2007). Direct intracerebral delivery of cintredekin besudotox (IL13-PE38QQR) in recurrent malignant glioma: a report by the Cintredekin Besudotox Intraparenchymal Study Group. *J Clin Oncol* **25**: 837-844.

92. Saydam, O, Glauser, DL, Heid, I, Turkeri, G, Hilbe, M, Jacobs, AH*, et al.* (2005). Herpes simplex virus 1 amplicon vector-mediated siRNA targeting epidermal growth factor receptor inhibits growth of human glioma cells in vivo. *Mol Ther* **12**: 803-812.

93. Kock, N, Kasmieh, R, Weissleder, R, and Shah, K (2007). Tumor therapy mediated by lentiviral expression of shBcl-2 and S-TRAIL. *Neoplasia* **9**: 435-442.

94.   Liu, XL, Zhao, D, Sun, DP, Wang, Y, Li, Y, Qiu, FQ, *et al.* (2012). Adenovirus-mediated delivery of CALR and MAGE-A3 inhibits invasion and angiogenesis of glioblastoma cell line U87. *J Exp Clin Cancer Res* **31**: 8.

95.   Kambara, H, Okano, H, Chiocca, EA, and Saeki, Y (2005). An oncolytic HSV-1 mutant expressing ICP34.5 under control of a nestin promoter increases survival of animals even when symptomatic from a brain tumor. *Cancer Res* **65**: 2832-2839.

96.   Natsume, A, and Yoshida, J (2008). Gene therapy for high-grade glioma: current approaches and future directions. *Cell Adh Migr* **2**: 186-191.

97.   Hunter, WD, Martuza, RL, Feigenbaum, F, Todo, T, Mineta, T, Yazaki, T, *et al.* (1999). Attenuated, replication-competent herpes simplex virus type 1 mutant G207: safety evaluation of intracerebral injection in nonhuman primates. *J Virol* **73**: 6319-6326.

98.   Markert, JM, Liechty, PG, Wang, W, Gaston, S, Braz, E, Karrasch, M, *et al.* (2009). Phase Ib trial of mutant herpes simplex virus G207 inoculated pre-and post-tumor resection for recurrent GBM. *Mol Ther* **17**: 199-207.

99.   Gambini, E, Reisoli, E, Appolloni, I, Gatta, V, Campadelli-Fiume, G, Menotti, L, *et al.* (2012). Replication-competent herpes simplex virus retargeted to HER2 as therapy for high-grade glioma. *Mol Ther* **20**: 994-1001.

100.   Geoerger, B, Grill, J, Opolon, P, Morizet, J, Aubert, G, Terrier-Lacombe, MJ, *et al.* (2002). Oncolytic activity of the E1B-55 kDa-deleted adenovirus ONYX-015 is independent of cellular p53 status in human malignant glioma xenografts. *Cancer Res* **62**: 764-772.

101.   Chiocca, EA, Abbed, KM, Tatter, S, Louis, DN, Hochberg, FH, Barker, F, *et al.* (2004). A phase I open-label, dose-escalation, multi-institutional trial of injection with an E1B-Attenuated adenovirus, ONYX-015, into the peritumoral region of recurrent malignant gliomas, in the adjuvant setting. *Mol Ther* **10**: 958-966.

102.   Kroeger, KM, Muhammad, AK, Baker, GJ, Assi, H, Wibowo, MK, Xiong, W, *et al.* (2010). Gene therapy and virotherapy: novel therapeutic approaches for brain tumors. *Discov Med* **10**: 293-304.

103.   Tai, CK, Wang, WJ, Chen, TC, and Kasahara, N (2005). Single-shot, multicycle suicide gene therapy by replication-competent retrovirus vectors achieves long-term survival benefit in experimental glioma. *Mol Ther* **12**: 842-851.

104.   Ferguson, SD, Ahmed, AU, Thaci, B, Mercer, RW, and Lesniak, MS (2010). Crossing the boundaries: stem cells and gene therapy. *Discov Med* **9**: 192-196.

105.   Fulci, G, Breymann, L, Gianni, D, Kurozomi, K, Rhee, SS, Yu, J, *et al.* (2006). Cyclophosphamide enhances glioma virotherapy by inhibiting innate immune responses. *Proc Natl Acad Sci USA* **103**: 12873-12878.

106.   Yoshida, J, and Mizuno, M (2003). Clinical gene therapy for brain tumors. Liposomal delivery of anticancer molecule to glioma. *J Neurooncol* **65**: 261-267.

107.   Zhou, J, Atsina, KB, Himes, BT, Strohbehn, GW, and Saltzman, WM (2012). Novel delivery strategies for glioblastoma. *Cancer J* **18**: 89-99.

108.   Gupta, B, Levchenko, TS, and Torchilin, VP (2007). TAT peptide-modified liposomes provide enhanced gene delivery to intracranial human brain tumor xenografts in nude mice. *Oncol Res* **16**: 351-359.

109.   Kato, T, Natsume, A, Toda, H, Iwamizu, H, Sugita, T, Hachisu, R, *et al.* (2010). Efficient delivery of liposome-mediated MGMT-siRNA reinforces the cytotoxity of temozolomide in GBM-initiating cells. *Gene Ther* **17**: 1363-1371.

110.   Natsume, A, Mizuno, M, Ryuke, Y, and Yoshida, J (1999). Antitumor effect and cellular immunity activation by murine interferon-beta gene transfer against intracerebral glioma in mouse. *Gene Ther* **6**: 1626-1633.

111.   Natsume, A, Tsujimura, K, Mizuno, M, Takahashi, T, and Yoshida, J (2000). IFN-beta gene therapy induces systemic antitumor immunity against malignant glioma. *J Neurooncol* **47**: 117-124.

112.   Yagi, K, Hayashi, Y, Ishida, N, Ohbayashi, M, Ohishi, N, Mizuno, M, *et al.* (1994). Interferon-beta endogenously produced by intratumoral injection of cationic liposome-encapsulated gene: cytocidal effect on glioma transplanted into nude mouse brain. *Biochem Mol Biol Int* **32**: 167-171.

113.   Yoshida, J, Mizuno, M, Fujii, M, Kajita, Y, Nakahara, N, Hatano, M, *et al.* (2004). Human gene therapy for malignant gliomas (glioblastoma multiforme and anaplastic astrocytoma) by in vivo transduction with human interferon beta gene using cationic liposomes. *Hum Gene Ther* **15**: 77-86.

114.   Ren, H, Boulikas, T, Lundstrom, K, Soling, A, Warnke, PC, and Rainov, NG (2003). Immunogene therapy of recurrent glioblastoma multiforme with a liposomally encapsulated replication-incompetent Semliki forest virus vector carrying the human interleukin-12 gene--a phase I/II clinical protocol. *J Neurooncol* **64**: 147-154.

115. Liu, X, Madhankumar, AB, Slagle-Webb, B, Sheehan, JM, Surguladze, N, and Connor, JR (2011). Heavy chain ferritin siRNA delivered by cationic liposomes increases sensitivity of cancer cells to chemotherapeutic agents. *Cancer Res* **71**: 2240-2249.
116. Saw, PE, Ko, YT, and Jon, S (2010). Efficient Liposomal Nanocarrier-mediated Oligodeoxynucleotide Delivery Involving Dual Use of a Cell-Penetrating Peptide as a Packaging and Intracellular Delivery Agent. *Macromol Rapid Commun* **31**: 1155-1162.
117. Jin, J, Bae, KH, Yang, H, Lee, SJ, Kim, H, Kim, Y*, et al.* (2011). In vivo specific delivery of c-Met siRNA to glioblastoma using cationic solid lipid nanoparticles. *Bioconjug Chem* **22**: 2568-2572.
118. Zhan, C, Wei, X, Qian, J, Feng, L, Zhu, J, and Lu, W (2012). Co-delivery of TRAIL gene enhances the anti-glioblastoma effect of paclitaxel in vitro and in vivo. *J Control Release* **160**: 630-636.
119. Li, J, Gu, B, Meng, Q, Yan, Z, Gao, H, Chen, X*, et al.* (2011). The use of myristic acid as a ligand of polyethylenimine/DNA nanoparticles for targeted gene therapy of glioblastoma. *Nanotechnology* **22**: 435101.
120. Wang, XL, Nguyen, T, Gillespie, D, Jensen, R, and Lu, ZR (2008). A multifunctional and reversibly polymerizable carrier for efficient siRNA delivery. *Biomaterials* **29**: 15-22.
121. Wang, XL, Ramusovic, S, Nguyen, T, and Lu, ZR (2007). Novel polymerizable surfactants with pH-sensitive amphiphilicity and cell membrane disruption for efficient siRNA delivery. *Bioconjug Chem* **18**: 2169-2177.
122. Wang, XL, Xu, R, Wu, X, Gillespie, D, Jensen, R, and Lu, ZR (2009). Targeted systemic delivery of a therapeutic siRNA with a multifunctional carrier controls tumor proliferation in mice. *Mol Pharm* **6**: 738-746.
123. Veiseh, O, Kievit, FM, Fang, C, Mu, N, Jana, S, Leung, MC*, et al.* (2010). Chlorotoxin bound magnetic nanovector tailored for cancer cell targeting, imaging, and siRNA delivery. *Biomaterials* **31**: 8032-8042.
124. Aboody, KS, Brown, A, Rainov, NG, Bower, KA, Liu, S, Yang, W*, et al.* (2000). Neural stem cells display extensive tropism for pathology in adult brain: evidence from intracranial gliomas. *Proc Natl Acad Sci USA* **97**: 12846-12851.
125. Nakamizo, A, Marini, F, Amano, T, Khan, A, Studeny, M, Gumin, J*, et al.* (2005). Human bone marrow-derived mesenchymal stem cells in the treatment of gliomas. *Cancer Res* **65**: 3307-3318.
126. Nakamura, K, Ito, Y, Kawano, Y, Kurozumi, K, Kobune, M, Tsuda, H*, et al.* (2004). Antitumor effect of genetically engineered mesenchymal stem cells in a rat glioma model. *Gene Ther* **11**: 1155-1164.
127. Cheng, P, Gao, ZQ, Liu, YH, and Xue, YX (2009). Platelet-derived growth factor BB promotes the migration of bone marrow-derived mesenchymal stem cells towards C6 glioma and up-regulates the expression of intracellular adhesion molecule-1. *Neurosci Lett* **451**: 52-56.
128. Schmidt, NO, Przylecki, W, Yang, W, Ziu, M, Teng, Y, Kim, SU*, et al.* (2005). Brain tumor tropism of transplanted human neural stem cells is induced by vascular endothelial growth factor. *Neoplasia* **7**: 623-629.
129. Gottlieb, DI (2002). Large-scale sources of neural stem cells. *Annu Rev Neurosci* **25**: 381-407.
130. Tocci, A, and Forte, L (2003). Mesenchymal stem cell: use and perspectives. *Hematol J* **4**: 92-96.
131. Zuk, PA, Zhu, M, Ashjian, P, De Ugarte, DA, Huang, JI, Mizuno, H*, et al.* (2002). Human adipose tissue is a source of multipotent stem cells. *Mol Biol Cell* **13**: 4279-4295.
132. Kim, SM, Woo, JS, Jeong, CH, Ryu, CH, Lim, JY, and Jeun, SS (2012). Effective combination therapy for malignant glioma with TRAIL-secreting mesenchymal stem cells and lipoxygenase inhibitor MK886. *Cancer Res* **72**: 4807-4817.
133. Dembinski, JL, Spaeth, EL, Fueyo, J, Gomez-Manzano, C, Studeny, M, Andreeff, M*, et al.* (2010). Reduction of nontarget infection and systemic toxicity by targeted delivery of conditionally replicating viruses transported in mesenchymal stem cells. *Cancer Gene Ther* **17**: 289-297.
134. Sonabend, AM, Ulasov, IV, Tyler, MA, Rivera, AA, Mathis, JM, and Lesniak, MS (2008). Mesenchymal stem cells effectively deliver an oncolytic adenovirus to intracranial glioma. *Stem Cells* **26**: 831-841.
135. Tyler, MA, Ulasov, IV, Sonabend, AM, Nandi, S, Han, Y, Marler, S*, et al.* (2009). Neural stem cells target intracranial glioma to deliver an oncolytic adenovirus in vivo. *Gene Ther* **16**: 262-278.
136. Aboody, KS, Najbauer, J, and Danks, MK (2008). Stem and progenitor cell-mediated tumor selective gene therapy. *Gene Ther* **15**: 739-752.
137. Kosztowski, T, Zaidi, HA, and Quinones-Hinojosa, A (2009). Applications of neural and mesenchymal stem cells in the treatment of gliomas. *Expert Rev Anticancer Ther* **9**: 597-612.
138. Sanai, N, Alvarez-Buylla, A, and Berger, MS (2005). Neural stem cells and the origin of gliomas. *N Engl J Med* **353**: 811-822.
139. Nduom, EK, Hadjipanayis, CG, and Van Meir, EG (2012). Glioblastoma cancer stem-like cells: implications for pathogenesis and treatment. *Cancer J* **18**: 100-106.

176

140. Hadjipanayis, CG, and Van Meir, EG (2009). Brain cancer propagating cells: biology, genetics and targeted therapies. *Trends Mol Med* **15**: 519-530.
141. Galli, R, Binda, E, Orfanelli, U, Cipelletti, B, Gritti, A, De Vitis, S*, et al.* (2004). Isolation and characterization of tumorigenic, stem-like neural precursors from human glioblastoma. *Cancer Res* **64**: 7011-7021.
142. Singh, SK, Hawkins, C, Clarke, ID, Squire, JA, Bayani, J, Hide, T*, et al.* (2004). Identification of human brain tumour initiating cells. *Nature* **432**: 396-401.
143. Liu, G, Yuan, X, Zeng, Z, Tunici, P, Ng, H, Abdulkadir, IR*, et al.* (2006). Analysis of gene expression and chemoresistance of CD133+ cancer stem cells in glioblastoma. *Mol Cancer* **5**: 67.
144. Salmaggi, A, Boiardi, A, Gelati, M, Russo, A, Calatozzolo, C, Ciusani, E*, et al.* (2006). Glioblastoma-derived tumorospheres identify a population of tumor stem-like cells with angiogenic potential and enhanced multidrug resistance phenotype. *Glia* **54**: 850-860.
145. Bao, S, Wu, Q, McLendon, RE, Hao, Y, Shi, Q, Hjelmeland, AB*, et al.* (2006). Glioma stem cells promote radioresistance by preferential activation of the DNA damage response. *Nature* **444**: 756-760.
146. Uchida, N, Buck, DW, He, D, Reitsma, MJ, Masek, M, Phan, TV*, et al.* (2000). Direct isolation of human central nervous system stem cells. *Proc Natl Acad Sci USA* **97**: 14720-14725.
147. Eulalio, A, Behm-Ansmant, I, Schweizer, D, and Izaurralde, E (2007). P-body formation is a consequence, not the cause, of RNA-mediated gene silencing. *Mol Cell Biol* **27**: 3970-3981.
148. Wilusz, CJ, and Wilusz, J (2004). Bringing the role of mRNA decay in the control of gene expression into focus. *Trends Genet* **20**: 491-497.
149. Lee, RC, Feinbaum, RL, and Ambros, V (1993). The C. elegans heterochronic gene lin-4 encodes small RNAs with antisense complementarity to lin-14. *Cell* **75**: 843-854.
150. Fire, A, Xu, S, Montgomery, MK, Kostas, SA, Driver, SE, and Mello, CC (1998). Potent and specific genetic interference by double-stranded RNA in Caenorhabditis elegans. *Nature* **391**: 806-811.
151. Reinhart, BJ, and Bartel, DP (2002). Small RNAs correspond to centromere heterochromatic repeats. *Science* **297**: 1831.
152. Aravin, AA, Hannon, GJ, and Brennecke, J (2007). The Piwi-piRNA pathway provides an adaptive defense in the transposon arms race. *Science* **318**: 761-764.
153. Filipowicz, W, Bhattacharyya, SN, and Sonenberg, N (2008). Mechanisms of post-transcriptional regulation by microRNAs: are the answers in sight? *Nat Rev Genet* **9**: 102-114.
154. Croce, CM (2009). Causes and consequences of microRNA dysregulation in cancer. *Nat Rev Genet* **10**: 704-714.
155. Calin, GA, and Croce, CM (2006). MicroRNA signatures in human cancers. *Nat Rev Cancer* **6**: 857-866.
156. Esquela-Kerscher, A, and Slack, FJ (2006). Oncomirs - microRNAs with a role in cancer. *Nat Rev Cancer* **6**: 259-269.
157. Kloosterman, WP, and Plasterk, RH (2006). The diverse functions of microRNAs in animal development and disease. *Dev Cell* **11**: 441-450.
158. Altuvia, Y, Landgraf, P, Lithwick, G, Elefant, N, Pfeffer, S, Aravin, A*, et al.* (2005). Clustering and conservation patterns of human microRNAs. *Nucleic Acids Res* **33**: 2697-2706.
159. Kim, YK, and Kim, VN (2007). Processing of intronic microRNAs. *EMBO J* **26**: 775-783.
160. Rodriguez, A, Griffiths-Jones, S, Ashurst, JL, and Bradley, A (2004). Identification of mammalian microRNA host genes and transcription units. *Genome Res* **14**: 1902-1910.
161. Cai, X, Hagedorn, CH, and Cullen, BR (2004). Human microRNAs are processed from capped, polyadenylated transcripts that can also function as mRNAs. *RNA* **10**: 1957-1966.
162. Kim, VN (2005). MicroRNA biogenesis: coordinated cropping and dicing. *Nat Rev Mol Cell Biol* **6**: 376-385.
163. Ruby, JG, Jan, CH, and Bartel, DP (2007). Intronic microRNA precursors that bypass Drosha processing. *Nature* **448**: 83-86.
164. Sibley, CR, Seow, Y, Saayman, S, Dijkstra, KK, El Andaloussi, S, Weinberg, MS*, et al.* (2012). The biogenesis and characterization of mammalian microRNAs of mirtron origin. *Nucleic Acids Res* **40**: 438-448.
165. Berezikov, E, Chung, WJ, Willis, J, Cuppen, E, and Lai, EC (2007). Mammalian mirtron genes. *Mol Cell* **28**: 328-336.
166. Shomron, N, and Levy, C (2009). MicroRNA-biogenesis and Pre-mRNA splicing crosstalk. *J Biomed Biotechnol* **2009**: 594678.
167. Meister, G, Landthaler, M, Patkaniowska, A, Dorsett, Y, Teng, G, and Tuschl, T (2004). Human Argonaute2 mediates RNA cleavage targeted by miRNAs and siRNAs. *Mol Cell* **15**: 185-197.

168.   Perron, MP, and Provost, P (2008). Protein interactions and complexes in human microRNA biogenesis and function. *Front Biosci* **13**: 2537-2547.
169.   Schwarz, DS, Hutvagner, G, Du, T, Xu, Z, Aronin, N, and Zamore, PD (2003). Asymmetry in the assembly of the RNAi enzyme complex. *Cell* **115**: 199-208.
170.   Bartel, DP (2004). MicroRNAs: genomics, biogenesis, mechanism, and function. *Cell* **116**: 281-297.
171.   Plante, I, and Provost, P (2006). Hypothesis: a role for fragile X mental retardation protein in mediating and relieving microRNA-guided translational repression? *J Biomed Biotechnol* **2006**: 16806.
172.   Ambros, V (2004). The functions of animal microRNAs. *Nature* **431**: 350-355.
173.   Hutvagner, G, and Zamore, PD (2002). A microRNA in a multiple-turnover RNAi enzyme complex. *Science* **297**: 2056-2060.
174.   Liu, X, Fortin, K, and Mourelatos, Z (2008). MicroRNAs: biogenesis and molecular functions. *Brain Pathol* **18**: 113-121.
175.   Brennecke, J, Stark, A, Russell, RB, and Cohen, SM (2005). Principles of microRNA-target recognition. *PLoS Biol* **3**: e85.
176.   Kiriakidou, M, Nelson, PT, Kouranov, A, Fitziev, P, Bouyioukos, C, Mourelatos, Z*, et al.* (2004). A combined computational-experimental approach predicts human microRNA targets. *Genes Dev* **18**: 1165-1178.
177.   Fabian, MR, and Sonenberg, N (2012). The mechanics of miRNA-mediated gene silencing: a look under the hood of miRISC. *Nat Struct Mol Biol* **19**: 586-593.
178.   Behm-Ansmant, I, Rehwinkel, J, Doerks, T, Stark, A, Bork, P, and Izaurralde, E (2006). mRNA degradation by miRNAs and GW182 requires both CCR4:NOT deadenylase and DCP1:DCP2 decapping complexes. *Genes Dev* **20**: 1885-1898.
179.   Eulalio, A, Huntzinger, E, and Izaurralde, E (2008). GW182 interaction with Argonaute is essential for miRNA-mediated translational repression and mRNA decay. *Nat Struct Mol Biol* **15**: 346-353.
180.   Richter, JD, and Sonenberg, N (2005). Regulation of cap-dependent translation by eIF4E inhibitory proteins. *Nature* **433**: 477-480.
181.   Lopez-Lastra, M, Rivas, A, and Barria, MI (2005). Protein synthesis in eukaryotes: the growing biological relevance of cap-independent translation initiation. *Biol Res* **38**: 121-146.
182.   Mokrejs, M, Vopalensky, V, Kolenaty, O, Masek, T, Feketova, Z, Sekyrova, P*, et al.* (2006). IRESite: the database of experimentally verified IRES structures (www.iresite.org). *Nucleic Acids Res* **34**: D125-130.
183.   Filipowicz, W, Jaskiewicz, L, Kolb, FA, and Pillai, RS (2005). Post-transcriptional gene silencing by siRNAs and miRNAs. *Curr Opin Struct Biol* **15**: 331-341.
184.   Humphreys, DT, Westman, BJ, Martin, DI, and Preiss, T (2005). MicroRNAs control translation initiation by inhibiting eukaryotic initiation factor 4E/cap and poly(A) tail function. *Proc Natl Acad Sci USA* **102**: 16961-16966.
185.   Mathonnet, G, Fabian, MR, Svitkin, YV, Parsyan, A, Huck, L, Murata, T*, et al.* (2007). MicroRNA inhibition of translation initiation in vitro by targeting the cap-binding complex eIF4F. *Science* **317**: 1764-1767.
186.   Kiriakidou, M, Tan, GS, Lamprinaki, S, De Planell-Saguer, M, Nelson, PT, and Mourelatos, Z (2007). An mRNA m7G cap binding-like motif within human Ago2 represses translation. *Cell* **129**: 1141-1151.
187.   Frank, F, Fabian, MR, Stepinski, J, Jemielity, J, Darzynkiewicz, E, Sonenberg, N*, et al.* (2011). Structural analysis of 5'-mRNA-cap interactions with the human AGO2 MID domain. *EMBO Rep* **12**: 415-420.
188.   Kinch, LN, and Grishin, NV (2009). The human Ago2 MC region does not contain an eIF4E-like mRNA cap binding motif. *Biol Direct* **4**: 2.
189.   Chekulaeva, M, Mathys, H, Zipprich, JT, Attig, J, Colic, M, Parker, R*, et al.* (2011). miRNA repression involves GW182-mediated recruitment of CCR4-NOT through conserved W-containing motifs. *Nat Struct Mol Biol* **18**: 1218-1226.
190.   Fabian, MR, Cieplak, MK, Frank, F, Morita, M, Green, J, Srikumar, T*, et al.* (2011). miRNA-mediated deadenylation is orchestrated by GW182 through two conserved motifs that interact with CCR4-NOT. *Nat Struct Mol Biol* **18**: 1211-1217.
191.   Cooke, A, Prigge, A, and Wickens, M (2010). Translational repression by deadenylases. *J Biol Chem* **285**: 28506-28513.
192.   Braun, JE, Huntzinger, E, Fauser, M, and Izaurralde, E (2011). GW182 proteins directly recruit cytoplasmic deadenylase complexes to miRNA targets. *Mol Cell* **44**: 120-133.
193.   Chendrimada, TP, Finn, KJ, Ji, X, Baillat, D, Gregory, RI, Liebhaber, SA*, et al.* (2007). MicroRNA silencing through RISC recruitment of eIF6. *Nature* **447**: 823-828.

194. Fabian, MR, Mathonnet, G, Sundermeier, T, Mathys, H, Zipprich, JT, Svitkin, YV, *et al.* (2009). Mammalian miRNA RISC recruits CAF1 and PABP to affect PABP-dependent deadenylation. *Mol Cell* **35**: 868-880.

195. Guo, H, Ingolia, NT, Weissman, JS, and Bartel, DP (2010). Mammalian microRNAs predominantly act to decrease target mRNA levels. *Nature* **466**: 835-840.

196. Maroney, PA, Yu, Y, Fisher, J, and Nilsen, TW (2006). Evidence that microRNAs are associated with translating messenger RNAs in human cells. *Nat Struct Mol Biol* **13**: 1102-1107.

197. Nottrott, S, Simard, MJ, and Richter, JD (2006). Human let-7a miRNA blocks protein production on actively translating polyribosomes. *Nat Struct Mol Biol* **13**: 1108-1114.

198. Petersen, CP, Bordeleau, ME, Pelletier, J, and Sharp, PA (2006). Short RNAs repress translation after initiation in mammalian cells. *Mol Cell* **21**: 533-542.

199. Hendrickson, DG, Hogan, DJ, McCullough, HL, Myers, JW, Herschlag, D, Ferrell, JE, *et al.* (2009). Concordant regulation of translation and mRNA abundance for hundreds of targets of a human microRNA. *PLoS Biol* **7**: e1000238.

200. Anderson, JS, and Parker, RP (1998). The 3' to 5' degradation of yeast mRNAs is a general mechanism for mRNA turnover that requires the SKI2 DEVH box protein and 3' to 5' exonucleases of the exosome complex. *EMBO J* **17**: 1497-1506.

201. Parker, R, and Song, H (2004). The enzymes and control of eukaryotic mRNA turnover. *Nat Struct Mol Biol* **11**: 121-127.

202. Eulalio, A, Behm-Ansmant, I, and Izaurralde, E (2007). P bodies: at the crossroads of post-transcriptional pathways. *Nat Rev Mol Cell Biol* **8**: 9-22.

203. Baek, D, Villen, J, Shin, C, Camargo, FD, Gygi, SP, and Bartel, DP (2008). The impact of microRNAs on protein output. *Nature* **455**: 64-71.

204. Selbach, M, Schwanhausser, B, Thierfelder, N, Fang, Z, Khanin, R, and Rajewsky, N (2008). Widespread changes in protein synthesis induced by microRNAs. *Nature* **455**: 58-63.

205. Giraldez, AJ, Mishima, Y, Rihel, J, Grocock, RJ, Van Dongen, S, Inoue, K, *et al.* (2006). Zebrafish MiR-430 promotes deadenylation and clearance of maternal mRNAs. *Science* **312**: 75-79.

206. Wu, L, Fan, J, and Belasco, JG (2006). MicroRNAs direct rapid deadenylation of mRNA. *Proc Natl Acad Sci USA* **103**: 4034-4039.

207. Chu, CY, and Rana, TM (2006). Translation repression in human cells by microRNA-induced gene silencing requires RCK/p54. *PLoS Biol* **4**: e210.

208. Su, H, Meng, S, Lu, Y, Trombly, MI, Chen, J, Lin, C, *et al.* (2011). Mammalian hyperplastic discs homolog EDD regulates miRNA-mediated gene silencing. *Mol Cell* **43**: 97-109.

209. Aleman, LM, Doench, J, and Sharp, PA (2007). Comparison of siRNA-induced off-target RNA and protein effects. *RNA* **13**: 385-395.

210. Bazzini, AA, Lee, MT, and Giraldez, AJ (2012). Ribosome profiling shows that miR-430 reduces translation before causing mRNA decay in zebrafish. *Science* **336**: 233-237.

211. Djuranovic, S, Nahvi, A, and Green, R (2012). miRNA-mediated gene silencing by translational repression followed by mRNA deadenylation and decay. *Science* **336**: 237-240.

212. Cougot, N, Babajko, S, and Seraphin, B (2004). Cytoplasmic foci are sites of mRNA decay in human cells. *J Cell Biol* **165**: 31-40.

213. Sheth, U, and Parker, R (2003). Decapping and decay of messenger RNA occur in cytoplasmic processing bodies. *Science* **300**: 805-808.

214. Parker, R, and Sheth, U (2007). P bodies and the control of mRNA translation and degradation. *Mol Cell* **25**: 635-646.

215. Bhattacharyya, SN, Habermacher, R, Martine, U, Closs, EI, and Filipowicz, W (2006). Relief of microRNA-mediated translational repression in human cells subjected to stress. *Cell* **125**: 1111-1124.

216. Kedersha, N, Stoecklin, G, Ayodele, M, Yacono, P, Lykke-Andersen, J, Fritzler, MJ, *et al.* (2005). Stress granules and processing bodies are dynamically linked sites of mRNP remodeling. *J Cell Biol* **169**: 871-884.

217. Hwang, HW, Wentzel, EA, and Mendell, JT (2007). A hexanucleotide element directs microRNA nuclear import. *Science* **315**: 97-100.

218. Alvarez-Garcia, I, and Miska, EA (2005). MicroRNA functions in animal development and human disease. *Development* **132**: 4653-4662.

219. Stark, A, Brennecke, J, Bushati, N, Russell, RB, and Cohen, SM (2005). Animal MicroRNAs confer robustness to gene expression and have a significant impact on 3'UTR evolution. *Cell* **123**: 1133-1146.

220. Liu, N, and Olson, EN (2010). MicroRNA regulatory networks in cardiovascular development. *Dev Cell* **18**: 510-525.

221. Gangaraju, VK, and Lin, H (2009). MicroRNAs: key regulators of stem cells. *Nat Rev Mol Cell Biol* **10**: 116-125.
222. O'Connell, RM, Rao, DS, Chaudhuri, AA, and Baltimore, D (2010). Physiological and pathological roles for microRNAs in the immune system. *Nat Rev Immunol* **10**: 111-122.
223. Moore, KJ, Rayner, KJ, Suarez, Y, and Fernandez-Hernando, C (2010). microRNAs and cholesterol metabolism. *Trends Endocrinol Metab* **21**: 699-706.
224. Poy, MN, Eliasson, L, Krutzfeldt, J, Kuwajima, S, Ma, X, Macdonald, PE*, et al.* (2004). A pancreatic islet-specific microRNA regulates insulin secretion. *Nature* **432**: 226-230.
225. Lecellier, CH, Dunoyer, P, Arar, K, Lehmann-Che, J, Eyquem, S, Himber, C*, et al.* (2005). A cellular microRNA mediates antiviral defense in human cells. *Science* **308**: 557-560.
226. Johnson, CD, Esquela-Kerscher, A, Stefani, G, Byrom, M, Kelnar, K, Ovcharenko, D*, et al.* (2007). The let-7 microRNA represses cell proliferation pathways in human cells. *Cancer Res* **67**: 7713-7722.
227. Jovanovic, M, and Hengartner, MO (2006). miRNAs and apoptosis: RNAs to die for. *Oncogene* **25**: 6176-6187.
228. Small, EM, and Olson, EN (2011). Pervasive roles of microRNAs in cardiovascular biology. *Nature* **469**: 336-342.
229. Nelson, PT, Wang, WX, and Rajeev, BW (2008). MicroRNAs (miRNAs) in neurodegenerative diseases. *Brain Pathol* **18**: 130-138.
230. Pandey, AK, Agarwal, P, Kaur, K, and Datta, M (2009). MicroRNAs in diabetes: tiny players in big disease. *Cell Physiol Biochem* **23**: 221-232.
231. Calin, GA, Dumitru, CD, Shimizu, M, Bichi, R, Zupo, S, Noch, E*, et al.* (2002). Frequent deletions and down-regulation of micro- RNA genes miR15 and miR16 at 13q14 in chronic lymphocytic leukemia. *Proc Natl Acad Sci USA* **99**: 15524-15529.
232. Calin, GA, Sevignani, C, Dumitru, CD, Hyslop, T, Noch, E, Yendamuri, S*, et al.* (2004). Human microRNA genes are frequently located at fragile sites and genomic regions involved in cancers. *Proc Natl Acad Sci USA* **101**: 2999-3004.
233. Carmell, MA, Xuan, Z, Zhang, MQ, and Hannon, GJ (2002). The Argonaute family: tentacles that reach into RNAi, developmental control, stem cell maintenance, and tumorigenesis. *Genes Dev* **16**: 2733-2742.
234. Karube, Y, Tanaka, H, Osada, H, Tomida, S, Tatematsu, Y, Yanagisawa, K*, et al.* (2005). Reduced expression of Dicer associated with poor prognosis in lung cancer patients. *Cancer Sci* **96**: 111-115.
235. Kumar, MS, Lu, J, Mercer, KL, Golub, TR, and Jacks, T (2007). Impaired microRNA processing enhances cellular transformation and tumorigenesis. *Nat Genet* **39**: 673-677.
236. Lu, J, Getz, G, Miska, EA, Alvarez-Saavedra, E, Lamb, J, Peck, D*, et al.* (2005). MicroRNA expression profiles classify human cancers. *Nature* **435**: 834-838.
237. Volinia, S, Calin, GA, Liu, CG, Ambs, S, Cimmino, A, Petrocca, F*, et al.* (2006). A microRNA expression signature of human solid tumors defines cancer gene targets. *Proc Natl Acad Sci USA* **103**: 2257-2261.
238. Calin, GA, Ferracin, M, Cimmino, A, Di Leva, G, Shimizu, M, Wojcik, SE*, et al.* (2005). A MicroRNA signature associated with prognosis and progression in chronic lymphocytic leukemia. *N Engl J Med* **353**: 1793-1801.
239. Yanaihara, N, Caplen, N, Bowman, E, Seike, M, Kumamoto, K, Yi, M*, et al.* (2006). Unique microRNA molecular profiles in lung cancer diagnosis and prognosis. *Cancer Cell* **9**: 189-198.
240. Cimmino, A, Calin, GA, Fabbri, M, Iorio, MV, Ferracin, M, Shimizu, M*, et al.* (2005). miR-15 and miR-16 induce apoptosis by targeting BCL2. *Proc Natl Acad Sci USA* **102**: 13944-13949.
241. Ambs, S, Prueitt, RL, Yi, M, Hudson, RS, Howe, TM, Petrocca, F*, et al.* (2008). Genomic profiling of microRNA and messenger RNA reveals deregulated microRNA expression in prostate cancer. *Cancer Res* **68**: 6162-6170.
242. Roccaro, AM, Sacco, A, Thompson, B, Leleu, X, Azab, AK, Azab, F*, et al.* (2009). MicroRNAs 15a and 16 regulate tumor proliferation in multiple myeloma. *Blood* **113**: 6669-6680.
243. Akao, Y, Nakagawa, Y, and Naoe, T (2006). let-7 microRNA functions as a potential growth suppressor in human colon cancer cells. *Biol Pharm Bull* **29**: 903-906.
244. Iorio, MV, Ferracin, M, Liu, CG, Veronese, A, Spizzo, R, Sabbioni, S*, et al.* (2005). MicroRNA gene expression deregulation in human breast cancer. *Cancer Res* **65**: 7065-7070.
245. Esquela-Kerscher, A, Trang, P, Wiggins, JF, Patrawala, L, Cheng, A, Ford, L*, et al.* (2008). The let-7 microRNA reduces tumor growth in mouse models of lung cancer. *Cell Cycle* **7**: 759-764.
246. Johnson, SM, Grosshans, H, Shingara, J, Byrom, M, Jarvis, R, Cheng, A*, et al.* (2005). RAS is regulated by the let-7 microRNA family. *Cell* **120**: 635-647.

247. Lee, YS, and Dutta, A (2007). The tumor suppressor microRNA let-7 represses the HMGA2 oncogene. *Genes Dev* **21**: 1025-1030.
248. Sampson, VB, Rong, NH, Han, J, Yang, Q, Aris, V, Soteropoulos, P*, et al.* (2007). MicroRNA let-7a down-regulates MYC and reverts MYC-induced growth in Burkitt lymphoma cells. *Cancer Res* **67**: 9762-9770.
249. Xiong, Y, Fang, JH, Yun, JP, Yang, J, Zhang, Y, Jia, WH*, et al.* (2010). Effects of microRNA-29 on apoptosis, tumorigenicity, and prognosis of hepatocellular carcinoma. *Hepatology* **51**: 836-845.
250. Fabbri, M, Garzon, R, Cimmino, A, Liu, Z, Zanesi, N, Callegari, E*, et al.* (2007). MicroRNA-29 family reverts aberrant methylation in lung cancer by targeting DNA methyltransferases 3A and 3B. *Proc Natl Acad Sci USA* **104**: 15805-15810.
251. Nana-Sinkam, SP, and Croce, CM (2012). Clinical applications for microRNAs in cancer. *Clin Pharmacol Ther* **93**: 98-104.
252. Garzon, R, Calin, GA, and Croce, CM (2009). MicroRNAs in Cancer. *Annu Rev Med* **60**: 167-179.
253. He, L, Thomson, JM, Hemann, MT, Hernando-Monge, E, Mu, D, Goodson, S*, et al.* (2005). A microRNA polycistron as a potential human oncogene. *Nature* **435**: 828-833.
254. Ota, A, Tagawa, H, Karnan, S, Tsuzuki, S, Karpas, A, Kira, S*, et al.* (2004). Identification and characterization of a novel gene, C13orf25, as a target for 13q31-q32 amplification in malignant lymphoma. *Cancer Res* **64**: 3087-3095.
255. Mendell, JT (2008). miRiad roles for the miR-17-92 cluster in development and disease. *Cell* **133**: 217-222.
256. Dews, M, Homayouni, A, Yu, D, Murphy, D, Sevignani, C, Wentzel, E*, et al.* (2006). Augmentation of tumor angiogenesis by a Myc-activated microRNA cluster. *Nat Genet* **38**: 1060-1065.
257. O'Donnell, KA, Wentzel, EA, Zeller, KI, Dang, CV, and Mendell, JT (2005). c-Myc-regulated microRNAs modulate E2F1 expression. *Nature* **435**: 839-843.
258. Ivanovska, I, Ball, AS, Diaz, RL, Magnus, JF, Kibukawa, M, Schelter, JM*, et al.* (2008). MicroRNAs in the miR-106b family regulate p21/CDKN1A and promote cell cycle progression. *Mol Cell Biol* **28**: 2167-2174.
259. Bloomston, M, Frankel, WL, Petrocca, F, Volinia, S, Alder, H, Hagan, JP*, et al.* (2007). MicroRNA expression patterns to differentiate pancreatic adenocarcinoma from normal pancreas and chronic pancreatitis. *JAMA* **297**: 1901-1908.
260. Meng, F, Henson, R, Wehbe-Janek, H, Ghoshal, K, Jacob, ST, and Patel, T (2007). MicroRNA-21 regulates expression of the PTEN tumor suppressor gene in human hepatocellular cancer. *Gastroenterology* **133**: 647-658.
261. Selcuklu, SD, Donoghue, MT, and Spillane, C (2009). miR-21 as a key regulator of oncogenic processes. *Biochem Soc Trans* **37**: 918-925.
262. Gabriely, G, Yi, M, Narayan, RS, Niers, JM, Wurdinger, T, Imitola, J*, et al.* (2011). Human glioma growth is controlled by microRNA-10b. *Cancer Res* **71**: 3563-3572.
263. Ma, L, Teruya-Feldstein, J, and Weinberg, RA (2007). Tumour invasion and metastasis initiated by microRNA-10b in breast cancer. *Nature* **449**: 682-688.
264. Baffa, R, Fassan, M, Volinia, S, O'Hara, B, Liu, CG, Palazzo, JP*, et al.* (2009). MicroRNA expression profiling of human metastatic cancers identifies cancer gene targets. *J Pathol* **219**: 214-221.
265. Tan, HX, Wang, Q, Chen, LZ, Huang, XH, Chen, JS, Fu, XH*, et al.* (2010). MicroRNA-9 reduces cell invasion and E-cadherin secretion in SK-Hep-1 cell. *Med Oncol* **27**: 654-660.
266. Ciafre, SA, Galardi, S, Mangiola, A, Ferracin, M, Liu, CG, Sabatino, G*, et al.* (2005). Extensive modulation of a set of microRNAs in primary glioblastoma. *Biochem Biophys Res Commun* **334**: 1351-1358.
267. Liu, Y, Zhao, J, Zhang, PY, Zhang, Y, Sun, SY, Yu, SY*, et al.* (2012). MicroRNA-10b targets E-cadherin and modulates breast cancer metastasis. *Med Sci Monit* **18**: BR299-308.
268. Hossain, A, Kuo, MT, and Saunders, GF (2006). Mir-17-5p regulates breast cancer cell proliferation by inhibiting translation of AIB1 mRNA. *Mol Cell Biol* **26**: 8191-8201.
269. Cheng, AM, Byrom, MW, Shelton, J, and Ford, LP (2005). Antisense inhibition of human miRNAs and indications for an involvement of miRNA in cell growth and apoptosis. *Nucleic Acids Res* **33**: 1290-1297.
270. Felli, N, Fontana, L, Pelosi, E, Botta, R, Bonci, D, Facchiano, F*, et al.* (2005). MicroRNAs 221 and 222 inhibit normal erythropoiesis and erythroleukemic cell growth via kit receptor down-modulation. *Proc Natl Acad Sci USA* **102**: 18081-18086.
271. Garofalo, M, Di Leva, G, Romano, G, Nuovo, G, Suh, SS, Ngankeu, A*, et al.* (2009). miR-221&222 regulate TRAIL resistance and enhance tumorigenicity through PTEN and TIMP3 downregulation. *Cancer Cell* **16**: 498-509.

272. Nakamura, T, Canaani, E, and Croce, CM (2007). Oncogenic All1 fusion proteins target Drosha-mediated microRNA processing. *Proc Natl Acad Sci U S A* **104**: 10980-10985.
273. Jones, PA, and Baylin, SB (2007). The epigenomics of cancer. *Cell* **128**: 683-692.
274. Esteller, M (2007). Cancer epigenomics: DNA methylomes and histone-modification maps. *Nat Rev Genet* **8**: 286-298.
275. Weber, B, Stresemann, C, Brueckner, B, and Lyko, F (2007). Methylation of human microRNA genes in normal and neoplastic cells. *Cell Cycle* **6**: 1001-1005.
276. Saito, Y, Liang, G, Egger, G, Friedman, JM, Chuang, JC, Coetzee, GA*, et al.* (2006). Specific activation of microRNA-127 with downregulation of the proto-oncogene BCL6 by chromatin-modifying drugs in human cancer cells. *Cancer Cell* **9**: 435-443.
277. Toyota, M, Suzuki, H, Sasaki, Y, Maruyama, R, Imai, K, Shinomura, Y*, et al.* (2008). Epigenetic silencing of microRNA-34b/c and B-cell translocation gene 4 is associated with CpG island methylation in colorectal cancer. *Cancer Res* **68**: 4123-4132.
278. Saito, Y, Suzuki, H, Tsugawa, H, Nakagawa, I, Matsuzaki, J, Kanai, Y*, et al.* (2009). Chromatin remodeling at Alu repeats by epigenetic treatment activates silenced microRNA-512-5p with downregulation of Mcl-1 in human gastric cancer cells. *Oncogene* **28**: 2738-2744.
279. Brueckner, B, Stresemann, C, Kuner, R, Mund, C, Musch, T, Meister, M*, et al.* (2007). The human let-7a-3 locus contains an epigenetically regulated microRNA gene with oncogenic function. *Cancer Res* **67**: 1419-1423.
280. Bandres, E, Agirre, X, Bitarte, N, Ramirez, N, Zarate, R, Roman-Gomez, J*, et al.* (2009). Epigenetic regulation of microRNA expression in colorectal cancer. *Int J Cancer* **125**: 2737-2743.
281. Scott, GK, Mattie, MD, Berger, CE, Benz, SC, and Benz, CC (2006). Rapid alteration of microRNA levels by histone deacetylase inhibition. *Cancer Res* **66**: 1277-1281.
282. Iorio, MV, and Croce, CM (2012). microRNA involvement in human cancer. *Carcinogenesis* **33**: 1126-1133.
283. Chang, TC, Wentzel, EA, Kent, OA, Ramachandran, K, Mullendore, M, Lee, KH*, et al.* (2007). Transactivation of miR-34a by p53 broadly influences gene expression and promotes apoptosis. *Mol Cell* **26**: 745-752.
284. He, L, He, X, Lim, LP, de Stanchina, E, Xuan, Z, Liang, Y*, et al.* (2007). A microRNA component of the p53 tumour suppressor network. *Nature* **447**: 1130-1134.
285. Fabbri, M, Bottoni, A, Shimizu, M, Spizzo, R, Nicoloso, MS, Rossi, S*, et al.* (2011). Association of a microRNA/TP53 feedback circuitry with pathogenesis and outcome of B-cell chronic lymphocytic leukemia. *JAMA* **305**: 59-67.
286. Hussain, SP, and Harris, CC (1998). Molecular epidemiology of human cancer: contribution of mutation spectra studies of tumor suppressor genes. *Cancer Res* **58**: 4023-4037.
287. Chang, TC, Zeitels, LR, Hwang, HW, Chivukula, RR, Wentzel, EA, Dews, M*, et al.* (2009). Lin-28B transactivation is necessary for Myc-mediated let-7 repression and proliferation. *Proc Natl Acad Sci USA* **106**: 3384-3389.
288. Mott, JL, Kurita, S, Cazanave, SC, Bronk, SF, Werneburg, NW, and Fernandez-Zapico, ME (2010). Transcriptional suppression of mir-29b-1/mir-29a promoter by c-Myc, hedgehog, and NF-kappaB. *J Cell Biochem* **110**: 1155-1164.
289. Assanah, M, Lochhead, R, Ogden, A, Bruce, J, Goldman, J, and Canoll, P (2006). Glial progenitors in adult white matter are driven to form malignant gliomas by platelet-derived growth factor-expressing retroviruses. *J Neurosci* **26**: 6781-6790.
290. Shao, M, Rossi, S, Chelladurai, B, Shimizu, M, Ntukogu, O, Ivan, M*, et al.* (2011). PDGF induced microRNA alterations in cancer cells. *Nucleic Acids Res* **39**: 4035-4047.
291. Takamizawa, J, Konishi, H, Yanagisawa, K, Tomida, S, Osada, H, Endoh, H*, et al.* (2004). Reduced expression of the let-7 microRNAs in human lung cancers in association with shortened postoperative survival. *Cancer Res* **64**: 3753-3756.
292. Caramuta, S, Egyhazi, S, Rodolfo, M, Witten, D, Hansson, J, Larsson, C*, et al.* (2010). MicroRNA expression profiles associated with mutational status and survival in malignant melanoma. *J Invest Dermatol* **130**: 2062-2070.
293. Merritt, WM, Lin, YG, Han, LY, Kamat, AA, Spannuth, WA, Schmandt, R*, et al.* (2008). Dicer, Drosha, and outcomes in patients with ovarian cancer. *N Engl J Med* **359**: 2641-2650.
294. Giovannetti, E, Funel, N, Peters, GJ, Del Chiaro, M, Erozenci, LA, Vasile, E*, et al.* (2010). MicroRNA-21 in pancreatic cancer: correlation with clinical outcome and pharmacologic aspects underlying its role in the modulation of gemcitabine activity. *Cancer Res* **70**: 4528-4538.
295. Liu, R, Chen, X, Du, Y, Yao, W, Shen, L, Wang, C*, et al.* (2012). Serum microRNA expression profile as a biomarker in the diagnosis and prognosis of pancreatic cancer. *Clin Chem* **58**: 610-618.

296. Gao, W, Lu, X, Liu, L, Xu, J, Feng, D, and Shu, Y (2012). MiRNA-21: a biomarker predictive for platinum-based adjuvant chemotherapy response in patients with non-small cell lung cancer. *Cancer Biol Ther* **13**: 330-340.

297. Schetter, AJ, Leung, SY, Sohn, JJ, Zanetti, KA, Bowman, ED, Yanaihara, N*, et al.* (2008). MicroRNA expression profiles associated with prognosis and therapeutic outcome in colon adenocarcinoma. *JAMA* **299**: 425-436.

298. Garzon, R, Volinia, S, Liu, CG, Fernandez-Cymering, C, Palumbo, T, Pichiorri, F*, et al.* (2008). MicroRNA signatures associated with cytogenetics and prognosis in acute myeloid leukemia. *Blood* **111**: 3183-3189.

299. Marcucci, G, Radmacher, MD, Maharry, K, Mrozek, K, Ruppert, AS, Paschka, P*, et al.* (2008). MicroRNA expression in cytogenetically normal acute myeloid leukemia. *N Engl J Med* **358**: 1919-1928.

300. Novakova, J, Slaby, O, Vyzula, R, and Michalek, J (2009). MicroRNA involvement in glioblastoma pathogenesis. *Biochem Biophys Res Commun* **386**: 1-5.

301. Sana, J, Hajduch, M, Michalek, J, Vyzula, R, and Slaby, O (2011). MicroRNAs and glioblastoma: roles in core signalling pathways and potential clinical implications. *J Cell Mol Med* **15**: 1636-1644.

302. Zhang, Y, Dutta, A, and Abounader, R (2012). The role of microRNAs in glioma initiation and progression. *Front Biosci* **17**: 700-712.

303. Yang, HS, Jansen, AP, Komar, AA, Zheng, X, Merrick, WC, Costes, S*, et al.* (2003). The transformation suppressor Pdcd4 is a novel eukaryotic translation initiation factor 4A binding protein that inhibits translation. *Mol Cell Biol* **23**: 26-37.

304. Goke, R, Barth, P, Schmidt, A, Samans, B, and Lankat-Buttgereit, B (2004). Programmed cell death protein 4 suppresses CDK1/cdc2 via induction of p21(Waf1/Cip1). *Am J Physiol Cell Physiol* **287**: C1541-1546.

305. Papagiannakopoulos, T, Shapiro, A, and Kosik, KS (2008). MicroRNA-21 targets a network of key tumor-suppressive pathways in glioblastoma cells. *Cancer Res* **68**: 8164-8172.

306. Gabriely, G, Wurdinger, T, Kesari, S, Esau, CC, Burchard, J, Linsley, PS*, et al.* (2008). MicroRNA 21 promotes glioma invasion by targeting matrix metalloproteinase regulators. *Mol Cell Biol* **28**: 5369-5380.

307. Loffler, D, Brocke-Heidrich, K, Pfeifer, G, Stocsits, C, Hackermuller, J, Kretzschmar, AK*, et al.* (2007). Interleukin-6 dependent survival of multiple myeloma cells involves the Stat3-mediated induction of microRNA-21 through a highly conserved enhancer. *Blood* **110**: 1330-1333.

308. Rahaman, SO, Harbor, PC, Chernova, O, Barnett, GH, Vogelbaum, MA, and Haque, SJ (2002). Inhibition of constitutively active Stat3 suppresses proliferation and induces apoptosis in glioblastoma multiforme cells. *Oncogene* **21**: 8404-8413.

309. Tchirkov, A, Khalil, T, Chautard, E, Mokhtari, K, Veronese, L, Irthum, B*, et al.* (2007). Interleukin-6 gene amplification and shortened survival in glioblastoma patients. *Br J Cancer* **96**: 474-476.

310. Fujita, S, Ito, T, Mizutani, T, Minoguchi, S, Yamamichi, N, Sakurai, K*, et al.* (2008). miR-21 Gene expression triggered by AP-1 is sustained through a double-negative feedback mechanism. *J Mol Biol* **378**: 492-504.

311. Ribas, J, Ni, X, Haffner, M, Wentzel, EA, Salmasi, AH, Chowdhury, WH*, et al.* (2009). miR-21: an androgen receptor-regulated microRNA that promotes hormone-dependent and hormone-independent prostate cancer growth. *Cancer Res* **69**: 7165-7169.

312. Talotta, F, Cimmino, A, Matarazzo, MR, Casalino, L, De Vita, G, D'Esposito, M*, et al.* (2009). An autoregulatory loop mediated by miR-21 and PDCD4 controls the AP-1 activity in RAS transformation. *Oncogene* **28**: 73-84.

313. Seike, M, Goto, A, Okano, T, Bowman, ED, Schetter, AJ, Horikawa, I*, et al.* (2009). MiR-21 is an EGFR-regulated anti-apoptotic factor in lung cancer in never-smokers. *Proc Natl Acad Sci USA* **106**: 12085-12090.

314. Davis, BN, Hilyard, AC, Lagna, G, and Hata, A (2008). SMAD proteins control DROSHA-mediated microRNA maturation. *Nature* **454**: 56-61.

315. Gillies, JK, and Lorimer, IA (2007). Regulation of p27Kip1 by miRNA 221/222 in glioblastoma. *Cell Cycle* **6**: 2005-2009.

316. le Sage, C, Nagel, R, Egan, DA, Schrier, M, Mesman, E, Mangiola, A*, et al.* (2007). Regulation of the p27(Kip1) tumor suppressor by miR-221 and miR-222 promotes cancer cell proliferation. *EMBO J* **26**: 3699-3708.

317. Gonzalez, T, Seoane, M, Caamano, P, Vinuela, J, Dominguez, F, and Zalvide, J (2003). Inhibition of Cdk4 activity enhances translation of p27kip1 in quiescent Rb-negative cells. *J Biol Chem* **278**: 12688-12695.

318.   Huse, JT, Brennan, C, Hambardzumyan, D, Wee, B, Pena, J, Rouhanifard, SH*, et al.* (2009). The PTEN-regulating microRNA miR-26a is amplified in high-grade glioma and facilitates gliomagenesis in vivo. *Genes Dev* **23**: 1327-1337.

319.   Kim, H, Huang, W, Jiang, X, Pennicooke, B, Park, PJ, and Johnson, MD (2010). Integrative genome analysis reveals an oncomir/oncogene cluster regulating glioblastoma survivorship. *Proc Natl Acad Sci USA* **107**: 2183-2188.

320.   O'Connor, L, Strasser, A, O'Reilly, LA, Hausmann, G, Adams, JM, Cory, S*, et al.* (1998). Bim: a novel member of the Bcl-2 family that promotes apoptosis. *EMBO J* **17**: 384-395.

321.   Pellikainen, JM, and Kosma, VM (2007). Activator protein-2 in carcinogenesis with a special reference to breast cancer--a mini review. *Int J Cancer* **120**: 2061-2067.

322.   Godlewski, J, Nowicki, MO, Bronisz, A, Williams, S, Otsuki, A, Nuovo, G*, et al.* (2008). Targeting of the Bmi-1 oncogene/stem cell renewal factor by microRNA-128 inhibits glioma proliferation and self-renewal. *Cancer Res* **68**: 9125-9130.

323.   Zhang, Y, Chao, T, Li, R, Liu, W, Chen, Y, Yan, X*, et al.* (2009). MicroRNA-128 inhibits glioma cells proliferation by targeting transcription factor E2F3a. *J Mol Med (Berl)* **87**: 43-51.

324.   Sparmann, A, and van Lohuizen, M (2006). Polycomb silencers control cell fate, development and cancer. *Nat Rev Cancer* **6**: 846-856.

325.   Kefas, B, Godlewski, J, Comeau, L, Li, Y, Abounader, R, Hawkinson, M*, et al.* (2008). microRNA-7 inhibits the epidermal growth factor receptor and the Akt pathway and is down-regulated in glioblastoma. *Cancer Res* **68**: 3566-3572.

326.   Guessous, F, Zhang, Y, Kofman, A, Catania, A, Li, Y, Schiff, D*, et al.* (2010). microRNA-34a is tumor suppressive in brain tumors and glioma stem cells. *Cell Cycle* **9**: 1031-1036.

327.   Li, Y, Guessous, F, Zhang, Y, Dipierro, C, Kefas, B, Johnson, E*, et al.* (2009). MicroRNA-34a inhibits glioblastoma growth by targeting multiple oncogenes. *Cancer Res* **69**: 7569-7576.

328.   Roth, P, Wischhusen, J, Happold, C, Chandran, PA, Hofer, S, Eisele, G*, et al.* (2011). A specific miRNA signature in the peripheral blood of glioblastoma patients. *J Neurochem* **118**: 449-457.

329.   Ilhan-Mutlu, A, Wagner, L, Wohrer, A, Furtner, J, Widhalm, G, Marosi, C*, et al.* (2012). Plasma MicroRNA-21 concentration may be a useful biomarker in glioblastoma patients. *Cancer Invest* **30**: 615-621.

330.   Ilhan-Mutlu, A, Wagner, L, Wohrer, A, Jungwirth, S, Marosi, C, Fischer, P*, et al.* (2012). Blood alterations preceding clinical manifestation of glioblastoma. *Cancer Invest* **30**: 625-629.

331.   Baraniskin, A, Kuhnhenn, J, Schlegel, U, Maghnouj, A, Zollner, H, Schmiegel, W*, et al.* (2011). Identification of microRNAs in the cerebrospinal fluid as biomarker for the diagnosis of glioma. *Neuro Oncol* **14**: 29-33.

332.   Lakomy, R, Sana, J, Hankeova, S, Fadrus, P, Kren, L, Lzicarova, E*, et al.* (2011). MiR-195, miR-196b, miR-181c, miR-21 expression levels and O-6-methylguanine-DNA methyltransferase methylation status are associated with clinical outcome in glioblastoma patients. *Cancer Sci* **102**: 2186-2190.

333.   Guan, Y, Mizoguchi, M, Yoshimoto, K, Hata, N, Shono, T, Suzuki, SO*, et al.* (2010). MiRNA-196 is upregulated in glioblastoma but not in anaplastic astrocytoma and has prognostic significance. *Clin Cancer Res* **16**: 4289-4297.

334.   Zhang, W, Zhang, J, Hoadley, K, Kushwaha, D, Ramakrishnan, V, Li, S*, et al.* (2012). miR-181d: a predictive glioblastoma biomarker that downregulates MGMT expression. *Neuro Oncol* **14**: 712-719.

335.   Marquez, RT, and McCaffrey, AP (2008). Advances in microRNAs: implications for gene therapists. *Hum Gene Ther* **19**: 27-38.

336.   Esau, CC (2008). Inhibition of microRNA with antisense oligonucleotides. *Methods* **44**: 55-60.

337.   Lee, YS, Kim, HK, Chung, S, Kim, KS, and Dutta, A (2005). Depletion of human micro-RNA miR-125b reveals that it is critical for the proliferation of differentiated cells but not for the down-regulation of putative targets during differentiation. *J Biol Chem* **280**: 16635-16641.

338.   Kloosterman, WP, Lagendijk, AK, Ketting, RF, Moulton, JD, and Plasterk, RH (2007). Targeted inhibition of miRNA maturation with morpholinos reveals a role for miR-375 in pancreatic islet development. *PLoS Biol* **5**: e203.

339.   Gantier, MP, McCoy, CE, Rusinova, I, Saulep, D, Wang, D, Xu, D*, et al.* (2011). Analysis of microRNA turnover in mammalian cells following Dicer1 ablation. *Nucleic Acids Res* **39**: 5692-5703.

340.   Lee, Y, Hur, I, Park, SY, Kim, YK, Suh, MR, and Kim, VN (2006). The role of PACT in the RNA silencing pathway. *EMBO J* **25**: 522-532.

341.   Zhang, B, and Farwell, MA (2008). microRNAs: a new emerging class of players for disease diagnostics and gene therapy. *J Cell Mol Med* **12**: 3-21.

342. Boutla, A, Delidakis, C, and Tabler, M (2003). Developmental defects by antisense-mediated inactivation of micro-RNAs 2 and 13 in Drosophila and the identification of putative target genes. *Nucleic Acids Res* **31**: 4973-4980.

343. Hutvagner, G, Simard, MJ, Mello, CC, and Zamore, PD (2004). Sequence-specific inhibition of small RNA function. *PLoS Biol* **2**: E98.

344. Krutzfeldt, J, Rajewsky, N, Braich, R, Rajeev, KG, Tuschl, T, Manoharan, M*, et al.* (2005). Silencing of microRNAs in vivo with 'antagomirs'. *Nature* **438**: 685-689.

345. Esau, C, Davis, S, Murray, SF, Yu, XX, Pandey, SK, Pear, M*, et al.* (2006). miR-122 regulation of lipid metabolism revealed by in vivo antisense targeting. *Cell Metab* **3**: 87-98.

346. Davis, S, Lollo, B, Freier, S, and Esau, C (2006). Improved targeting of miRNA with antisense oligonucleotides. *Nucleic Acids Res* **34**: 2294-2304.

347. Orom, UA, Kauppinen, S, and Lund, AH (2006). LNA-modified oligonucleotides mediate specific inhibition of microRNA function. *Gene* **372**: 137-141.

348. Davis, S, Propp, S, Freier, SM, Jones, LE, Serra, MJ, Kinberger, G*, et al.* (2009). Potent inhibition of microRNA in vivo without degradation. *Nucleic Acids Res* **37**: 70-77.

349. Nielsen, PE, Egholm, M, Berg, RH, and Buchardt, O (1991). Sequence-selective recognition of DNA by strand displacement with a thymine-substituted polyamide. *Science* **254**: 1497-1500.

350. Fabbri, E, Brognara, E, Borgatti, M, Lampronti, I, Finotti, A, Bianchi, N*, et al.* (2011). miRNA therapeutics: delivery and biological activity of peptide nucleic acids targeting miRNAs. *Epigenomics* **3**: 733-745.

351. Torres, AG, Fabani, MM, Vigorito, E, Williams, D, Al-Obaidi, N, Wojciechowski, F*, et al.* (2011). Chemical structure requirements and cellular targeting of microRNA-122 by peptide nucleic acids anti-miRs. *Nucleic Acids Res* **40**: 2152-2167.

352. Shiraishi, T, Nielsen, P.E. (2009). Cellular bioavailability of peptide nucleic acids (PNAs) conjugated to cell penetrating peptides. In: *Delivery technologies for biopharmaceuticals: peptides, proteins, nucleic acids and vaccines*. John Wiley and Sons Ltd.

353. Babar, IA, Cheng, CJ, Booth, CJ, Liang, X, Weidhaas, JB, Saltzman, WM*, et al.* (2012). Nanoparticle-based therapy in an in vivo microRNA-155 (miR-155)-dependent mouse model of lymphoma. *Proc Natl Acad Sci USA* **109**: E1695-1704.

354. Ebert, MS, Neilson, JR, and Sharp, PA (2007). MicroRNA sponges: competitive inhibitors of small RNAs in mammalian cells. *Nat Methods* **4**: 721-726.

355. Kluiver, J, Gibcus, JH, Hettinga, C, Adema, A, Richter, MK, Halsema, N*, et al.* (2012). Rapid generation of microRNA sponges for microRNA inhibition. *PLoS One* **7**: e29275.

356. Franco-Zorrilla, JM, Valli, A, Todesco, M, Mateos, I, Puga, MI, Rubio-Somoza, I*, et al.* (2007). Target mimicry provides a new mechanism for regulation of microRNA activity. *Nat Genet* **39**: 1033-1037.

357. Ebert, MS, and Sharp, PA (2010). Emerging roles for natural microRNA sponges. *Curr Biol* **20**: R858-861.

358. Poliseno, L (2012). Pseudogenes: newly discovered players in human cancer. *Sci Signal* **5**: re5.

359. Li, T, Li, D, Sha, J, Sun, P, and Huang, Y (2009). MicroRNA-21 directly targets MARCKS and promotes apoptosis resistance and invasion in prostate cancer cells. *Biochem Biophys Res Commun* **383**: 280-285.

360. Si, ML, Zhu, S, Wu, H, Lu, Z, Wu, F, and Mo, YY (2007). miR-21-mediated tumor growth. *Oncogene* **26**: 2799-2803.

361. Hatley, ME, Patrick, DM, Garcia, MR, Richardson, JA, Bassel-Duby, R, van Rooij, E*, et al.* (2010). Modulation of K-Ras-dependent lung tumorigenesis by MicroRNA-21. *Cancer Cell* **18**: 282-293.

362. Park, JK, Lee, EJ, Esau, C, and Schmittgen, TD (2009). Antisense inhibition of microRNA-21 or -221 arrests cell cycle, induces apoptosis, and sensitizes the effects of gemcitabine in pancreatic adenocarcinoma. *Pancreas* **38**: e190-199.

363. Basu, A, Alder, H, Khiyami, A, Leahy, P, Croce, CM, and Haldar, S (2011). MicroRNA-375 and MicroRNA-221: Potential Noncoding RNAs Associated with Antiproliferative Activity of Benzyl Isothiocyanate in Pancreatic Cancer. *Genes Cancer* **2**: 108-119.

364. Park, JK, Kogure, T, Nuovo, GJ, Jiang, J, He, L, Kim, JH*, et al.* (2011). miR-221 silencing blocks hepatocellular carcinoma and promotes survival. *Cancer Res* **71**: 7608-7616.

365. Ma, L, Reinhardt, F, Pan, E, Soutschek, J, Bhat, B, Marcusson, EG*, et al.* (2010). Therapeutic silencing of miR-10b inhibits metastasis in a mouse mammary tumor model. *Nat Biotechnol* **28**: 341-347.

366. Bader, AG, Brown, D, and Winkler, M (2010). The promise of microRNA replacement therapy. *Cancer Res* **70**: 7027-7030.

367. Henry, JC, Azevedo-Pouly, AC, and Schmittgen, TD (2011). MicroRNA replacement therapy for cancer. *Pharm Res* **28**: 3030-3042.
368. Behlke, MA (2008). Chemical modification of siRNAs for in vivo use. *Oligonucleotides* **18**: 305-319.
369. Choung, S, Kim, YJ, Kim, S, Park, HO, and Choi, YC (2006). Chemical modification of siRNAs to improve serum stability without loss of efficacy. *Biochem Biophys Res Commun* **342**: 919-927.
370. Prakash, TP, Allerson, CR, Dande, P, Vickers, TA, Sioufi, N, Jarres, R*, et al.* (2005). Positional effect of chemical modifications on short interference RNA activity in mammalian cells. *J Med Chem* **48**: 4247-4253.
371. Kitade, Y, and Akao, Y (2010). MicroRNAs and their therapeutic potential for human diseases: microRNAs, miR-143 and -145, function as anti-oncomirs and the application of chemically modified miR-143 as an anti-cancer drug. *J Pharmacol Sci* **114**: 276-280.
372. Hamm, S, Latz, E, Hangel, D, Muller, T, Yu, P, Golenbock, D*, et al.* (2010). Alternating 2'-O-ribose methylation is a universal approach for generating non-stimulatory siRNA by acting as TLR7 antagonist. *Immunobiology* **215**: 559-569.
373. Chorn, G, Klein-McDowell, M, Zhao, L, Saunders, MA, Flanagan, WM, Willingham, AT*, et al.* (2012). Single-stranded microRNA mimics. *RNA* **18**: 1796-1804.
374. Esau, CC, and Monia, BP (2007). Therapeutic potential for microRNAs. *Adv Drug Deliv Rev* **59**: 101-114.
375. Liu, YP, and Berkhout, B (2011). miRNA cassettes in viral vectors: problems and solutions. *Biochim Biophys Acta* **1809**: 732-745.
376. McManus, MT, Petersen, CP, Haines, BB, Chen, J, and Sharp, PA (2002). Gene silencing using micro-RNA designed hairpins. *RNA* **8**: 842-850.
377. Sibley, CR, Seow, Y, and Wood, MJ (2010). Novel RNA-based strategies for therapeutic gene silencing. *Mol Ther* **18**: 466-476.
378. Grimm, D, and Kay, MA (2007). RNAi and gene therapy: a mutual attraction. *Hematology Am Soc Hematol Educ Program*: 473-481.
379. Grimm, D, Wang, L, Lee, JS, Schurmann, N, Gu, S, Borner, K*, et al.* (2010). Argonaute proteins are key determinants of RNAi efficacy, toxicity, and persistence in the adult mouse liver. *J Clin Invest* **120**: 3106-3119.
380. Boudreau, RL, Martins, I, and Davidson, BL (2009). Artificial microRNAs as siRNA shuttles: improved safety as compared to shRNAs in vitro and in vivo. *Mol Ther* **17**: 169-175.
381. McBride, JL, Boudreau, RL, Harper, SQ, Staber, PD, Monteys, AM, Martins, I*, et al.* (2008). Artificial miRNAs mitigate shRNA-mediated toxicity in the brain: implications for the therapeutic development of RNAi. *Proc Natl Acad Sci USA* **105**: 5868-5873.
382. Jackson, AL, Burchard, J, Schelter, J, Chau, BN, Cleary, M, Lim, L*, et al.* (2006). Widespread siRNA "off-target" transcript silencing mediated by seed region sequence complementarity. *RNA* **12**: 1179-1187.
383. Sun, X, Rogoff, HA, and Li, CJ (2008). Asymmetric RNA duplexes mediate RNA interference in mammalian cells. *Nat Biotechnol* **26**: 1379-1382.
384. Liu, C, Kelnar, K, Liu, B, Chen, X, Calhoun-Davis, T, Li, H*, et al.* (2011). The microRNA miR-34a inhibits prostate cancer stem cells and metastasis by directly repressing CD44. *Nat Med* **17**: 211-215.
385. Tazawa, H, Tsuchiya, N, Izumiya, M, and Nakagama, H (2007). Tumor-suppressive miR-34a induces senescence-like growth arrest through modulation of the E2F pathway in human colon cancer cells. *Proc Natl Acad Sci USA* **104**: 15472-15477.
386. Li, L, Xie, X, Luo, J, Liu, M, Xi, S, Guo, J*, et al.* (2012). Targeted expression of miR-34a using the T-VISA system suppresses breast cancer cell growth and invasion. *Mol Ther* **20**: 2326-2334.
387. Elmen, J, Lindow, M, Silahtaroglu, A, Bak, M, Christensen, M, Lind-Thomsen, A*, et al.* (2008). Antagonism of microRNA-122 in mice by systemically administered LNA-antimiR leads to up-regulation of a large set of predicted target mRNAs in the liver. *Nucleic Acids Res* **36**: 1153-1162.
388. Lanford, RE, Hildebrandt-Eriksen, ES, Petri, A, Persson, R, Lindow, M, Munk, ME*, et al.* (2010). Therapeutic silencing of microRNA-122 in primates with chronic hepatitis C virus infection. *Science* **327**: 198-201.
389. Jopling, CL, Yi, M, Lancaster, AM, Lemon, SM, and Sarnow, P (2005). Modulation of hepatitis C virus RNA abundance by a liver-specific MicroRNA. *Science* **309**: 1577-1581.
390. Lindow, M, and Kauppinen, S (2012). Discovering the first microRNA-targeted drug. *J Cell Biol* **199**: 407-412.
391. Bader, AG (2012). miR-34 - a microRNA replacement therapy is headed to the clinic. *Front Genet* **3**: 120.

392. Banks, WA, Farr, SA, Butt, W, Kumar, VB, Franko, MW, and Morley, JE (2001). Delivery across the blood-brain barrier of antisense directed against amyloid beta: reversal of learning and memory deficits in mice overexpressing amyloid precursor protein. *J Pharmacol Exp Ther* **297**: 1113-1121.

393. Catuogno, S, Esposito, CL, Quintavalle, C, Condorelli, G, de Franciscis, V, and Cerchia, L (2012). Nucleic acids in human glioma treatment: innovative approaches and recent results. *J Signal Transduct* **2012**: 735135.

394. Du, L, Kayali, R, Bertoni, C, Fike, F, Hu, H, Iversen, PL*, et al.* (2011). Arginine-rich cell-penetrating peptide dramatically enhances AMO-mediated ATM aberrant splicing correction and enables delivery to brain and cerebellum. *Hum Mol Genet* **20**: 3151-3160.

395. Xia, H, Mao, Q, Paulson, HL, and Davidson, BL (2002). siRNA-mediated gene silencing in vitro and in vivo. *Nat Biotechnol* **20**: 1006-1010.

396. Lu, PY, Xie, F, and Woodle, MC (2005). In vivo application of RNA interference: from functional genomics to therapeutics. *Adv Genet* **54**: 117-142.

397. Tong, AW (2006). Small RNAs and non-small cell lung cancer. *Curr Mol Med* **6**: 339-349.

398. Uprichard, SL, Boyd, B, Althage, A, and Chisari, FV (2005). Clearance of hepatitis B virus from the liver of transgenic mice by short hairpin RNAs. *Proc Natl Acad Sci USA* **102**: 773-778.

399. Kota, J, Chivukula, RR, O'Donnell, KA, Wentzel, EA, Montgomery, CL, Hwang, HW*, et al.* (2009). Therapeutic microRNA delivery suppresses tumorigenesis in a murine liver cancer model. *Cell* **137**: 1005-1017.

400. Trang, P, Medina, PP, Wiggins, JF, Ruffino, L, Kelnar, K, Omotola, M*, et al.* (2010). Regression of murine lung tumors by the let-7 microRNA. *Oncogene* **29**: 1580-1587.

401. Bonci, D, Coppola, V, Musumeci, M, Addario, A, Giuffrida, R, Memeo, L*, et al.* (2008). The miR-15a-miR-16-1 cluster controls prostate cancer by targeting multiple oncogenic activities. *Nat Med* **14**: 1271-1277.

402. Lee, SJ, Kim, SJ, Seo, HH, Shin, SP, Kim, D, Park, CS*, et al.* (2012). Over-expression of miR-145 enhances the effectiveness of HSVtk gene therapy for malignant glioma. *Cancer Lett* **320**: 72-80.

403. Wang, X, Han, L, Zhang, A, Wang, G, Jia, Z, Yang, Y*, et al.* (2011). Adenovirus-mediated shRNAs for co-repression of miR-221 and miR-222 expression and function in glioblastoma cells. *Oncol Rep* **25**: 97-105.

404. Leber, MF, Bossow, S, Leonard, VH, Zaoui, K, Grossardt, C, Frenzke, M*, et al.* (2011). MicroRNA-sensitive oncolytic measles viruses for cancer-specific vector tropism. *Mol Ther* **19**: 1097-1106.

405. Lee, CY, Rennie, PS, and Jia, WW (2009). MicroRNA regulation of oncolytic herpes simplex virus-1 for selective killing of prostate cancer cells. *Clin Cancer Res* **15**: 5126-5135.

406. Skalsky, RL, and Cullen, BR (2011). Reduced expression of brain-enriched microRNAs in glioblastomas permits targeted regulation of a cell death gene. *PLoS One* **6**: e24248.

407. Pramanik, D, Campbell, NR, Karikari, C, Chivukula, R, Kent, OA, Mendell, JT*, et al.* (2011). Restitution of tumor suppressor microRNAs using a systemic nanovector inhibits pancreatic cancer growth in mice. *Mol Cancer Ther* **10**: 1470-1480.

408. Chen, Y, Zhu, X, Zhang, X, Liu, B, and Huang, L (2010). Nanoparticles modified with tumor-targeting scFv deliver siRNA and miRNA for cancer therapy. *Mol Ther* **18**: 1650-1656.

409. Trang, P, Wiggins, JF, Daige, CL, Cho, C, Omotola, M, Brown, D*, et al.* (2011). Systemic delivery of tumor suppressor microRNA mimics using a neutral lipid emulsion inhibits lung tumors in mice. *Mol Ther* **19**: 1116-1122.

410. Guan, J, Fujimoto, KL, Sacks, MS, and Wagner, WR (2005). Preparation and characterization of highly porous, biodegradable polyurethane scaffolds for soft tissue applications. *Biomaterials* **26**: 3961-3971.

411. Yang, YP, Chien, Y, Chiou, GY, Cherng, JY, Wang, ML, Lo, WL*, et al.* (2012). Inhibition of cancer stem cell-like properties and reduced chemoradioresistance of glioblastoma using microRNA145 with cationic polyurethane-short branch PEI. *Biomaterials* **33**: 1462-1476.

412. Liu, XY, Ho, WY, Hung, WJ, and Shau, MD (2009). The characteristics and transfection efficiency of cationic poly (ester-co-urethane) - short chain PEI conjugates self-assembled with DNA. *Biomaterials* **30**: 6665-6673.

413. Bala, I, Hariharan, S, and Kumar, MN (2004). PLGA nanoparticles in drug delivery: the state of the art. *Crit Rev Ther Drug Carrier Syst* **21**: 387-422.

414. Pettit, MW, Griffiths, P, Ferruti, P, and Richardson, SC (2011). Poly(amidoamine) polymers: soluble linear amphiphilic drug-delivery systems for genes, proteins and oligonucleotides. *Ther Deliv* **2**: 907-917.

415. Ren, Y, Kang, CS, Yuan, XB, Zhou, X, Xu, P, Han, L*, et al.* (2010). Co-delivery of as-miR-21 and 5-FU by poly(amidoamine) dendrimer attenuates human glioma cell growth in vitro. *J Biomater Sci Polym Ed* **21**: 303-314.

416. D'Emanuele, A, and Attwood, D (2005). Dendrimer-drug interactions. *Adv Drug Deliv Rev* **57**: 2147-2162.

417. Khasraw, M. and Lassman, A.B. (2010) Advances in the treatment of malignant gliomas. *Curr Oncol Rep*, **12**, 26-33.

418. Bartel, D.P. and Chen, C.Z. (2004) Micromanagers of gene expression: the potentially widespread influence of metazoan microRNAs. *Nat Rev Genet*, **5**, 396-400.

419 Hank, N.C., Shapiro, J.R. and Scheck, A.C. (2006) Over-representation of specific regions of chromosome 22 in cells from human glioma correlate with resistance to 1,3-bis(2-chloroethyl)-1-nitrosourea. *BMC Cancer*, **6**, 2.

420 Lena, A., Rechichi, M., Salvetti, A., Bartoli, B., Vecchio, D., Scarcelli, V., Amoroso, R., Benvenuti, L., Gagliardi, R., Gremigni, V. *et al.* (2009) Drugs targeting the mitochondrial pore act as cytotoxic and cytostatic agents in temozolomide-resistant glioma cells. *J Transl Med*, **7**, 13.

421 Prados, M.D., Lamborn, K.R., Chang, S., Burton, E., Butowski, N., Malec, M., Kapadia, A., Rabbitt, J., Page, M.S., Fedoroff, A. *et al.* (2006) Phase 1 study of erlotinib HCl alone and combined with temozolomide in patients with stable or recurrent malignant glioma. *Neuro Oncol*, **8**, 67-78.

422 Lawler, S. and Chiocca, E.A. (2009) Emerging functions of microRNAs in glioblastoma. *J Neurooncol*, **92**, 297-306.

423 Silber, J., Lim, D.A., Petritsch, C., Persson, A.I., Maunakea, A.K., Yu, M., Vandenberg, S.R., Ginzinger, D.G., James, C.D., Costello, J.F. *et al.* (2008) miR-124 and miR-137 inhibit proliferation of glioblastoma multiforme cells and induce differentiation of brain tumor stem cells. *BMC Med*, **6**, 14.

424 Morris, P.G. and Abrey, L.E. (2010) Novel targeted agents for platelet-derived growth factor receptor and c-KIT in malignant gliomas. *Target Oncol*, **5**, 193-200.

425 Lei, L., Sonabend, A.M., Guarnieri, P., Soderquist, C., Ludwig, T., Rosenfeld, S., Bruce, J.N. and Canoll, P. (2011), In *PLoS One*, Vol. 6, pp. e20041.

426 Chan, J.A., Krichevsky, A.M. and Kosik, K.S. (2005) MicroRNA-21 is an antiapoptotic factor in human glioblastoma cells. *Cancer Res*, **65**, 6029-6033.

427 Conti, A., Aguennouz, M., La Torre, D., Tomasello, C., Cardali, S., Angileri, F.F., Maio, F., Cama, A., Germano, A., Vita, G. *et al.* (2009) miR-21 and 221 upregulation and miR-181b downregulation in human grade II-IV astrocytic tumors. *J Neurooncol*, **93**, 325-332.

428 Zhu, S., Wu, H., Wu, F., Nie, D., Sheng, S. and Mo, Y.Y. (2008) MicroRNA-21 targets tumor suppressor genes in invasion and metastasis. *Cell Res*, **18**, 350-359.

429 Trabulo, S., Resina, S., Simoes, S., Lebleu, B. and Pedroso de Lima, M.C. (2010) A non-covalent strategy combining cationic lipids and CPPs to enhance the delivery of splice correcting oligonucleotides. *J Control Release*, **145**, 149-158.

430 Lu, Z., Liu, M., Stribinskis, V., Klinge, C.M., Ramos, K.S., Colburn, N.H. and Li, Y. (2008) MicroRNA-21 promotes cell transformation by targeting the programmed cell death 4 gene. *Oncogene*, **27**, 4373-4379.

431 Ak, P. and Levine, A.J. (2010) p53 and NF-kappaB: different strategies for responding to stress lead to a functional antagonism. *FASEB J*, **24**, 3643-3652.

432 Stiewe, T. (2007) The p53 family in differentiation and tumorigenesis. *Nat Rev Cancer*, **7**, 165-168.

433 Kim, S., Han, J., Lee, S.K., Hur, S.M., Koo, M., Cho, D.H., Bae, S.Y., Choi, M.Y., Shin, I., Yang, J.H. *et al.* (2010) Pifithrin-alpha, an inhibitor of p53 transactivation, up-regulates COX-2 expression through an MAPK-dependent pathway. *Pharmacology*, **86**, 313-319.

434 Murphy, P.J., Galigniana, M.D., Morishima, Y., Harrell, J.M., Kwok, R.P., Ljungman, M. and Pratt, W.B. (2004) Pifithrin-alpha inhibits p53 signaling after interaction of the tumor suppressor protein with hsp90 and its nuclear translocation. *J Biol Chem*, **279**, 30195-30201.

435 Fan, S., Qi, M., Yu, Y., Li, L., Yao, G., Tashiro, S., Onodera, S. and Ikejima, T. (2012) P53 activation plays a crucial role in silibinin induced ROS generation via PUMA and JNK. *Free Radic Res*, **46**, 310-319.

436 Strosznajder, R.P., Jesko, H., Banasik, M. and Tanaka, S. (2005) Effects of p53 inhibitor on survival and death of cells subjected to oxidative stress. *J Physiol Pharmacol*, **56 Suppl 4**, 215-221.

437 Rocha, S., Campbell, K.J., Roche, K.C. and Perkins, N.D. (2003) The p53-inhibitor pifithrin-alpha inhibits firefly luciferase activity in vivo and in vitro. *BMC Mol Biol*, **4**, 9.

438 Tergaonkar, V. and Perkins, N.D. (2007) p53 and NF-kappaB crosstalk: IKKalpha tips the balance. *Mol Cell*, **26**, 158-159.

439 Ben-Neriah, Y. and Karin, M. (2011) Inflammation meets cancer, with NF-kappaB as the matchmaker. *Nat Immunol*, **12**, 715-723.

440   Heinzelmann, J., Henning, B., Sanjmyatav, J., Posorski, N., Steiner, T., Wunderlich, H., Gajda, M.R. and Junker, K. (2011) Specific miRNA signatures are associated with metastasis and poor prognosis in clear cell renal cell carcinoma. *World J Urol*, **29**, 367-373.

441   Zhang, H., Li, Y. and Lai, M. (2010) The microRNA network and tumor metastasis. *Oncogene*, **29**, 937-948.

442   Asangani, I.A., Rasheed, S.A., Nikolova, D.A., Leupold, J.H., Colburn, N.H., Post, S. and Allgayer, H. (2008) MicroRNA-21 (miR-21) post-transcriptionally downregulates tumor suppressor Pdcd4 and stimulates invasion, intravasation and metastasis in colorectal cancer. *Oncogene*, **27**, 2128-2136.

443   Zhu, S., Si, M.L., Wu, H. and Mo, Y.Y. (2007) MicroRNA-21 targets the tumor suppressor gene tropomyosin 1 (TPM1). *J Biol Chem*, **282**, 14328-14336.

444   Gaur, A.B., Holbeck, S.L., Colburn, N.H. and Israel, M.A. (2011) Downregulation of Pdcd4 by mir-21 facilitates glioblastoma proliferation in vivo. *Neuro Oncol*, **13**, 580-590.

445   Lino, M.M. and Merlo, A. (2010) PI3Kinase signaling in glioblastoma. *J Neurooncol*, **103**, 417-427.

446   Zhou, X., Ren, Y., Moore, L., Mei, M., You, Y., Xu, P., Wang, B., Wang, G., Jia, Z., Pu, P. *et al.* (2010) Downregulation of miR-21 inhibits EGFR pathway and suppresses the growth of human glioblastoma cells independent of PTEN status. *Lab Invest*, **90**, 144-155.

447   Gao, F., Zhang, P., Zhou, C., Li, J., Wang, Q., Zhu, F., Ma, C., Sun, W. and Zhang, L. (2007) Frequent loss of PDCD4 expression in human glioma: possible role in the tumorigenesis of glioma. *Oncol Rep*, **17**, 123-128.

448   Yang, H.S., Jansen, A.P., Nair, R., Shibahara, K., Verma, A.K., Cmarik, J.L. and Colburn, N.H. (2001) A novel transformation suppressor, Pdcd4, inhibits AP-1 transactivation but not NF-kappaB or ODC transactivation. *Oncogene*, **20**, 669-676.

449   Chen, Y., Liu, W., Chao, T., Zhang, Y., Yan, X., Gong, Y., Qiang, B., Yuan, J., Sun, M. and Peng, X. (2008) MicroRNA-21 down-regulates the expression of tumor suppressor PDCD4 in human glioblastoma cell T98G. *Cancer Lett*, **272**, 197-205.

450   Corsten, M.F., Miranda, R., Kasmieh, R., Krichevsky, A.M., Weissleder, R. and Shah, K. (2007) MicroRNA-21 knockdown disrupts glioma growth in vivo and displays synergistic cytotoxicity with neural precursor cell delivered S-TRAIL in human gliomas. *Cancer Res*, **67**, 8994-9000.

451   Ren, Y., Kang, C.S., Yuan, X.B., Zhou, X., Xu, P., Han, L., Wang, G.X., Jia, Z., Zhong, Y., Yu, S. *et al.* (2010) Co-delivery of as-miR-21 and 5-FU by poly(amidoamine) dendrimer attenuates human glioma cell growth in vitro. *J Biomater Sci Polym Ed*, **21**, 303-314.

452   Ren, Y., Zhou, X., Mei, M., Yuan, X.B., Han, L., Wang, G.X., Jia, Z.F., Xu, P., Pu, P.Y. and Kang, C.S. (2010) MicroRNA-21 inhibitor sensitizes human glioblastoma cells U251 (PTEN-mutant) and LN229 (PTEN-wild type) to taxol. *BMC Cancer*, **10**, 27.

453   Banker, G. and Goslin, K. (1998) *Culturing nerve cells (Second Edition)*. The MIT Press, Cambridge, MA.

454   de Almeida, L.P., Ross, C.A., Zala, D., Aebischer, P. and Deglon, N. (2002) Lentiviral-mediated delivery of mutant huntingtin in the striatum of rats induces a selective neuropathology modulated by polyglutamine repeat size, huntingtin expression levels, and protein length. *J Neurosci*, **22**, 3473-3483.

455   Alves, S., Nascimento-Ferreira, I., Dufour, N., Hassig, R., Auregan, G., Nobrega, C., Brouillet, E., Hantraye, P., Pedroso de Lima, M.C., Deglon, N. *et al.* (2010) Silencing ataxin-3 mitigates degeneration in a rat model of Machado-Joseph disease: no role for wild-type ataxin-3? *Hum Mol Genet*, **19**, 2380-2394.

456   Cardoso, A.L., Guedes, J.R., Pereira de Almeida, L. and Pedroso de Lima, M.C. (2012) miR-155 modulates microglia-mediated immune response by down-regulating SOCS-1 and promoting cytokine and nitric oxide production. *Immunology*, **135**, 73-88.

457   Lee, H., Choi, H.J., Kang, C.S., Lee, H.J., Lee, W.S. and Park, C.S. (2012) Expression of miRNAs and PTEN in endometrial specimens ranging from histologically normal to hyperplasia and endometrial adenocarcinoma. *Mod Pathol.*

458   Pfaffl, M.W. (2001), In *Nucleic Acids Res*, Vol. 29, pp. e45.

459   Ferreira, R., Xapelli, S., Santos, T., Silva, A.P., Cristovao, A., Cortes, L. and Malva, J.O. (2010) Neuropeptide Y modulation of interleukin-1{beta} (IL-1{beta})-induced nitric oxide production in microglia. *J Biol Chem*, **285**, 41921-41934.

460   Pena, J.T., Sohn-Lee, C., Rouhanifard, S.H., Ludwig, J., Hafner, M., Mihailovic, A., Lim, C., Holoch, D., Berninger, P., Zavolan, M. *et al.* (2009) miRNA in situ hybridization in formaldehyde and EDC-fixed tissues. *Nat Methods*, **6**, 139-141.

461   O'Brien, J., Wilson, I., Orton, T. and Pognan, F. (2000) Investigation of the Alamar Blue (resazurin) fluorescent dye for the assessment of mammalian cell cytotoxicity. *Eur J Biochem*, **267**, 5421-5426.

462   Benjamini, Y., Hochberg, Y. (1995) Controlling the false discovery rate - a practical and powerful approach to multiple testing. *Journal of the Royal Statistical Society. Series B (Methodological)*, **57**, 289-300.

463.   Costa, PM, Cardoso, AL, Nobrega, C, Pereira de Almeida, LF, Bruce, JN, Canoll, P*, et al.* (2012). MicroRNA-21 silencing enhances the cytotoxic effect of the antiangiogenic drug sunitinib in glioblastoma. *Hum Mol Genet* **22**: 904-918.

464.   Dong, CG, Wu, WK, Feng, SY, Wang, XJ, Shao, JF, and Qiao, J (2012). Co-inhibition of microRNA-10b and microRNA-21 exerts synergistic inhibition on the proliferation and invasion of human glioma cells. *Int J Oncol* **41**: 1005-1012.

465.   Qian, X, Ren, Y, Shi, Z, Long, L, Pu, P, Sheng, J*, et al.* (2012). Sequence-dependent synergistic inhibition of human glioma cell lines by combined temozolomide and miR-21 inhibitor gene therapy. *Mol Pharm* **9**: 2636-2645.

466.   Cardoso, AL, Simoes, S, de Almeida, LP, Plesnila, N, Pedroso de Lima, MC, Wagner, E*, et al.* (2008). Tf-lipoplexes for neuronal siRNA delivery: a promising system to mediate gene silencing in the CNS. *J Control Release* **132**: 113-123.

467.   Hutterer, M, Gunsilius, E, and Stockhammer, G (2006). Molecular therapies for malignant glioma. *Wien Med Wochenschr* **156**: 351-363.

468.   Kanai, R, Rabkin, SD, Yip, S, Sgubin, D, Zaupa, CM, Hirose, Y*, et al.* (2011). Oncolytic virus-mediated manipulation of DNA damage responses: synergy with chemotherapy in killing glioblastoma stem cells. *J Natl Cancer Inst* **104**: 42-55.

469.   Gomes-da-Silva, LC, Santos, AO, Bimbo, LM, Moura, V, Ramalho, JS, Pedroso de Lima, MC*, et al.* (2012). Toward a siRNA-containing nanoparticle targeted to breast cancer cells and the tumor microenvironment. *Int J Pharm* **434**: 9-19.

470.   Judge, AD, Robbins, M, Tavakoli, I, Levi, J, Hu, L, Fronda, A*, et al.* (2009). Confirming the RNAi-mediated mechanism of action of siRNA-based cancer therapeutics in mice. *J Clin Invest* **119**: 661-673.

471.   Mendonca, LS, Firmino, F, Moreira, JN, Pedroso de Lima, MC, and Simoes, S (2010). Transferrin receptor-targeted liposomes encapsulating anti-BCR-ABL siRNA or asODN for chronic myeloid leukemia treatment. *Bioconjug Chem* **21**: 157-168.

472.   Mamelak, AN, and Jacoby, DB (2007). Targeted delivery of antitumoral therapy to glioma and other malignancies with synthetic chlorotoxin (TM-601). *Expert Opin Drug Deliv* **4**: 175-186.

473.   Veiseh, O, Sun, C, Fang, C, Bhattarai, N, Gunn, J, Kievit, F*, et al.* (2009). Specific targeting of brain tumors with an optical/magnetic resonance imaging nanoprobe across the blood-brain barrier. *Cancer Res* **69**: 6200-6207.

474.   Deshane, J, Garner, CC, and Sontheimer, H (2003). Chlorotoxin inhibits glioma cell invasion via matrix metalloproteinase-2. *J Biol Chem* **278**: 4135-4144.

475.   Aguilar-Morante, D, Morales-Garcia, JA, Sanz-SanCristobal, M, Garcia-Cabezas, MA, Santos, A, and Perez-Castillo, A (2010). Inhibition of glioblastoma growth by the thiadiazolidinone compound TDZD-8. *PLoS One* **5**: e13879.

476.   Pedroso de Lima, MC, Simoes, S, Pires, P, Faneca, H, and Duzgunes, N (2001). Cationic lipid-DNA complexes in gene delivery: from biophysics to biological applications. *Adv Drug Deliv Rev* **47**: 277-294.

477.   Semple, SC, Klimuk, SK, Harasym, TO, Dos Santos, N, Ansell, SM, Wong, KF*, et al.* (2001). Efficient encapsulation of antisense oligonucleotides in lipid vesicles using ionizable aminolipids: formation of novel small multilamellar vesicle structures. *Biochim Biophys Acta* **1510**: 152-166.

478.   Zimmermann, TS, Lee, AC, Akinc, A, Bramlage, B, Bumcrot, D, Fedoruk, MN*, et al.* (2006). RNAi-mediated gene silencing in non-human primates. *Nature* **441**: 111-114.

479.   Morrissey, DV, Lockridge, JA, Shaw, L, Blanchard, K, Jensen, K, Breen, W*, et al.* (2005). Potent and persistent in vivo anti-HBV activity of chemically modified siRNAs. *Nat Biotechnol* **23**: 1002-1007.

480.   Li, SD, and Huang, L (2008). Pharmacokinetics and biodistribution of nanoparticles. *Mol Pharm* **5**: 496-504.

481.   Remaut, K, Lucas, B, Braeckmans, K, Demeester, J, and De Smedt, SC (2007). Pegylation of liposomes favours the endosomal degradation of the delivered phosphodiester oligonucleotides. *J Control Release* **117**: 256-266.

482.   Santos, AO, da Silva, LC, Bimbo, LM, de Lima, MC, Simoes, S, and Moreira, JN (2010). Design of peptide-targeted liposomes containing nucleic acids. *Biochim Biophys Acta* **1798**: 433-441.

483.   Moreira, JN, Gaspar, R, and Allen, TM (2001). Targeting Stealth liposomes in a murine model of human small cell lung cancer. *Biochim Biophys Acta* **1515**: 167-176.

484. Bartlett, DW, Su, H, Hildebrandt, IJ, Weber, WA, and Davis, ME (2007). Impact of tumor-specific targeting on the biodistribution and efficacy of siRNA nanoparticles measured by multimodality in vivo imaging. *Proc Natl Acad Sci U S A* **104**: 15549-15554.

485. de Wolf, HK, Snel, CJ, Verbaan, FJ, Schiffelers, RM, Hennink, WE, and Storm, G (2007). Effect of cationic carriers on the pharmacokinetics and tumor localization of nucleic acids after intravenous administration. *Int J Pharm* **331**: 167-175.

486. Trabulo, S, Cardoso, AM, Santos-Ferreira, T, Cardoso, AL, Simoes, S, and Pedroso de Lima, MC (2011). Survivin silencing as a promising strategy to enhance the sensitivity of cancer cells to chemotherapeutic agents. *Mol Pharm* **8**: 1120-1131.

487. Lyons, SA, O'Neal, J, and Sontheimer, H (2002). Chlorotoxin, a scorpion-derived peptide, specifically binds to gliomas and tumors of neuroectodermal origin. *Glia* **39**: 162-173.

488. Xiong, Q, Wilson, WK, and Pang, J (2007). The Liebermann-Burchard reaction: sulfonation, desaturation, and rearrangment of cholesterol in acid. *Lipids* **42**: 87-96.

489. Moreira, JN, Ishida, T, Gaspar, R, and Allen, TM (2002). Use of the post-insertion technique to insert peptide ligands into pre-formed stealth liposomes with retention of binding activity and cytotoxicity. *Pharm Res* **19**: 265-269.

490. Schneider, CA, Rasband, WS, and Eliceiri, KW (2012). NIH Image to ImageJ: 25 years of image analysis. *Nat Methods* **9**: 671-675.

491. Costa, PM, Cardoso, AL, Pereira de Almeida, LF, Bruce, JN, Canoll, P, and Pedroso de Lima, MC (2012). PDGF-B-mediated downregulation of miR-21: new insights into PDGF signaling in glioblastoma. *Hum Mol Genet*. **21**: 5118-5130.

492. Nagarajan, R.P. and Costello, J.F. (2009) Epigenetic mechanisms in glioblastoma multiforme. *Semin. Cancer Biol.*, **19**, 188-197.

493. Hermanson, M., Funa, K., Hartman, M., Claesson-Welsh, L., Heldin, C.H., Westermark, B. and Nister, M. (1992) Platelet-derived growth factor and its receptors in human glioma tissue: expression of messenger RNA and protein suggests the presence of autocrine and paracrine loops. *Cancer Res.*, **52**, 3213-3219.

494. Armstrong, R.C., Harvath, L. and Dubois-Dalcq, M.E. (1990) Type 1 astrocytes and oligodendrocyte-type 2 astrocyte glial progenitors migrate toward distinct molecules. *J. Neurosci. Res.*, **27**, 400-407.

495. Frost, E.E., Zhou, Z., Krasnesky, K. and Armstrong, R.C. (2009) Initiation of oligodendrocyte progenitor cell migration by a PDGF-A activated extracellular regulated kinase (ERK) signaling pathway. *Neurochem. Res.*, **34**, 169-181.

496. Uhrbom, L., Hesselager, G., Nister, M. and Westermark, B. (1998) Induction of brain tumors in mice using a recombinant platelet-derived growth factor B-chain retrovirus. *Cancer Res.*, **58**, 5275-5279.

497. Assanah, M.C., Bruce, J.N., Suzuki, S.O., Chen, A., Goldman, J.E. and Canoll, P. (2009) PDGF stimulates the massive expansion of glial progenitors in the neonatal forebrain. *Glia*, **57**, 1835-1847.

498. Masui, K., Suzuki, S.O., Torisu, R., Goldman, J.E., Canoll, P. and Iwaki, T. (2010) Glial progenitors in the brainstem give rise to malignant gliomas by platelet-derived growth factor stimulation. *Glia*, **58**, 1050-1065.

499. Calzolari, F. and Malatesta, P. (2010) Recent insights into PDGF-induced gliomagenesis. *Brain Pathol.*, **20**, 527-538.

500. Torisu, R., Suzuki, S.O., Masui, K., Yoshimoto, K., Mizoguchi, M., Hashizume, M., Canoll, P., Goldman, J.E., Sasaki, T. and Iwaki, T. (2011) Persistent roles of signal transduction of platelet-derived growth factor B in genesis, growth, and anaplastic transformation of gliomas in an in-vivo serial transplantation model. *Brain Tumor Pathol.*, **28**, 33-42.

501. Cannell, I.G., Kong, Y.W. and Bushell, M. (2008) How do microRNAs regulate gene expression? *Biochem. Soc. Trans.*, **36**, 1224-1231.

502. Dweep, H., Sticht, C., Pandey, P. and Gretz, N. (2011) miRWalk--database: prediction of possible miRNA binding sites by "walking" the genes of three genomes. *J. Biomed. Inform.*, **44**, 839-847.

503. Sirotkin, A.V., Laukova, M., Ovcharenko, D., Brenaut, P. and Mlyncek, M. (2010) Identification of microRNAs controlling human ovarian cell proliferation and apoptosis. *J. Cell. Physiol.*, **223**, 49-56.

504. King, J.C., Lu, Q.Y., Li, G., Moro, A., Takahashi, H., Chen, M., Go, V.L., Reber, H.A., Eibl, G. and Hines, O.J. (2012) Evidence for activation of mutated p53 by apigenin in human pancreatic cancer. *Biochim. Biophys. Acta*, **1823**, 593-604.

505. Waters, F.J., Shavlakadze, T., McIldowie, M.J., Piggott, M.J. and Grounds, M.D. (2010) Use of pifithrin to inhibit p53-mediated signalling of TNF in dystrophic muscles of mdx mice. *Mol. Cell Biochem.*, **337**, 119-131.

506. Chang, K.W., Liu, C.J., Chu, T.H., Cheng, H.W., Hung, P.S., Hu, W.Y. and Lin, S.C. (2008) Association between high miR-211 microRNA expression and the poor prognosis of oral carcinoma. *J. Dent. Res.*, **87**, 1063-1068.

507. Quintavalle, M., Elia, L., Condorelli, G. and Courtneidge, S.A. (2010) MicroRNA control of podosome formation in vascular smooth muscle cells in vivo and in vitro. *J. Cell Biol.*, **189**, 13-22.

508. Goff, L.A., Boucher, S., Ricupero, C.L., Fenstermacher, S., Swerdel, M., Chase, L.G., Adams, C.C., Chesnut, J., Lakshmipathy, U. and Hart, R.P. (2008) Differentiating human multipotent mesenchymal stromal cells regulate microRNAs: prediction of microRNA regulation by PDGF during osteogenesis. *Exp. Hematol.*, **36**, 1354-1369.

509. Folini, M., Gandellini, P., Longoni, N., Profumo, V., Callari, M., Pennati, M., Colecchia, M., Supino, R., Veneroni, S., Salvioni, R. *et al.* (2010) miR-21: an oncomir on strike in prostate cancer. *Mol. Cancer.*, **9**, 12.

510. Rask, L., Balslev, E., Jorgensen, S., Eriksen, J., Flyger, H., Moller, S., Hogdall, E., Litman, T. and Nielsen, B.S. (2011) High expression of miR-21 in tumor stroma correlates with increased cancer cell proliferation in human breast cancer. *APMIS*, **119**, 663-673.

511. Hong, L., Lai, M., Chen, M., Xie, C., Liao, R., Kang, Y.J., Xiao, C., Hu, W.Y., Han, J. and Sun, P. (2010) The miR-17-92 cluster of microRNAs confers tumorigenicity by inhibiting oncogene-induced senescence. *Cancer Res.*, **70**, 8547-8557.

512. Chen, L., Li, C., Zhang, R., Gao, X., Qu, X., Zhao, M., Qiao, C., Xu, J. and Li, J. (2011) miR-17-92 cluster microRNAs confers tumorigenicity in multiple myeloma. *Cancer Lett.*, **309**, 62-70.

513. Olive, V., Jiang, I. and He, L. (2010) mir-17-92, a cluster of miRNAs in the midst of the cancer network. *Int. J. Biochem. Cell Biol.*, **42**, 1348-1354.

514. Schraivogel, D., Weinmann, L., Beier, D., Tabatabai, G., Eichner, A., Zhu, J.Y., Anton, M., Sixt, M., Weller, M., Beier, C.P. *et al.* (2011) CAMTA1 is a novel tumour suppressor regulated by miR-9/9* in glioblastoma stem cells. *EMBO J.*, **30**, 4309-4322.

515. Srinivasan, S., Patric, I.R. and Somasundaram, K. (2011) A ten-microRNA expression signature predicts survival in glioblastoma. *PLoS One*, **6**, e17438.

516. Yang, G., Zhang, R., Chen, X., Mu, Y., Ai, J., Shi, C., Liu, Y., Sun, L., Rainov, N.G., Li, H. *et al.* (2011) MiR-106a inhibits glioma cell growth by targeting E2F1 independent of p53 status. *J. Mol. Med. (Berl)*, **89**, 1037-1050.

517. Landais, S., Landry, S., Legault, P. and Rassart, E. (2007) Oncogenic potential of the miR-106-363 cluster and its implication in human T-cell leukemia. *Cancer Res.*, **67**, 5699-5707.

518. Lee, S.T., Chu, K., Oh, H.J., Im, W.S., Lim, J.Y., Kim, S.K., Park, C.K., Jung, K.H., Lee, S.K., Kim, M. *et al.* (2011) Let-7 microRNA inhibits the proliferation of human glioblastoma cells. *J. Neurooncol.*, **102**, 19-24.

519. Acunzo, M., Visone, R., Romano, G., Veronese, A., Lovat, F., Palmieri, D., Bottoni, A., Garofalo, M., Gasparini, P., Condorelli, G. *et al.* (2012) miR-130a targets MET and induces TRAIL-sensitivity in NSCLC by downregulating miR-221 and 222. *Oncogene*, **31**, 634-642.

520. Zhang, L., Volinia, S., Bonome, T., Calin, G.A., Greshock, J., Yang, N., Liu, C.G., Giannakakis, A., Alexiou, P., Hasegawa, K. *et al.* (2008) Genomic and epigenetic alterations deregulate microRNA expression in human epithelial ovarian cancer. *Proc. Natl. Acad. Sci. U S A*, **105**, 7004-7009.

521. Chan, M.C., Hilyard, A.C., Wu, C., Davis, B.N., Hill, N.S., Lal, A., Lieberman, J., Lagna, G. and Hata, A. (2010) Molecular basis for antagonism between PDGF and the TGFbeta family of signalling pathways by control of miR-24 expression. *EMBO J.*, **29**, 559-573.

522. Sumazin, P., Yang, X., Chiu, H.S., Chung, W.J., Iyer, A., Llobet-Navas, D., Rajbhandari, P., Bansal, M., Guarnieri, P., Silva, J. *et al.* (2011) An extensive microRNA-mediated network of RNA-RNA interactions regulates established oncogenic pathways in glioblastoma. *Cell*, **147**, 370-381.

523. White, N.M., Fatoohi, E., Metias, M., Jung, K., Stephan, C. and Yousef, G.M. (2011) Metastamirs: a stepping stone towards improved cancer management. *Nat. Rev. Clin. Oncol.*, **8**, 75-84.

524. Vandesompele, J., De Preter, K., Pattyn, F., Poppe, B., Van Roy, N., De Paepe, A. and Speleman, F. (2002) Accurate normalization of real-time quantitative RT-PCR data by geometric averaging of multiple internal control genes. *Genome Biol.*, **3**, RESEARCH0034.

525. Lu, J. and Tsourkas, A. (2009) Imaging individual microRNAs in single mammalian cells in situ. *Nucleic Acids Res.*, **37**, e100.